

# BIOINORGANICS

Synthetic growth factors for bone regeneration

Zeinab Tahmasebi Birgani



**BIOINORGANICS**  
**SYNTHETIC GROWTH FACTORS FOR**  
**BONE REGENERATION**

**Zeinab Tahmasebi Birgani**

## Composition of the graduation committee:

*Chairman and Secretary* Prof.dr. Ir. J.W.M. Hilgenkamp

*Promoters* Prof.dr. P. Habibovic  
Prof.dr. C.A. van Blitterswijk

*Members* Prof.dr. H.B.J. Karperien  
Prof.dr. J.E. ten Elshof  
Prof.dr. J. de Boer  
Prof.dr. M. Bohner  
Dr. J.J.J.P. van den Beucken  
Dr. F. De Groot-Barrere

**MIRA**  
BIOMEDICAL TECHNOLOGY  
AND TECHNICAL MEDICINE

UNIVERSITY OF TWENTE.



The work described in this thesis was carried out in the department of Tissue Regeneration, MIRA Institute for Biomedical Technology and Technical Medicine, University of Twente, the Netherlands.

This research was funded by the research program of the BioMedical Materials institute, co-funded by the Dutch Ministry of Economic Affairs, Agriculture and Innovation.

Bioinorganics: Synthetic growth factors for bone regeneration

PhD thesis, University of Twente, Enschede

ISBN: 978-90-365-4153-4

DOI: 10.3990/1.9789036541534

Copyright ©Z. Tahmasebi Birgani

Published by: Z. Tahmasebi Birgani

Cover design: Z. Tahmasebi Birgani

Printed by: Gildeprint, Enschede

**BIOINORGANICS**  
**SYNTHETIC GROWTH FACTORS FOR**  
**BONE REGENERATION**

DISSERTATION

to obtain  
the degree of doctor at University of Twente,  
on the authority of the rector magnificus,  
Prof.dr. H. Brinksma,  
on account of the decision of the graduation committee,  
to be publicly defended  
on Wednesday, July 6<sup>th</sup>, 2016 at 12:45

by

**Zeinab Tahmasebi Birgani**

Born on 16 July 1985  
In Andimeshk, Iran.

This dissertation has been approved by:

Prof.dr. P. Habibovic

Prof.dr. C.A. van Blitterswijk

**This work is dedicated to my parents,  
for their support and inspiration for me,  
to grow into the person who I am today.**

این پایان نامه را به پدر و مادرم تقدیم می‌کنم،  
برای حمایت‌ها و تشویق‌هایشان،  
که باعث شد من این انسانی باشم که امروز هستم.



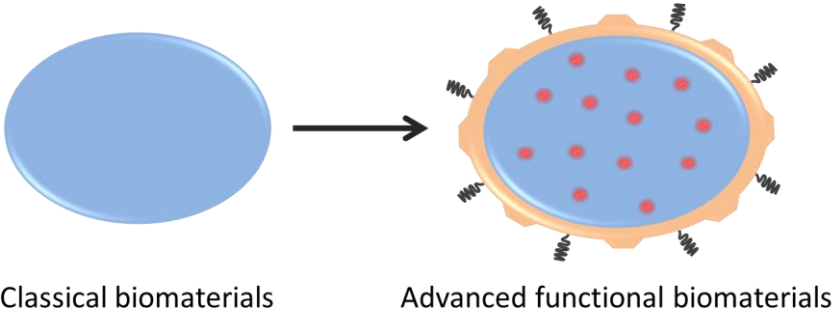
# Contents

<b>Chapter 1</b>	
Introduction: Biomaterials	<b>1</b>
<b>Chapter 2</b>	
Calcium phosphate ceramics with inorganic additives	<b>11</b>
<b>Chapter 3</b>	
Monolithic calcium phosphate/poly(lactic acid) composite versus calcium phosphate-coated poly(lactic acid) for support of osteogenic differentiation of human mesenchymal stromal cells	<b>63</b>
<b>Chapter 4</b>	
Human mesenchymal stromal cells response to biomimetic octacalcium phosphate containing strontium	<b>87</b>
<b>Chapter 5</b>	
Combinatorial incorporation of fluoride and cobalt ions into calcium phosphates to stimulate osteogenesis and angiogenesis	<b>117</b>
<b>Chapter 6</b>	
Stimulatory effect of cobalt ions incorporated into calcium phosphate coatings on neovascularization in an in vivo intramuscular model in goats	<b>149</b>
<b>Chapter 7</b>	
Poly(lactic acid) microspheres for local delivery of bioinorganics for applications in bone regeneration	<b>173</b>
<b>Chapter 8</b>	
General discussion and future perspective	<b>195</b>

<b>Summary</b>	<b>206</b>
<b>Samenvatting</b>	<b>208</b>
<b>Acknowledgement</b>	<b>210</b>
<b>Publications</b>	<b>212</b>

# Chapter 1

## Introduction: Biomaterials



## 1.1. Biomaterials

Biomaterials are defined as “materials intended to interface with biological systems to evaluate, treat, augment or replace any tissues, organs or functions of the body” [1].

Biomaterials have been categorized based on their chemical composition (metals, ceramics, polymers and their composites), origin (natural or synthetic), form (bulk materials, particulates, injectables, etc.), degradation behavior (permanent or degradable) and even based on the time period in which they were developed [2-5].

From an engineering point of view, the approaches that have been undertaken to develop biomaterials were determinant for the progression of the field. These approaches have shown an evolutionary path from conventional, passive materials that were used to anatomically replace damaged tissues or organs, to advanced functional biomaterials, which actively play a role in the restoration of the normal function of the damaged organ or tissue. This chapter summarizes the evolution of the approaches for developing biomaterials, introduces the main approach that was followed in the research described here and gives an outline of this thesis.

## 1.2. Classical biomaterials

The archeological efforts have demonstrated that the interactions of foreign non-biologic materials with the human body date back to prehistorical time. However, sea shell- and metal-based dental replacements are probably the first examples of biomaterials that were intentionally used for medical reasons. Suture materials, used for closing large wounds, are another example of the existence of the concept of biomaterials in early history [3], when the correct terminology and proper criteria for selecting, producing and using biomaterials did not exist, yet.

Further development of biomaterials was entangled with the recognition of the concepts of biocompatibility and bio(re)activity. The understanding of such concepts resulted in an improved success rate of the implanted biomaterials [3-4]. It also opened the door to the use of a wide range of the materials including metals, ceramics and especially polymers [4-5] in many more applications such as intraocular lenses, artificial organs, orthopedic and dental implants, cardiovascular implants, etc. [3]. The development of these conventional medical devices, which were used to anatomically replace and passively take over the

function of the damaged tissue or organ, was largely based on the properties that available materials could offer. The criteria for the desired biomaterials were defined by the clinical need. By searching among the existing materials, the material that qualified most criteria was then selected for producing the medical device or implant. Efforts put in design of the material properties were limited. While many of the biomaterials from the category of classical biomaterials are inert and non-degradable, examples exist of bioactive and degradable biomaterials that have been developed using the conventional approaches. These materials have been introduced in 1970's upon realizing that many of the clinical applications require materials that interact with the human body or are degradable in time [2].

### **1.3. Advanced functional biomaterials**

Further progress in basic knowledge of the clinical needs has revealed that for many clinical applications, biomaterials are needed which can aid restoration of one or more natural functions of damaged tissues. Such developments have set the stage for the next generation of biomaterials, the so-called functional biomaterials.

Functionality of a biomaterial is simply defined as the fitness for use in a clinical need [2]. In the context of biomaterials development, functional or advanced functional biomaterials are defined as the ones with added functionalities, which inherently do not exist in the material.

While the conventional methods were dependent on finding a biomaterial that offers the desired properties, the functional biomaterials are formulated and fabricated based on the required criteria via either processing-driven or design-driven approaches [6].

The processing-driven approaches aim at varying natural properties of the biomaterials in a controlled manner by changing and manipulating the processing parameters. The use of sintering conditions to control microstructure of ceramic materials, which in turn affects their bioactivity in orthopedic applications is a simple example of such an approach [7].

Design-driven approaches are based on the fundamental knowledge of the interactions between individual material properties and the biological system [6]. Here, the advanced biomaterials are developed by combining different types of materials and technologies, to develop implantable constructs with superior properties and/or improved functionality. Examples of such an approach include

the use of surface modification techniques [8] or the combinations of two or more biomaterials in the form of coatings [9-10] or monolithic and assembled composites [11-12]. Another example is the application of microtechnology techniques, such as soft embossing, to develop polymers with (surface) structural properties of ceramic materials [6].

#### **1.4. Functional biomaterials for bone regeneration**

Several methods have been used for developing functional materials for bone repair and regeneration. Incorporation of the appropriate cues into the carrier material that induce or stimulate new bone formation, such as surface topographical features, recreation of the topographical context of native extracellular matrix and application of peptides have been introduced as approaches for enhancing biofunctionality of biomaterials for bone regeneration [13-14].

Stabilizing osteogenic differentiation-related growth factors onto and delivering them from bone graft substitutes is another promising approach to improve bone regenerative potential of biomaterials. This includes the addition of compounds that directly stimulate new bone formation (e.g. osteoinductive bone morphogenetic proteins 2 and 7) or those that are indirectly involved in bone regeneration by stimulating other relevant process such as vascularization [15-16]. Such biological growth factors are usually proteins and their use is associated with high cost and stability issues. Therefore, increasing effort are invested in developing alternatives to such growth factors, in the form of small molecules and bioinorganics. Bioinorganics are simple, inorganic compounds, which are often present in the human body in trace amounts, and are known to be important in normal functioning of organs and tissues [17]. In their role of therapeutics, or compounds used to stimulate regenerative processes, bioinorganics are often referred to as “synthetic growth factors” owing to their inorganic nature [17].

##### **1.4.1. Bioinorganics-based biomaterials for bone regeneration**

Initial interest in application of bioinorganics as potential therapeutics stems from epidemiological and nutritional studies, which showed the effects of changes in the systemic ion levels, on normal functioning of organs and tissues [17]. Inspired by the composition of inorganic phase of bone, being itself a carbonated-apatite

that contains considerable amounts of bioinorganics such as sodium, fluoride, chloride, magnesium, strontium, zinc, copper, etc. [18], these bioinorganic ions have emerged in the past decades as a potential therapeutic option for bone regeneration [18]. Although the existing data about bioinorganics and their direct and indirect effects on bone formation and remodeling have demonstrated their potential as effective and inexpensive therapeutic factors, the research in this area is still in its infancy. The exact underlying mechanisms of the observed effects of selected bioinorganics on bone metabolism are not fully understood and are considered an important topic for fundamental research. While systemic delivery of bioinorganics, including oral administration, has been employed clinically, recent research efforts have been invested in local, controlled delivery of these compounds.

#### **1.4.2. Strategies for local delivery of bioinorganics**

Currently, the common strategies to locally deliver bioinorganics relevant to bone regeneration are based on their incorporation into bone graft substitutes, such as CaPs or bioactive glasses [19-20].

CaPs possess a strong ability to host foreign ions in their structure. The level of substitution of calcium or phosphate ions by another ion is largely dependent on the properties of the dopant, such as its atomic radius [21]. The release of the ion from such a material is dependent on both the efficiency of substitution and the solubility of the ceramic phase [22-23]. Similar to CaPs, silicate- and phosphate-based glasses are commonly used for local delivery of bioinorganics to aid bone repair and regeneration. The degradation rate of this class of materials can be controlled over several orders of magnitude by alteration of the glass composition [24], which is important in order to keep the amount released within the therapeutic window. By incorporating bioinorganics into CaPs and bioglasses, they become a structural component of the ceramic. As such, they can significantly affect the physicochemical properties of the host material, including crystallinity, solubility and mechanical properties. Furthermore, the release of the bioinorganic of interest is always accompanied by the release of other constituents of the carrier material. It is therefore difficult to distinguish between the direct chemical effects of the bioinorganic, from the indirect effects caused by the modification of the physicochemical properties of the carrier material upon incorporation of the bioinorganic.

Unlike CaPs and bioactive glasses, incorporation of bioinorganics into polymeric biomaterials has only been explored in a limited number of studies [25], despite the fact that these materials offer much more flexibility for controlled local delivery. For example, polymer-based delivery platforms offer a more controlled system for studying the effects of single ions or a selected combination of ions. Furthermore, combinations of polymers with bioinorganics and ceramics opens new possibilities in improving various functionalities of synthetic bone graft substitutes, while retaining their synthetic character.

### 1.5. Outline of this thesis

To date, research and development of bioinorganics-functionalized bone graft substitutes is associated with a number of scientific questions, such as:

- Which bioinorganic or combination of bioinorganics is best suited for bone regeneration?
- What concentrations of the bioinorganics are efficient and non-toxic in this application?
- What are the mechanisms of actions of the bioinorganics for enhancing bone regeneration?
- What material is the best to be used as carrier for bioinorganics?
- How do bioinorganics affect the physicochemical properties of the host material?
- What are the boons and banes of bioinorganics-modified bone graft substitutes as compared to the existing bone graft substitutes such as biological growth factors-based systems?
- ...

The aim of this thesis is to provide the answers to some of these questions, which will contribute to the knowledge required to develop successful, comprehensive synthetic substitutes for patient's own bone that is still considered the gold standard in bone regenerative strategies.

Following this introduction, **Chapter 2** of this thesis presents an overview of the roles of bioinorganics in natural bone formation and remodeling and reviews the current position of CaP ceramics with bioinorganic additives in bone regenerative strategies. Furthermore, it critically discusses the safety of some of the commonly used bioinorganics in such applications and gives some future perspective of the field.

In **Chapter 3**, two different methods of combining a polymer with CaP ceramic, i.e. a biomimetic coating method and a physical powder mixing method, are compared. The aim of this study is to investigate the effect of each phase on the osteogenic differentiation of human mesenchymal stromal cells (hMSCs), a clinically relevant cell type for bone regeneration, and to develop the best carrier for bioinorganics to be used in the studies described rest of the thesis.

In **Chapter 4**, the validated CaP coatings are used as carriers for strontium ( $\text{Sr}^{2+}$ ) ions to study their effect on growth and osteogenic differentiation of hMSCs.  $\text{Sr}^{2+}$  was selected for its proven role as an anti-osteoporotic agent. For assessing the efficiency of the CaPs with bioinorganic additives, the results of this experiment are compared to those in which  $\text{Sr}^{2+}$  ions were directly added to the medium in comparable concentrations.

**Chapter 5** investigates the possibility of combinatorial incorporation of bioinorganics into CaPs to simultaneously affect different biological processes related to bone regeneration. In this chapter, the biological response of hMSCs to fluoride ( $\text{F}^-$ ) and cobalt ( $\text{Co}^{2+}$ ) ions, individually or in combination is studied by direct supplementation to cell culture medium or by incorporating them into CaP coatings used as cell culture substrates. The rationale for using these two elements was their proven positive effect on osteogenesis and angiogenesis, respectively,

While **Chapters 3 to 5** focus on the in vitro effects of bioinorganics on the osteogenic/angiogenic differentiation of hMSCs, **Chapter 6** describes an in vivo study. In this chapter, the effect of  $\text{Co}^{2+}$  incorporation into CaPs coatings deposited on poly(lactic acid) particles is assessed on neo-vascularization in an intramuscular goat model.

A proof of principle for the use of polymeric microspheres as a carrier for bioinorganics is presented in **Chapter 7**. This study shows the possibilities that such a system offers as a platform for testing the biological effects of individual or cocktails of bioinorganics. It furthermore explores the use of microspheres for local delivery of bioinorganics and as new bone grafts substitutes.

Finally, **Chapter 8** is dedicated to an overall discussion of the data presented in the experimental chapters of this thesis and contains a number of concluding remarks.

## References

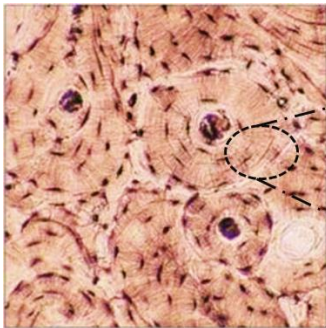
1. D. Williams, *Essential biomaterials science*, Cambridge University Press, Cambridge (2014).
2. C.A.C. Zavaglia and M.H. Prado da Silva, Feature article: Biomaterials, Reference Module in Materials Science and Materials Engineering, doi:10.1016/B978-0-12-803581-8.04109-6 (2016).
3. B.D. Ratner, *A History of biomaterials*, Editors: B.D. Ratner, A.S. Hoffman, F.J. Schoen, J.E. Lemons, Biomaterials Science (Third Edition), Academic Press, Oxford (2013) Xli-Liil.
4. I. Kulinetz, *Biomaterials and their applications in medicine*, Editors: S.F. Amato, R.M. Ezzell Jr, Regulatory Affairs for Biomaterials and Medical Devices, Woodhead Publishing, Cambridge (2015) 1–10.
5. G. Binyamin, B.M. Shafi, C.M. Mery, *Biomaterials: A primer for surgeons*, *Seminars in Pediatric Surgery* 15 (2006) 276–283.
6. C. Danoux, L. Sun, G. Koçer, Z. Tahmasebi Birgani, D. Barata, J. Barralet, C. van Blitterswijk, R. Truckenmüller, P. Habibovic, Development of highly functional biomaterials by decoupling and recombining material properties, *Advanced Materials* 28 (2016) 1803–1808.
7. H. Yuan, H. Fernandes, P. Habibovic, J. de Boer, A.M.C. Barradas, A. de Ruyter, W.R. Walsh, C.A. van Blitterswijk, J.D. de Bruijn, Osteoinductive ceramics as a synthetic alternative to autologous bone grafting, *PNAS* 107 2010 (13614–13619).
8. R. Williams, *Surface modification of biomaterials*, Woodhead Publishing, Cambridge (2011).
9. B.J. McEntire, B.S. Bal, M.N. Rahaman, J. Chevalier, G. Pezzotti, Ceramics and ceramic coatings in orthopaedics, *Journal of the European Ceramic Society* 35 (2015) 4327–4369.
10. R.A. Surmenev, M.A. Surmeneva, A.A. Ivanova, Significance of calcium phosphate coatings for the enhancement of new bone osteogenesis – A review, *Acta Biomaterialia* 10 (2014) 557–579.
11. S. Ramakrishna, J. Mayer, E. Wintermantel, K.W. Leong, Biomedical applications of polymer-composite materials: a review, *Composites Science and Technology* (2001) 1189–1224.
12. R.A. Pérez, J. Won, J.C. Knowles, H. Kim, Naturally and synthetic smart composite biomaterials for tissue regeneration, *Advanced Drug Delivery Reviews* 65 (2013) 471–496.
13. M.M. Stevens, Biomaterials for bone tissue engineering, *Materials Today* 11 (2008) 18–25.
14. F.R. Maia, S.J. Bidarra, P.L. Granja, C.C. Barrias, Functionalization of biomaterials with small osteoinductive moieties, *Acta Biomaterialia* 9 (2013) 8773–8789.
15. P.S. Lienemann, M.P. Lutolf, M. Ehrbar, Biomimetic hydrogels for controlled biomolecule delivery to augment bone regeneration, *Advanced drug delivery reviews* 64 (2012) 1078–1089.
16. T.N. Vo, F.K. Kasper, A.G. Mikos, Strategies for controlled delivery of growth factors and cells for bone regeneration, *Advanced drug delivery reviews* 64 (2012) 1292–1309.
17. P. Habibovic, J.E. Barralet, *Bioinorganics and biomaterials: Bone repair*. *Acta Biomaterialia* 7 (2011) 3013–3026.
18. A. Bigi, G. Cojazzi, S. Panzavolta, A. Ripamonti, N. Roveri, M. Romanello, K. Noris Suarez, L. Moro, Chemical and structural characterization of the mineral phase from cortical and trabecular bone. *Journal of inorganic biochemistry* 68 (1997) 45–51.
19. S. Bose, G. Fielding, S. Tarafder, A. Bandyopadhyay, Trace element doping in calcium phosphate ceramics to Understand osteogenesis and angiogenesis, *Trends in Biotechnology* 31 (2013) doi:10.1016/j.tibtech.2013.06.005.
20. A. Hoppe, N.S. Güldal, A.R. Boccaccini, A review of the biological response to ionic dissolution products from bioactive glasses and glass-ceramics, *Biomaterials* 32 (2011) 2757–2774.
21. W. Habraken, P. Habibovic, M. Epple, M. Böhner, Calcium phosphates in biomedical applications: Materials for the future?, *Materials Today* 19 (2016) 69–87.
22. S. Patnirapong, P. Habibovic, P.V. Hauschka, Effects of soluble cobalt and cobalt incorporated into calcium phosphate layers on osteoclast differentiation and activation, *Biomaterials* 30 (2009) 548–555.
23. C. Lindahl, W. Xia, J. Lausmaa, H. Engqvist, Incorporation of active ions into calcium phosphate coatings, their release behavior and mechanism, *Biomedical Materials* 7 (2012) 045018.

24. J.C. Knowles, Phosphate based glasses for biomedical applications. *Journal of Materials Chemistry* 13 (2003) 2395-2401.
25. H. Maeda, T.Kasuga, Preparation of poly (lactic acid) composite hollow spheres containing calcium carbonates, *Acta Biomaterialia* 2 (2006) 403-408.

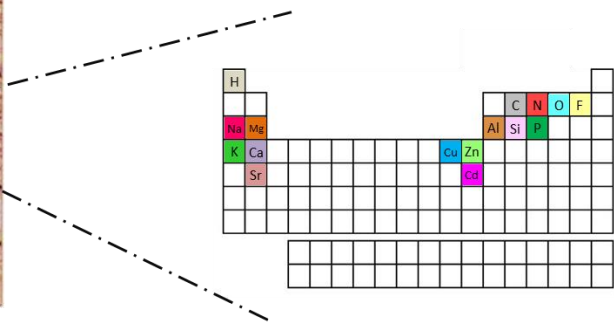


## Chapter 2

### Calcium phosphate ceramics with inorganic additives



Bone Tissue



## **Abstract**

The use of inorganic compounds as synthetic growth factors is a promising approach for improving the biological properties of existing synthetic bone graft substitutes such as calcium phosphates. In this chapter we have described some of the inorganic additives that may improve the capabilities of calcium phosphates, and help bridge the gap towards autograft's performance known as gold standard for bone regeneration. This chapter focuses on the specific roles of bioinorganics in processes related to bone formation and resorption and how these modify the biological properties of calcium phosphates, and finally provides insight into the future of this field.

## 2.1. Introduction

Regenerative medicine is a broad field that aims to restore, rather than replace, the function of damaged and degraded organs and tissues. This exciting field has shown great potential to date, and is becoming increasingly important due to an aging population. In the areas of orthopedic and craniomaxillofacial surgery there is a high demand for bone regeneration strategies and materials. Tumor removal, infections, trauma, as well as spinal fusion, are frequently performed surgeries in the clinic where a bone graft may be needed. Currently, there are many options for the treatment of bone defects, including natural bone grafts, synthetic bone graft substitutes, and tissue-engineered constructs (Figure 1).

## 2.2. Bone

Bone is a highly specialized, hierarchical form of connective tissue that performs many functions within the body. Muscles and tendons attach to bone to facilitate skeletal locomotion, bone provides a rigid structure to protect vital organs of the cranial and thoracic cavities, and is storage pool of differentiated and multipotent cells within the bone marrow. In addition to these functions, bone also acts as a reservoir for calcium and phosphate, available for the homeostatic regulation of these elements throughout the body [1].

Morphologically, two forms of bone exist, being cortical and cancellous bone. Cortical bone has a dense, low porosity structure that forms complete bones, or as an outer shell of the porous cancellous bone. Cancellous bone can be found within the epiphyses of long bone, or bone within the ribs and spine. Cancellous bone has a highly porous structure (>75%), with numerous interconnected small bone trabeculae that orient themselves according to the loading environment.

Bone comprises several cell types, predominantly osteoblasts, bone lining cells, osteocytes, and osteoclasts. Osteoblasts and bone lining cells originate from local or migrating osteoprogenitor cells of mesenchymal origin, with the main function of osteoblasts being osteoid deposition. This organic, mainly collagen matrix, is mineralized as the bone matures, which embeds the osteoblast within the mineralized matrix, transforming the osteoblast into an osteocyte. The larger multinucleated osteoclasts, of hematopoietic origin, are responsible for the

resorption of bone. This ongoing matrix formation by osteoblasts, and matrix resorption by osteoclasts, forms the basis of the continual remodeling of bone.

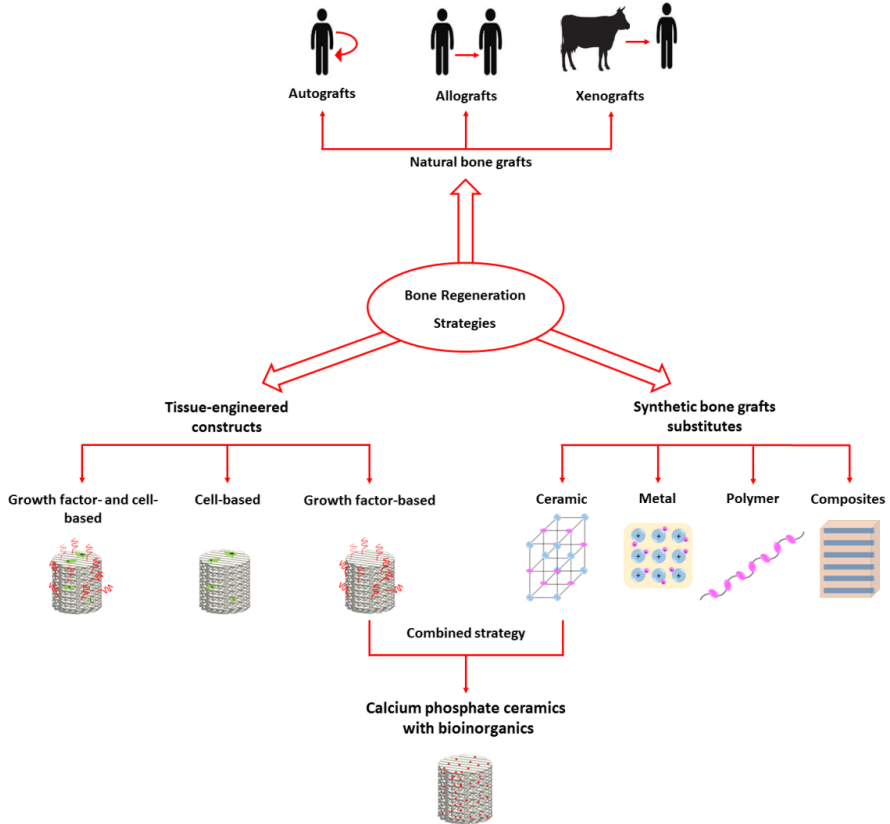


Figure 1. An overview of the current strategies in bone repair and regeneration. Calcium phosphates combined with bioinorganics represents the coordination between ceramic scaffolds and growth factors. In this case, bioinorganics perform the cell signaling function of biological growth factors.

By weight, bone contains approximately 60% mineral, 10% water, and 30% organic matrix. Type I collagen constitutes ~90% of the organic matrix, with the remaining 10% made up of proteoglycans and numerous noncollagenous

proteins, such as osteocalcin, osteopontin, osteonectin, bone sialoprotein, decorin, and biglycan [2, 3].

The mineral, inorganic component of bone mineral consists of a non-stoichiometric AB-type carbonated apatite, with the exact composition varying depending on the location and function in the body, and age. Carbonate is the most abundant substitute in biological apatite crystal lattice, accounting for 2–8 wt% of total bone mineral content [4, 5]. Apart from calcium, phosphate, and carbonate, the inorganic phase of bone also contains a great number of inorganic compounds in varying quantities. Therefore, the strong interest exists in incorporating inorganic elements with calcium phosphates (CaPs).

## **2.3. Current methods in bone regeneration**

### **2.3.1. Natural bone grafts**

Autograft is the well-established gold standard for bone defect healing, due to it meeting the majority of requirements for successful bone regeneration. These requirements are traditionally grouped as: osteoconductive, which facilitates cell attachment and infiltration through the porous structure; osteoinductive, by providing signaling molecules capable of initiating osteogenic differentiation of osteoblast precursors; and osteogenic, by directly supplying the relevant osteogenic and osteoprogenitor cells [6-10].

Despite the bone healing efficacy of autograft, several drawbacks are associated with its use. These include additional surgical procedures, increased risk of infection, increased blood loss, limited quantity, and donor-site hypersensitivity or morbidity [6, 8, 9, 11-15].

Other natural bone grafts, including allografts and xenografts, are available in greater quantities, but their basic performance is inferior to that of autografts [9, 14, 16-18]. Further, processing of these materials is required to limit detrimental host immunogenic responses [19, 20].

### **2.3.2. Synthetic bone graft substitutes**

Synthetic bone graft substitutes present an attractive alternative to natural bone grafts. Many of these materials are available in unlimited quantities, with off the shelf availability. More importantly, these materials can be selected and tailored

to avoid negative immunogenic responses, and in many cases even provide benefit to the local environment. Three material types have all been used in orthopedic devices and as bone graft substitutes, being metals, polymers, and ceramics, and their combinations thereof. Of these, CaP based ceramic materials are of particular interest for bone regeneration.

### **2.3.2.1. Calcium phosphate ceramics**

CaP ceramics possess a chemical composition similar to that of bone and tooth mineral. In addition to their excellent biocompatibility, their bioactivity provides another dimension of functionality. As reviewed by Damien and Parsons [8], various CaP biomaterials have shown distinct clinical success. Hydroxyapatites (HA), either derived from natural sources, such as coral and bovine bone, or of synthetic origin, have been successfully used for clinical applications. Owing to its low resorption rate, HA has proven to be a good material for alveolar ridge augmentation, pulp capping, and filling of periodontal defects. Conversely, the use of autologous bone, which is resorbable, has been found to be less than optimal in such cases. Within the field of orthopedics, porous HA blocks have been used for filling bone defects remaining after tumor excision, as well as in spinal fusion of vertebral bodies. Tricalcium phosphate (TCP) is another widely used ceramic, particularly in applications where a greater rate of material degradation is required. Dental applications of TCPs include the filling of defects due to periodontal loss, as well as repairing cleft palates. In orthopedics, TCP has been used in for many augmenting bone defects, and also in cases of spinal fusions. A ceramic receiving more recent attention is biphasic calcium phosphates (BCP), consisting of HA and TCP. By altering the ratio of HA to TCP, variable rates of degradation can be achieved. In addition to the uses mentioned herein, BCP has been clinically tested to aid in the treatment of patient with scoliosis, and for the filling of bone defects after tumor removal. While many phases of CaPs are available, this feature is only one facet of the performance of CaPs.

Currently, CaP ceramics can be produced in various forms including particles, dense and porous scaffolds [21, 22], and in many more defined shapes using additive manufacturing techniques [23]. Their microstructure known to play an important role in the bioactivity of CaP ceramics in vivo, can be modified by

controlling the production process parameters [24]. Figure 2 shows an example of CaP ceramic particles (a), macro- (b) and micro-structure (c) of porous CaP ceramic, and its bonding to bone (d), which is indicative of the material's bioactivity.

An important limitation of ceramics is their intrinsic brittleness. As a major function of bone is based on its mechanical properties, restoring this is essential to restore the bone's function. However, due to the brittle nature of CaPs, their application is limited in load-bearing applications. To overcome this limitation, and tailor the graft's properties, combinations with both metals and polymers are possible [25-32]. Although, while such composites or coatings may be mechanically beneficial, these will inherently change the bioactivity potential, making the balance between multiple considerations important for such bone graft substitutes.

### **2.3.3. Tissue engineering**

Despite intensive research and continuous improvements of synthetic biomaterials, to date there is still no equivalent to autograft. The osteoconductivity of bone graft substitutes is generally inferior, and their mechanical properties are commonly an issue to overcome [8, 16, 33-35]. Tissue engineering, originally defined by Langer and Vacanti [36], as an "interdisciplinary field that applies principles of engineering and life sciences toward the development of biological substitutes that restore, maintain, or improve tissue function", has been considered a promising technique to develop successful alternatives to autograft. To achieve this goal, classical tissue engineering approaches rely on the concept of incorporating cells, scaffolds and signals, in an attempt to construct materials with properties and function similar to that of natural tissue.

In relation to bone tissue engineering, rather than using a bioactive CaP ceramic that resembles bone mineral, an additional step is made to add cells and/or growth factors to the ceramic, creating thereby a construct that resembles both the mineral and organic components of bone. Bone tissue engineering constructs most often consist of a synthetic carrier loaded with molecules or proteins capable of providing favorable cell signals, and osteogenic cell precursors [36].

To date, numerous growth factors have been identified and subsequently produced by recombinant gene technology. Most notably, these include bone morphogenetic proteins (BMPs) and other members of the transforming growth factor  $\beta$  (TGF- $\beta$ ) family, fibroblast growth factors (FGFs), platelet-derived growth factors (PDGFs), and insulin-derived growth factors (IGFs). Multiple studies have shown that such growth factors have several stimulatory and regulating effects on cells from the osteoblastic lineage. These *in vivo* studies have demonstrated that some factors can induce bone formation and/or stimulate bone healing. Kirker-Head has reviewed the application of BMPs in a number of animal models at various orthotopic sites, such as in spinal fusions, long bone defects, mandibular and cranial bone defects, fracture healing, as well as periodontal regeneration, alveolar ridge augmentation, and osseointegration of dental implants [37]. In addition, various preclinical and clinical studies have shown positive effects of BMPs in nonunions and segmental defects, such as in tibial [38, 39] and femoral defects [40].

The combination of autologous cells with carriers is another way to produce tissue-engineered hybrids. Various cell types such as calvarial [40, 41] and periosteal cells [42, 43], osteoblasts of trabecular bone [44, 45], chondrocytes [46], and vascular pericytes [47] have been tested as potential sources of bone-forming cells. Nevertheless, the most widely used source of osteogenic cells is bone marrow. Bone marrow has been recognized as a source of osteoprogenitor cells able to differentiate towards bone-forming cells when cultured under appropriate conditions [48-51]. In addition, bone marrow has been shown to be the most abundant source of osteoprogenitor cells, which possess high proliferative ability and great capacity for differentiation [52, 53]. Studies in rodents have demonstrated the feasibility of the tissue-engineered hybrids, consisting of a carrier and bone marrow stromal cells, implanted in both ectopic [54, 55] and orthotopic sites [54-58]. In larger animals, there are many studies that demonstrate the biological performance of the tissue-engineered hybrids, also in ectopic [59-61] and orthotopic sites [62-64]. In a small number of studies in which cell-based tissue-engineered constructs have been tested in humans, the results obtained have had varying degrees of success [65].

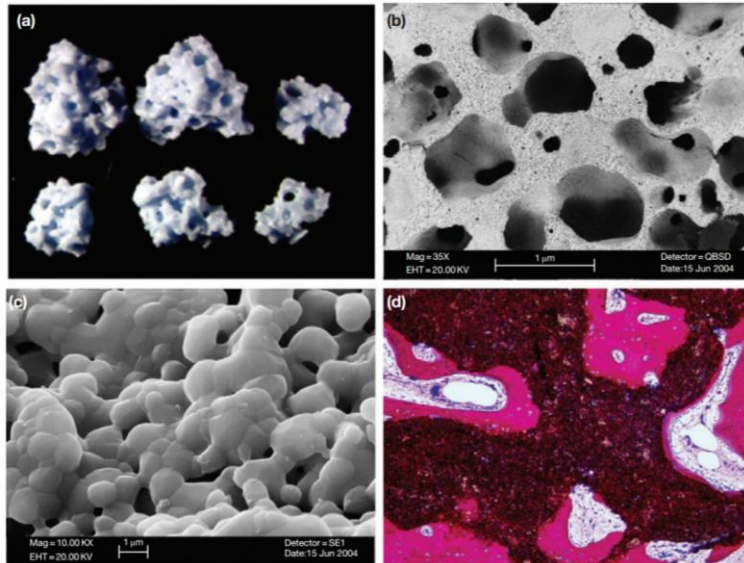


Figure 2. Calcium phosphate ceramic: (a) digital micrograph showing ceramic particles, (b) low magnification scanning electron microscopy micrograph of an open porous macrostructure, (c) high magnification scanning electron microscopy micrograph showing microstructure with ceramic grains among which micropores are found, and (d) light microscopy micrograph of a histological slide showing bone that has formed inside the ceramic pores and is in close contact with ceramic surface.

Although both growth factors-based and cell-based tissue-engineered constructs have shown the capability to enhance bone formation when implanted orthotopically, their biological performance is largely dependent on the construct carrier. For example, when BMPs are implanted without a carrier, they are reported to diffuse too rapidly to be able to induce or to enhance new bone formation. Further, the amount of BMP necessary to achieve a certain dose in vivo is also carrier dependent [66-68]. Similarly, a suitable carrier is a prerequisite for the success of a cell-based tissue-engineered construct. Further, the findings of the clinically relevant studies suggest that the effect of tissue engineering is moderate and may be irrelevant at long-term implantation intervals. The tissue-engineering technique is also associated with some drawbacks. The production of recombinant growth factors, collection and transport of the biopsies, and culture

of autologous cells are some of the many factors that make tissue-engineering time, money, and labor consuming.

## 2.4. Improvement of synthetic bone graft substitutes

From this overview of the current status of bone regeneration strategies, the following summary can be made: (1) autologous bone is the gold standard with regard to biological performance, but its limited availability and other issues creates a need for comprehensive alternatives; (2) synthetic bone graft substitutes have a great advantage of being available in large quantities off-the-shelf and relatively inexpensive, but their current biological performance is inferior to autograft; and (3) tissue engineering is a strategy with great possibilities, but owing to its complexity, extensive research is needed before tissue engineering can be widely applied in the clinic.

For material scientists, a real challenge lies in the improvement of the biological performance of the existing bone graft substitutes, while retaining their synthetic character. In this chapter, the potential use of inorganic additives to bone graft substitutes will be discussed as 'synthetic growth factors' (Figure 1). These inorganic additives are compounds found in bone mineral as trace elements. As mentioned previously, the inorganic component of bone is a nonstoichiometric HA, mainly consisting of calcium (36.6 wt%), phosphorus (17.1 wt%), and carbonate (4.8 wt%). In addition, a number of other components are also found in bone minerals, such as sodium (1 wt%), potassium (0.07 wt%), fluorine (0.1 wt%), chlorine (0.1 wt%), magnesium (0.6 wt%), and strontium (0.05 wt%) [69]. In an early work by Becker and coworkers, a presence of aluminium, copper, iron, manganese, lead, silicon, tin, vanadium, and zinc has also been determined in human bone [70]. In 1997, El-Amri and El-Kabroun used neutron activation analysis and showed that also barium and bromine are present in human bone [71]. Most of these elements have an effect on properties of bone mineral, such as its mechanical and degradation properties. In addition, a number of these elements can influence processes of angiogenesis, bone formation, and remodeling, all of which are of importance in the field of bone regeneration. One of the best examples of trace elements used in bone regeneration and bone-related diseases is the clinical use of strontium ranelate in patients with

osteoporosis. However, there is also evidence that other elements can influence processes related to bone formation and remodeling. Here, three metallic components (cations), namely, zinc, copper, and strontium, and two nonmetallic components (anions) of bone, namely, fluoride and carbonate, are discussed in relation to their potential use for bone regeneration. The occurrence of these five ions in bone is summarized in Table 1. Their importance will be discussed in regards to bone metabolism, and a literature review will be given on their effect on the processes related to bone formation and remodeling. Furthermore, a number of methods will be discussed on how these elements can be incorporated into CaP-based ceramics. This continues with an overview of studies in which ceramics with additives have been tested for bone formation and resorption. Finally, some future perspectives in the search for and investigations of 'synthetic growth factors' will be given.

## **2.5. Trace elements in bone metabolism and processes related to bone formation**

### **2.5.1. Zinc**

The amount of zinc in the human body is relatively low, between 1.4 and 2.3 g, at a biochemical level; however, its importance has been proven in a number of physiological processes [72]. Zinc is required for the activity of over 300 metalloenzymes, including those involved in nucleic acid and protein synthesis, cellular replication, immune function, and antioxidant systems [73]. It is a constituent of various enzymes and proteins such as alkaline phosphatase (ALP), lactate dehydrogenase (LDH) and carbonic anhydrase, steroid hormone receptors, and transcription factors [74, 75].

Around 1400 zinc-finger proteins exist that participate in the genetic expression of a range of proteins [76]. The amount of zinc in bone is relatively high as compared to that in other tissues. As reviewed by Colhoun and coworkers, human bone ash contains between 150 and 250  $\mu\text{g g}^{-1}$  zinc, depending on the location in body. Zinc deficiency is associated with a number of skeletal anomalies in fetal and postnatal development, such as depressed bone age, which can be treated with zinc supplementation. It was demonstrated that nutritional zinc deficiency results in a decrease of zinc concentrations in bone.

Table 1. Occurrence of zinc, copper, strontium, fluoride, and carbonate in bone

Element	Content
Zinc	60–85 ppm (in ash of human cortical bone) [70] 153–266 ppm (in ash of various human bones) [72] 54–315 ppm (in lyophilized human bone) [71]
Copper	5 ppm (in ash of human cortical bone) [70]
Strontium	62–130 ppm (in ash of human cortical bone) [70] 11–418 ppm (in lyophilized human bone) [71]
Fluoride	0.1 wt% (in mineral of bovine cortical bone) [69] 0.08–0.69 wt% (in ash of human iliac crest bone) [9]
Carbonate	4.8 wt% (in mineral of bovine cortical bone) [69] 5.1–5.8 wt% (ash of human iliac crest bone) [77]

Early studies indicated an increase in the uptake of zinc in the region of bone healing, in particular, when in close proximity to the sites of calcification, as well as during ectopic bone formation, suggesting the influence of zinc in osteogenesis [72]. The role of zinc within bone has been shown to be twofold: (1) zinc plays a structural role in the bone matrix that consist of HA crystals, which contain zinc complexed with fluoride and (2) zinc is involved in the stimulation of bone formation by osteoblasts and inhibition of bone resorption by osteoclasts [78]. Yamaguchi and coworkers, for example, showed an increase in Runx-2, osteoprotegerin, and regucalcin mRNA expression by MC3T3-E1 osteoblast-like cells in the presence of zinc sulfate, at concentrations of  $10^{-6}$ – $10^{-4}$  M [79]. More recently, Kwun and colleagues showed that zinc deficiency reduced the osteogenic activity of MC3T3-E1 cells in vitro. This deficiency decreases bone marker gene transcription through reduced and delayed Runx-2 expression, and by a reduction of extracellular matrix mineralization through a decrease in ALP activity [80]. The effect of zinc on human osteoblast-like cell line SaOS-2 was also

investigated, and it was observed that both ALP expression and the formation of mineral nodules were stimulated in the presence of zinc, at concentrations of 1 and 10  $\mu\text{M}$ , but inhibited at concentrations higher than 25  $\mu\text{M}$  [81]. When primary murine bone marrow stromal cells and osteoblast were treated with zinc at concentrations of  $10^{-9}$  M and lower, no effect was observed on proliferation, and an inhibitory effect was shown on both osteogenic and adipogenic differentiation [82].

As recently reviewed by Yamaguchi, zinc has been shown to have an inhibitory effect on bone resorption in tissue culture systems in vitro and to suppress osteoclastogenesis of osteoclastic cells derived from the bone marrow [83].

### 2.5.2. Copper

Copper deficiency is generally associated with syndromes of anemia and pancytopenia, as well as with neuro-degeneration in humans and other mammals. In the metabolism of the skeleton, copper performs a key catalytic function in the first step of the maturation of collagen to form stable fibrils [84, 85].

This effect can be attributed primarily to the copper-dependent enzyme lysyl oxidase, for which copper acts as cofactor. Lysyl oxidase is required for the formation of lysine-derived cross-links in collagen and elastin [86]. Several reports suggested that mild copper deficiency may contribute to bone defects such as osteoporotic-like lesions and bone fragility in humans and animals [87, 88], as well as to a variety of bone developmental defects in preterm infants [89]. Oral supplementation with copper, however, resulted in complete healing of fractures and an improvement in other bone defects [89].

Copper was shown to affect both the proliferation and differentiation behavior of mesenchymal stem cells (MSCs) in vitro. It decreased the proliferation rate of MSCs and induced an increase in their differentiation towards the osteogenic and adipogenic lineages [90]. Copper was also reported to affect the timing ALP activity expression, which reached its maximum earlier than in the controls without copper.

Copper also plays a role in the inhibition of bone resorption through its action as a cofactor for superoxidase dismutase, an antioxidant enzyme containing a zinc

and a copper atom, which acts as a free radical scavenger, neutralizing the superoxide radicals produced by osteoclasts during bone resorption [78]. While an inhibition in osteoclast function was observed in copper-deficient animals [91], Wilson suggested that higher concentrations of copper in cell culture medium ( $10^{-5}$  M copper sulfate) reduced bone resorption and inhibited hydroxyproline, protein, and DNA synthesis in vitro [92].

In a number of studies, copper was also shown to have an effect on angiogenesis, a process that is of great importance in bone regeneration. Angiogenesis is essential for the survival of osteoblasts, as well as for the regulation of fracture healing and bone remodeling [93, 94].

Previous reports have also shown that copper can enhance growth of endothelial cells in vivo [95-97], and copper found in wound tissues is known to be involved in the generation of free radicals during tissue regeneration [98].

### **2.5.3. Strontium**

Strontium is, similar to calcium, a group IIa element and, from a chemical point of view, they behave similarly. Although strontium is not an essential trace element, a substantial amount of research has been performed on its properties and effects due to its chemical analogy to calcium. Strontium is a bone-seeking element, of which 98% in the human body can be found in the skeleton [99]. It is therefore not surprising that among the trace metals present in human bone, strontium was the only one that was correlated with bone compressive strength [100, 101]. Strontium was shown to have dose-dependent effects on bone formation, which was further affected by the presence or absence of renal failure. While low doses (0.19–0.34% in drinking water during 9 weeks) were reported to improve the vertebral bone density and stimulate bone formation in rats with normal renal function [102-104], high doses (> 0.4% in drinking water) were shown to have deleterious effects on bone mineralization [102, 103].

However, in animals with chronic renal failure, 0.34% of strontium (as chloride compound) in drinking water induced a bone lesion histologically characterized as osteomalacia [105]. This and further studies on a similar model showed that the effect of strontium is complex and dose dependent.

Similarly, a dose-dependent effect of strontium was also observed in cell culture experiments. Studies with primary osteoblasts isolated from fetal rat calvaria showed that at low doses ( $1 \mu\text{g ml}^{-1}$  strontium in the culture medium), reduced nodule formation occurred in the presence of intact mineralization. At an intermediate concentration ( $5 \mu\text{g ml}^{-1}$ ), no effect was observed, while at high concentrations ( $20\text{--}100 \mu\text{g ml}^{-1}$ ), intact nodule formation was accompanied by reduced mineralization [106].

Strontium was also shown to reduce excessive bone resorption in rats with osteopenia, which was associated with a decrease in the number of osteoclasts [107]. Further, Baron and Tsouderos showed that a strontium salt, Sr12911, dissolved into the culture medium, inhibited osteoclast differentiation and osteoclast activity in a dose-dependent manner, without affecting the attachment of the osteoclast [108].

As mentioned before, current clinical use of strontium ranelate for treatment of osteoporosis is an excellent example of the application of inorganic trace elements in bone-related conditions. The dual anabolic and antiresorptive role of strontium ranelate has been described *in vitro* [109]. As recently reviewed by O'Donnell and coworkers, there is evidence that supports the efficacy of strontium ranelate in reducing vertebral and nonvertebral fractures in postmenopausal osteoporotic women, and in increasing bone matrix density in postmenopausal women with and without osteoporosis [110, 111].

In addition to the chemical interplay, Blake and Fogelman, and Chavassieux et al. have previously suggested that strontium ranelate prevents osteoporotic fractures through physical effects associated with an increase in bone hardness due to  $\text{Sr}^{2+}$  ionic substitution [112, 113].

#### **2.5.4. Fluoride**

Fluoride has been recognized as an important ion in mineralized tissues, such as teeth and bone, for over a century. Initial attention was paid to environmental overexposure to this element as a cause of crippling bone disease. However, research that followed led to some major clinical successes, in particular, in dentistry with eradication of endemic dental fluorosis worldwide and a successful water and topical fluoridation program that has reduced prevalence of dental

caries [114]. The role of fluoride in the prevention and control of dental caries in both humans and animals has been shown to be predominant in the maturation stage of enamel formation [115-119]. Fluoride was also found to be the single most effective agent for increasing bone volume in the osteoporotic skeleton [120] and an effective anabolic agent to increase spinal bone density by increasing bone formation and mineralization [121, 122].

Similar to strontium, fluoride was shown to have a dose related effect on bone formation. Low doses of fluoride (50 mg sodium fluoride daily) increased the trabecular bone density of osteoporotic patients [123-126], whereas a dose of 75 mg day<sup>-1</sup> had no beneficial effects on bone mineral density in postmenopausal women [125]. Fluoride intake of 0.8 mg kg<sup>-1</sup> also stimulated bone formation in rats [104]. The complex and dose-dependent effects of fluoride, together with reports of an increase in occurrence of osteoporotic hip fractures related to regular fluoride intake, were important reasons for the lack of major achievements of fluoride treatment within orthopedics.

Dose-dependent effects of fluoride have also been observed in vitro. Bellows et al. demonstrated an increase in proliferation of fetal rat calvarial osteoblasts with increasing dose of sodium fluoride in cell culture medium in concentrations between 10 and 500 µM, with higher concentrations being cytotoxic [127]. A positive effect of 10 µM sodium fluoride on proliferation in culture medium was also observed on embryonic chick calvarial cells, while no effect was found in human osteoblast cultures [114]. Recently, a dose-dependent effect of sodium fluoride was found on the proliferation and differentiation of caprine osteoblasts. At concentrations below 10<sup>-5</sup> M of sodium fluoride in cell culture medium, cell proliferation and ALP expression were enhanced, whereas above this dose, apoptosis occurred and a decrease in ALP expression was observed [128]. Burgener and coworkers suggested that fluoride enhances protein tyrosine phosphorylation in osteoblast-like cells UMR-106, by enhancing tyrosine kinase activity, postulating that this signal transduction pathway is involved in the osteogenic effect of fluoride [129].

The effect of fluoride on the behavior of osteoclasts has been reported in a study where rabbit primary osteoclasts were cultured on thin slices of bovine bone. Sodium fluoride in concentrations of 0.5–1.0 mM in medium decreased the number of resorption lacunae made by individual osteoclasts, as well as the

resorbed area per osteoclast [130]. It was further shown that suppression of the resorption was enhanced by increasing the sodium fluoride concentration of the cell culture medium [131].

### 2.5.5. Carbonate

Carbonate, together with calcium and phosphate, is a major constituent of bone mineral. This makes it an interesting potential compound for the treatment of damaged and degraded bone tissue. Bone mineral of most mammals contains between about 2 and 8 wt% carbonate [5, 69, 132], depending on the age of the individual [132]. Type B carbonated apatite ( $\text{CO}_3^{2-}$  for  $\text{PO}_4^{3-}$ -substitution, coupled with  $\text{Na}^+$  for  $\text{Ca}^{2+}$  substitution) prevails in biological apatites [132]. A small amount of  $\text{CO}_3^{2-}$  is believed to be a substituent for  $\text{OH}^-$  groups, known as type A substitution [133]. Type A to type B ratio in biological apatites is between 0.7 and 0.9 [134]. Introducing carbonate groups in the structure of HA mineral, in general, results in a decrease of crystallinity and increase of solubility in vitro and in vivo [135]. Direct addition of carbonate to the cell culture medium will mainly affect its pH, which is of relatively little interest. Carbonate will therefore be discussed in more detail in the section on CaP ceramics with inorganic additives.

## 2.6. Inorganic additives in calcium phosphate ceramics

### 2.6.1. Methods of preparation

A great advantage of inorganic additives, in comparison with organic compounds such as growth factors, is their thermal stability. That implies that inorganic additives do not require physiological conditions to retain their stability and functionality. However, although standard methods of preparation can often be used, processes sometimes need adaptations for various additives to be efficiently incorporated into a CaP ceramic. The method of incorporation determines the way an element is a part of the ceramic and therewith also the release profile and the efficiency of the element upon release.

Powder preparation is often a first step in the process of ceramic production. Depending on the desired ceramic type, the produced powder then undergoes a number of subsequent processes. For sintered, porous, or dense ceramics, for example, calcination, slurry preparation, drying, and sintering are frequently the

steps following powder preparation. In the case of nonsintered ceramics or cements, powder is often mixed with a liquid phase to initiate setting of cement. A great number of different coating techniques have been used to coat the surfaces of the implants with a CaP ceramic layer. The most widely used coating method is plasma-spraying [136, 137], however alternative methods such as double decomposition [138], biomimetic [139-142], electrolytic deposition [143], sol-gel [144-146], laser [147-149], magnetic sputtering [136], and hydrothermal coating [150-152] have garnered interest in the past few decades. For a number of these methods, powder is a starting point. For others, precipitation of the coating directly from a solution is a part of the process.

Inorganic additives are frequently incorporated into a ceramic during the process of powder production, either by addition of a salt into the solution from which CaP phase is precipitated, or by adding a precursor containing the additive of choice into a sol-gel process. Another way of additive incorporation is in the later stage of ceramic processing, by a solid-state reaction. In this case, a ceramic powder, such as HA or  $\beta$ -TCP, is mixed with a salt of choice, followed by heating at high temperatures, which allows incorporation of the inorganic additive into the ceramic powder.

Metallic ion additives can be doped into the crystal lattice, which is one of the most widely used methods of incorporation. A maximum exists for the amount of dopant that can be added, above which impurities are formed.

Zinc, for example, is often incorporated into  $\beta$ -TCP ceramics and results in the stabilization of the crystal lattice [153, 154]. Other examples of methods used for preparation of zinc incorporated CaPs are an adapted coprecipitation process [153, 155], sol-gel reactions with zinc nitrite as a precursor [156] and solid-state reactions [154] can be indicated.

Similar to zinc, various methods have been used to obtain strontium-doped CaPs, such as solid-state reaction of strontium carbonate, ammonium phosphate with  $\beta$ -TCP powders, followed by heat treatment [154]. Strontium has also been added to HA powders, either by a coprecipitation process or sol-gel method [157, 158].

In contrast to zinc and strontium doping, a relatively limited amount of work has been done on copper doping of CaP ceramics. Examples of the methods used include solid-state reaction [159] and precipitation from ionic solutions [142].

Fluorinated apatite powders can be readily made by adding a fluoride donor during CaP precipitation process, whereby  $F^-$  substitutes the  $OH^-$  [160-162], leading to a reduction in crystal size and an increase in structure stability [69, 77]. Synthetic carbonated apatite type A ( $CO_3^{2-}$  for  $OH^-$  substitution) has been successfully produced by using a time-consuming process of sintering HA powder under  $CO_2$  supply, or by soaking HA powder in an aqueous solution saturated with  $CO_2$  [69].

Preparation of type B ( $CO_3^{2-}$  for  $PO_4^{3-}$  substitution, coupled with  $Na^+$  for  $Ca^{2+}$  substitution) or type AB, is more complex and occurs predominantly via closely controlled aqueous precipitation reactions [163-167].

### 2.6.2. Safety of bioinorganics

The use of bioinorganics for regenerative medicine applications, by using both systemic delivery systems and local delivery from biomaterials, has been one of the most studied topics in this field in the past decades. However, the issue of the safety of using bioinorganics is one of the most important to address.

While comprehensive research for analyzing the safety and toxicity of the bioinorganic-based systems is still demanded, in a number of studies the toxic or undesired inhibitory effects of bioinorganics using *in vitro* models have been reported. The results of these studies suggested that the safety or toxicity of the bioinorganics is dependent on the species, the duration of use, and most importantly on the dose of bioinorganic [168].

In 1989, Borovansky and Riley [169] reported the cytotoxicity of the zinc ions for several cell lines, and at the concentration of approximately 1.25 M. Different levels of zinc salts have been also reported as cytotoxic dependent on the species used for testing, including prokaryote cells, algae, invertebrates and marine animals, as summarized by Ni' Shu'illeabha'ín et al. [170]. Conversely, Nilsson [171] has shown that lower concentrations of zinc ions (0.5-2 mM) resumed the proliferation of Ciliate Tetrahymena, which is a known model cell system in cytotoxicology.

In the context of bone cells, exposure of zinc ions dissolved in cell culture medium (up to 100 mM) or as a coating has been followed by normal growth of the cells [79, 81]. When incorporated into CaPs, lower concentrations of zinc did not

2

compromise the growth of osteoblastic cells, whereas CaPs with more than 1 wt% of zinc significantly reduced the cell proliferation [155, 172]. Consistently, CaPs with zinc content of higher than 3 wt% caused inflammation at the implant sites [173].

Schumacher et al. [174] have shown that the ionic concentration of up to 1mM of strontium ions in cell culture medium is not only safe to be exposed to hMSCs, but it also increases cell viability. However, concentrations equal to or higher than 5mM in cell medium substantially decreased cell viability. Similarly, Er et al. [175] observed the short-term and long-term cytotoxicity of strontium ranelate for human periodontal ligament fibroblast cells at concentrations higher than approximately 20 mM, while the concentrations of 10 and 5 mM were reported safe for this cell type.

Toxic damage to cells caused by the incorporation of strontium into CaPs has not been observed. This may be due to low concentrations of doping, and limited dissolution of CaPs, which result in releasing strontium ions in cell culture medium or implantation sites at concentrations much lower than toxicity thresholds. In this context, Schumacher and Gelinsky [176] have recently reviewed the material characteristics of strontium modified calcium phosphate cements (CPCs) and stated that strontium modification does not induce cytotoxicity. According to this review, a positive effect of the strontium doping and/or the strontium ions released from the strontium-modified CPCs was found on cell proliferation and osteogenic differentiation of various cell types. These included MG63 (human osteoblast-like cell line), hMSCs and MC3T3-E1 (murine pre-osteoblast cell line). Only in one case a mild cytotoxic effect of strontium ions on the murine connective tissue cell line (L929) was detected at higher concentrations of doping [176, 177].

Similarly, in other forms of CaPs, the cell viability and growth was not negatively compromised by incorporation of strontium, unless at high concentration of impregnation [142, 178, 179].

Similar to strontium, cytotoxic effects of copper have been recognized at relatively high dosages. In vitro cell culture experiments have shown a significant antiproliferative effect for copper-containing complexes against several human cancer cell lines. Furthermore, a mild and severe antiproliferative effect on human umbilical vein endothelial (HUVECs) cells was observed at doses higher

than 50 and 200  $\mu\text{M}$  of copper compounds, respectively [180]. Emphasizing the role of the source of ion, copper ions in the form of  $\text{CuSO}_4$  up to the level 500  $\mu\text{M}$  were shown to increase the proliferation of HUVECs. Furthermore, in vivo studies have not reported any toxic effect of copper ions administered as salts ( $\text{CuSO}_4$ ), directly or incorporated into biomaterials [96, 97, 181]. Combined with CaP carriers, copper ions did not cause any toxicity up to approximately 250  $\mu\text{g}$  in an in vivo model, while In vivo vascularization and wound tissue ingrowth were sensitive to the concentration of  $\text{CuSO}_4$ , being enhanced at specific concentrations [182].

As with other bioinorganics, in vitro studies have shown a dose-dependent effect of fluoride on proliferation of various relevant cell types. Sodium fluoride levels up to 500  $\mu\text{M}$ , for example, were shown to be safe for exposing to rat calvaria cells, while concentrations higher than 1 mM significantly reduced cell viability, suggesting cell cytotoxicity caused by fluoride ions at this concentration [127]. Using a cell based quantitative evaluation of the MTT assay, Qu et al. [128] showed that sodium fluoride at concentrations of 100  $\mu\text{M}$  and 1 mM suppressed cell proliferation and induced apoptosis in caprine osteoblasts. Regarding incorporation into CaPs, fluoride ions modification was shown to promote viability and proliferation of various cell types [142, 183-187]. A slight suppression of cell growth was observed in studies at high concentrations of the  $\text{F}^-$  doping, which is unlikely to be related to the release of the ions from the CaPs to cell culture medium, considering that no negative effect on cell viability was observed in the presence of similar concentrations of fluoride ions directly added to cell culture medium [188]. It is notable that fluoride substitution may substantially influence the physicochemical properties of CaPs, which can indirectly affect the cell attachment and viability [142, 188].

Regarding carbonated CaPs, although release of carbonate may result in pH reduction in cell microenvironment, previous studies reported a normal or enhanced proliferation of bone cells on carbonated CaPs [189-191]. Furthermore, no toxic effect has been found upon implantation of carbonated CaPs in animals [192-194].

The results summarized above emphasize the role of an administered dose of bioinorganics as a dominant factor for their safety or cytotoxicity. It is important to note that this is also dependent on the carrier used, as this influences the

release profile of bioinorganics, and their final dose exposed to cells or living tissues.

### **2.6.3. Biological performance of ceramics containing inorganic additives**

In many studies, it has been demonstrated that bioinorganics, added as soluble ions or incorporated into bone graft substitutes such as CaPs, can directly alter the cells due to the change in chemistry. These influences are caused by the essential roles of the ions in cell signaling pathways related to osteoblastogenesis and mineralization, osteoclastogenesis and bone resorption, and angiogenesis and vascularization [195]. In this section, release profiles of the inorganic additives from the ceramics are discussed in physiological conditions, as well as their effect in *in vitro* and *in vivo* systems related to bone formation and remodeling. Furthermore, the biological effects of the bioinorganics described below have been also illustrated in Figure 3.

#### **2.6.3.1. Zinc**

Studies on the *in vitro* release profiles of zinc for the zinc-incorporated  $\beta$ -TCP in simulated body fluid (SBF) showed an initial burst release, followed by a sustained release over a longer period of time. The amount of zinc released increased with the increasing zinc content of the ceramic ranging from 0.6 to 6 wt% [196]. The rate of zinc release was shown to increase when the calcium content of the release medium was decreased [196].

In a study by Tas et al. it was demonstrated that a presence of zinc in  $\beta$ -TCP in concentrations of 2900 and 4100 ppm increased viability of murine osteoblast-like cells, whereas further increase in zinc content had an opposite effect. ALP activity of these cells was found to reach its maximum on ceramics containing 4100 ppm zinc [197]. Dose-dependent effects on osteoblastic cell attachment and growth were observed in both zinc-containing HA and  $\beta$ -TCP, with a positive effect up to 1.5 wt% and a negative effect above this level, possibly due to the toxic effects on cells [198, 199].

Ito and colleagues also reported a more pronounced MC3T3-E1 osteoblasts proliferation *in vitro* for ZnTCP/HA ceramics with zinc content ranging from 0.6

and 1.2 wt% as compared to the control [153], which was consistent with other *in vitro* reports [172, 200].

The proliferation of the MC3T3-E1 osteoblasts and their ALP activity were enhanced when 10 wt% Zn incorporated CaP was used to prepare CPCs [201]. Similarly, Huang et al. showed that MC3T3-E1 cells cultured on calcium silicate/zinc-doped HA featured improved adhesion, proliferation and expression of ALP than those cultured on phase-pure HA [202].

Resorption by mature osteoclasts of Zn incorporated  $\beta$ -TCP with zinc concentrations of 0.316 wt% and especially 0.633 wt%, was lower than resorption of pure TCP, possibly due to an increase in the apoptosis of osteoclasts [155, 203]. At a zinc level of 0.633 wt%, the number of apoptotic osteoclasts was 2.8 times higher than on pure TCP after 24 h of culture. These findings were consistent with the laser microscopic measurement experiments on osteoclastic resorption pits, which showed that ZnTCP slightly reduced the resorption area by 15.5%, remarkably reduced the depth of resorption pits by 25.4%, and therewith the volume of resorption pits by 53.9% compared to pure TCP [204].

*In vivo* studies in rabbit femora showed that 0.316 wt% of zinc was the optimum concentration at which the largest area of new bone was formed, in both Zn-TCP and Zn-TCP/HA, whereas zinc content of 0.633 wt% was too high, enlarging the medullary cavity area by stimulated bone resorption [205]. Interestingly, the optimum zinc content *in vivo* was much lower than the zinc amount needed to exert a positive effect of osteoblast proliferation *in vitro* [153].

Incorporation of silica ( $\text{SiO}_2$ ) and zinc oxide (ZnO) into three dimensional printed  $\beta$ -TCP scaffolds increased the capacity of the scaffolds for early bone formation in a bicortical femur defect in a murine model, by modulating collagen I and osteocalcin production. Furthermore, mechanical interlocking between the scaffold and the host bone tissue was stronger than the force it took to fracture the bone for both pure and doped samples, after only 4 weeks of implantation [206].

In a more recent study it was shown that Zn- $\beta$ -TCP enhanced the ALP activity of hMSCs, the effect that was dependent on Zn content in TCP. It was also observed that zinc could influence both the activity and the formation of multinucleated giant cells. Furthermore, after a 12-week implantation in the muscles of dogs, the formation of the new bone increased with increasing zinc content in Zn-TCP up to

52% bone in the free space, while no bone formation was observed in  $\beta$ -TCP without zinc [207].

### 2.6.3.2. Copper

Copper-containing CaP ceramics have not been extensively investigated with regard to their bioactivity in bone regeneration; however, simple adsorption of copper ions on a CaP ceramic prepared at room temperature showed a positive effect on angiogenesis *in vitro* and *in vivo* [181, 182]. This is an interesting finding because poor vascularization is considered an important reason for failure in timely and complete regeneration of critically sized bone defects.

Copper ions were shown to influence the response of osteoblastic and osteoclastic cells to CaP too. While copper-incorporated CaP coatings had a mild inhibitory effect on osteoblast differentiation, a significant decrease in resorptive activity of osteoclasts was observed on such coatings as compared to the ones without the ion additive [142].

The copper-incorporated HA coatings also exhibited good cytocompatibility and had no toxicity toward MC3T3-E1 at low concentrations [208, 209]. Copper-incorporated CaP materials are also frequently studied as antimicrobial surfaces [208-210].

Lysenko et al. have observed that BCP granules doped with 0.5–1 at.% silver and 0.25–0.5 at.% copper stimulated bone tissue repair in a bone defect in rats [210]. *In vitro* bioactivity studies in SBF showed that strontium-HA, with a strontium content below 10 mol%, showed a more pronounced apatite layer formation on the surface than pure HA, which can be attributed to a higher dissolution rate of the strontium -containing ceramic [211, 212].

### 2.6.3.3. Strontium

A similar observation was made in strontium-containing TCP [213]. Experiments with osteoprecursor cells (OPC1) showed that both the attachment and proliferation were increased in HA-containing 20 mol% strontium as compared to the control without the additive. Increases in ALP and osteopontin were also seen, suggesting that strontium stimulated osteogenic differentiation of OPC1 cells [212]. Similar findings were also obtained in a study where osteoblast-like

cells were cultured on strontium-substituted CaPs [142, 178, 214-216]. Pulsed-laser deposition was successfully used to apply a coating of strontium-doped HA, prepared by an aqueous precipitation method, on metallic substrates. Osteogenic differentiation of human osteosarcoma cell line MG-63 was stimulated by strontium (3–7 at.% in the coating), whereas proliferation of osteoclasts was negatively affected [179].

Schumacher et al. [174] observed that in indirect and direct cell culture experiments with strontium-incorporated CPCs, the proliferation and osteogenic proliferation of hMSCs was significantly enhanced compared to the cement without strontium. Expression of osteogenic markers and formation of mineralization nodules were also substantially increased in rat primary osteoblast cells when cultured on the strontium-substituted HA ceramics [217, 218]. Similar observations were found in other studies [178, 219, 220].

Strontium incorporation in CaPs was demonstrated to promote the secretion and mRNA expression of angiogenic growth factors from cultured endothelial cells and to reduce the proliferation and resorption activity of the cultured osteoclasts, too [142, 221].

Injection of strontium-containing CPC into rabbit iliac crest cancellous bone revealed that strontium-HA stimulated the formation of osteoblast and osteoid layers, and hence new bone formation [222].

Implantation of CPCs with and without strontium incorporation in rats for 6 weeks revealed that strontium addition to the cements significantly increased the bone formation in the fracture defect zone along with the increase in the expression of the bone formation-related proteins at the implantation site [223]. Similar observations were obtained by implanting other strontium-added CaP-based biomaterials [224, 225].

Gu et al. [226] suggested that strontium-containing CaPs could accelerate bone formation through stimulating the secretion of VEGF and bFGF from osteoblasts. It was also shown that strontium-containing apatite/polylactide composites enhanced bone formation in osteopenic rabbits [227]. Furthermore, Kuang et al. [228] found that the local release of strontium from CPC accelerated soft tissue tendon graft healing within the bone tunnels in rabbits.

#### 2.6.3.4. Fluoride

Fluorinated HA showed a positive effect on proliferation and osteogenic differentiation of cells. In a study by Wang and coworkers, MG-63 cells were cultured on fluorinated HA coatings produced by a sol-gel dipping method. Positive effect of fluoride on cell attachment, as well as ALP and osteocalcin production, was observed in a certain concentration range [229], at which the ceramic coating had the lowest solubility. A positive effect of fluoride on cell proliferation and osteogenic differentiation was also observed when SaOS-2 rat osteosarcoma cells were cultured on fluorinated HA disks in comparison to fluoride-free controls [230]. MC3T3-E1 osteoblasts also showed improved proliferation when cultured on fluorinated HA coatings, compared to the cells cultured on phase-pure HA coatings or titanium implants [231].

Proliferation of MSCs and expression of the osteogenic biomarkers was enhanced when cultured on fluorinated CaPs [188, 232]. Furthermore fluoride ions, supplemented in cell medium or released from CaPs, substantially improved the mineralization of these cells [188]. Similarly, positive effects of fluoride modification on osteogenic properties of CaPs were observed [187, 233, 234]. Yang et al. [142] also observed that fluoride incorporation into CaP coatings reduced the resorptive activity of osteoclasts.

In a study by Inoue and coworkers, fluorinated apatite ceramics were tested in a short-term implantation model in rat tibia. A more pronounced bone formation was observed in fluoride-containing ceramic compared to a non-sintered calcium-deficient apatite ceramic [235]. Lalk et al. [236] implanted magnesium alloy sponges without and with addition of fluoride and CaP coatings in the femur of rabbits. After analyzing the implants within 24 weeks, it was concluded that sponges with fluoride addition were superior in biocompatibility and characterized them as more suitable candidates for bone replacement.

#### 2.6.3.5. Carbonate

Redey and coworkers showed a poor attachment and low collagen production of human primary osteoblasts on carbonated apatite ceramic as compared to that on HA ceramic, possibly caused by the difference in wettability between the two

ceramics [191]. This is in agreement with other reports showing a positive correlation between surface energy and attachment of cells [237-239].

After initial cell attachment, however, no significant differences were found in further proliferation of the cells between carbonated and pure HA ceramic. Kannan et al. also showed that proliferation of osteoblastic-like cells could be either delayed or accelerated upon addition of different doses of carbonate to CaPs while the same proliferation level was reached in all the samples at later time points [240]. Furthermore, carbonate was shown to enable the pre-osteoblastic differentiation of the cells [240-242].

Similar to osteoblast attachment, osteoclast attachment was more pronounced on carbonate-free ceramics compared to the carbonated one, while no difference was observed on the spreading of cells after initial attachment [190]. Doi et al. showed that carbonated apatite was resorbed by osteoclasts in 2-day cultures, while HA remained unresorbed, suggesting that the presence of carbonate may play a crucial role in osteoclastic resorption [243], which was in accordance with the results obtained in an in vivo experiment in rats [194]. A possible reason could be the released carbonate stimulates carbonic anhydrase activity and hence promotes acid secretion by osteoclasts [244]. Additionally, Spence and coworkers observed an increase in osteoclastic resorption with an increase of carbonate content in an HA ceramic [245], while Yang et al. [142] observed the opposite results. In an in vivo study in rabbits by Landi and coworkers, a higher amount of new bone formation was found in sintered carbonated apatite ceramic compared to the pure HA ceramic [193]. An increase in the amount of newly formed bone with increasing carbonate content in an apatite ceramic was also observed in a rat femur model [192]. In a critical-size iliac wing model in goats, it was shown that an increase in carbonate content of a ceramic does not necessarily lead to more bone formation if other ceramic properties are not controlled [246]. Recent in vivo experiments revealed the potential of carbonated CaP-based bone graft substitutes for bone regeneration. Borkowski et al. [247], for example, prepared a carbonated apatite-glucan composite and after implantation in rabbit tibia observed that this carbonated composite enabled the full regeneration of bone tissue after 6 months. It was also reported that the transplantation of MSCs with carbonated-apatite particles regenerated the bone defects in artificial jaw cleft in dogs [248].

#### 2.6.4. Effect of inorganic additives on ceramic properties

2

An indirect mechanism through which bioinorganics incorporated into bone graft substitute materials may influence the cell fate is by modifying the physicochemical properties of the host materials. Upon incorporation into the CaPs, the bioinorganics may cause changes in the crystal lattice structure and lattice parameters, therefore resulting in changes in the crystal morphology, and directional crystal growth at the microstructure level. Surface topographical parameters including surface morphology, surface porosity and roughness are important physicochemical parameters, which can substantially direct the cell attachment, growth and differentiation. It is worth mentioning that the physicochemical properties of the CaPs are substantially dependent on one another and small changes in one may determine considerable changes in another. Figure 4. Illustrates some of these physicochemical properties of CaPs, their interactive relations and their possible changes upon addition of bioinorganics.

Effects of incorporation of inorganic additives on the physicochemical and structural properties of CaP ceramics, and consequently their biological behavior, are largely dependent on the way an additive is incorporated into the crystal lattice. A few examples of these structural changes are listed below.

Incorporation of zinc into the CaP crystal lattice occurs by substitution of calcium ions. It has been shown that zinc incorporation decreases the lattice parameters due to its lower ionic radius as compared to calcium ion; however, there have also been reports suggesting an increase in the lattice parameters, at higher zinc contents [249-251]. It has been shown that with an increase in zinc content, the solubility of TCP decreases [252]. It is notable that controversial results have been observed in other studies plausibly due to differences in production methods [253-255]. Crystallinity of the CaPs was also shown to be compromised upon incorporation of zinc ions [249, 253].

Similar to the effects of zinc incorporation, the dependence of unit cell parameters on the copper concentration in the copper incorporated CaPs has been reported, also due to the lower ionic radius of copper as compared with that of the calcium [256, 257].

Substitution of calcium by strontium in CaPs was shown to influence their lattice parameters because of the slightly larger ionic radius of strontium compared with that of calcium [106, 154, 213, 258, 259]. Furthermore, this substitution resulted in an increased solubility of the ceramic [211].

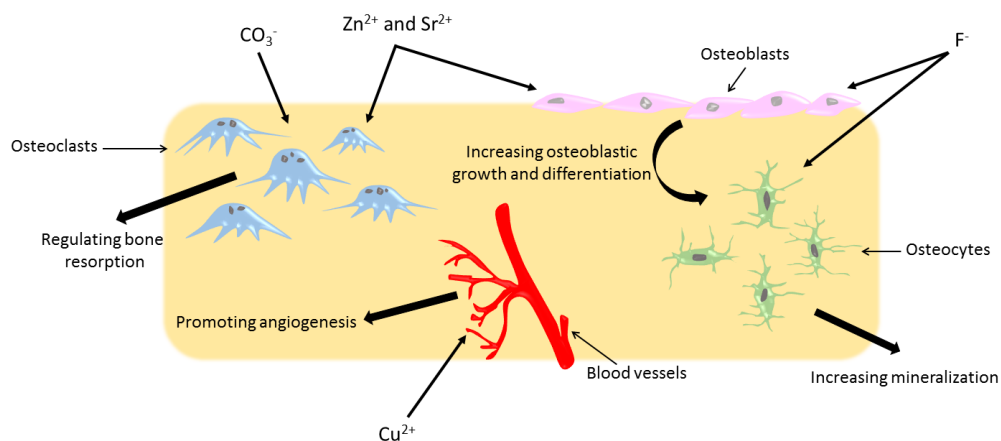


Figure 3. Role of different bioinorganics on various mechanisms involved in bone formation and remodeling including osteoblastogenesis, osteoclastogenesis and angiogenesis.

Replacement of hydroxide group with fluoride in an apatite lattice can bring about a reduction in the volume of the unit cell, and a concomitant increase in structure stability [69, 260-264].

Dissolution tests have shown that solubility decreased with the increase in fluoride content [229, 262, 265, 266].

An increase of carbonate content in a carbonated apatite by both A and B substitution, resulted in contraction of a-axis and expansion of c-axis of the unit cell, and therefore, in a decrease in crystal size and an increase in crystal strain, which in turn resulted in a higher solubility [267, 268].

Figure 5, as an example of the structural changes upon ionic substitution in CaPs, shows microstructure of an HA and a carbonated apatite ceramic, produced using

a similar method, from which it is obvious that even a carbonate content of approximately 5 wt% leads to a great decrease of the grain size of the ceramic.

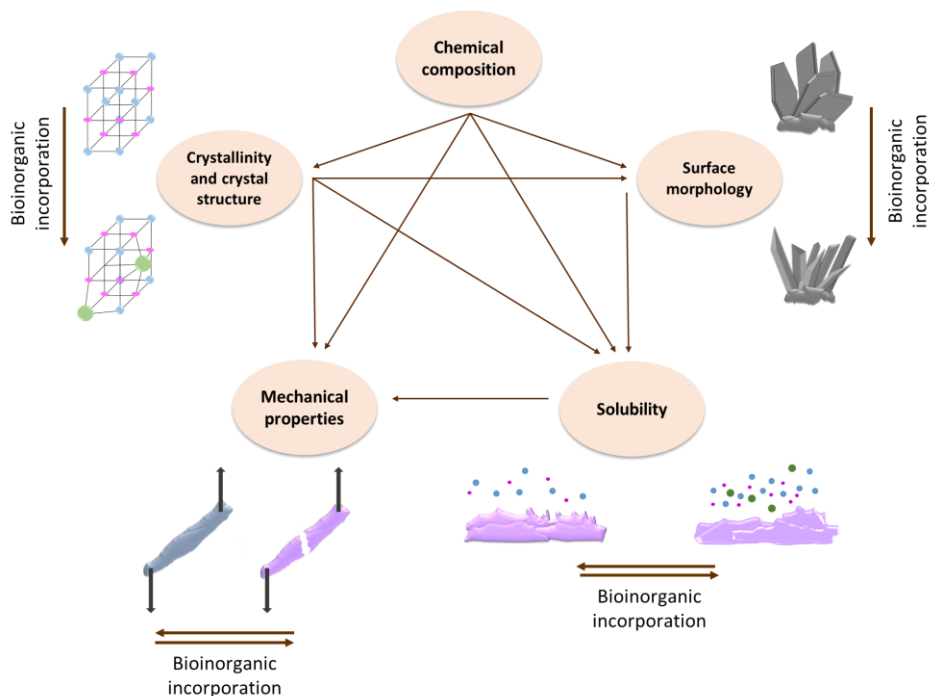


Figure 4. Examples of physicochemical properties of CaPs influenced by ionic substitution and their interactive relations.

### 2.6.5. Incorporation of multiple elements into CaPs

As discussed above, the incorporation of a single trace element into CaP-based synthetic bone grafts has demonstrated positive results to date. The results of many studies suggest that the incorporation of bioinorganics into CaPs mimics the physicochemical properties of the mineral component of natural bone, and this triggers different mechanisms involved in bone remodeling and formation processes. On the other hand, the CaP mineral that exists within bone contains a combination of bioinorganics in trace quantities [5]. Therefore, it is reasonable to hypothesize that incorporating multiple bioinorganics into CaP-based bone graft

substitutes may further enhance the biological performance [269]. Hence, the idea of incorporating a cocktail of bioinorganics into CaPs is gaining popularity, although there are only a few studies completed on this topic. Many studies in this field have focused on the changes in physicochemical, structural and mechanical properties of CaPs upon incorporation of multiple bioinorganics, showing that the desired properties of the CaPs can be obtained by manipulating the combination and dose of the bioinorganics [270-273]. For example, Bose et al. [270] studied the mechanical properties of  $\beta$ -TCP into which different double and triple combinations of magnesium-, silicon- and strontium ions were incorporated and showed that all combinations of the bioinorganics reduced the compressive strength of dry TCPs. However, the presence of the cocktails of bioinorganics preserved the mechanical strength of the TCPs in SBF. They also observed that incorporating these multiple bioinorganics into CaPs increased the bioactivity and formation of an apatite-like phase on the surface of the implant [270].

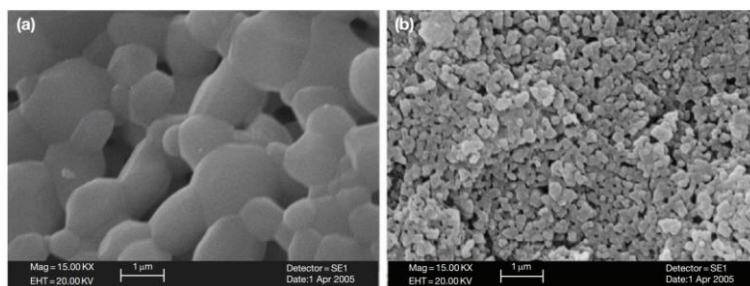


Figure 5. High magnification scanning electron microscopy micrographs showing microstructure of (a) hydroxyapatite and (b) type B carbonated apatite ceramic containing about 4 wt% carbonate, produced using a similar process. Note a significant decrease in crystal size in presence of carbonate.

The role of incorporating multiple bioinorganics on enhancing osteogenic properties of bone graft substitutes has been also studied *in vitro* and *in vivo*. For instance, the addition of magnesium and strontium ions to bone graft substitutes have resulted in decreased *in vitro* osteoclastogenesis, expression of osteoblastic markers in human bone derived cells, and finally have led to enhanced

mineralization and bone formation when implanted in a rat femoral defect model [274, 275]. Doping combinations of zinc and silicon in  $\beta$ -TCP scaffolds, similar to the cocktail of magnesium and strontium, also resulted in accelerated bone healing compared to undoped scaffolds. Simultaneous incorporation of fluoride and carbonate into apatites led to inhibition of osteoclast proliferation and pit formation in vitro as compared to that in pure HA and carbonated apatites, whereas in vivo, faster bone remodeling was observed [276].-Other combinations of multiple elements were also found to be of influence on osteoclasts and osteoblasts and therefore, on bone resorption and formation respectively [276-278].

In a few studies, the incorporation of combinations of more than two bioinorganics has been attempted; however, little data is available on the biologic response to the modified CaPs. Yang et al. [279] have taken a medium throughput approach, in which silicon, magnesium, strontium and zinc ions were incorporated into octacalcium phosphate microbeads of different sizes, as individual or cocktails in different doses. Upon a subcutaneous implantation in rats, the beads containing a cocktail of bioinorganics showed excellent biocompatibility, as well as higher neovascularization when compared to the beads without bioinorganic incorporation. Furthermore, beads with a cocktail of bioinorganics showed higher bone formation compared to the empty octacalcium phosphate beads after 6 weeks implantation in femur defects in rats [279].

These studies introduced the incorporation of multiple bioinorganics into CaP-based bone graft substitutes as another promising strategy for improving the field of bone regeneration. While offering much potential, developing this strategy is associated with great difficulties at the research level considering that developing an optimum formulation of the bioinorganic cocktail requires large-sized experiments.

## **2.7. Future perspectives: Mechanistic studies and high-throughput screening systems**

We foresee two important developments in the field of bioinorganics for regenerative medicine, one aimed at decoupling direct chemical effect of bioinorganics from the indirect effects it has on the carrier material including

surface topography, and the other at high-throughput systems for discovering optimum combinations of bioinorganics.

In the context of bone regeneration, it has been shown that certain topographical cues induce *in vitro* osteogenic differentiation. Dalby et al., for example, stimulated MSCs to produce mineralization in an *in vitro* environment by culturing them on nano-scale surface topographies [280]. Other studies with similar approaches have also shown that surfaces with micro- and nano- topographies featuring pit, pillar and groove arrays may be able to regulate cell fate. It was shown that cells respond to the patterned surfaces with a different behavior in terms of cell attachment, growth or differentiation, than when cultured on flat, unpatterned surfaces [281-285].

Finding and producing the optimum surface topography for dictating the desired cell fate requires comprehensive and in depth research. In the case of CaPs with bioinorganic incorporation, one obstacle for understanding the role of surface topography on cell and tissue biologic response is to individually recognize and decouple the impacts of surface morphology and chemistry. This is important since both chemical composition and surface morphology may be modified upon incorporation. Danoux et al. have recently attempted to develop a design-driven approach for decoupling and recombining inherent properties of CaP materials such as chemistry and surface topography, aiming at increasing the knowledge of interactions of biomaterial and biological systems. This is with the purpose of opening new doors towards developing advanced functional materials. In this approach, they produced CaP crystals with various chemical compositions and surface topographies, and utilized them for fabricating the replica of the crystals featuring the exact surface topographies into neutral polymers (decoupling step). The replicas were then later coated with a thin layer of CaP or titanium in order to show the possibility of recombining chemistry and surface topography [286]. Similar approaches can be used for decoupling the physicochemical properties of CaP materials with bioinorganic incorporation, and may be able to shed light on the individual role of each property on determining cell fate. Similarly, replacing CaPs as carriers of bioinorganics by other materials, such as polymers, will be useful for decoupling the effect of the bioinorganic of interest from that of other ions present in CaPs [287].

Incorporation of single and multiple bioinorganics presents a promising approach for controlling and enhancing the performance of CaP-based bone graft substitutes. However, studying the effect of several elements is associated with many difficulties. This results in a dramatic increase in the size and number of experiments needed to identify potential combinations and concentrations of elements. Therefore, there is a demand for new tools, which can provide systematic and high-throughput approaches for screening the effects of multiple elements in varying concentrations and formulations.

Microfluidic devices, for example, can provide platforms for screening the effects of small molecules, such as bioinorganic ions in combination, as well as varying, continuous concentrations at a single cell level. This would increase the throughput of the experiments by utilizing parallelization, multiplexing and automation. Such platforms offer other advantages as compared to conventional cell culture and bioassay techniques such as close temporal and spatial control over fluids and physical parameters, and integration of sensors for direct readouts [288, 289]. As an example, Harink et al. [288, 290] have developed a microfluidic chamber that allows the generation of four orthogonal, overlapping and stable gradients of soluble small molecules, and this supports the normal attachment and growth of different cell types. Such platforms can be used for generating overlapping continuous gradient concentrations of several bioinorganics, and can help to study the impact of countless formulations of bioinorganics on the cell biologic responses simultaneously.

Chemical library systems using (micro)well array platforms offer another approach that has been previously used for discovering novel pharmaceuticals and optimizing the microenvironment of the cells for tissue regeneration and stem cell engineering applications [291, 292]. An automated micro-array platform can also be a powerful toolbox for analyzing a chemical library of bioinorganics both as soluble salt and incorporated into bone graft substitutes. The platform can be designed to study various formulations of the bioinorganics based on an image or chemical signal readout.

Both of the high-throughput approaches introduced above have been previously used in preliminary in vivo studies in micro-organisms such as zebrafish [292-295]. Similarly, they can be also utilized to study the impact of bioinorganics on formation of zebrafish skeletal system.

The extensive potential of these approaches for fast and accurate analysis in controlled microenvironmental conditions, combined with the possibility of performing preliminary *in vivo* screens, demonstrates the promise of these platforms for carrying out systemic biological evaluations of bioinorganics for bone regeneration applications. This would help to speed up the discovery of promising bioinorganic combinations, and help to bridge the gap towards autograft.

## 2.8. Concluding remarks

Improving the biological performance of bone graft substitutes remains a challenge. Incorporation of inorganic additives into CaPs with the aim to develop a comprehensive synthetic alternative to patient's own bone is a complex matter, as has been demonstrated in the previous sections. The preparation, characterization, and assessments of safety and biological activity of ceramics-containing zinc, copper, strontium, fluoride, and carbonate, respectively, have been discussed. The incorporation of these additives into CaP bone graft substitutes not only adds an additional element into the structure that can exert a certain function, but also changes intrinsic properties of the recipient material. The way and the efficiency of incorporation are dependent on the method used. These in turn affect the release profile of the incorporated additive, and also the solubility of the recipient itself; these all affect the behavior of osteoblasts and osteoclasts *in vitro*, as well as the *in vivo* bone formation and remodeling.

As already mentioned, these are some general remarks about the effects of various additives on properties and efficiency of the existing bone graft substitutes. Due to variations in the preparation and characterization methods and assessment of biological performance of these materials, a comparison among the studies and the results obtained is difficult, and hence general conclusions cannot be drawn. Thus, it behooves the field of biomaterials research to utilize generally accepted, standard methods of study, such that *in vitro* behavior and *in vivo* performance can be correlated. We also suggest that high-throughput study concepts have their place in biomaterials research, such as in the context of quantifying the effect of ionic substitutions within the apatite lattice.

## References

1. D.W. Fawcett and W. Bloom, A Textbook of Histology 11 ed. 1986, PA Saunders Philadelphia.
2. P. Derkx, A.L. Nigg, F.T. Bosman, D.H. Birkenhäger-Frenkel, A.B. Houtsmuller, H.A.P. Pols, J.P.T.M. van Leeuwen, Immunolocalization and Quantification of Noncollagenous Bone Matrix Proteins In Methylnmethacrylate-Embedded Adult Human Bone In Combination With Histomorphometry. *Bone*, 22 (1998) 367-373.
3. S.C. Marks, D.C. Hermey Jr., J.P. Bilezikian, L.G. Raisz, G.A. Rodan, Principles of Bone Biology 1996, USA Academic Press San Diego.
4. M.R. van der Harst, P.A.J. Brama, C.H.A. van de Lest, G.H. Kiers, J. DeGroot, P.R. van Weeren, An integral biochemical analysis of the main constituents of articular cartilage, subchondral and trabecular bone. *Osteoarthritis and Cartilage*, 12 (2004) 752-761.
5. A. Bigi, G. Cojazzi, S. Panzavolta, A. Ripamonti, N. Roveri, M. Romanello, K. Noris Suarez, L. Moro, Chemical and structural characterization of the mineral phase from cortical and trabecular bone. *J Inorg Biochem*, 68 (1997) 45-51.
6. K.L. Brown and R.L. Cruess, Bone and cartilage transplantation in orthopaedic surgery. A review. *The Journal of Bone & Joint Surgery*, 64 (1982) 270-279.
7. C.N. Cornell and J.M. Lane, Current understanding of osteoconduction in bone regeneration. *Clin Orthop Relat Res*, (1998) S267-73.
8. C.J. Damien and J.R. Parsons, Bone graft and bone graft substitutes: a review of current technology and applications. *J Appl Biomater*, 2 (1991) 187-208.
9. J.M. Lane, E. Tomin, M.P. Bostrom, Biosynthetic bone grafting. *Clin Orthop Relat Res*, (1999) S107-17.
10. M.R. Urist, Bone: formation by autoinduction. *Science*, 150 (1965) 893-9.
11. E.D. Arrington, W.J. Smith, H.G. Chambers, A.L. Bucknell, N.A. Davino, Complications of iliac crest bone graft harvesting. *Clin Orthop Relat Res*, (1996) 300-9.
12. A.G. Coombes and M.C. Meikle, Resorbable synthetic polymers as replacements for bone graft. *Clin Mater*, 17 (1994) 35-67.
13. S.P. Cowley and L.D. Anderson, Hernias through donor sites for iliac-bone grafts. *The Journal of Bone & Joint Surgery*, 65 (1983) 1023-1025.
14. D.J. Prolo and J.J. Rodrigo, Contemporary bone graft physiology and surgery. *Clin Orthop Relat Res*, 200 (1985) 322-42.
15. E.M. Younger and M.W. Chapman, Morbidity at bone graft donor sites. *J Orthop Trauma*, 3 (1989) 192-5.
16. M.L. Anderson, W.J. Dhert, J.D. de Bruijn, R.A. Dalmeijer, H. Leenders, C.A. van Blitterswijk, A.J. Verbout, Critical size defect in the goat's os ilium. A model to evaluate bone grafts and substitutes. *Clin Orthop Relat Res*, (1999) 231-9.
17. J. Oikarinen and L.K. Korhonen, The bone inductive capacity of various bone transplanting materials used for treatment of experimental bone defects. *Clin Orthop Relat Res*, 140 (1979) 208-15.
18. S.A. Oklund, D.J. Prolo, R.V. Gutierrez, S.E. King, Quantitative comparisons of healing in cranial fresh autografts, frozen autografts and processed autografts, and allografts in canine skull defects. *Clin Orthop Relat Res*, 205 (1986) 269-91.
19. J.W. Brantigan, B.W. Cunningham, K. Warden, P.C. McAfee, A.D. Steffee, Compression strength of donor bone for posterior lumbar interbody fusion. *Spine (Phila Pa 1976)*, 18 (1993) 1213-21.
20. M.R. Urist, B.F. Silverman, K. Buring, F.L. Dubuc, J.M. Rosenberg, The bone induction principle. *Clin Orthop Relat Res*, 53 (1967) 243-83.

21. P. Habibovic, M.C. Kruyt, M.V. Juhl, S. Clyens, R. Martinetti, L. Dolcini, N. Theilgaard, C.A. van Blitterswijk, Comparative in vivo study of six hydroxyapatite-based bone graft substitutes. *J Orthop Res*, 26 (2008) 1363-70.
22. D. Le Nihouannen, G. Daculsi, A. Saffarzadeh, O. Gauthier, S. Delplace, P. Pilet, P. Layrolle, Ectopic bone formation by microporous calcium phosphate ceramic particles in sheep muscles. *Bone*, 36 (2005) 1086-93.
23. P. Habibovic, U. Gbureck, C.J. Doillon, D.C. Bassett, C.A. van Blitterswijk, J.E. Barralet, Osteoconduction and osteoinduction of low-temperature 3D printed bioceramic implants. *Biomaterials*, 29 (2008) 944-53.
24. P. Habibovic, H. Yuan, C.M. van der Valk, G. Meijer, C.A. van Blitterswijk, K. de Groot, 3D microenvironment as essential element for osteoinduction by biomaterials. *Biomaterials*, 26 (2005) 3565-75.
25. B. Ben-Nissan, C. Chai, K. Gross, Effect of solution ageing on sol-gel hydroxyapatite coatings. *Bioceramics*, 10 (1997) 175-178.
26. P. Ducheyne, W. Van Raemdonck, J.C. Heughebaert, M. Heughebaert, Structural analysis of hydroxyapatite coatings on titanium. *Biomaterials*, 7 (1986) 97-103.
27. L.I. Havelin, L.B. Engesaeter, B. Espehaug, O. Furnes, S.A. Lie, S.E. Vollset, The Norwegian Arthroplasty Register: 11 years and 73,000 arthroplasties. *Acta Orthop Scand*, 71 (2000) 337-53.
28. J.L. Ong, L.C. Lucas, W.R. Lacefield, E.D. Rigney, Structure, solubility and bond strength of thin calcium phosphate coatings produced by ion beam sputter deposition. *Biomaterials*, 13 (1992) 249-254.
29. Y. Liu, E.B. Hunziker, P. Layrolle, J.D. De Bruijn, K. De Groot, Bone morphogenetic protein 2 incorporated into biomimetic coatings retains its biological activity. *Tissue Eng*, 10 (2004) 101-8.
30. L. Guan and J.E. Davies, Preparation and characterization of a highly macroporous biodegradable composite tissue engineering scaffold. *Journal of Biomedical Materials Research Part A*, 71A (2004) 480-487.
31. L.D. Zardiackas, R.D. Teasdall, R.J. Black, G.S. Jones, K.R. St John, L.D. Dillon, J.L. Hughes, Torsional properties of healed canine diaphyseal defects grafted with a fibrillar collagen and hydroxyapatite/tricalcium phosphate composite. *J Appl Biomater*, 5 (1994) 277-83.
32. R. Zhang and P.X. Ma, Poly( $\alpha$ -hydroxyl acids)/hydroxyapatite porous composites for bone-tissue engineering. I. Preparation and morphology. *Journal of Biomedical Materials Research*, 44 (1999) 446-455.
33. T.J. Blokhuis, B.W. Wippermann, F.C. den Boer, A. van Lingen, P. Patka, F.C. Bakker, H.J. Haarman, Resorbable calcium phosphate particles as a carrier material for bone marrow in an ovine segmental defect. *J Biomed Mater Res*, 51 (2000) 369-75.
34. S.D. Boden, G.J. Martin, Jr., M. Morone, J.L. Ugbo, L. Titus, W.C. Hutton, The use of coralline hydroxyapatite with bone marrow, autogenous bone graft, or osteoinductive bone protein extract for posterolateral lumbar spine fusion. *Spine (Phila Pa 1976)*, 24 (1999) 320-7.
35. T.A. Zdeblick, M.E. Cooke, D.N. Kunz, D. Wilson, R.P. McCabe, Anterior cervical discectomy and fusion using a porous hydroxyapatite bone graft substitute. *Spine (Phila Pa 1976)*, 19 (1994) 2348-57.
36. R. Langer and J.P. Vacanti, Tissue engineering. *Science*, 260 (1993) 920-6.
37. C.A. Kirker-Head, Potential applications and delivery strategies for bone morphogenetic proteins. *Adv Drug Deliv Rev*, 43 (2000) 65-92.

38. R.G. Geesink, N.H. Hoefnagels, S.K. Bulstra, Osteogenic activity of OP-1 bone morphogenetic protein (BMP-7) in a human fibular defect. *J Bone Joint Surg Br*, 81 (1999) 710-8.
39. E.E. Johnson, M.R. Urist, G.A. Finerman, Bone morphogenetic protein augmentation grafting of resistant femoral nonunions. A preliminary report. *Clin Orthop Relat Res*, (1988) 257-65.
40. E.E. Johnson and M.R. Urist, Human bone morphogenetic protein allografting for reconstruction of femoral nonunion. *Clin Orthop Relat Res*, (2000) 61-74.
41. Y. Wada, H. Kataoka, S. Yokose, T. Ishizuya, K. Miyazono, Y.H. Gao, Y. Shibasaki, A. Yamaguchi, Changes in Osteoblast Phenotype During Differentiation of Enzymatically Isolated Rat Calvaria Cells. *Bone*, 22 (1998) 479-485.
42. Y. Miura and S.W. O'Driscoll, Culturing periosteum in vitro: the influence of different sizes of explants - Dose-response for transforming growth factor-beta 1 (TGF- $\beta$ 1). *J Bone Miner Res*, 7 (1998) 453-457.
43. A. Takushima, Y. Kitano, K. Harii, Osteogenic Potential of Cultured Periosteal Cells in a Distracted Bone Gap in Rabbits. *Journal of Surgical Research*, 78 (1998) 68-77.
44. R. GUNDLE, C.J. JOYNER, J.T. TRIFFITT Interactions of human osteoprogenitors with porous ceramic following diffusion chamber implantation in a xenogeneic host. *Journal of Materials Science: Materials in Medicine*, 8 (1997) 519-523.
45. P.G. Robey and J.D. Termine, Human bone cells in vitro. *Calcif Tissue Int*, 37 (1985) 453-60.
46. S.P. Bruder and B.S. Fox, Tissue engineering of bone. Cell based strategies. *Clin Orthop Relat Res*, (1999) S68-83.
47. M.J. Doherty, B.A. Ashton, S. Walsh, J.N. Beresford, M.E. Grant, A.E. Canfield, Vascular Pericytes Express Osteogenic Potential In Vitro and In Vivo. *Journal of Bone and Mineral Research*, 13 (1998) 828-838.
48. A.J. Friedenstein, R.K. Chailakhyan, U.V. Gerasimov, Bone marrow osteogenic stem cells: in vitro cultivation and transplantation in diffusion chambers. *Cell Tissue Kinet*, 20 (1987) 263-72.
49. C. Maniopoulos, J. Sodek, A.H. Melcher, Bone formation in vitro by stromal cells obtained from bone marrow of young adult rats. *Cell and Tissue Research*, 254 (1988) 317-330.
50. H. Ohgushi and M. Okumura, Osteogenic capacity of rat and human marrow cells in porous ceramics: Experiments in athymic (nude) mice. *Acta Orthopaedica Scandinavica*, 61 (1990) 431-434.
51. M. Owen, Marrow stromal stem cells. *J Cell Sci Suppl*, 10 (1988) 63-76.
52. J.N. Beresford, Osteogenic stem cells and the stromal system of bone and marrow. *Clin Orthop Relat Res*, (1989) 270-80.
53. G.F. Muschler, C. Boehm, K. Easley, Aspiration to obtain osteoblast progenitor cells from human bone marrow: the influence of aspiration volume. *J Bone Joint Surg Am*, 79 (1997) 1699-709.
54. J.A. Allay, J.E. Dennis, S.E. Haynesworth, M.K. Majumdar, D.W. Clapp, L.D. Shultz, A.I. Caplan, S.L. Gerson, LacZ and interleukin-3 expression in vivo after retroviral transduction of marrow-derived human osteogenic mesenchymal progenitors. *Hum Gene Ther*, 8 (1997) 1417-27.
55. A.J. Friedenstein, N.W. Latzinik, A.G. Grosheva, U.F. Gorskaya, Marrow microenvironment transfer by heterotopic transplantation of freshly isolated and cultured cells in porous sponges. *Exp Hematol*, 10 (1982) 217-27.
56. S.P. Bruder, A.A. Kurth, M. Shea, W.C. Hayes, N. Jaiswal, S. Kadiyala, Bone regeneration by implantation of purified, culture-expanded human mesenchymal stem cells. *J Orthop Res*, 16 (1998) 155-62.
57. Q. Cui, Z. Ming Xiao, G. Balian, G.J. Wang, Comparison of lumbar spine fusion using mixed and cloned marrow cells. *Spine (Phila Pa 1976)*, 26 (2001) 2305-10.

58. P.H. Krebsbach, M.H. Mankani, K. Satomura, S.A. Kuznetsov, P.G. Robey, Repair of craniotomy defects using bone marrow stromal cells. *Transplantation*, 66 (1998) 1272-8.
59. K. Anselme, B. Noël, B. Flautre, M.C. Blary, C. Delecourt, M. Descamps, P. Hardouin, Association of porous hydroxyapatite and bone marrow cells for bone regeneration. *Bone*, 25 (1999) 51S-54S.
60. M.C. Kruyt, J.D. de Bruijn, C.E. Wilson, F.C. Oner, C.A. van Blitterswijk, A.J. Verbout, W.J. Dhert, Viable osteogenic cells are obligatory for tissue-engineered ectopic bone formation in goats. *Tissue Eng*, 9 (2003) 327-36.
61. M.C. Kruyt, W.J. Dhert, C. Oner, C.A. van Blitterswijk, A.J. Verbout, J.D. de Bruijn, Optimization of bone-tissue engineering in goats. *J Biomed Mater Res B Appl Biomater*, 69 (2004) 113-20.
62. S.P. Bruder, K.H. Kraus, V.M. Goldberg, S. Kadiyala, The effect of implants loaded with autologous mesenchymal stem cells on the healing of canine segmental bone defects. *J Bone Joint Surg Am*, 80 (1998) 985-96.
63. M.C. Kruyt, W.J. Dhert, H. Yuan, C.E. Wilson, C.A. van Blitterswijk, A.J. Verbout, J.D. de Bruijn, Bone tissue engineering in a critical size defect compared to ectopic implantations in the goat. *J Orthop Res*, 22 (2004) 544-51.
64. H. Petite, V. Viateau, W. Bensaid, A. Meunier, C. de Pollak, M. Bourguignon, K. Oudina, L. Sedel, G. Guillemain, Tissue-engineered bone regeneration. *Nat Biotechnol*, 18 (2000) 959-63.
65. G.J. Meijer, J.D. de Bruijn, R. Koole, C.A. van Blitterswijk, Cell-based bone tissue engineering. *PLoS Med*, 4 (2007) e9.
66. S.D. Boden, Bioactive factors for bone tissue engineering. *Clin Orthop Relat Res*, (1999) S84-94.
67. J.O. Hollinger, H. Uludag, S.R. Winn, Sustained release emphasizing recombinant human bone morphogenetic protein-2. *Adv Drug Deliv Rev*, 31 (1998) 303-318.
68. S.R. Winn, H. Uludag, J.O. Hollinger, Carrier systems for bone morphogenetic proteins. *Clin Orthop Relat Res*, 367 (1999) S95-106.
69. J.C. Elliot, *Structure and Chemistry of the Apatites and Other Calcium Orthophosphates 1994*, Amsterdam Elsevier
70. R.O. Becker, J.A. Spadaro, E.W. Berg, The trace elements of human bone. *J Bone Joint Surg Am*, 50 (1968) 326-34.
71. F.A. El-Amri and M.A.R. El-Kabroun, Trace element concentrations in human bone using instrumental neutron activation analysis. *Journal of Radioanalytical and Nuclear Chemistry*, 217 (1997) 205-207.
72. N.R. Calhoun, J.C. Smith, Jr., K.L. Becker, The role of zinc in bone metabolism. *Clin Orthop Relat Res*, (1974) 212-34.
73. P.I. Oteiza and G.G. Mackenzie, Zinc, oxidant-triggered cell signaling, and human health. *Mol Aspects Med*, 26 (2005) 245-55.
74. B.L. Vallee and D.S. Auld, Zinc coordination, function, and structure of zinc enzymes and other proteins. *Biochemistry*, 29 (1990) 5647-59.
75. B.L. Vallee and K.H. Falchuk, The biochemical basis of zinc physiology. *Physiol Rev*, 73 (1993) 79-118.
76. A.S. Prasad, B. Bao, F.W. Beck, O. Kucuk, F.H. Sarkar, Antioxidant effect of zinc in humans. *Free Radic Biol Med*, 37 (2004) 1182-90.
77. M.D. Grynpas, Fluoride effects on bone crystals. *J Bone Miner Res*, 5 Suppl 1 (1990) S169-75.
78. N.M. Lowe, N.M. Lowe, W.D. Fraser, M.J. Jackson, Is there a potential therapeutic value of copper and zinc for osteoporosis? *Proc Nutr Soc*, 61 (2002) 181-5.

79. M. Yamaguchi, M. Goto, S. Uchiyama, T. Nakagawa, Effect of zinc on gene expression in osteoblastic MC3T3-E1 cells: enhancement of Runx2, OPG, and regucalcin mRNA expressions. *Mol Cell Biochem*, 312 (2008) 157-66.
80. I.S. Kwun, Y.E. Cho, R.A. Lomeda, H.I. Shin, J.Y. Choi, Y.H. Kang, J.H. Beattie, Zinc deficiency suppresses matrix mineralization and retards osteogenesis transiently with catch-up possibly through Runx 2 modulation. *Bone*, 46 (2010) 732-41.
81. A. Cerovic, I. Miletic, S. Sobajic, D. Blagojevic, M. Radusinovic, A. El-Sohehy, Effects of zinc on the mineralization of bone nodules from human osteoblast-like cells. *Biol Trace Elem Res*, 116 (2007) 61-71.
82. T. Wang, J.C. Zhang, Y. Chen, P.G. Xiao, M.S. Yang, Effect of zinc ion on the osteogenic and adipogenic differentiation of mouse primary bone marrow stromal cells and the adipocytic trans-differentiation of mouse primary osteoblasts. *J Trace Elem Med Biol*, 21 (2007) 84-91.
83. M. Yamaguchi, Role of nutritional zinc in the prevention of osteoporosis. *Mol Cell Biochem*, 338 (2010) 241-54.
84. B.L. O'Dell, Roles for iron and copper in connective tissue biosynthesis. *Philos Trans R Soc Lond B Biol Sci*, 294 (1981) 91-104.
85. D. Tinker, N. Romero, R. Rucker, L. Hurley, C. Keen, B. Lonnerdal, R. Rucker, *Trace Element in Man and Animals 1988* New York Plenum
86. R.B. Rucker, T. Kosonen, M.S. Clegg, A.E. Mitchell, B.R. Rucker, J.Y. Uriu-Hare, C.L. Keen, Copper, lysyl oxidase, and extracellular matrix protein cross-linking. *Am J Clin Nutr*, 67 (1998) 996s-1002s.
87. J.M. Howell and A.N. Davison, The copper content and cytochrome oxidase activity of tissues from normal and swayback lambs. *Biochemical Journal*, 72 (1959) 365-368.
88. J.J. Strain, A reassessment of diet and osteoporosis--possible role for copper. *Med Hypotheses*, 27 (1988) 333-8.
89. C.R. Paterson, Osteogenesis imperfecta and other bone disorders in the differential diagnosis of unexplained fractures. *Journal of the Royal Society of Medicine*, 83 (1990) 72-74.
90. O. Fromigué, P.J. Marie, A. Lomri, Bone morphogenetic protein-2 and transforming growth factor- $\beta$ 2 interact to modulate human bone marrow stromal cell proliferation and differentiation. *Journal of Cellular Biochemistry*, 68 (1998) 411-426.
91. H. Rico, Minerals and osteoporosis. *Osteoporos Int*, 2 (1991) 20-5.
92. T. Wilson, J.M. Katz, D.H. Gray, Inhibition of active bone resorption by copper. *Calcif Tissue Int*, 33 (1981) 35-9.
93. E.F. Eriksen, G.Z. Eghbali-Fatourehchi, S. Khosla, Remodeling and vascular spaces in bone. *J Bone Miner Res*, 22 (2007) 1-6.
94. H. Ito, M. Koefoed, P. Tiypatanaputi, K. Gromov, J.J. Goater, J. Carmouche, X. Zhang, P.T. Rubery, J. Rabinowitz, R.J. Samulski, T. Nakamura, K. Soballe, R.J. O'Keefe, B.F. Boyce, E.M. Schwarz, Remodeling of cortical bone allografts mediated by adherent rAAV-RANKL and VEGF gene therapy. *Nature medicine*, 11 (2005) 291-297.
95. G.F. Hu, Copper stimulates proliferation of human endothelial cells under culture. *J Cell Biochem*, 69 (1998) 326-35.
96. A. Parke, P. Bhattacharjee, R.M. Palmer, N.R. Lazarus, Characterization and quantification of copper sulfate-induced vascularization of the rabbit cornea. *The American Journal of Pathology*, 130 (1988) 173-178.
97. C.K. Sen, S. Khanna, M. Venojarvi, P. Trikha, E.C. Ellison, T.K. Hunt, S. Roy, Copper-induced vascular endothelial growth factor expression and wound healing. *Am J Physiol Heart Circ Physiol*, 282 (2002) H1821-7.

98. B. Halliwell and J.M. Gutteridge, Role of free radicals and catalytic metal ions in human disease: an overview. *Methods Enzymol*, 186 (1990) 1-85.
99. S. Skoryna, Metabolic aspects of the pharmacologic uses of the trace elements in human subjects with specific reference to stable Sr. *Trace Substances and Environmental Health* 18 (1984) 3-23
100. P. Ammann, I. Badoud, S. Barraud, R. Dayer, R. Rizzoli, Strontium Ranelate Treatment Improves Trabecular and Cortical Intrinsic Bone Tissue Quality, a Determinant of Bone Strength. *Journal of Bone and Mineral Research*, 22 (2007) 1419-1425.
101. S.D. Bain, C. Jerome, V. Shen, I. Dupin-Roger, P. Ammann, Strontium ranelate improves bone strength in ovariectomized rat by positively influencing bone resistance determinants. *Osteoporosis International*, 20 (2009) 1417-1428.
102. M.D. Grynpas and P.J. Marie, Effects of low doses of strontium on bone quality and quantity in rats. *Bone*, 11 (1990) 313-9.
103. P.J. Marie, M.T. Garba, M. Hott, L. Miravet, Effect of low doses of stable strontium on bone metabolism in rats. *Miner Electrolyte Metab*, 11 (1985) 5-13.
104. P.J. Marie and M. Hott, Short-term effects of fluoride and strontium on bone formation and resorption in the mouse. *Metabolism*, 35 (1986) 547-51.
105. I. Schrooten, W. Cabrera, W.G. Goodman, S. Dauwe, L.V. Lamberts, R. Marynissen, W. Dorrine, M.E. De Broe, P.C. D'Haese, Strontium causes osteomalacia in chronic renal failure rats. *Kidney Int*, 54 (1998) 448-56.
106. S.C. Verberckmoes, M.E. De Broe, P.C. D'Haese, Dose-dependent effects of strontium on osteoblast function and mineralization. *Kidney Int*, 64 (2003) 534-43.
107. P.J. Marie, M. Hott, D. Modrowski, C. De Pollak, J. Guillemain, P. Deloffre, Y. Tsouderos, An uncoupling agent containing strontium prevents bone loss by depressing bone resorption and maintaining bone formation in estrogen-deficient rats. *J Bone Miner Res*, 8 (1993) 607-15.
108. R. Baron and Y. Tsouderos, In vitro effects of S12911-2 on osteoclast function and bone marrow macrophage differentiation. *Eur J Pharmacol*, 450 (2002) 11-7.
109. E. Canalis, A. Giustina, J.P. Bilezikian, Mechanisms of anabolic therapies for osteoporosis. *N Engl J Med*, 357 (2007) 905-16.
110. S. O'Donnell, A. Cranney, G.A. Wells, J.D. Adachi, J.Y. Reginster, Strontium ranelate for preventing and treating postmenopausal osteoporosis. *Cochrane Database Syst Rev*, (2006) Cd005326.
111. P.J. Meunier, C. Roux, E. Seeman, S. Ortolani, J.E. Badurski, T.D. Spector, J. Cannata, A. Balogh, E.M. Lemmel, S. Pors-Nielsen, R. Rizzoli, H.K. Genant, J.Y. Reginster, The effects of strontium ranelate on the risk of vertebral fracture in women with postmenopausal osteoporosis. *N Engl J Med*, 350 (2004) 459-68.
112. G.M. Blake and I. Fogelman, Bone: Strontium ranelate does not have an anabolic effect on bone. *Nat Rev Endocrinol*, 9 (2013) 696-7.
113. P. Chavassieux, P.J. Meunier, J.P. Roux, N. Portero-Muzy, M. Pierre, R. Chapurlat, Bone histomorphometry of transiliac paired bone biopsies after 6 or 12 months of treatment with oral strontium ranelate in 387 osteoporotic women: randomized comparison to alendronate. *J Bone Miner Res*, 29 (2014) 618-28.
114. L.G.R. M. Kleerekoper . J.P. Bilezikian , G.A. Rodan *Principles of Bone Biology* 1996, San Diego Academic Press.
115. A. Richards, Nature and mechanisms of dental fluorosis in animals. *J Dent Res*, 69 (1990) 701-5; discussion 721.

116. A. Richards, J. Kragstrup, K. Josephsen, O. Fejerskov, Dental fluorosis developed in post-secretory enamel. *J Dent Res*, 65 (1986) 1406-9.
117. U. Kierdorf, H. Kierdorf, F. Sedlacek, O. Fejerskov, Structural changes in fluorosed dental enamel of red deer (*Cervus elaphus* L.) from a region with severe environmental pollution by fluorides. *Journal of Anatomy*, 188 (1996) 183-195.
118. M.J. Larsen, E. Kirkegaard, S. Poulsen, O. Fejerskov, Enamel Fluoride, Dental Fluorosis and Dental Caries among Immigrants to and Permanent Residents of Five Danish Fluoride Areas. *Caries Research*, 20 (1986) 349-355.
119. G. Suckling, D.C. Thurley, D.G. Nelson, The macroscopic and scanning electron-microscopic appearance and microhardness of the enamel, and the related histological changes in the enamel organ of erupting sheep incisors resulting from a prolonged low daily dose of fluoride. *Arch Oral Biol*, 33 (1988) 361-73.
120. S.M. Farley, J.E. Wergedal, L.C. Smith, M.W. Lundy, J.R. Farley, D.J. Baylink, Fluoride therapy for osteoporosis: characterization of the skeletal response by serial measurements of serum alkaline phosphatase activity. *Metabolism: clinical and experimental*, 36 (1987) 211-218.
121. S. Gabuda, A. Gaidash, S. Kozlova, N. Allan, Structural forms of fluorides in bone tissue of animals under chronic fluoride intoxication. *Journal of Structural Chemistry*, 47 (2006).
122. E.J. Mackie, Osteoblasts: novel roles in orchestration of skeletal architecture. *Int J Biochem Cell Biol*, 35 (2003) 1301-5.
123. D. Briancon and P.J. Meunier, Treatment of osteoporosis with fluoride, calcium, and vitamin D. *Orthop Clin North Am*, 12 (1981) 629-48.
124. N. Mamelle, P.J. Meunier, R. Dusan, M. Guillaume, J.L. Martin, A. Gaucher, A. Prost, G. Zeigler, P. Netter, Risk-benefit ratio of sodium fluoride treatment in primary vertebral osteoporosis. *Lancet*, 2 (1988) 361-5.
125. B.L. Riggs , S.F. Hodgson , W.M. O'Fallon , E.Y.S. Chao , H.W. Wahner , J.M. Muhs , S.L. Cedel , L.J.I. Melon Effect of Fluoride Treatment on the Fracture Rate in Postmenopausal Women with Osteoporosis. *New England Journal of Medicine*, 322 (1990) 802-809.
126. B.L. Riggs , E. Seeman , S.F. Hodgson , D.R. Taves , W.M. O'Fallon Effect of the Fluoride/Calcium Regimen on Vertebral Fracture Occurrence in Postmenopausal Osteoporosis. *New England Journal of Medicine*, 306 (1982) 446-450.
127. C.G. Bellows, J.N. Heersche, J.E. Aubin, The effects of fluoride on osteoblast progenitors in vitro. *J Bone Miner Res*, 5 (1990) S101-5.
128. W.J. Qu, D.B. Zhong, P.F. Wu, J.F. Wang, B. Han, Sodium fluoride modulates caprine osteoblast proliferation and differentiation. *J Bone Miner Metab*, 26 (2008) 328-34.
129. D. Burgener, J.P. Bonjour, J. Caverzasio, Fluoride increases tyrosine kinase activity in osteoblast-like cells: regulatory role for the stimulation of cell proliferation and Pi transport across the plasma membrane. *J Bone Miner Res*, 10 (1995) 164-71.
130. A. Okuda, J. Kanehisa, J.N. Heersche, The effects of sodium fluoride on the resorptive activity of isolated osteoclasts. *J Bone Miner Res*, 5 (1990) S115-20.
131. M.L. Taylor, E. Maconnachie, K. Frank, A. Boyde, S.J. Jones, The effect of fluoride on the resorption of dentine by osteoclasts In Vitro. *Journal of Bone and Mineral Research*, 5 (1990) S121-S130.
132. R.Z. Legeros, Calcium Phosphates in Oral Biology and Medicine. 1991, Basel, Switzerland Karger.
133. J.C. Elliot, D.W. Holcomb, R.A. Young, Infrared determination of the degree of substitution of hydroxyl by carbonate ions in human dental enamel. *Calcified Tissue International*, 37 (1985) 372-375.

134. C. Rey, B. Collins, T. Goehl, I.R. Dickson, M.J. Glimcher, The carbonate environment in bone mineral: a resolution-enhanced Fourier Transform Infrared Spectroscopy Study. *Calcif Tissue Int*, 45 (1989) 157-64.
135. R.Z. Legeros, O.R. Trautz, J.P. Legeros, E. Klein, W.P. Shirra, Apatite crystallites: effects of carbonate on morphology. *Science*, 155 (1967) 1409-11.
136. C. Massaro, M.A. Baker, F. Cosentino, P.A. Ramires, S. Klose, E. Milella, Surface and biological evaluation of hydroxyapatite-based coatings on titanium deposited by different techniques. *Journal of Biomedical Materials Research*, 58 (2001) 651-657.
137. G. Willmann, Coating of Implants with Hydroxyapatite – Material Connections between Bone and Metal. *Advanced Engineering Materials*, 1 (1999) 95-105.
138. G. Bonel, J.C. Heughebaert, M. Heughebaert, J.L. Lacout, A. Lebugle, Apatitic calcium orthophosphates and related compounds for biomaterials preparation. *Ann N Y Acad Sci*, 523 (1988) 115-30.
139. F. Barrere, P. Layrolle, C.A. van Blitterswijk, K. de Groot, Biomimetic calcium phosphate coatings on Ti6Al4V: a crystal growth study of octacalcium phosphate and inhibition by Mg<sup>2+</sup> and HCO<sub>3</sub>. *Bone*, 25 (1999) 107s-111s.
140. F. Barrere, C.A. van Blitterswijk, K. de Groot, P. Layrolle, Influence of ionic strength and carbonate on the Ca-P coating formation from SBFx5 solution. *Biomaterials*, 23 (2002) 1921-30.
141. S. Patntirapong, P. Habibovic, P.V. Hauschka, Effects of soluble cobalt and cobalt incorporated into calcium phosphate layers on osteoclast differentiation and activation. *Biomaterials*, 30 (2009) 548-55.
142. L. Yang, S. Perez-Amodio, F.Y. Barrere-de Groot, V. Everts, C.A. van Blitterswijk, P. Habibovic, The effects of inorganic additives to calcium phosphate on in vitro behavior of osteoblasts and osteoclasts. *Biomaterials*, 31 (2010) 2976-89.
143. T. Kokubo, H. Kushitani, Y. Abe, T. Yamamuro, Apatite coating on various substrates in simulated body fluids  
*Bioceramics*, 2 ( 1989) 235-242
144. H.W. Kim, Y.H. Koh, L.H. Li, S. Lee, H.E. Kim, Hydroxyapatite coating on titanium substrate with titania buffer layer processed by sol-gel method. *Biomaterials*, 25 (2004) 2533-8.
145. D.M. Liu, T. Troczynski, W.J. Tseng, Water-based sol-gel synthesis of hydroxyapatite: process development. *Biomaterials*, 22 (2001) 1721-30.
146. E.S. Thian, K.A. Khor, N.H. Loh, S.B. Tor, Processing of HA-coated Ti–6Al–4V by a ceramic slurry approach: an in vitro study. *Biomaterials*, 22 (2001) 1225-1232.
147. L. Cleries, J.M. Fernandez-Pradas, J.L. Morenza, Bone growth on and resorption of calcium phosphate coatings obtained by pulsed laser deposition. *J Biomed Mater Res*, 49 (2000) 43-52.
148. L. Cleries, J.M. Fernandez-Pradas, J.L. Morenza, Behavior in simulated body fluid of calcium phosphate coatings obtained by laser ablation. *Biomaterials*, 21 (2000) 1861-5.
149. J.M. Fernandez-Pradas, L. Cleries, E. Martinez, G. Sardin, J. Esteve, J.L. Morenza, Influence of thickness on the properties of hydroxyapatite coatings deposited by KrF laser ablation. *Biomaterials*, 22 (2001) 2171-5.
150. H. Ishizawa, M. Fujino, M. Ogino, Histomorphometric evaluation of the thin hydroxyapatite layer formed through anodization followed by hydrothermal treatment. *Journal of Biomedical Materials Research*, 35 (1997) 199-206.
151. H. Ishizawa and M. Ogino, Formation and characterization of anodic titanium oxide films containing Ca and P. *J Biomed Mater Res*, 29 (1995) 65-72.

152. H. Ishizawa and M. Ogino, Characterization of thin hydroxyapatite layers formed on anodic titanium oxide films containing Ca and P by hydrothermal treatment. *J Biomed Mater Res*, 29 (1995) 1071-9.
153. A. Ito, K. Ojima, H. Naito, N. Ichinose, T. Tateishi, Preparation, solubility, and cytocompatibility of zinc-releasing calcium phosphate ceramics. *J Biomed Mater Res*, 50 (2000) 178-83.
154. A. Bigi, E. Foresti, M. Gandolfi, M. Gazzano, N. Roveri, Isomorphous substitutions in  $\beta$ -tricalcium phosphate: The different effects of zinc and strontium. *Journal of Inorganic Biochemistry*, 66 (1997) 259-265.
155. A. Ito, H. Kawamura, M. Otsuka, M. Ikeuchi, H. Ohgushi, K. Ishikawa, K. Onuma, N. Kanzaki, Y. Sogo, N. Ichinose, Zinc-releasing calcium phosphate for stimulating bone formation. *Materials Science and Engineering: C*, 22 (2002) 21-25.
156. E. Jallot, J.M. Nedelec, A.S. Grimault, E. Chassot, A. Grandjean-Laquerriere, P. Laquerriere, D. Laurent-Maquin, STEM and EDXS characterisation of physico-chemical reactions at the periphery of sol-gel derived Zn-substituted hydroxyapatites during interactions with biological fluids. *Colloids Surf B Biointerfaces*, 42 (2005) 205-10.
157. Z.Y. Li, W.M. Lam, C. Yang, B. Xu, G.X. Ni, S.A. Abbah, K.M.C. Cheung, K.D.K. Luk, W.W. Lu, Chemical composition, crystal size and lattice structural changes after incorporation of strontium into biomimetic apatite. *Biomaterials*, 28 (2007) 1452-1460.
158. A. Balamurugan, G. Balossier, P. Torres, J. Michel, J.M.F. Ferreira, Sol-gel synthesis and spectrometric structural evaluation of strontium substituted hydroxyapatite. *Materials Science and Engineering: C*, 29 (2009) 1006-1009.
159. A.A. Belik, O.V. Yanov, B.I. Lazoryak, Synthesis and crystal structure of  $\text{Ca}_9\text{Cu}_{1.5}(\text{PO}_4)_7$  and reinvestigation of  $\text{Ca}_9.5\text{Cu}(\text{PO}_4)_7$ . *Materials Research Bulletin*, 36 (2001) 1863-1871.
160. M. Okazaki, Y. Miake, H. Tohda, T. Yanagisawa, T. Matsumoto, J. Takahashi, Functionally graded fluoridated apatites. *Biomaterials*, 20 (1999) 1421-6.
161. M. Okazaki, Y. Miake, H. Tohda, T. Yanagisawa, J. Takahashi, Fluoridated apatite synthesized using a multi-step fluoride supply system. *Biomaterials*, 20 (1999) 1303-7.
162. N. Bouslama, F. Ben Ayed, J. Bouaziz, Effect of fluorapatite additive on densification and mechanical properties of tricalcium phosphate. *J Mech Behav Biomed Mater*, 3 (2010) 2-13.
163. D.G. Nelson and J.D. Featherstone, Preparation, analysis, and characterization of carbonated apatites. *Calcif Tissue Int*, 34 (1982) S69-81.
164. M. Vignoles, G. Bonel, R.A. Young, Occurrence of nitrogenous species in precipitated B-type carbonated hydroxyapatites. *Calcif Tissue Int*, 40 (1987) 64-70.
165. Y. Doi, Y. Moriwaki, T. Aoba, M. Okazaki, J. Takahashi, K. Joshin, Carbonate apatites from aqueous and non-aqueous media studied by ESR, IR, and X-ray diffraction: effect of  $\text{NH}_4^+$  ions on crystallographic parameters. *J Dent Res*, 61 (1982) 429-34.
166. I.R. Gibson and W. Bonfield, Novel synthesis and characterization of an AB-type carbonate-substituted hydroxyapatite. *J Biomed Mater Res*, 59 (2002) 697-708.
167. E. Landi, A. Tampieri, G. Celotti, L. Vichi, M. Sandri, Influence of synthesis and sintering parameters on the characteristics of carbonate apatite. *Biomaterials*, 25 (2004) 1763-70.
168. P. Habibovic and J.E. Barralet, Bioinorganics and biomaterials: bone repair. *Acta Biomater*, 7 (2011) 3013-26.
169. J. Borovansky and P.A. Riley, Cytotoxicity of zinc in vitro. *Chem Biol Interact*, 69 (1989) 279-91.
170. S. Ni Shuilleabhain, C. Mothersill, D. Sheehan, N.M. O'Brien, O.H. J, F.N. Van Pelt, M. Davoren, In vitro cytotoxicity testing of three zinc metal salts using established fish cell lines. *Toxicol In Vitro*, 18 (2004) 365-76.

171. J.R. NILSSON, How Cytotoxic is Zinc? A Study on Effects of Zinc on Cell Proliferation, Endocytosis, and Fine Structure of the Ciliate Tetrahymena. *Acta Protozool*, 42 (2003) 19-29.
172. Y. Sogo, T. Sakurai, K. Onuma, A. Ito, The most appropriate (Ca+Zn)/P molar ratio to minimize the zinc content of ZnTCP/HAP ceramic used in the promotion of bone formation. *Journal of Biomedical Materials Research*, 62 (2002) 457-463.
173. X. Li, Y. Sogo, A. Ito, H. Mutsuzaki, N. Ochiai, T. Kobayashi, S. Nakamura, K. Yamashita, R.Z. LeGeros, The optimum zinc content in set calcium phosphate cement for promoting bone formation in vivo. *Materials science & engineering. C, Materials for biological applications*, 29 (2009) 969-975.
174. M. Schumacher, A. Lode, A. Helth, M. Gelinsky, A novel strontium(II)-modified calcium phosphate bone cement stimulates human-bone-marrow-derived mesenchymal stem cell proliferation and osteogenic differentiation in vitro. *Acta Biomater*, 9 (2013) 9547-57.
175. K. Er, Z.A. Polat, F. Ozan, T. Tasdemir, U. Sezer, S.H. Siso, Cytotoxicity analysis of strontium ranelate on cultured human periodontal ligament fibroblasts: a preliminary report. *J Formos Med Assoc*, 107 (2008) 609-15.
176. M. Schumacher and M. Gelinsky, Strontium modified calcium phosphate cements - approaches towards targeted stimulation of bone turnover. *Journal of Materials Chemistry B*, 3 (2015) 4626-4640.
177. D. Guo, K. Xu, X. Zhao, Y. Han, Development of a strontium-containing hydroxyapatite bone cement. *Biomaterials*, 26 (2005) 4073-83.
178. S.S. Singh, A. Roy, B.E. Lee, J. Ohodnicki, A. Loghmanian, I. Banerjee, P.N. Kumta, A study of strontium doped calcium phosphate coatings on AZ31. *Mater Sci Eng C Mater Biol Appl*, 40 (2014) 357-65.
179. C. Capuccini, P. Torricelli, F. Sima, E. Boanini, C. Ristoscu, B. Bracci, G. Socol, M. Fini, I.N. Mihailescu, A. Bigi, Strontium-substituted hydroxyapatite coatings synthesized by pulsed-laser deposition: In vitro osteoblast and osteoclast response. *Acta Biomaterialia*, 4 (2008) 1885-1893.
180. V. Gandin, A. Trenti, M. Porchia, F. Tisato, M. Giorgetti, I. Zanusso, L. Trevisi, C. Marzano, Homoleptic phosphino copper(i) complexes with in vitro and in vivo dual cytotoxic and anti-angiogenic activity. *Metallomics*, 7 (2015) 1497-1507.
181. C. Gerard, L.J. Bordeleau, J. Barralet, C.J. Doillon, The stimulation of angiogenesis and collagen deposition by copper. *Biomaterials*, 31 (2010) 824-31.
182. J. Barralet, U. Gbureck, P. Habibovic, E. Vorndran, C. Gerard, C.J. Doillon, Angiogenesis in calcium phosphate scaffolds by inorganic copper ion release. *Tissue Eng Part A*, 15 (2009) 1601-9.
183. H.W. Kim, H.E. Kim, J.C. Knowles, Fluor-hydroxyapatite sol-gel coating on titanium substrate for hard tissue implants. *Biomaterials*, 25 (2004) 3351-8.
184. H.W. Kim, Y.M. Kong, C.J. Bae, Y.J. Noh, H.E. Kim, Sol-gel derived fluor-hydroxyapatite biocoatings on zirconia substrate. *Biomaterials*, 25 (2004) 2919-26.
185. J. Li, Y. Song, S. Zhang, C. Zhao, F. Zhang, X. Zhang, L. Cao, Q. Fan, T. Tang, In vitro responses of human bone marrow stromal cells to a fluoridated hydroxyapatite coated biodegradable Mg-Zn alloy. *Biomaterials*, 31 (2010) 5782-8.
186. J. Wang, Y. Chao, Q. Wan, Z. Zhu, H. Yu, Fluoridated hydroxyapatite coatings on titanium obtained by electrochemical deposition. *Acta Biomaterialia*, 5 (2009) 1798-1807.
187. B.D. Hahn, Y.L. Cho, D.S. Park, J.J. Choi, J. Ryu, J.W. Kim, C.W. Ahn, C. Park, H.E. Kim, S.G. Kim, Effect of fluorine addition on the biological performance of hydroxyapatite coatings on Ti by aerosol deposition. *J Biomater Appl*, 27 (2013) 587-94.

188. Z. Tahmasebi Birgani, N. Gharraee, C.A. van Blitterswijk, P. Habibovic, Combinatorial incorporation of fluoride and cobalt ions into calcium phosphates to stimulate osteogenesis and angiogenesis. *Biomedical Materials*, 11 (2016) 015020.
189. B. Li, X. Chen, B. Guo, X. Wang, H. Fan, X. Zhang, Fabrication and cellular biocompatibility of porous carbonated biphasic calcium phosphate ceramics with a nanostructure. *Acta Biomater*, 5 (2009) 134-43.
190. S.A. Redey, S. Razzouk, C. Rey, D. Bernache-Assollant, G. Leroy, M. Nardin, G. Cournot, Osteoclast adhesion and activity on synthetic hydroxyapatite, carbonated hydroxyapatite, and natural calcium carbonate: Relationship to surface energies. *Journal of Biomedical Materials Research*, 45 (1999) 140-147.
191. S.A. Redey, M. Nardin, D. Bernache-Assollant, C. Rey, P. Delannoy, L. Sedel, P.J. Marie, Behavior of human osteoblastic cells on stoichiometric hydroxyapatite and type A carbonate apatite: role of surface energy. *J Biomed Mater Res*, 50 (2000) 353-64.
192. L.G. Ellies, J.M. Carter, J.R. Natiella, J.D. Featherstone, D.G. Nelson, Quantitative analysis of early in vivo tissue response to synthetic apatite implants. *J Biomed Mater Res*, 22 (1988) 137-48.
193. E. Landi, G. Celotti, G. Logroscino, A. Tampieri, Carbonated hydroxyapatite as bone substitute. *Journal of the European Ceramic Society*, 23 (2003) 2931-2937.
194. M. Hasegawa, Y. Doi, A. Uchida, Cell-mediated bioresorption of sintered carbonate apatite in rabbits. *J Bone Joint Surg Br*, 85 (2003) 142-7.
195. S. Bose, G. Fielding, S. Tarafder, A. Bandyopadhyay, Understanding of dopant-induced osteogenesis and angiogenesis in calcium phosphate ceramics. *Trends in Biotechnology*, 31 (2013) 594-605.
196. J.E. Barralet, S.M. Best, W. Bonfield, Effect of sintering parameters on the density and microstructure of carbonate hydroxyapatite. *Journal of Materials Science: Materials in Medicine*, 11 (2000) 719-724.
197. A. Cuneyt Tas, S.B. Bhaduri, S. Jalota, Preparation of Zn-doped  $\beta$ -tricalcium phosphate ( $\beta$ -Ca<sub>3</sub>(PO<sub>4</sub>)<sub>2</sub>) bioceramics. *Materials Science and Engineering: C*, 27 (2007) 394-401.
198. T.J. Webster, C. Ergun, R.H. Doremus, R. Bizios, Hydroxylapatite with substituted magnesium, zinc, cadmium, and yttrium. II. Mechanisms of osteoblast adhesion. *J Biomed Mater Res*, 59 (2002) 312-7.
199. A. Bandyopadhyay, E.A. Withey, J. Moore, S. Bose, Influence of ZnO doping in calcium phosphate ceramics. *Materials Science and Engineering: C*, 27 (2007) 14-17.
200. M. Ikeuchi, A. Ito, Y. Dohi, H. Ohgushi, H. Shimaoka, K. Yonemasu, T. Tateishi, Osteogenic differentiation of cultured rat and human bone marrow cells on the surface of zinc-releasing calcium phosphate ceramics. *Journal of Biomedical Materials Research Part A*, 67A (2003) 1115-1122.
201. S. Horiuchi, M. Hiasa, A. Yasue, K. Sekine, K. Hamada, K. Asaoka, E. Tanaka, Fabrications of zinc-releasing biocement combining zinc calcium phosphate to calcium phosphate cement. *Journal of the Mechanical Behavior of Biomedical Materials*, 29 (2014) 151-160.
202. Y. Huang, H. Zhang, H. Qiao, X. Nian, X. Zhang, W. Wang, X. Zhang, X. Chang, S. Han, X. Pang, Anticorrosive effects and in vitro cytocompatibility of calcium silicate/zinc-doped hydroxyapatite composite coatings on titanium. *Applied Surface Science*, 357, Part B (2015) 1776-1784.
203. Y. Yamada, A. Ito, M. Sakane, S. Miyakawa, T. Uemura, Laser microscopic measurement of osteoclastic resorption pits on biomaterials. *Materials Science and Engineering: C*, 27 (2007) 762-766.

204. Y. Yamada, A. Ito, H. Kojima, M. Sakane, S. Miyakawa, T. Uemura, R.Z. LeGeros, Inhibitory effect of Zn<sup>2+</sup> in zinc-containing beta-tricalcium phosphate on resorbing activity of mature osteoclasts. *J Biomed Mater Res A*, 84 (2008) 344-52.
205. H. Kawamura, A. Ito, S. Miyakawa, P. Layrolle, K. Ojima, N. Ichinose, T. Tateishi, Stimulatory effect of zinc-releasing calcium phosphate implant on bone formation in rabbit femora. *J Biomed Mater Res*, 50 (2000) 184-90.
206. G. Fielding and S. Bose, SiO<sub>2</sub> and ZnO dopants in three-dimensionally printed tricalcium phosphate bone tissue engineering scaffolds enhance osteogenesis and angiogenesis in vivo. *Acta Biomaterialia*, 9 (2013) 9137-9148.
207. X. Luo, D. Barbieri, N. Davison, Y. Yan, J.D. de Bruijn, H. Yuan, Zinc in calcium phosphate mediates bone induction: In vitro and in vivo model. *Acta Biomaterialia*, 10 (2014) 477-485.
208. Y. Huang, X. Zhang, R. Zhao, H. Mao, Y. Yan, X. Pang, Antibacterial efficacy, corrosion resistance, and cytotoxicity studies of copper-substituted carbonated hydroxyapatite coating on titanium substrate. *Journal of Materials Science*, 50 (2015) 1688-1700.
209. Y. Huang, X. Zhang, H. Mao, T. Li, R. Zhao, Y. Yan, X. Pang, Osteoblastic cell responses and antibacterial efficacy of Cu/Zn co-substituted hydroxyapatite coatings on pure titanium using electrodeposition method. *RSC Advances*, 5 (2015) 17076-17086.
210. O. Lysenko, O. Dubok, A. Borysenko, O. Shinkaruk, The biological properties of the silver- and copper-doped ceramic biomaterial. *Journal of Nanoparticle Research*, 17 (2015).
211. J. Christoffersen, M.R. Christoffersen, N. Kolthoff, O. Barenholdt, Effects of strontium ions on growth and dissolution of hydroxyapatite and on bone mineral detection. *Bone*, 20 (1997) 47-54.
212. W. Xue, J.L. Moore, H.L. Hosick, S. Bose, A. Bandyopadhyay, W.W. Lu, K.M. Cheung, K.D. Luk, Osteoprecursor cell response to strontium-containing hydroxyapatite ceramics. *J Biomed Mater Res A*, 79 (2006) 804-14.
213. S.J. Saint-Jean, C.L. Camire, P. Nevsten, S. Hansen, M.P. Ginebra, Study of the reactivity and in vitro bioactivity of Sr-substituted alpha-TCP cements. *J Mater Sci Mater Med*, 16 (2005) 993-1001.
214. H.W. Kim, Y.H. Koh, Y.M. Kong, J.G. Kang, H.E. Kim, Strontium substituted calcium phosphate biphasic ceramics obtained by a powder precipitation method. *J Mater Sci Mater Med*, 15 (2004) 1129-34.
215. Y. Huang, Y. Yan, X. Pang, Q. Ding, S. Han, Bioactivity and corrosion properties of gelatin-containing and strontium-doped calcium phosphate composite coating. *Applied Surface Science*, 282 (2013) 583-589.
216. W. Zhang, Y. Shen, H. Pan, K. Lin, X. Liu, B.W. Darvell, W.W. Lu, J. Chang, L. Deng, D. Wang, W. Huang, Effects of strontium in modified biomaterials. *Acta Biomaterialia*, 7 (2011) 800-808.
217. G.X. Ni, Z.P. Yao, G.T. Huang, W.G. Liu, W.W. Lu, The effect of strontium incorporation in hydroxyapatite on osteoblasts in vitro. *J Mater Sci Mater Med*, 22 (2011) 961-7.
218. E. Boanini, P. Torricelli, M. Fini, A. Bigi, Osteopenic bone cell response to strontium-substituted hydroxyapatite. *J Mater Sci Mater Med*, 22 (2011) 2079-88.
219. H. Zhou, S. Kong, Y. Pan, Z. Zhang, L. Deng, Microwave-assisted fabrication of strontium doped apatite coating on Ti6Al4V. *Mater Sci Eng C Mater Biol Appl*, 56 (2015) 174-80.
220. C.F. Marques, A. Lemos, S.I. Vieira, O.A.B. da Cruz e Silva, A. Bettencourt, J.M.F. Ferreira, Antibiotic-loaded Sr-doped porous calcium phosphate granules as multifunctional bone grafts. *Ceramics International*, 42 (2016) 2706-2716.
221. X. Wang, Y. Wang, L. Li, Z. Gu, H. Xie, X. Yu, Stimulations of strontium-doped calcium polyphosphate for bone tissue engineering to protein secretion and mRNA expression of the

- angiogenic growth factors from endothelial cells in vitro. *Ceramics International*, 40 (2014) 6999-7005.
222. C.T. Wong, W.W. Lu, W.K. Chan, K.M. Cheung, K.D. Luk, D.S. Lu, A.B. Rabie, L.F. Deng, J.C. Leong, In vivo cancellous bone remodeling on a strontium-containing hydroxyapatite (sr-HA) bioactive cement. *J Biomed Mater Res A*, 68 (2004) 513-21.
  223. U. Thormann, S. Ray, U. Sommer, T. Elkhassawna, T. Rehling, M. Hundgeburth, A. Henss, M. Rohnke, J. Janek, K.S. Lips, C. Heiss, G. Schlewitz, G. Szalay, M. Schumacher, M. Gelinsky, R. Schnettler, V. Alt, Bone formation induced by strontium modified calcium phosphate cement in critical-size metaphyseal fracture defects in ovariectomized rats. *Biomaterials*, 34 (2013) 8589-98.
  224. M. Baier, P. Staudt, R. Klein, U. Sommer, R. Wenz, I. Grafe, P.J. Meeder, P.P. Nawroth, C. Kasperk, Strontium enhances osseointegration of calcium phosphate cement: a histomorphometric pilot study in ovariectomized rats. *J Orthop Surg Res*, 8 (2013) 16.
  225. H. Xie, J. Wang, C. Li, Z. Gu, Q. Chen, L. Li, Application of strontium doped calcium polyphosphate bioceramic as scaffolds for bone tissue engineering. *Ceramics International*, 39 (2013) 8945-8954.
  226. Z. Gu, X. Zhang, L. Li, Q. Wang, X. Yu, T. Feng, Acceleration of segmental bone regeneration in a rabbit model by strontium-doped calcium polyphosphate scaffold through stimulating VEGF and bFGF secretion from osteoblasts. *Mater Sci Eng C Mater Biol Appl*, 33 (2013) 274-81.
  227. X. Luo, D. Barbieri, R. Duan, H. Yuan, J.D. Bruijn, Strontium-containing apatite/poly lactide composites enhance bone formation in osteopenic rabbits. *Acta Biomater*, 26 (2015) 331-7.
  228. G.M. Kuang, W.P. Yau, W.W. Lu, K.Y. Chiu, Local application of strontium in a calcium phosphate cement system accelerates healing of soft tissue tendon grafts in anterior cruciate ligament reconstruction: experiment using a rabbit model. *Am J Sports Med*, 42 (2014) 2996-3002.
  229. Y. Wang, S. Zhang, X. Zeng, L.L. Ma, W. Weng, W. Yan, M. Qian, Osteoblastic cell response on fluoridated hydroxyapatite coatings. *Acta Biomater*, 3 (2007) 191-7.
  230. H. Qu and M. Wei, The effect of fluoride contents in fluoridated hydroxyapatite on osteoblast behavior. *Acta Biomaterialia*, 2 (2006) 113-119.
  231. Y. Huang, Q. Ding, X. Pang, S. Han, Y. Yan, Corrosion behavior and biocompatibility of strontium and fluorine co-doped electrodeposited hydroxyapatite coatings. *Applied Surface Science*, 282 (2013) 456-462.
  232. J. Li, Y. Song, S. Zhang, C. Zhao, F. Zhang, X. Zhang, L. Cao, Q. Fan, T. Tang, In vitro responses of human bone marrow stromal cells to a fluoridated hydroxyapatite coated biodegradable Mg-Zn alloy. *Biomaterials*, 31 (2010) 5782-5788.
  233. Y. Shiwaku, T. Anada, H. Yamazaki, Y. Honda, S. Morimoto, K. Sasaki, O. Suzuki, Structural, morphological and surface characteristics of two types of octacalcium phosphate-derived fluoride-containing apatitic calcium phosphates. *Acta Biomater*, 8 (2012) 4417-25.
  234. M. Ohno, K. Kimoto, T. Toyoda, K. Kawata, H. Arakawa, Fluoride-treated bio-resorbable synthetic nonceramic [corrected] hydroxyapatite promotes proliferation and differentiation of human osteoblastic MG-63 cells. *J Oral Implantol*, 39 (2013) 154-60.
  235. M. Inoue, H. Nagatsuka, H. Tsujigiwa, M. Inoue, R.Z. LeGeros, T. Yamamoto, N. Nagai, In vivo effect of fluoride-substituted apatite on rat bone. *Dent Mater J*, 24 (2005) 398-402.
  236. M. Lalk, J. Reifenrath, N. Angrisani, A. Bondarenko, J.-M. Seitz, P.P. Mueller, A. Meyer-Lindenberg, Fluoride and calcium-phosphate coated sponges of the magnesium alloy AX30 as bone grafts: a comparative study in rabbits. *Journal of Materials Science: Materials in Medicine*, 24 (2012) 417-436.

237. A. Dekker, K. Reitsma, T. Beugeling, A. Bantjes, J. Feijen, W.G. van Aken, Adhesion of endothelial cells and adsorption of serum proteins on gas plasma-treated polytetrafluoroethylene. *Biomaterials*, 12 (1991) 130-8.
238. J.M. Schakenraad, H.J. Busscher, C.R. Wildevuur, J. Arends, Thermodynamic aspects of cell spreading on solid substrata. *Cell Biophys*, 13 (1988) 75-91.
239. T.G. van Kooten, J.M. Schakenraad, H.C. van der Mei, H.J. Busscher, Influence of substratum wettability on the strength of adhesion of human fibroblasts. *Biomaterials*, 13 (1992) 897-904.
240. S. Kannan, S.I. Vieira, S.M. Olhero, P.M. Torres, S. Pina, O.A. da Cruz e Silva, J.M. Ferreira, Synthesis, mechanical and biological characterization of ionic doped carbonated hydroxyapatite/beta-tricalcium phosphate mixtures. *Acta Biomater*, 7 (2011) 1835-43.
241. H.W. Tong, M. Wang, Z.Y. Li, W.W. Lu, Electrospinning, characterization and in vitro biological evaluation of nanocomposite fibers containing carbonated hydroxyapatite nanoparticles. *Biomed Mater*, 5 (2010) 054111.
242. A. Rupani, L.A. Hidalgo-Bastida, F. Rutten, A. Dent, I. Turner, S. Cartmell, Osteoblast activity on carbonated hydroxyapatite. *J Biomed Mater Res A*, 100 (2012) 1089-96.
243. Y. Doi, H. Iwanaga, T. Shibutani, Y. Moriwaki, Y. Iwayama, Osteoclastic responses to various calcium phosphates in cell cultures. *Journal of Biomedical Materials Research*, 47 (1999) 424-433.
244. R.E. Anderson, W.S. Jee, D.M. Woodbury, Stimulation of carbonic anhydrase in osteoclasts by parathyroid hormone. *Calcif Tissue Int*, 37 (1985) 646-50.
245. G. Spence, N. Patel, R. Brooks, W. Bonfield, N. Rushton, Osteoclastogenesis on hydroxyapatite ceramics: The effect of carbonate substitution. *Journal of Biomedical Materials Research Part A*, 92A (2010) 1292-1300.
246. P. Habibovic, M.V. Juhl, S. Clyens, R. Martinetti, L. Dolcini, N. Theilgaard, C.A. van Blitterswijk, Comparison of two carbonated apatite ceramics in vivo. *Acta Biomater*, 6 (2010) 2219-26.
247. L. Borkowski, M. Pawlowska, R.P. Radzki, M. Bienko, I. Polkowska, A. Belcarz, M. Karpinski, T. Slowik, L. Matuszewski, A. Slosarczyk, G. Ginalska, Effect of a carbonated HAP/beta-glucan composite bone substitute on healing of drilled bone voids in the proximal tibial metaphysis of rabbits. *Mater Sci Eng C Mater Biol Appl*, 53 (2015) 60-7.
248. M. Yoshioka, K. Tanimoto, Y. Tanne, K. Sumi, T. Awada, N. Oki, M. Sugiyama, Y. Kato, K. Tanne, Bone regeneration in artificial jaw cleft by use of carbonated hydroxyapatite particles and mesenchymal stem cells derived from iliac bone. *Int J Dent*, 2012 (2012) 352510.
249. M. Li, X. Xiao, R. Liu, C. Chen, L. Huang, Structural characterization of zinc-substituted hydroxyapatite prepared by hydrothermal method. *J Mater Sci Mater Med*, 19 (2008) 797-803.
250. F. Ren, R. Xin, X. Ge, Y. Leng, Characterization and structural analysis of zinc-substituted hydroxyapatites. *Acta Biomaterialia*, 5 (2009) 3141-3149.
251. S. Kannan, F. Goetz-Neunhoffer, J. Neubauer, J.M.F. Ferreira, Ionic Substitutions in Biphasic Hydroxyapatite and  $\beta$ -Tricalcium Phosphate Mixtures: Structural Analysis by Rietveld Refinement. *Journal of the American Ceramic Society*, 91 (2008) 1-12.
252. A. Ito, H. Kawamura, S. Miyakawa, P. Layrolle, N. Kanzaki, G. Treboux, K. Onuma, S. Tsutsumi, Resorbability and solubility of zinc-containing tricalcium phosphate. *J Biomed Mater Res*, 60 (2002) 224-31.
253. T.J. Webster, E.A. Massa-Schlueter, J.L. Smith, E.B. Slamovich, Osteoblast response to hydroxyapatite doped with divalent and trivalent cations. *Biomaterials*, 25 (2004) 2111-21.
254. A. Ito, H. Kawamura, S. Miyakawa, P. Layrolle, R. Aomori, S. Tsutsumi, Resorbability Reduction by the Incorporation of Zinc into Tricalcium Phosphate. *Key Engineering Materials*, 199 (2001) 192-195.

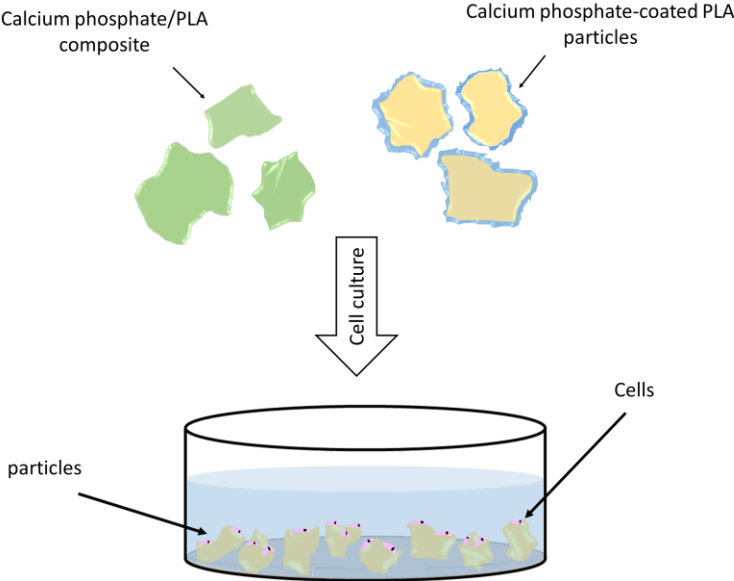
255. I. Mayer and J.D.B. Featherstone, Dissolution studies of Zn-containing carbonated hydroxyapatites. *Journal of Crystal Growth*, 219 (2000) 98-101.
256. R.D. Shannon and C.T. Prewitt, Effective ionic radii in oxides and fluorides. *Acta Crystallographica Section B*, 25 (1969) 925-946.
257. I. Gutowska, Z. Machoy, B. Machaliński, The role of bivalent metals in hydroxyapatite structures as revealed by molecular modeling with the HyperChem software. *Journal of Biomedical Materials Research Part A*, 75A (2005) 788-793.
258. S. Kannan, S. Pina, J.M.F. Ferreira, Formation of Strontium-Stabilized  $\beta$ -Tricalcium Phosphate from Calcium-Deficient Apatite. *Journal of the American Ceramic Society*, 89 (2006) 3277-3280.
259. X. Wang and J. Ye, Variation of crystal structure of hydroxyapatite in calcium phosphate cement by the substitution of strontium ions. *J Mater Sci Mater Med*, 19 (2008) 1183-6.
260. T. Aoba, The effect of fluoride on apatite structure and growth. *Crit Rev Oral Biol Med*, 8 (1997) 136-53.
261. M.H. Fathi and E.M. Zahrani, Fabrication and characterization of fluoridated hydroxyapatite nanopowders via mechanical alloying. *Journal of Alloys and Compounds*, 475 (2009) 408-414.
262. Y. Chen and X. Miao, Thermal and chemical stability of fluorohydroxyapatite ceramics with different fluorine contents. *Biomaterials*, 26 (2005) 1205-10.
263. L.M. Rodriguez-Lorenzo, J.N. Hart, K.A. Gross, Influence of fluorine in the synthesis of apatites. Synthesis of solid solutions of hydroxy-fluorapatite. *Biomaterials*, 24 (2003) 3777-85.
264. K. Cheng, W. Weng, H. Wang, S. Zhang, In vitro behavior of osteoblast-like cells on fluoridated hydroxyapatite coatings. *Biomaterials*, 26 (2005) 6288-95.
265. M.I. Kay, R.A. Young, A.S. Posner, Crystal Structure of Hydroxyapatite. *Nature*, 204 (1964) 1050-1052.
266. J. Harrison, A.J. Melville, J.S. Forsythe, B.C. Muddle, A.O. Trounson, K.A. Gross, R. Mollard, Sintered hydroxyfluorapatites--IV: The effect of fluoride substitutions upon colonisation of hydroxyapatites by mouse embryonic stem cells. *Biomaterials*, 25 (2004) 4977-86.
267. R. Legeros, Apatites in Biological Systems. *Progressive Crystal Growth Characterization*, 4 (1981) 1-45
268. A.A. Baig, J.L. Fox, R.A. Young, Z. Wang, J. Hsu, W.I. Higuchi, A. Chhetry, H. Zhuang, M. Otsuka, Relationships among carbonated apatite solubility, crystallite size, and microstrain parameters. *Calcif Tissue Int*, 64 (1999) 437-49.
269. S. Bose, G. Fielding, S. Tarafder, A. Bandyopadhyay, Trace element doping in calcium phosphate ceramics to Understand osteogenesis and angiogenesis. *Trends in biotechnology*, 31 (2013) 10.1016/j.tibtech.2013.06.005.
270. S. Bose, S. Tarafder, S.S. Banerjee, N.M. Davies, A. Bandyopadhyay, Understanding in vivo response and mechanical property variation in MgO, SrO and SiO<sub>2</sub> doped beta-TCP. *Bone*, 48 (2011) 1282-90.
271. B. Badraoui, A. Aissa, A. Bigi, M. Debbabi, M. Gazzano, Synthesis and characterization of Sr(10-x)Cdx(PO<sub>4</sub>)<sub>6</sub>Y<sub>2</sub> (Y = OH and F): A comparison of apatites containing two divalent cations. *Materials Research Bulletin*, 44 (2009) 522-530.
272. M.S. Sader, K. Lewis, G.A. Soares, R.Z. LeGeros, Simultaneous incorporation of magnesium and carbonate in apatite: effect on physico-chemical properties. *Materials Research*, 16 (2013) 779-784.
273. F. Yao, J.P. LeGeros, R.Z. LeGeros, Simultaneous incorporation of carbonate and fluoride in synthetic apatites: Effect on crystallographic and physico-chemical properties. *Acta Biomaterialia*, 5 (2009) 2169-2177.

274. S. Tarafder, N.M. Davies, A. Bandyopadhyay, S. Bose, 3D printed tricalcium phosphate scaffolds: Effect of SrO and MgO doping on osteogenesis in a rat distal femoral defect model. *Biomater Sci*, 1 (2013) 1250-1259.
275. S. Bodhak, S. Bose, A. Bandyopadhyay, Influence of MgO, SrO, and ZnO Dopants on Electro-Thermal Polarization Behavior and In Vitro Biological Properties of Hydroxyapatite Ceramics. *Journal of the American Ceramic Society*, 94 (2011) 1281-1288.
276. F. Yao and J.P. LeGeros, Carbonate and fluoride incorporation in synthetic apatites: Comparative effect on physico-chemical properties and in vitro bioactivity in fetal bovine serum. *Materials Science and Engineering C*, 30 (2010) 423-430.
277. M. Roy, G. Fielding, A. Bandyopadhyay, S. Bose, Effects of Zinc and Strontium Substitution in Tricalcium Phosphate on Osteoclast Differentiation and Resorption. *Biomater Sci*, 1 (2013) 74-82.
278. H. Zreiqat, Y. Ramaswamy, C. Wu, A. Paschalidis, Z. Lu, B. James, O. Birke, M. McDonald, D. Little, C.R. Dunstan, The incorporation of strontium and zinc into a calcium-silicon ceramic for bone tissue engineering. *Biomaterials*, 31 (2010) 3175-84.
279. X. Yang, L. Zhang, X. Chen, G. Yang, L. Zhang, C. Gao, H. Yang, Z. Gou, Trace element-incorporating octacalcium phosphate porous beads via polypeptide-assisted nanocrystal self-assembly for potential applications in osteogenesis. *Acta Biomater*, 8 (2012) 1586-96.
280. M.J. Dalby, N. Gadegaard, R. Tare, A. Andar, M.O. Riehle, P. Herzyk, C.D.W. Wilkinson, R.O.C. Oreffo, The control of human mesenchymal cell differentiation using nanoscale symmetry and disorder. *Nat Mater*, 6 (2007) 997-1003.
281. M. Estevez, E. Martinez, S.J. Yarwood, M.J. Dalby, J. Samitier, Adhesion and migration of cells responding to microtopography. *J Biomed Mater Res A*, 103 (2015) 1659-68.
282. A. Wilkinson, R.N. Hewitt, L.E. McNamara, D. McCloy, R.M. Dominic Meek, M.J. Dalby, Biomimetic microtopography to enhance osteogenesis in vitro. *Acta Biomater*, 7 (2011) 2919-25.
283. J. Yang, L.E. McNamara, N. Gadegaard, E.V. Alakpa, K.V. Burgess, R.M. Meek, M.J. Dalby, Nanotopographical induction of osteogenesis through adhesion, bone morphogenic protein cosignaling, and regulation of microRNAs. *ACS Nano*, 8 (2014) 9941-53.
284. J.R. Wang, S.F. Ahmed, N. Gadegaard, R.M. Meek, M.J. Dalby, S.J. Yarwood, Nanotopology potentiates growth hormone signalling and osteogenesis of mesenchymal stem cells. *Growth Horm IGF Res*, 24 (2014) 245-50.
285. D. Nadeem, C.A. Smith, M.J. Dalby, R.M. Meek, S. Lin, G. Li, B. Su, Three-dimensional CaP/gelatin lattice scaffolds with integrated osteoinductive surface topographies for bone tissue engineering. *Biofabrication*, 7 (2015) 015005.
286. C. Danoux, L. Sun, G. Kocer, Z.T. Birgani, D. Barata, J. Barralet, C. van Blitterswijk, R. Truckenmuller, P. Habibovic, Development of Highly Functional Biomaterials by Decoupling and Recombining Material Properties. *Adv Mater*, 28 (2016) 1803-8.
287. Z. Tahmasebi Birgani, B.J. Klotz, C.A. van Blitterswijk, P. Habibovic, Poly(lactic acid) microspheres for local delivery of bioinorganics for applications in bone regeneration. *Advanced Biomaterials and Devices in Medicine*, 1 (2014) 1-10.
288. B. Harink, S. Le Gac, D. Barata, C. van Blitterswijk, P. Habibovic, Microfluidic platform with four orthogonal and overlapping gradients for soluble compound screening in regenerative medicine research. *Electrophoresis*, 36 (2015) 475-84.
289. B. Harink, S. Le Gac, R. Truckenmuller, C. van Blitterswijk, P. Habibovic, Regeneration-on-a-chip? The perspectives on use of microfluidics in regenerative medicine. *Lab Chip*, 13 (2013) 3512-28.

290. B. Harink, S. Le Gac, D. Barata, C. van Blitterswijk, P. Habibovic, Microtiter plate-sized standalone chip holder for microenvironmental physiological control in gas-impermeable microfluidic devices. *Lab Chip*, 14 (2014) 1816-20.
291. Y. Mei, M. Goldberg, D. Anderson, The development of high-throughput screening approaches for stem cell engineering. *Curr Opin Chem Biol*, 11 (2007) 388-93.
292. Y. Xu, Y. Shi, S. Ding, A chemical approach to stem-cell biology and regenerative medicine. *Nature*, 453 (2008) 338-44.
293. D. Barata, C. van Blitterswijk, P. Habibovic, High-throughput screening approaches and combinatorial development of biomaterials using microfluidics. *Acta Biomater*, (2015).
294. L.I. Zon and R.T. Peterson, In vivo drug discovery in the zebrafish. *Nat Rev Drug Discov*, 4 (2005) 35-44.
295. E.M. Wielhouwer, S. Ali, A. Al-Afandi, M.T. Blom, M.B. Olde Riekerink, C. Poelma, J. Westerweel, J. Oonk, E.X. Vrouwe, W. Buesink, H.G.J. vanMil, J. Chicken, R. van 't Oever, M.K. Richardson, Zebrafish embryo development in a microfluidic flow-through system. *Lab on a Chip*, 11 (2011) 1815-1824.

# Chapter 3

## Monolithic calcium phosphate/poly(lactic acid) composite versus calcium phosphate-coated poly(lactic acid) for support of osteogenic differentiation of human mesenchymal stromal cells



## Abstract

Calcium phosphates (CaPs), extensively used synthetic bone graft substitutes, are often combined with other materials with the aim to overcome issues related to poor mechanical properties of most CaP ceramics. Thin ceramic coatings on metallic implants and polymer-ceramic composites are examples of such hybrid materials. Both the properties of the CaP used and the method of incorporation into a hybrid structure are determinant for the bioactivity of the final construct. In the present study, a monolithic composite comprising nano-sized CaP and poly(lactic acid) (PLA) and a CaP-coated PLA were comparatively investigated for their ability to support proliferation and osteogenic differentiation of bone marrow-derived human mesenchymal stromal cells (hMSCs). Both, the PLA/CaP composite, produced using physical mixing and extrusion and CaP-coated PLA, resulting from a biomimetic coating process at near-physiological conditions, supported proliferation of hMSCs with highest rates at PLA/CaP composite. Enzymatic alkaline phosphatase (ALP) activity as well as the mRNA expression of bone morphogenetic protein-2 (BMP2), osteopontin (OP) and osteocalcin (OC) were higher on the composite and coated polymer as compared to the PLA control, while no significant differences were observed between the two methods of combining CaP and PLA. The results of this study confirmed the importance of CaP in osteogenic differentiation while the exact properties and the method of incorporation into the hybrid material played a less prominent role.

### 3.1. Introduction

To overcome issues related to the use of natural bone grafts [1-2] and to satisfy a rapidly increasing need for successful and affordable strategies to treat damaged and diseased bone tissue [2-3], significant efforts are currently invested in developing synthetic alternatives to natural bone. While all three main material types, i.e. metals, ceramics and polymers, as well as their combinations have been used as bone graft substitutes, calcium phosphate (CaP) ceramics, varying in chemistry (hydroxyapatite, tricalcium phosphate, brushite, octacalcium phosphate, etc.) [4] and mode of application (sintered bulk ceramics, particles, injectable cements, etc.) [5-6] are the most widely used materials, owing to their chemical resemblance to bone mineral [7]. CaPs possess excellent biocompatibility in osseous environment [1-2, 5, 8], and more importantly, they are generally accepted as osteoconductive materials [9-10], with a subpopulation even being osteoinductive [11-13]. CaPs, however, suffer from intrinsic brittleness, which is an important limiting factor, particularly in load-bearing applications [14-15]. To overcome this issue, CaP ceramics have been combined with other materials, in particular polymers, in the bulk [14-25] or as surface coatings [8, 26]. For example, CaPs have been used to develop monolithic composites with poly( $\alpha$ -esters) such as poly(lactic acid) (PLA), poly(glycolic acid) (PGA) and their copolymers (PLGA) [17-20], protein based polymers including collagen [21] and gelatin [22-23], polysaccharides like chitosan [24] as well as synthetic co-polymers such as poly(ethylene oxide terephthalate)/poly(butylene terephthalate) (PEOT-PBT) [25]. Alternatively to conventional composites, physical assembly of the individual components [25] has been used to develop polymer-ceramic hybrids. Concerning coating techniques, classical methods for coating CaPs on substrates, such as plasma-spraying, have mainly been used to coat non-degradable permanent metallic implants to improve their bioactivity [8, 26, 27-29], for example in total hip arthroplasty. Nevertheless, examples of more subtle coating techniques exist, which are suitable for coating thermally less stable materials including polymers, such as biomimetic coating process [30-32], radio frequency (RF) magnetron sputtering [33], or pulse laser deposition [34].

Properties of a hybrid material, as well as its biological performance, are dependent on the properties of each of the components, as well as on the way they are combined. For example, degradation of a CaP/polymer composite depends on the physico-chemical properties of the ceramic (CaP phase, crystallinity, surface area, etc.), physico-chemical properties of the polymer

(composition, molecular weight, level of crosslinking etc.) as well as the way they are integrated into the final product (solvent-based mixing, physical mixing, coating, etc.).

In the current study, we hypothesized that direct contact between the CaP component of a CaP/polymer hybrid material and the biological environment is beneficial for the bioactivity of the hybrid. To test this, we have produced PLA particles and coated them with a thin layer of CaP by immersion into a saturated CaP solution, and compared them to composite particles produced by the extrusion of a PLA/nano-sized CaP mixture. Upon characterization of both particle types, bone marrow-derived human mesenchymal stromal cells (hMSCs) were cultured with the two materials, followed by the assessment of their proliferation and differentiation towards the osteogenic lineage.

## **3.2. Materials and Methods**

### **3.2.1. Materials production**

For this study, two hybrid materials consisting of CaP and PLA were produced: a monolithic composite PLA/CaP composite and a CaP-coated PLA. PLA without CaP served as control. The composite consisted of 50 wt.% amorphous poly(D,L-lactic acid) (PLA) (Purasorb PDL05, Purac, MW: 59000 g/mole) and 50 wt.% in-house produced nano-sized CaP apatite powder, prepared using a wet precipitation method as was described previously [18-20]. Briefly, the HA was precipitated in a mixture of aqueous solutions of  $(\text{NH}_4)_2\text{HPO}_4$  and  $\text{Ca}(\text{NO}_3)_2 \cdot 4\text{H}_2\text{O}$  at a pH above 10. The resulting precipitate was allowed to age overnight, washed and finally resuspended in acetone and allowed to dry. The composite was produced by extrusion using a twin-screw extruder with conical non-converging screws (Artecs BV, Enschede, The Netherlands). The PLA and CaP powder were mixed for 5 minutes in the extruder at 150 °C using the screw rotation speed of 100 rpm. The composite was extruded in the form of rods, which were ground and sieved to obtain composite particles in the range of 0.5-1 mm.

PLA particles were obtained using the same procedure of extrusion, grinding and sieving as described above for the PLA/CaP composite. The particles were either left uncoated or were coated with a CaP layer via a two-step biomimetic method similar to the one described earlier [35-36]. In short, the particles were first immersed in a concentrated Simulated Body Fluid (SBF 2.5x) with ionic content of 733.5 mM  $\text{Na}^{2+}$ , 7.5 mM  $\text{Mg}^{2+}$ , 12.5 mM  $\text{Ca}^{2+}$ , 720 mM  $\text{Cl}^-$ , 5 mM  $\text{HPO}_4^{2-}$  and 21

mM  $\text{HCO}_3^-$ , under stirring at 37 °C for three days, with daily refreshment. In the second step, the particles were incubated with a calcium phosphate solution (CPS) consisting of 140 mM  $\text{Na}^{2+}$ , 4 mM  $\text{Ca}^{2+}$ , 2 mM  $\text{HPO}_4^{2-}$  and 144 mM  $\text{Cl}^-$  (buffered at pH 7.4), while stirring at 37 °C for three days with two refreshments. The coated PLA particles were then washed three times with MilliQ water and dried at least overnight in an air oven at 37° C.

### 3.2.2. Material characterization

The surface morphology and elemental analysis of calcium, phosphorous and carbon were investigated on gold-sputtered PLA, PLA/CaP composite and CaP-coated PLA particles using scanning electron microscopy (SEM, XL-30 ESEM-FEG, Philips) in the secondary electron mode, coupled with energy dispersive X-ray spectroscopy analyzer (EDS, EDAX, AMETEK Materials Analysis Division) at the accelerator voltage of 10 KeV and working distance of 10 mm. The chemical composition of various particles was characterized using Fourier transform infrared spectroscopy (FTIR, Perkin-Elmer Spectrum 1000) in transmission mode and x-ray diffraction method (XRD, PANalytical X'Pert). Thermogravimetric analysis (TGA, STA 449 F3, NETZSCH) was performed in the temperature range of 35-1000 °C and the weight loss was calculated to determine the mineral content. The release of  $\text{Ca}^{2+}$  and inorganic phosphate (Pi) ions from different particles was analyzed in simulated physiological solution (SPS) containing 137 mmol/L  $\text{Na}^+$ , 177 mmol/L  $\text{Cl}^-$ , 50 mmol/L HEPES in MilliQ water and buffered at pH 7.3 over a period of three months.  $100 \pm 1$  mg of PLA, PLA/CaP composite or CaP-coated PLA particles were precisely weighed and immersed in 5 ml SPS in plastic tubes. The tubes were then placed in a shaking water bath at 37°C. At dedicated time points between 1 and 12 weeks, triplicates of each sample were removed from water bath and  $\text{Ca}^{2+}$  and Pi ion content of SPS was quantified using QuantiChrom™ Calcium assay kit (DICA-500, BioAssay Systems, USA) and QuantiChrom™ Phosphate assay kit (DIPI-500 BioAssay Systems, USA), respectively, according to manufacturer's protocols.

### 3.2.3. In vitro cell culture

hMSCs were isolated from bone marrow aspirates (5–20 ml) after written informed consent, as described previously [37-38]. Briefly, aspirates were resuspended using 20-gauge needles, plated at a density of  $5 \times 10^5$  cells per  $\text{cm}^2$ ,

and cultured in proliferation medium (consisting of  $\alpha$ -MEM (Gibco) supplemented with 10 v/v% fetal bovine serum (Lonza), 2 mM L-glutamine (Gibco), 0.2 mM ascorbic acid (Sigma), 62.69  $\mu\text{g}\cdot\text{ml}^{-1}$  penicillin, 100  $\mu\text{g}\cdot\text{ml}^{-1}$  streptomycin (Gibco) and 1  $\text{ng}\cdot\text{ml}^{-1}$  rhbFGF (AbDSerotec)). The medium was refreshed every 2-3 days. Cells were harvested at approximately 80% confluency for subculture until passage 3.

In an earlier study, hMSCs that were isolated and expanded using this method were shown to be positive for CD29, CD44, CD105, and CD166 which are typical markers of hMSCs, and to possess the potential to differentiate into the osteogenic lineage in vitro and to induce new bone formation in vivo [38].

Approximately 100  $\mu\text{l}$  of particles were placed in the wells of non-plasma treated 25-well plates with square-shaped bottom and sterilized with isopropanol prior to cell culture. To sterilize, the samples were washed three times with 100% isopropanol followed by 15 min of drying inside the flow cabinet after each washing step. In the last step of sterilization, 100% isopropanol was added to the samples and allowed to evaporate in the flow cabinet for at least 2 hours. The samples were then washed twice with sterile PBS, followed by an overnight incubation in 1 ml basic medium (proliferation medium without rhbFGF) in a humidified atmosphere at 37°C and 5% CO<sub>2</sub>.

The particles were then collected in one corner of the wells and 200000 hMSCs of passage 3 were seeded on the particles in approximately 50  $\mu\text{l}$  of basic cell culture medium. This seeding method and density were optimized based on a preliminary study (data not shown). To maximize the attachment of the cells on the particles, the wells were tilted and cells were allowed to attach for 4 hours. 1 ml of either basic medium or osteogenic medium (basic medium supplemented with 10 nM dexamethasone (Sigma)) was added to each well. The medium was refreshed every 3-4 days. Old medium was collected at each refreshment and the concentration of Ca<sup>2+</sup> was determined using QuantiChrom™ calcium assay kit.

Total DNA amount was assessed with CyQuant Cell Proliferation Assay kit (Invitrogen) at day 7 and 14 after washing the samples with PBS. After 3 freeze/thaw cycles at -80° C, 500  $\mu\text{l}$  lysis buffer (lysis buffer provided in the kit diluted in a buffer of NaCl-EDTA solution) was added to each well. The samples were ultra-sonicated and incubated at RT for 1 hour. After centrifugation, 100  $\mu\text{l}$  of the supernatant was mixed with the same volume of CyQuant GR dye in a 96 well micro-plate and incubated for 15 minutes. Fluorescence measurements for DNA quantification were performed at excitation and emission wavelengths of

480 and 520 nm, respectively, using a spectrophotometer (Perkin Elmer). ALP activity in the cultures was measured using a CDP-star kit (Roche Applied Science). 10  $\mu$ l of the supernatant was mixed with 40  $\mu$ l CDP-star reagent in a 96 well micro-plate and incubated for 30 min. After incubation, chemiluminescence measurements were completed at 466 nm. Results of the DNA assays are presented based on average  $\mu$ g of DNA detected in each condition. Results of ALP activity were normalized for DNA content of each culture and presented as the average of normalized ALP activity per  $\mu$ g of DNA for each condition.

Total RNA was isolated by using a combination of NucleoSpin<sup>®</sup> RNA II isolation kit and Trizol method, in accordance with the manufacturer's protocol. RNA was collected in RNase-free water and the total concentration was measured using nano-drop equipment (ND1000 spectrophotometer, Thermo Scientific). The cDNA of the cultures were then prepared using iScript kit (Bio-Rad) according to the manufacturer's protocol and diluted 10 times in RNase-free water to be used for quantitative real-time PCR (qPCR). The qPCR measurements were completed using Bio-Rad equipment using Syber green I master mix (Invitrogen) and the primer sequences (Sigma), which are listed in table 1. Expression of the osteogenic marker genes was normalized to GAPDH levels and fold induction was calculated by using the  $\Delta\Delta$ CT method. mRNA level of the desired genes in hMSCs cultured on treated tissue culture plates (TCPs) at the density of 10000 cells/cm<sup>2</sup> in basic cell culture medium for 7 days was also quantified and used for normalizing the results.

#### **3.2.4. Statistical analysis**

Statistical comparisons were performed using One-way Analysis of Variance (ANOVA) followed by a Tukey's multiple comparison post-hoc test. Error bars indicate one standard deviation. The level of significance was set at  $p < 0.05$ .

### **3.3. Results**

#### **3.3.1. Characterization of the hybrid materials**

Particles of both pure PLA and of the two hybrid materials were dense with an irregular shape and with a size ranging between 0.5 and 1 mm (Figure. 1. a1 – 1. c1). While the surface of pure PLA appeared smooth (Figure. 1. b1), PLA/CaP composite particles exhibited a more rough surface structure (Figure. 1. b2). CaP-

coated PLA particles were homogenously covered with a coating consisting of small plate-shaped crystals, giving it a rough surface morphology (Figure. 1. b3). The EDS spectrum of PLA particles exhibited only carbon (C) and oxygen (O) peaks (Figure. 1. a3). A reduction in the intensity of C peak was observed in the EDS spectra of both PLA/CaP composite and CaP-coated PLA particles whereas the intensity of the O peak increased in these samples. Moreover, the EDS spectra of the two hybrid materials exhibited calcium and phosphorus peaks, demonstrating the presence of a CaP phase in these samples (Figure. 1. b3-c3). The EDS elemental maps confirmed these results (Figure. 1. a4-c6). A uniform distribution of calcium and phosphorus were observed in the elemental maps of composite and coated PLA particles showing a homogenous distribution of CaP in the polymer matrix and a uniform surface coating, respectively.

Table 1. Primer sequences of the osteogenic genes, the expression of which was investigated using qPCR analysis.

Gene	Primer sequences
GAPDH (housekeeping gene)	5'-CCATGGTGTCTGAGCGATGT 5'-CGCTCTCTGCTCCTCCTGTT
Alkaline phosphatase (ALP)	5'-TTCAGCTCGTACTGCATGTC 5'-ACAAGCACTCCCCTTCATC
Runt-related transcription factor 2 (RUNX2)	5'-GGAGTGGACGAGGCAAGAGTTT 5'-AGCTTCTGTCTGTGCCTTCTGG
Bone sialoprotein (BSP)	5'-TCCCCTTCTCACTTTCATA 5'-CCCCACCTTTTGGGAAAAC
Bone morphogenetic protein 2 (BMP2)	5'-GCATCTGTTCTCGGAAAACCT 5'-ACTACCAGAAACGAGTGGGAA
Osteopontin (OP)	5'-CCAAGTAAGTCCAACGAAAG 5'-GGTGATGCCTCGTCTGTA
Osteocalcin (OC)	5'-CGCTGGGTCTTTCACTAC 5'-TGAGAGCCCTCACACTCCTC

The FTIR spectra and the XRD patterns of the PLA, PLA/CaP composite and CaP-coated PLA are shown in Figure. 2. The spectrum of PLA showed peaks at approximately  $1000-1100\text{ cm}^{-1}$ , corresponding to stretching mode of C-O bond. The peaks of C-H bond in bending and stretching modes were observed at approximately  $1370-1450$  and  $1950-2000\text{ cm}^{-1}$ , respectively.

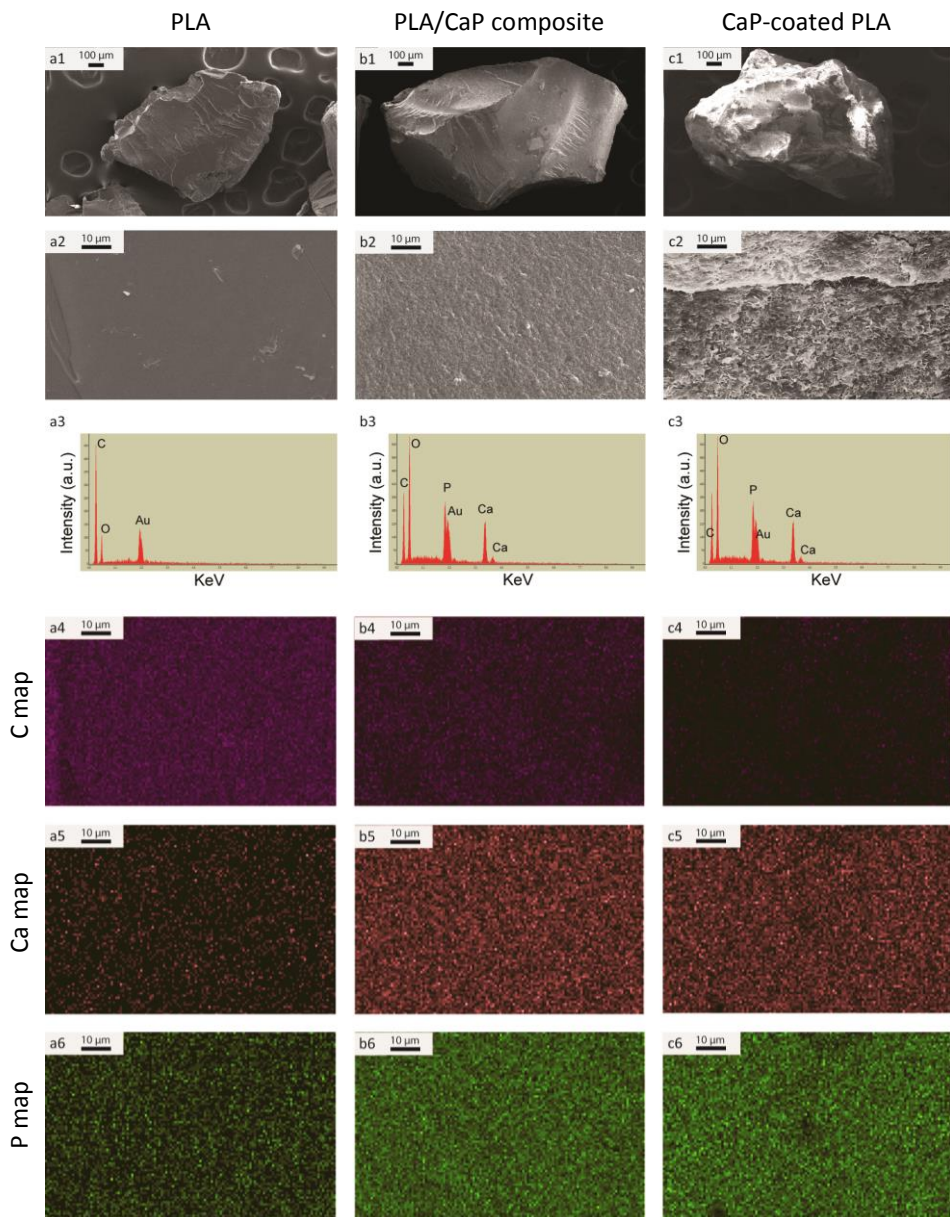


Figure. 1. SEM images at low (a1,b1,c1) and high (a2,b2,c2) magnification, EDS spectra (a3,b3,c3), carbon- (a4,b4,c4), calcium- (a5,b5,c5) and phosphorus (a6,b6,c6) elemental map of PLA, PLA/CaP composite and CaP-coated PLA, respectively. The PLA particles exhibited smooth surface, while the surface of the PLA/CaP composite appeared rougher with a homogenous distribution of CaP powder within the PLA matrix. A uniform CaP layer consisting of small, plate-shaped crystals was observed on PLA-coated particles. It should be noted that gold (Au) peak was observed in all the EDS spectra because the samples were gold-sputtered before SEM/EDS analysis.

A single peak that appeared at  $1750\text{ cm}^{-1}$  is attributed to stretching mode of C=O bond [39-40]. The PLA spectrum was in agreement with previously published data [18].

All peaks, typical of the PLA chemistry, were also found in the FTIR spectra of the two hybrid materials. A new band was observed around  $1000\text{ cm}^{-1}$ , probably due to the presence of  $\text{PO}_4^{3-}$ , the band of which appears at the similar wavelength [18-19]. The bands at  $560$  and  $604\text{ cm}^{-1}$  in the FTIR spectra of CaP-containing particles are also attributed to the P-O bond. Moreover, the hydroxyl bands at  $635$  and  $3565\text{ cm}^{-1}$  were detected in the spectrum of PLA/CaP composite suggesting the apatitic phase [18-19]. In the spectrum of the CaP-coated PLA, the hydroxyl band at  $3565\text{ cm}^{-1}$  appeared as a small shoulder on the  $\text{H}_2\text{O}$  band.

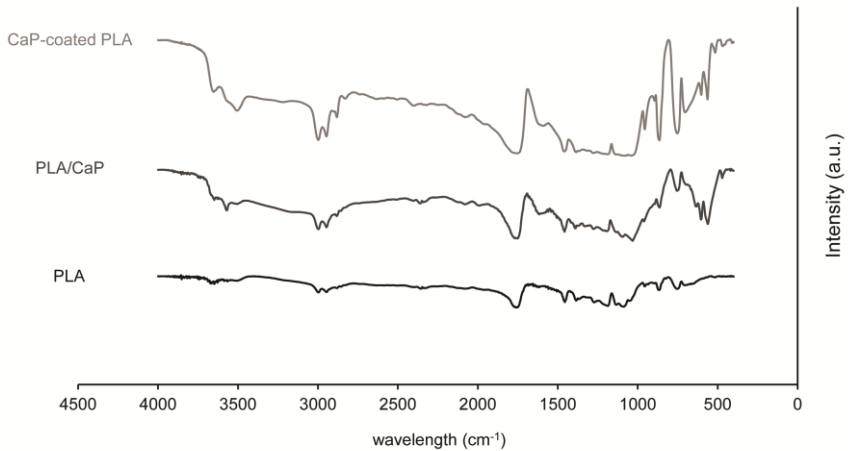
The XRD pattern of PLA particles did not show any distinguishable peaks, confirming the amorphous nature of the polymer. The XRD pattern of the PLA/CaP composite was in accordance with those obtained in previous studies, showing the presence of pure crystalline hydroxyapatite (HA) phase [18-19]. The most intense diffraction lines appeared at  $2\theta = 26, 31.9, 32.2, 33, 34.2, 29.9, 46.9$  and  $49.5^\circ$ , are attributed (002), (211), (112), (300), (202), (130), (222), and (213) crystalline planes in HA [41].

The XRD pattern of CaP-coated PLA showed less intense and broader peaks compared to the one of the composite material, confirming the formation of a less crystalline CaP phase. The most intense peak was observed at approximately  $4.9^\circ$ , which is attributed (010) crystalline plane of octacalcium phosphate (OCP). The small peak found at  $25.9^\circ$  corresponds to (002) plane in both OCP and HA structure [41-42]. The broad peak at about  $32^\circ$  is normally seen in the XRD pattern of OCP with a rather low intensity. The relatively high intensity of the peak at about  $32^\circ$  suggests the presence of an apatitic phase.

The TGA analysis (Figure. 3), performed in the temperature range  $35\text{-}1000^\circ\text{C}$ , showed a single drop in weight for all materials. The weight loss occurred in the approximate temperature range of  $300\text{-}400^\circ\text{C}$  and was calculated to be 98.9, 56 and 93.8% for PLA, PLA/CaP composite and CaP-coated PLA particles, respectively. Cumulative release of  $\text{Ca}^{2+}$  and  $\text{Pi}$  ions over a period of 12 weeks was investigated upon immersion of polymeric and hybrid particles in SPS (Figure. 4. a1-a2). A slight release of  $\text{Ca}^{2+}$  was measured in the solutions containing PLA particles at 1, 2, 3, and 6 weeks, possibly accidentally introduced to the solution during preparation, while no  $\text{Pi}$  ions were detected at any of the time points. A constant  $\text{Ca}^{2+}$  release to a maximum level of  $200\text{ }\mu\text{M}$  was detected for PLA/CaP composite particles until

week 3, after which a decrease to a concentration approximately 150  $\mu\text{M}$  was observed.

a



b

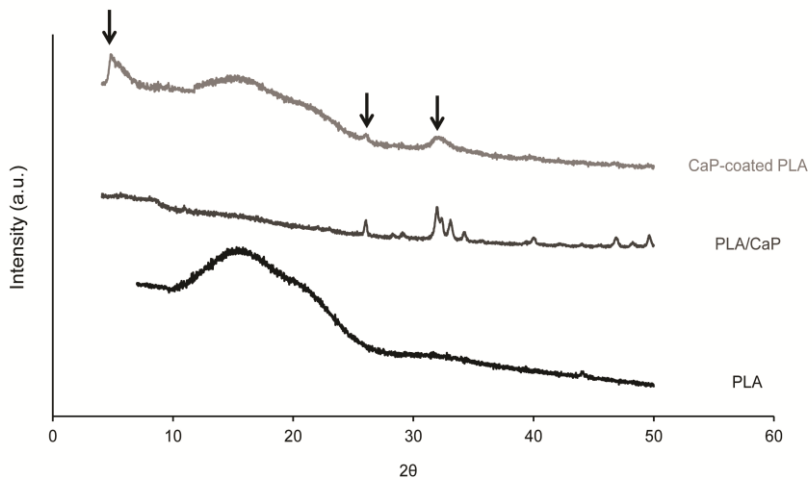


Figure. 2. FTIR spectra (a) and XRD patterns (b) of the PLA, PLA/CaP and CaP-coated PLA particles. The FTIR spectra of the two hybrid materials exhibited additional bands demonstrating the presence of CaP. The XRD patterns suggested the presence of a crystalline HA in the composite and a mixture of OCP (peaks shown by arrows) and apatite in the coated PLA.

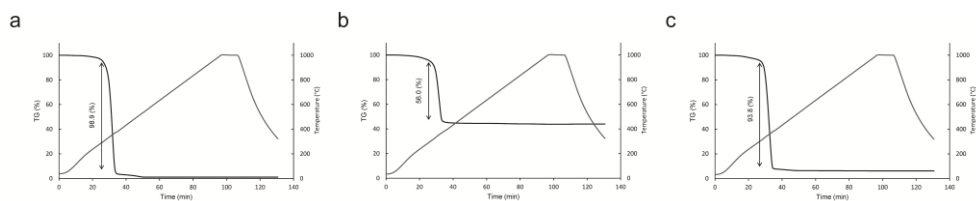


Figure 3. The TGA graphs showing weight loss of (a) PLA, (b) PLA/CaP and (c) CaP-coated PLA in the temperature range 35-1000 °C. A weight loss of 98.9, 56 and 93.8% were measured for PLA, PLA/CaP and CaP-coated PLA, respectively.

A linear increase in Pi ion concentration of PLA/CaP containing CPS was observed up to week 9, reaching a maximum concentration of 100  $\mu\text{M}$ . At week 12, the Pi ion level substantially decreased to 60  $\mu\text{M}$ . For the CaP-coated particles, an increasing release of  $\text{Ca}^{2+}$  up to 180  $\mu\text{M}$  was observed until week 2. This concentration remained constant for another week, and then linearly decreased to approximately 100  $\mu\text{M}$  at week 12. The Pi ion release profile of CaP-coated polymer showed an increase in concentration to 110  $\mu\text{M}$  in week 3, followed by a drop to approximately 80  $\mu\text{M}$  in the remaining experimental period.

The  $\text{Ca}^{2+}$  concentrations in time was also examined in the cell culture medium over a two-week period to investigate to which ionic concentrations the cells are exposed during culture. The  $\text{Ca}^{2+}$  concentration of the cell culture medium not containing any materials varied in the range of 1.7-2.0 mM over the two-week period.

Similar to the medium without materials, the  $\text{Ca}^{2+}$  concentration of the PLA-incubated medium showed variations in the range of 1.8-2.1 mM. A substantial decrease to approximately 300  $\mu\text{M}$  was detected in  $\text{Ca}^{2+}$  concentration after immersion of PLA/CaP composite particles in cell culture medium for 4 days, followed by a gradual increase to 600  $\mu\text{M}$ , at day 14. A slight decrease of approximately 200  $\mu\text{M}$  was observed in the  $\text{Ca}^{2+}$  concentration of the medium containing CaP-coated PLA particles at the first time point, a concentration that was comparable to that of the medium not containing any material. The  $\text{Ca}^{2+}$  level then increased in time, up to 2.5 mM at day 14.

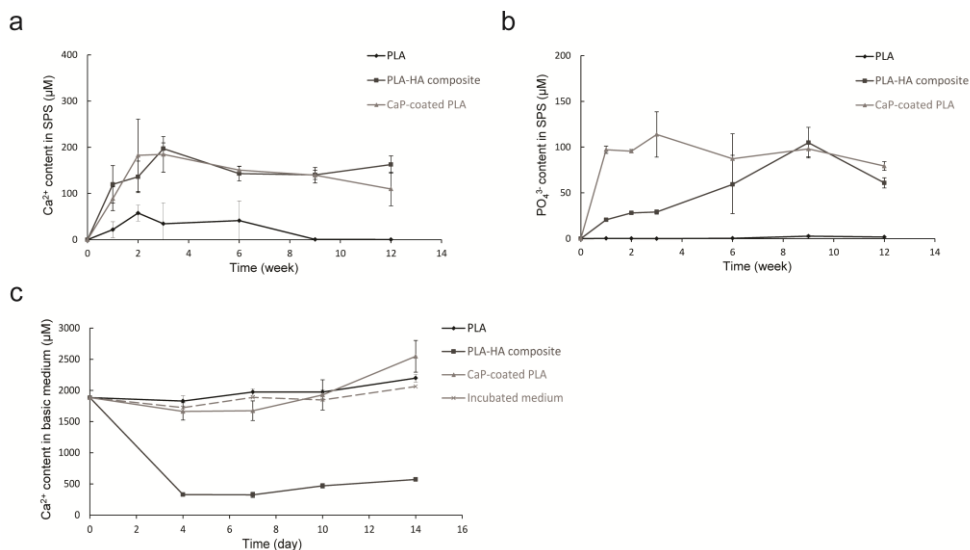


Figure 4. The Ca<sup>2+</sup> (a) and Pi ion (b) concentrations in SPS and the Ca<sup>2+</sup> (c) concentration in cell culture medium upon immersion of PLA, PLA/CaP and CaP-coated PLA particles. Both hybrid materials enriched the SPS solution with Ca<sup>2+</sup> and Pi ions at earlier time points, followed by a slight decrease of concentrations of both ions at later time points. Immersion of CaP-coated PLA in cell culture medium resulted in an initial decrease of Ca<sup>2+</sup> concentration, which was recovered at later time points. PLA/CaP composite particles depleted cell culture medium of the Ca<sup>2+</sup> ions, at all time points analyzed.

### 3.3.2. Response of hMSCs to hybrid materials

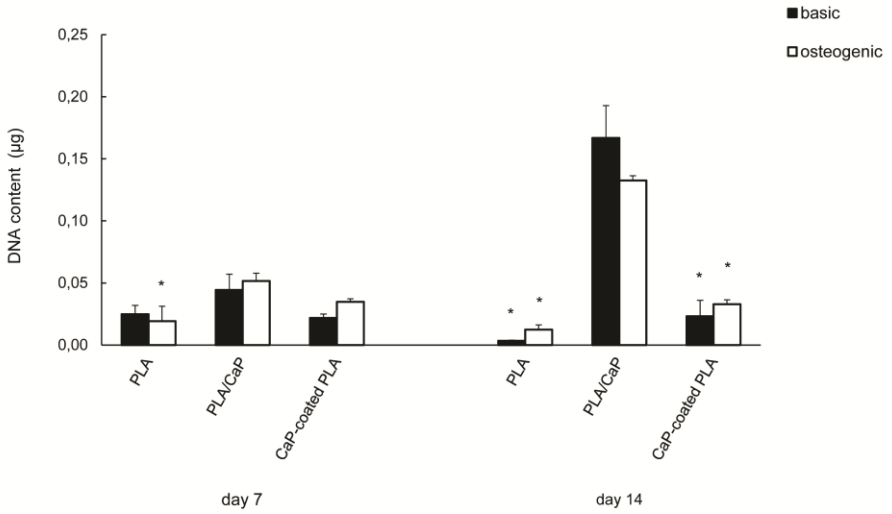
The DNA content of the hMSCs cultured on the PLA and the two hybrid samples was quantified at days 7 and 14 (Figure 5. a). At day 7, the DNA content of cells cultured on PLA/CaP composite was slightly higher as compared to PLA and CaP-coated PLA conditions in both media, however, the only significant difference was found between PLA/CaP composite and PLA particles, in osteogenic medium. At day 14, hMSCs cultured on CaP-coated PLA particles showed slightly higher DNA content compared to those cultured on PLA particles in both media, although this difference was not statistically significant. hMSCs cultured on composite, however, showed significantly higher DNA content compared to those cultured on PLA and coated PLA particles, both in basic and osteogenic medium. While only small, non-significant temporal increase in the DNA content of hMSCs cultured on PLA and coated PLA was observed, the DNA content of hMSCs cultured on PLA/CaP composite particles increased 3 to 4 times between days 7 and 14.

ALP activity of the hMSCs was also quantified and normalized for the DNA content (Figure. 5. b). At day 7, in both basic and osteogenic medium, both PLA/CaP composite and CaP-coated PLA samples showed higher ALP activity compared to PLA, however, this effect was significant only between CaP-coated PLA and PLA. ALP activity of hMSCs cultured on CaP-coated PLA was slightly higher than when the cells were cultured on PLA/CaP composite. At day 14, in basic medium, ALP activity measured on CaP-coated PLA was measured to be higher, although not significantly, than what was found on PLA and PLA/CaP composite samples. In osteogenic medium, both hybrid materials showed a significantly higher ALP activity than the pure polymer.

The mRNA expression of a panel of osteogenic markers including ALP, RUNX2, BSP, BMP2, OP and OC by hMSCs cultured on the three material types in either basic or osteogenic medium was analyzed after 7 and 14 days (Figure. 6. A-f). No significant differences in the ALP mRNA expression were observed among cells cultured on different materials, except at day 14 in basic medium, where PLA particles exhibited a higher ALP mRNA level as compared to the two hybrid materials. In general, the expression of the ALP gene was low at both time points and in both media, not exceeding a 1.5-fold change. At day 7, a significantly higher level of RUNX2 mRNA was measured on CaP-coated PLA as compared to PLA particles without CaP in osteogenic medium, while no differences were found at day 14.

At both time points, the expression of BMP2 and OP was higher in the hMSCs cultured on the two CaP-containing materials as compared to the cells cultured on PLA particles in basic medium. mRNA level of these two markers in osteogenic medium was in general low, however, a significant difference was observed in the expression of BMP2 between CaP-coated PLA and PLA particles at day 7. The mRNA level of OC was also higher in hMSCs cultured on CaP-containing particles compared to those cultured on PLA particles at both time points and in both media, although the only significant differences were observed between CaP-coated PLA and PLA particles at day 7 in basic medium.

a



b

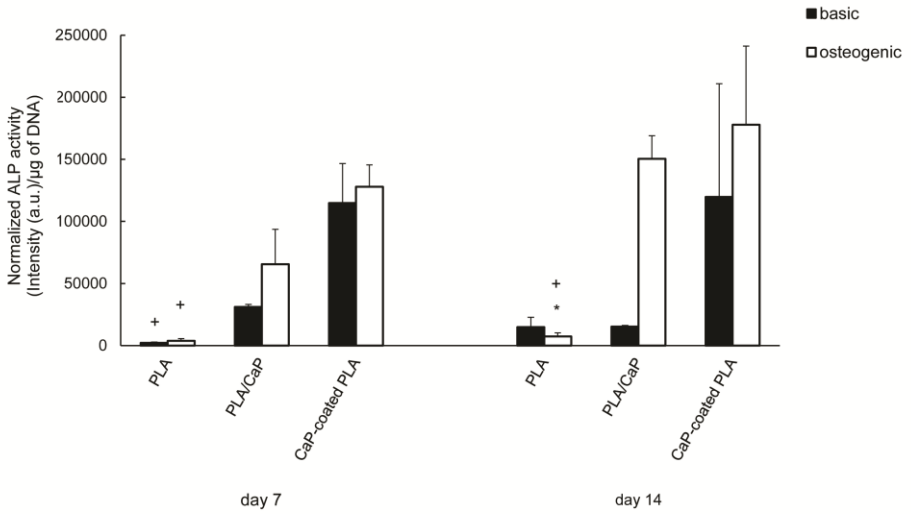


Figure 5. DNA content (a) and ALP activity (b) of hMSCs cultured on PLA, PLA/CaP and CaP-coated PLA particles. DNA content of hMSCs cultured on PLA/CaP particles was higher than that of hMSCs cultured on CaP-coated PLA and PLA particles. The ALP activity of the hMSCs was enhanced when cultured on the two hybrid materials as compared to the PLA control. # indicates  $p < 0.05$  when compared to PLA, \* indicated  $p < 0.05$  when compared to PLA/CaP composite and + indicates  $p < 0.05$ , when compared to CaP-coated PLA.

### 3.4. Discussion

In a search for successful synthetic alternatives to natural bone grafts, hybrid biomaterials are developed in which desired properties of the individual components are combined. In the current study, we have compared two hybrid materials consisting of CaP and PLA and investigated whether the method of combining the two, affects the response of hMSCs. While CaPs are widely used as bone graft substitutes owing to their resemblance to bone mineral [7] and related biocompatibility and bioactivity [1], polymers offer more diversity when it comes to mechanical properties [15-17].

An amorphous PLA with a relatively low molecular weight was selected for this study. PLA, being an aliphatic polyester, degrades by hydrolysis and the degradation profile of the polymeric phase has been shown to affect the degradation of hybrid materials, such as PLA/CaP composites [18]. Barbieri et al. [20] studied the role of the PLA molecular weight on mechanical and physicochemical properties of PLA/HA composite, similar to the one used in this study, as well as on their bone forming ability in vivo. The results revealed a higher fluid uptake by the composite prepared using low molecular weight PLA, resulting in release of more  $\text{Ca}^{2+}$  and  $\text{Pi}$  ions from and faster degradation of the composite. Moreover, heterotopic bone formation, or osteoinduction, which is considered an important characteristic of bone grafts and their substitutes, was only detected in the composites prepared with low molecular weight PLA.

To prepare monolithic composite in the current study, equal amounts of nano-sized CaP powder was mixed with PLA and extruded, a method that allowed preparation of a homogenous composite with a relatively high ceramic content. The TGA results demonstrated a mass loss of 56% in the composite material within the temperature range of 200-300°C. Within this temperature range, the organic component of the composite is expected to be completely burnt. No significant mass loss was observed at higher temperatures, indicating a total ceramic content to be 44%, which correlated well with the initial HA/PLA weight ratio used to produce the composite material. CaP content of PLA/CaP composites has been shown to substantially influence the mechanical properties of the composite [43-45]. On the other hand, the CaP content is also a critical factor determining degradation rate, bioactivity and bone forming ability of the composite, showing that indeed the properties of the individual components determine the properties of the hybrid material. Results of intramuscular implantation of PLA/HA composites with HA content varying from 0 to 40 wt% in

dogs showed that heterotopic bone formation only occurred in the composite containing 40 wt% of HA [19]. Heterotopic bone formation was also observed upon implantation of HA/PLA composite with weight ratio of 50/50 prepared by extrusion technique in sheep and dog animal models, while no bone formation was observed in PLA control implants [18,20].

A biomimetic method, involving immersion of polymeric particles into a solution containing  $\text{Ca}^{2+}$  and Pi ions under near-physiological conditions was used to deposit a homogenous layer on the polymer surface that was a mixture of OCP and apatite. Both these phases are biologically relevant, with carbonated apatite closely resembling the composition of bone mineral [7] and OCP being suggested as a precursor of biological apatite in hard tissue [46]. Both phases are also less stable than hydroxyapatite, showing a faster dissolution at neutral pH values [47]. In contrast to a relatively high CaP content of the monolithic composite, the TGA data showed that in CaP-coated particles, the mineral phase represented only 6.2 wt%.

Interestingly, despite this large difference in total mineral content between the two hybrid materials, upon immersion in SPS, a buffered solution, both materials showed a maximum release of approximately 200  $\mu\text{M}$  and 100  $\mu\text{M}$  of  $\text{Ca}^{2+}$  and Pi ions, respectively. Nevertheless, this concentration was more rapidly reached in CaP-coated PLA than in PLA/CaP composite, which can be related to both difference in CaP phase and the higher exposure of the CaP phase to the solution. While in the CaP-coated PLA, all CaP is on the surface, in the composite material, the majority of the mineral is in the bulk, and release of ions is dependent on the polymer degradation and the diffusion of the ions through the material bulk. In contrast to what was observed in SPS that, as-prepared, does not contain  $\text{Ca}^{2+}$  or Pi ions, in cell culture medium, a direct decrease of  $\text{Ca}^{2+}$  concentration was observed upon immersion of PLA/CaP composite particles or CaP-coated PLA particles, plausibly suggesting precipitation of a new CaP phase as was observed previously [48].

Regarding the differences in response of hMSCs to the two hybrid materials, with PLA without CaP as a control, cell proliferation on PLA/CaP composite particles was higher as compared to PLA. Previous results have shown that supplementing cell culture medium with 4, 7.8 and 8 mM  $\text{Ca}^{2+}$  increased the DNA content of hMSCs cultured on tissue culture plastic [49-50], suggesting a positive effects of  $\text{Ca}^{2+}$  ions on hMSCs proliferation.

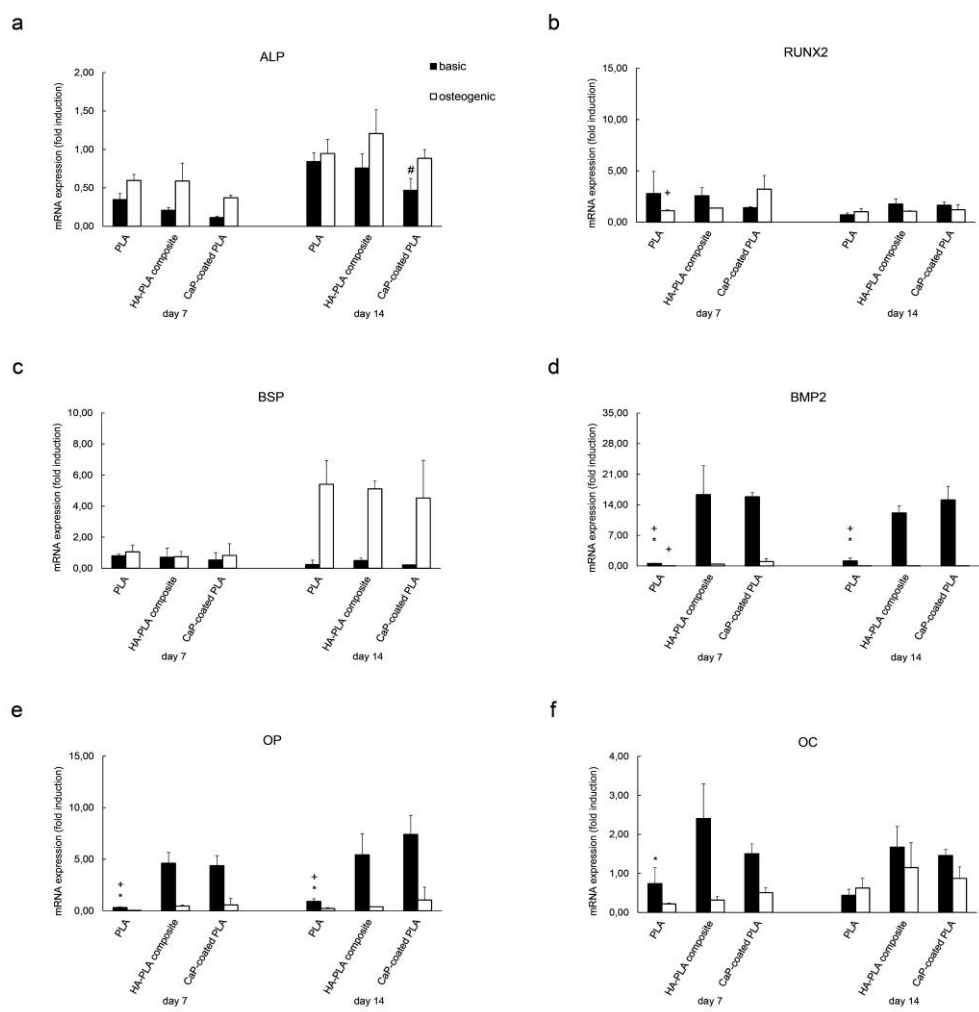


Figure 6. mRNA expression of ALP (a), RUNX2 (b), BSP (c), BMP2 (d), OP (e) and OC (f) in hMSCs cultured on PLA, PLA/CaP and CaP-coated PLA particles. Minor differences were detected in the mRNA expression of ALP, RUNX2 and BSP in hMSCs cultured on different materials. In contrast, the expression of BMP2, OP and OC genes was substantially higher in hMSCs cultured on PLA/CaP and CaP-coated PLA particles in comparison with PLA particles, in particular in basic cell culture medium. # indicates  $p < 0.05$  when compared to PLA, \* indicated  $p < 0.05$  when compared to PLA/CaP composite and + indicates  $p < 0.05$ , when compared to CaP-coated PLA.

In one of our previous studies [18], extruded PLA and PLA-HA composite with similar characteristics as used here were casted into pellets with a smooth

surface. In contrast to the present study, no differences in proliferation of hMSCs were observed between the polymer and composite material, which may be due to differences in total surface area between a 2D pellet and a 3D environment of a collection of particles. Furthermore, differences between the two studies could, for at least in a part, be caused by the physical differences between materials, such as the observed surface roughness.

Besides differences in proliferation of hMSCs as a result of presence of CaP, differences were also observed between the two types of hybrid materials. Cells cultured on PLA/CaP composite particles had a higher DNA content as compared to those cultured on CaP-coated PLA particles. Both differences in the chemical composition and topographical properties between these two materials may be responsible for this effect. This is in accordance with previous studies showing a more pronounced osteoblast attachment to an HA surface as compared to an OCP surface. Besides the difference in chemical composition and degradation properties, these two materials exhibited different grain size, which could also be of influence on cell attachment [51].

The ALP activity of hMSCs cultured on either PLA/CaP composite or CaP-coated PLA was higher as compared to that of cells cultured on PLA particles. Similarly, other studies also demonstrated a higher ALP activity of various cell types when cultured on PLA/CaP composite materials prepared using different techniques, in comparison with the polymer not containing the mineral phase [18,52-54]. Furthermore, Kim et al. [55] and Kung et al. [56] also observed that the ALP activity of bone marrow- and adipose-derived mesenchymal stem cells cultured on fibrous PLA meshes, the surface of which was covered with CaP, was significantly higher as compared to the culture on PLA samples without the ceramic. Danoux et al. [50] observed that the addition of 4 or 8  $\mu\text{M}$   $\text{Ca}^{2+}$ , or 4  $\mu\text{M}$  Pi ions to the cell culture medium enhanced the ALP activity of hMSCs. Furthermore, it was also shown that the individual release of these ions from only calcium-containing or only phosphate containing PLA particles increased the ALP activity of hMSCs compared to pure PLA particles. These results suggested that both  $\text{Ca}^{2+}$  and Pi ions released from the particles were responsible for promoting ALP activity in hMSCs.

Surprisingly, no effect of the hybrid materials on the mRNA level of ALP was detected, which may be explained by a transient peak expression of mRNA, in contrast to proteins, which are more stable. Similar to ALP, RUNX2 and BSP genes

were not influenced at mRNA level when the cells were cultured on different types of particles.

The expression of BMP2, OP and OC genes was substantially increased in hMSCs cultured on the PLA/CaP composite and CaP-coated PLA particles as compared to those cultured on PLA particles not containing CaP. These findings are in line with previously published studies, where the presence of CaP on electrospun PLA meshes had a positive effect on the expression of osteogenic markers such as collagen type I, OC and OP on stem cells from different origin [55-56]. Furthermore, it was previously shown that the expression of BMP2, OP and OC markers are significantly enhanced at elevated  $\text{Ca}^{2+}$  levels [49-50]. Although the  $\text{Ca}^{2+}$  level in the cell culture medium was shown to decrease in the presence of CaP-containing particles, it should be noted that the ionic concentration was measured in the bulk medium, not taking into account possible concentration differences between the bulk and the medium in close vicinity of the particle surface where cells are found, where  $\text{Ca}^{2+}$  concentration may be higher. Furthermore, apart from this chemical effect, the effect of physical surface properties of these materials, like roughness, surface area, etc. on differentiation of hMSCs should not be neglected, although these effects were not separately studied here.

No significant differences were observed in the expression of the osteogenic markers between hMSCs cultured on PLA/CaP composite and those cultured on CaP-coated PLA. The two hybrid materials differed in several properties including the phase, the amount and the availability in the CaP component, as well as the physical surface properties, which, taken together, resulted in a more pronounced decrease in concentration of  $\text{Ca}^{2+}$  and  $\text{Pi}$  ions in cell culture medium in the case of the monolithic composite as compared to the CaP-coated PLA. These differences however, were not reflected in the differentiation potential of hMSCs when cultured on the different materials suggesting that both methods of combining PLA and CaP can be used to enhance the osteogenic differentiation of hMSCs as compared to PLA without CaP.

### **3.5. Conclusion**

The results of the current study confirmed the beneficial effect of CaP regarding the osteogenic differentiation of hMSCs. This effect was independent of the method used to combine the CaP and the PLA component into a hybrid material,

i.e. generation of a monolithic composite or coating of the polymer with a ceramic layer.

## References

1. L. Yang, B. Harink, P. Habibovic, Calcium phosphate ceramics with inorganic additives. In: Paul Ducheyne, editor-in-chief. *Comprehensive biomaterials*. Elsevier Ltd; 2011. pp. 229-312.
2. B.F. Ricciardi and M.P. Bostrom, Bone graft substitutes: Claims and credibility. *Seminars in Arthroplasty* 24 (2013) 119-123.
3. M. Bohner, L. Galea, N. Doebelin, Calcium phosphate bone graft substitutes: Failures and hopes, *Journal of European Ceramic Society* 32 (2012) 2663-2671.
4. F. Barrère, C.A. van Blitterswijk, K. de Groot, Bone regeneration: molecular and cellular interactions with calcium phosphate ceramics, *International Journal of Nanomedicine* 1 (2006) 317-332.
5. S. Bose and S. Tarafder, Calcium phosphate ceramic systems in growth factor and drug delivery for bone tissue engineering: A review, *Acta Biomaterialia* 8 (2012) 1401-1421.
6. J Zhang, W Liu, V. Schnitzler, F. Tancret, J. Bouler, Calcium phosphate cements for bone substitution: Chemistry, handling and mechanical properties, *Acta Biomaterialia* 10 (2014) 1035-1049.
7. A. Bigi, G. Cojazzi, S. Panzavolta, A. Ripamonti, N. Roveri, M. Romanello, K. Noris Suarez, L. Moro, Chemical and structural characterization of the mineral phase from cortical and trabecular bone, *Journal of Inorganic Biochemistry* 68 (1997) 45-51.
8. R.A. Surmenev, M.A. Surmeneva, A.A. Ivanova, Significance of calcium phosphate coatings for the enhancement of new bone osteogenesis – A review, *Acta Biomaterialia* 10 (2014) 557-579.
9. R.Z. LeGeros, Properties of osteoconductive biomaterials: calcium phosphates, *Clinical Orthopaedic Related Research* 395 (2002) 81-98.
10. P. Habibovic, M.C. Kruyt, M.V. Juhl, S. Clyens, R. Martinetti, L. Dolcini, N. Theilgaard, C.A. van Blitterswijk, Comparative in vivo study of six hydroxyapatite-based bone graft substitutes, *Journal of Orthopedic Research* 26 (2008) 1363-1370.
11. H. Yuan, K. Kurashina, J.D. de Bruijn, Y. Li, K. de Groot, X. Zhang, A preliminary study on osteoinduction of two kinds of calcium phosphate ceramics, *Biomaterials* 20 (1999) 1799-1806.
12. H. Yuan, H. Fernandes, P. Habibovic, J. de Boer, A.M.C. Barradas, A. de Ruiter, W.R. Walsh, C.A. van Blitterswijk, J.D. de Bruijn, Osteoinductive ceramics as a synthetic alternative to autologous bone grafting, *Proceeding of National Academy of Sciences USA* 107 (2010) 13614-13619.
13. P. Habibovic, T.M. Sees, M.A. van den Doel, C.A. van Blitterswijk, K. de Groot Osteoinduction by biomaterials—Physicochemical and structural influences, *Biomedical Materials Research A* 77 (2006) 747-762.
14. A.J. Wagoner Johnson and B.A. Herschler, A review of the mechanical behavior of CaP and CaP/polymer composites for applications in bone replacement and repair, *Acta Biomaterialia* 7 (2011) 16-30.
15. C. Canal and M.P. Ginebra, Fibre-reinforced calcium phosphate cements: A review, *Journal of Mechanical Behavior of Biomedical Materials* 4 (2011) 1658-1671.
16. W.J.E.M. Habraken, J.G.C. Wolke, J.A. Jansen, Ceramic composites as matrices and scaffolds for drug delivery in tissue engineering, *Advanced Drug Delivery Review* 59 (2007) 234-248.
17. H. Zhou, J.G. Lawrence, S.B. Bhaduri, Fabrication aspects of PLA-CaP/PLGA-CaP composites for orthopedic applications: A review, *Acta Biomaterialia* 8 (2012) 1999-2016.
18. C.B. Danoux, D. Barbieri, H. Yuan, J.D. de Bruijn, C.A. van Blitterswijk, P. Habibovic, In vitro and in vivo bioactivity assessment of a polylactic acid/hydroxyapatite composite for bone regeneration, *Biomatter* 4 (2014) e27664 1-12.

19. D. Barbieri, A.J.S. Renard, J.D. de Bruijn, H. Yuan, Heterotopic Bone Formation by Nano-Apatite Containing Poly(D,L-Lactide) Composite, *European Cell and Materials* 19 (2010) 252-261.
20. D. Barbieri, H. Yuan, X. Luo, S. Fare, D.W. Grijpma, J.D. de Bruijn, Influence of polymer molecular weight in osteoinductive composites for bone tissue regeneration, *Acta Biomaterialia* 9 (2013) 9401-9431.
21. J.A. Inzana, D. Olvera, S.M. Fuller, J.P. Kelly, O.A. Graeve, E.M. Schwarz, S.L. Kates, H.A. Awad, 3D printing of composite calcium phosphate and collagen scaffolds for bone regeneration, *Biomaterials* 35 (2014) 4026-4034.
22. A. Bigi, B. Bracci, S. Panzavolta, Effect of added gelatin on the properties of calcium phosphate cement, *Biomaterials* 25 (2004) 2893-2899.
23. X. Zhang, Q. Cai, H. Liu, S. Zhang, Y. Wei, X. Yang, Y. Lin, Z. Yang, X. Deng, Calcium ion release and osteoblastic behavior of gelatin/beta-tricalcium phosphate composite nanofibers fabricated by electrospinning, *Materials Letter* 73 (2012) 172-175.
24. L. Pighinelli and M. Kucharska, Chitosan-hydroxyapatite composites, *Carbohydrate Polymers* 93 (2013) 256-262.
25. A. Nandakumar, C. Cruz, Mentink A, Z. Tahmasebi Birgani, L. Moroni, C. van Blitterswijk, P. Habibovic, Monolithic and assembled polymer-ceramic composites for bone regeneration, *Acta Biomaterialia* 9 (2013) 5708-5717.
26. P. Layrolle Calcium Phosphate Coatings. In: Paul Ducheyne, editor-in-chief. *Comprehensive biomaterials*. Elsevier Ltd; 2011. pp. 223-9.
27. P. Habibovic, J. Lia, C.M. van der Valk, G. Meijerc, P. Layrolle, C.A. van Blitterswijk, K. de Groot, Biological performance of uncoated and octacalcium phosphate-coated Ti6Al4V, *Biomaterials* 26 (2005) 23-36.
28. L. Xu, F. Pan, G. Yu, L. Yang, E. Zhang, K. Yang, In vitro and in vivo evaluation of the surface bioactivity of a calcium phosphate coated magnesium alloy, *Biomaterials* 30 (2009) 1512-1523.
29. S.C.G. Leeuwenburgh, J.G.C. Wolke, M.C. Siebers, J. Schoonman, J.A. Jansen, In vitro and in vivo reactivity of porous, electrosprayed calcium phosphate coatings, *Biomaterials* 27 (2006) 3368-3378.
30. A. Nandakumar, L. Yang, P. Habibovic, C. van Blitterswijk, Calcium Phosphate Coated Electrospun Fiber Matrices as Scaffolds for Bone Tissue Engineering, *Langmuir* 26 (2010) 7380-7387.
31. L. Yang, M. Hedhammar, T. Blom, K. Leifer, J. Johansson, P. Habibovic, C.A. van Blitterswijk, Biomimetic calcium phosphate coatings on recombinant spider silk fibres, *Biomedical Materials* (2010) doi: 10.1088/1748-6041/5/4/045002.
32. G. Wu, Y. Liu, T. Iizuka, E.B. Hunziker, Biomimetic Coating of Organic Polymers with a Protein-Functionalized Layer of Calcium Phosphate: The Surface Properties of the Carrier Influence Neither the Coating Characteristics Nor the Incorporation Mechanism or Release Kinetics of the Protein, *Tissue Engineering Part C: Methods* 16 (2010) 1255-1265.
33. B. Feddes, J.G.C. Wolke, A.M. Vredenberg, J.A. Jansen, Initial deposition of calcium phosphate ceramic on polyethylene and polydimethylsiloxane by RF magnetron sputtering deposition: the interface chemistry, *Biomaterials* 25 (2004) 633-639.
34. E.N. Bolbasov, I.N. Lapin, V.A. Svetlichnyi, Y.D. Lenivtseva, A. Malashicheva, Y. Malashichev, A.S. Golovkin, Y.G. Anissimov, S.I. Tverdokhlebov, The formation of calcium phosphate coatings by pulse laser deposition on the surface of polymeric ferroelectric, *Applied Surface Science* 349 (2015) 420-429.
35. L. Yang, S. Perez-Amodio, F.Y.F. Barre`re-de Groot, V. Everts, C.A. van Blitterswijk, P. Habibovic, The effects of inorganic additives to calcium phosphate on in vitro behavior of osteoblasts and osteoclasts, *Biomaterials* 31 (2010) 2976-2989.
36. S. Patntirapong, P. Habibovic, P.V. Hauschka, Effects of soluble cobalt and cobalt incorporated into calcium phosphate layers on osteoclast differentiation and activation, *Biomaterials* 30 (2009) 548-555.

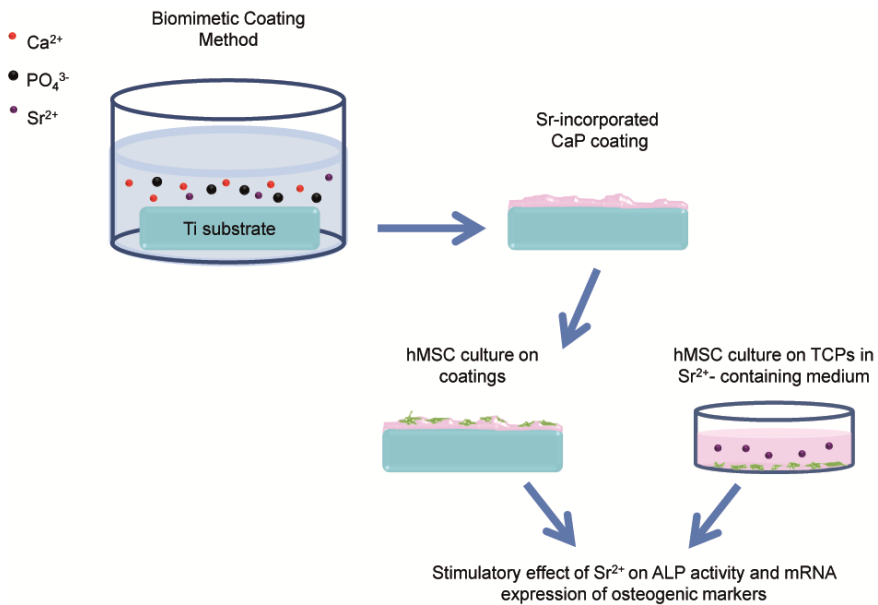
37. H. Fernandes, A. Mentink, R. Bank, R. Stoop, C. van Blitterswijk, J. de Boer, Endogenous Collagen Influences Differentiation of Human Multipotent Mesenchymal Stromal Cells, *Tissue Engineering: Part A* 16 (2010) 1693-1702.
38. S.K. Both, A.J.C. van der Muijsenberg, C.A. van Blitterswijk, C.A., J. de Boer, J.D. de Bruijn, A rapid and efficient method for expansion of human mesenchymal stem cells, *Tissue Engineering* 13 (1) (2007) 3-9.
39. B.W. Chieng, N.A. Ibrahim, W.M.Z.W. Yunus, M.Z. Hussein, Poly(lactic acid)/Poly(ethylene glycol) Polymer Nanocomposites: Effects of Graphene Nanoplatelets, *Polymers* 6 (2014) 93-104.
40. A. Jordá-Vilaplana, V. Fombuena, D. García-García, M.D. Samper, L. Sánchez-Nácher, Surface modification of polylactic acid (PLA) by air atmospheric plasma treatment, *European Polymer Journal* 58 (2014) 23–33.
41. R.K. Brundavanam, G.E. Jai Poinern, D. Fawcett, Modelling the Crystal Structure of a 30 nm Sized Particle based Hydroxyapatite Powder Synthesised under the Influence of Ultrasound Irradiation from X-ray powder Diffraction Data, *American Journal of Materials Science* 3 (2013) 84-90.
42. F. Barrère, P. Layrolle, C.A. van Blitterswijk, K. de Groot, Biomimetic coatings on titanium: a crystal growth study of octacalcium phosphate, *Journal of Materials Science: Materials in Medicine* 12 (2001) 529-534.
43. D. Barbieri, J.D. de Bruijn, X. Luo, S. Fare, D.W. Grijpma, H. Yuan, Controlling dynamic mechanical properties and degradation of composites for bone regeneration by means of filler content, *Journal of Mechanical Behavior of Biomedical Materials* 20 (2013) 162–172.
44. J. Russias, E. Saiz, R.K. Nalla, K. Gryn, R.O. Ritchie, A.P. Tomsia, Fabrication and mechanical properties of PLA/HA composites: A study of in vitro degradation, *Materials Science Engineering C* 6 (2006) 1289–1295.
45. N.C. Bleach, S.N. Nazhata, K.E. Tanner, M. Kellomaki, P. Tormala, Effect of filler content on mechanical and dynamic mechanical properties of particulate biphasic calcium phosphate-poly lactide composites, *Biomaterials* 23 (2002) 1579–1585.
46. O. Suzuki, Octacalcium phosphate (OCP)-based bone substitute materials, *Japanese Dental Science Reviews*, 49 (2013) 58-71.
47. S.V. Dorozhkin, Bioceramics of calcium orthophosphates, *Biomaterials* 31 (2010) 1465–1485.
48. A.M.C. Barradas, V. Monticone, M. Hulsman, C. Danoux, H. Fernandes, Z. Tahmasebi Birgani, F. Barre-re-de Groot, H. Yuan, M. Reinders, P. Habibovic, C. van Blitterswijk, J. de Boer, Molecular mechanisms of biomaterial-driven osteogenic differentiation in human mesenchymal stromal cells, *Integrative Biology* 5 (2013) 920-931.
49. A.M.C. Barradas, H.A.M. Fernandes, N. Groen, Y. Chai, J. Schrooten, J. van de Peppel, J.P.T.M. van Leeuwen, C.A. van Blitterswijk, J. de Boer, A calcium-induced signaling cascade leading to osteogenic differentiation of human bone marrow-derived mesenchymal stromal cells, *Biomaterials* 33 (2012) 205-215.
50. C.B.S.S. Danoux, D.C. Bassett, Z. Othman, A.I. Rodrigues, R.L. Reis, J.E. Barralet, C.A. van Blitterswijk, P. Habibovic, Elucidating the individual effects of calcium and phosphate ions on hMSCs by using composite materials, *Acta Biomaterialia* 17 (2015) 1-15.
51. W. Mróz, A. Bombalska, B. Budner, S. Burdyska, M. Jedynski, A. Prokopiuk, E. Menaszek, A. Scisłowska-Czarnecka, A. Niedzielska, K. Niedzielski, Comparative study of hydroxyapatite and octacalcium phosphate coatings deposited on metallic implants by PLD method, *Applied Physics A* 101 (2010) 713–716.
52. H. Kim, H. Lee, J.C. Knowles, Electrospinning biomedical nanocomposite fibers of hydroxyapatite/poly(lactic acid) for bone regeneration, *Journal of Biomedical Materials Research* 79A (2006) 643–649.
53. E. Tayton, M. Purcell, A. Aarvold, J.O. Smith, A. Briscoe, J.M. Kanczler, K.M. Shakesheff, S.M. Howdle, D.G. Dunlop, R.O.C. Oreffo, A comparison of polymer and polymer-hydroxyapatite

- composite tissue engineered scaffolds for use in bone regeneration. An in vitro and in vivo study, *Journal of Biomedical Materials Research* 102A (2014) 2613-2624.
54. S. Tanodekaew, S. Channasanon, P. Kaewkong, P. Uppanan, PLA-HA scaffolds: preparation and bioactivity, *Procedia Engineering* 59 (2013) 144 – 149.
  55. S. Kim, S. Oh, W. Lee, U.S. Shin, H. Kim, Poly(lactic acid) porous scaffold with calcium phosphate mineralized surface and bone marrow mesenchymal stem cell growth and differentiation, *Materials Science and Engineering C* 31 (2011) 612–619.
  56. F. Kung, C. Lin, W.T. Lai, Osteogenesis of human adipose-derived stem cells on hydroxyapatite-mineralized poly(lactic acid) nanofiber sheets, *Materials Science and Engineering C* 45 (2014) 578-588.

# Chapter 4

## Human mesenchymal stromal cells response to biomimetic octacalcium phosphate containing strontium

4



## Abstract

The incorporation of bioinorganics into synthetic biomaterials is a promising approach to improve the biological performance of bone graft substitutes, while still retaining their synthetic nature. Among these bioinorganics, strontium ions ( $\text{Sr}^{2+}$ ) have reported enhanced bone formation, and a reduced risk of bone fractures. While previous results have been encouraging, more detailed studies are needed in order to further develop specific applications. This study demonstrates the effects of  $\text{Sr}^{2+}$  on the osteogenic differentiation of human mesenchymal stromal cells (hMSCs) when introduced as either a dissolved salt, or incorporated into biomimetic calcium phosphate (CaP) coatings. Upon attachment, hMSCs seeded in the presence of higher  $\text{Sr}^{2+}$  concentrations presented with a more elongated shape as compared to the controls without  $\text{Sr}^{2+}$ . Both  $\text{Sr}^{2+}$  as a dissolved salt in the medium, or incorporated into CaP coatings, positively influenced hMSC alkaline phosphatase (ALP) activity in a dose-dependent manner. At the mRNA level, the expression of osteogenic markers ALP, bone sialoprotein (BSP), bone morphogenetic protein 2 (BMP2), osteopontin (OP) and osteoclastin (OC) were increased in the presence of  $\text{Sr}^{2+}$ , independent of the delivery method. Overall, this study demonstrates the positive effects of strontium on the osteogenic differentiation of human MSCs, and supports the use of strontium-incorporated CaPs for bone regeneration applications.

## 4.1. Introduction

Despite advances in orthopedic and dental surgery, the clinical management of bone defects continues to present challenges [1]. While autograft remains the gold standard for treating bone defects, issues such as limited quantity, donor site morbidity, and the requirement for an additional surgical site continue to encourage research into alternatives [2]. Synthetic bone graft substitutes have provided promising results to date, with calcium phosphates (CaPs) maintaining interest [2] due to their chemical similarities to the mineral phase of bone, being itself a non-stoichiometric carbonated apatite [3]. Despite this, the performance of synthetic bone grafts remains inferior to autograft. Several attempts have been made to improve the bone healing capacity of CaPs [4], including combining them with growth factors [5-7], cells [5, 8-9] and inorganic additives [10-12]. The incorporation of inorganic additives such as magnesium ( $Mg^{2+}$ ), copper ( $Cu^{2+}$ ), strontium ( $Sr^{2+}$ ), and fluoride (F) into synthetic bone grafts, is gaining popularity as these additives may directly induce changes in cells, for example via ion channels, potentially functioning as “synthetic growth factors”. The potential role of these bioinorganics in bone tissue, and their effects on bone formation, are comprehensively summarized by Habibovic and Barralet [13], Yang et al. [4], and Boanini et al [10].

While many elements have been shown to influence bone regeneration, the role of strontium is particularly interesting due to its relatively high presence within healthy bone. Approximately 99% of the strontium within the body is found within bone, with its quantity being positively correlated to the compressive strength of bone [13-14]. Strontium ranelate is currently used for treatment and management of osteoporotic bone [15-18], with its use reported to reduce the risk of fracture in postmenopausal osteoporotic bone [15], and increase bone mineral density [16].

To date, several studies have investigated the effects of local  $Sr^{2+}$  delivery on osteogenesis and bone formation. Promising results have been obtained when strontium was incorporated into synthetic bone grafts, including bioactive glasses [19-21], titanium implants [22-23], calcium silicates [24], and CaPs [1, 11, 25-31]. In vitro studies have previously demonstrated that strontium incorporation into CaPs resulted in a dose-dependent effect on osteoblast and osteoclast growth and activity [11, 25-29]. This effect has also been demonstrated using ovariectomized rats, where the ion release from  $Sr^{2+}$ -doped CaPs resulted in increased new bone formation [29] and improved osseointegration [30].

While the addition of strontium ions to CaP bone graft substitutes has provided positive results to date, a deeper understanding of the mechanisms and function of strontium is still lacking. Such information is needed to convert this potential into applicable products. To further elucidate the specific role of strontium in bone healing, this study investigated the effect of  $\text{Sr}^{2+}$  on hMSCs in two conditions. In the first condition,  $\text{Sr}^{2+}$  ions were delivered to the cells as a dissolved salt, in order to understand its direct effect on hMSCs. In comparison, and with the aim to assess a degradable CaP as a delivery vehicle for this ion, the second condition used a two-step biomimetic approach to incorporate  $\text{Sr}^{2+}$  at varying concentrations into crystalline CaP coatings, which were deposited in titanium substrate. For both conditions, cell responses were studied using proliferation and osteogenic differentiation marker expression, and changes in hMSC morphology. Overall, this study was undertaken to elucidate the specific mechanisms or strontium-induced osteogenesis, and therefore, improve the efficacy of calcium phosphates as bone graft substitutes

## 4.2. Materials and methods

### 4.2.1. Coating preparation

Commercially pure Titanium (cp Ti grade 4) was used as a substrate for the CaP coatings. The Ti sheet was cut into  $1 \times 1 \text{ cm}^2$  pieces and grit-blasted using alumina beads with a diameter of  $250 \mu\text{m}$  in order to reach a Ra roughness of  $1.3 \pm 0.1 \mu\text{m}$ . A 2-step biomimetic coating approach was used to prepare the coatings, as previously described [11, 32]. Briefly, the surface of the Ti plates were coated with a thin amorphous CaP layer by vertical immersion in a supersaturated simulated body fluid (SBF) for 24 hours at  $37^\circ\text{C}$ . This solution, containing NaCl,  $\text{CaCl}_2 \cdot 2\text{H}_2\text{O}$ ,  $\text{MgCl}_2 \cdot 6\text{H}_2\text{O}$ ,  $\text{NaHCO}_3$  and  $\text{Na}_2\text{HPO}_4 \cdot 2\text{H}_2\text{O}$  salts (Sigma, Table 1) was prepared under mildly acidic conditions by dissolution of  $\text{CO}_2$  gas. The pre-calcified Ti plates were then immersed for 48 hours at  $37^\circ\text{C}$  in a calcium phosphate solution (CPS) containing NaCl,  $\text{CaCl}_2 \cdot 2\text{H}_2\text{O}$  and  $\text{Na}_2\text{HPO}_4 \cdot 2\text{H}_2\text{O}$  salts (Sigma, Table 1) that was buffered at pH 7.4 by addition of tris-hydroxymethylaminomethane (Tris) and 1M HCL (Sigma). A stock solution of strontium acetate (Sigma) in a Tris buffer (pH=7.4) with concentration of 100 mM was prepared. In order to incorporate strontium into CaP coatings, appropriate volumes of  $\text{Sr}^{2+}$  stock solution were combined with the CPS solution to reach varying concentrations of  $\text{Sr}^{2+}$  in CPS (0, 10 and 1000

μM). The CPS solution was refreshed after 24 hours. The coatings were then washed three times with MilliQ water and dried overnight at 37°C in an air oven.

Table 1. Ionic content of concentrated SBF and CPS solutions used for preparation of the coatings.

Solution	Na <sup>+</sup>	Mg <sup>2+</sup>	Ca <sup>2+</sup>	Cl <sup>-</sup>	HPO <sub>4</sub> <sup>2-</sup>	HCO <sub>3</sub> <sup>-</sup>
Concentrated SBF	733.5	7.5	12.5	720	5	21
CPS	140	0	4	144	2	0

#### 4.2.2. Coating characterization

The chemistry of the mineral phase was characterized by Fourier transform infrared spectroscopy (FTIR, Perkin-Elmer Spectrum 1000) and x-ray diffraction (XRD, Miniflex, Rigaku). The morphology of the mineral films, and the presence and distribution of calcium, phosphorus and strontium were investigated scanning electron microscopy (SEM, XL-30 ESEM-FEG, Philips), coupled with energy dispersive X-ray spectroscopy analyzer (EDS, EDAX, AMETEK Materials Analysis Division). Quantification of the data was achieved using the TEAM™ EDS V2.2 software provided by the EDS manufacturer. The Ca/P, Sr/P, (Ca+Sr)/P and Sr/Ca ratios were calculated upon analysis.

Additionally, the coatings were dissolved in ultrapure nitric acid and the Sr<sup>2+</sup> content of the coating was measured using inductively coupled plasma mass spectrometry (ICP-MS, Agilent 7700 ICP-MS, Agilent Technologies).

#### 4.2.3. Cell subculture

hMSCs were isolated from bone marrow aspirates (5–20 ml) obtained from 2 donors after written informed consent. Isolation procedure and full characterization of the cells have been described previously [33-34]. In short, aspirates were resuspended using 20 G needles, plated at a density of 5x10<sup>5</sup> cells per cm<sup>2</sup>, and cultured in proliferation medium (consisting of α-MEM (Gibco) supplemented with 10% fetal bovine serum (Lonza), 2 mM L-glutamine (Gibco), 0.2 mM ascorbic acid (Sigma), 100 U ml<sup>-1</sup> penicillin and 100 μg ml<sup>-1</sup> streptomycin

(Gibco) and  $1 \text{ ng ml}^{-1}$  rhbFGF (AbDSerotec)). The medium was refreshed every 2-3 days. Cells were harvested at approximately 80% confluency for subculture until they reached passage 3.

#### 4.2.4. Cell culture

In the first step of cell culture, hMSCs of passage 3 from the 2 donors were seeded on treated tissue culture plates (TCPs) at a density of  $10000 \text{ cells/cm}^2$  (for DNA, ALP and qPCR assays) or at  $2500 \text{ cells/cm}^2$  (for imaging cell morphology) in approximately  $50 \mu\text{l}$  of basic medium ( $\alpha$ -MEM (Gibco) supplemented with 10% fetal bovine serum (Lonza), 2 mM L-glutamine (Gibco), 0.2 mM ascorbic acid (Sigma),  $100 \text{ U ml}^{-1}$  penicillin and  $100 \mu\text{g ml}^{-1}$  streptomycin (Gibco)). After seeding, 1 ml of either basic or osteogenic medium (basic medium supplemented with 10 nM dexamethasone (Sigma)) was added to each well. Appropriate volumes of  $\text{Sr}^{2+}$  stock was added to each well to reach  $\text{Sr}^{2+}$  concentrations of 0, 10 and  $1000 \mu\text{M}$  in cell culture medium. The medium was refreshed every 2-3 days.

In parallel, hMSCs of 2 donors were cultured on coated Ti plates. CaP coatings were sterilized with ethanol prior to cell culture. To sterilize, the samples were placed in a sterile non-treated well plate and washed three times with 70% ethanol followed by 15 min of drying inside the flow cabinet after each washing step. In the last step of sterilization, 100% ethanol was added to the samples and allowed to evaporate in the flow cabinet for at least 2 hours. The plates were then washed twice with sterile PBS, followed by an overnight incubation in a 5%  $\text{CO}_2$  humid atmosphere at  $37^\circ\text{C}$  after the addition of 1 ml basic medium.

hMSCs of passage 3 from 2 donors were seeded on the coated Ti plates at a density of  $10000 \text{ cells/cm}^2$  (for DNA, ALP and qPCR assays) or  $2500 \text{ cells/cm}^2$  (for imaging cell morphology) in approximately  $50 \mu\text{l}$  of basic medium and allowed to attach to the coatings for 4 hours, after which 1 ml of either basic or osteogenic medium was slowly added to each well. The medium was refreshed every 2-3 days. Cell medium was collected at each refreshment point and concentrations of Ca and Sr in basic cell medium were then measured using ICP-MS, at each refreshment point up to 7 days.

#### 4.2.5. Cell morphology

At day 1 after cell seeding, the cells cultured on TCPs and CaP coatings were washed with PBS and fixed with a buffer of 4% paraformaldehyde (pH=7.4) for 30

minutes. The cells cultured on TCPs and CaP coatings were then permeabilized with 0.1% Triton X-100 in PBS solution for 10 minutes, washed with PBS and blocked for 30 minutes in a blocking solution (2% bovine serum albumin (BSA) and 0.1 v/v% Tween 20 in PBS). Subsequently, Alexa Fluor 594 antibody (Invitrogen) diluted in blocking buffer was added to the cells to stain the cell cytoskeleton, and incubated at room temperature in dark for 1 hour. After incubation, cells were washed with PBS, and DAPI antibody (Sigma-Aldrich/Fluka) diluted in PBS was added for 10 minutes. The cells were then washed with PBS and imaged using a fluorescent microscope (E600, Nikon) (The data is not shown for cells cultured on CaP coatings).

6 pairs of immunofluorescent images obtained in blue and red channels (for Dapi and Phalloidin antibodies, respectively) were used for quantifying cell shape parameters. The data was analyzed in CellProfiler software as was described previously [35] and cell area and eccentricity parameters were selected to assess the changes in cell morphology upon introduction of  $\text{Sr}^{2+}$ . Cell area shows the total number of pixels located in the cell area. Eccentricity shows morphological elongation and measures the deviation of a conic section from a circle, with eccentricity being equal to zero for a circle and one for a parabola [36].

After fixation, the cells cultured on CaP coatings were also dehydrated by addition of alcohol series (70%, 80%, 90% and 100%, 30 min per concentration) and dried using a critical point drier (CPD 030, Balzers). The samples were then gold sputtered and imaged using SEM. Two independent experiments with  $n=2$  for each condition were performed.

#### **4.2.6. DNA content and ALP activity quantification**

Total DNA was assessed with CyQuant Cell Proliferation Assay kit (Invitrogen). After 3 freeze/thaw cycles at  $-80^{\circ}\text{C}$ , 500  $\mu\text{l}$  lysis buffer (lysis buffer provided in the kit diluted in a buffer of NaCl-EDTA solution) was added to each well. The samples were ultra-sonicated and incubated at room temperature for 1 hour. After centrifugation, 100  $\mu\text{l}$  of the supernatant was mixed with the same volume of CyQuant GR dye in a 96 well micro-plate and incubated for 15 min. Fluorescence measurements for DNA quantification were done at excitation and emission wavelengths of 480 and 520 nm, respectively, using a spectrophotometer (Perkin Elmer). ALP activity in the cultures was measured using a CDP-star kit (Roche Applied Science). 10  $\mu\text{l}$  of the supernatant was mixed with 40  $\mu\text{l}$  CDP-star reagent in a 96 well micro-plate and incubated for 30 min.

After incubation, chemiluminescence measurements were completed at 466 nm. Results of the DNA assays are presented based on average  $\mu\text{g}$  of DNA detected in each condition. Results of ALP activity were normalized per DNA content of each culture and presented as the average of normalized ALP activity per  $\mu\text{g}$  of DNA for each condition. Two independent experiments with  $n=3$  for each condition were performed for DNA and ALP analyses, and the results of one representative experiment are presented here.

#### **4.2.7. RNA extraction and gene expression (qPCR) assay**

Total RNA was isolated by using a NucleoSpin<sup>®</sup> RNA II isolation kit (Macherey Nagel) for cells cultured on TCPs and in combination with NucleoSpin<sup>®</sup> RNA II isolation kit and Trizol method, in accordance with the manufacturer's protocol. RNA was collected in RNase-free water and the total concentration was measured using nano-drop measurement equipment (ND1000 spectrophotometer, Thermo Scientific). The cDNA of the cultures were then prepared using an iScript kit (Bio-Rad) according to the manufacturer's protocol and diluted 10 times in RNase-free water to be used for quantitative real-time PCR (qPCR). The qPCR measurements were completed using Bio-Rad equipment using Syber green I master mix (Invitrogen) and the primer sequences (Sigma) which are listed in table 2. Expression of the osteogenic marker genes were normalized to GAPDH levels and fold inductions were calculated by using  $\Delta\Delta\text{CT}$  method. hMSCs cultured on TCPs in basic medium for 7 days were used as calibrator. Two independent experiments with  $n=3$  for each condition were performed for the qPCR analysis, and the results of one representative experiment are presented here.

#### **4.2.8. Statistical analysis**

Statistical comparisons were performed using One-way Analysis of Variance (ANOVA) followed by a Tukey's multiple comparison post-hoc test. Error bars indicate one standard deviation. For all figures, the following p-values apply: \* $p < 0.05$ .

Table 2. Primer sequence of the osteogenic genes investigated.

Gene	Primer sequences
GAPDH (housekeeping gene)	5'-CCATGGTGTCTGAGCGATG 5'-CGCTCTCTGCTCCTCTGTT
Alkaline phosphatase (ALP)	5'-TTCAGCTCGTACTGCATGTC 5'-ACAAGCACTCCCACTTCATC
Bone morphogenetic protein 2 (BMP2)	5'-GCATCTGTTCTCGAAAAACCT 5'-ACTACCAGAAACGAGTGGGAA
Bone sialoprotein (BSP)	5'-TCCCGTTCTCATTTCATA 5'-CCCCACCTTTTGGGAAAAC
Osteocalcin (OC)	5'-CGCCTGGGTCTCTCACTAC 5'-TGAGAGCCCTCACACTCCTC
Osteopontin (OP)	5'-CCAAGTAAGTCCAACGAAAG 5'-GGTGATGTCCTCGTCTGTA

## 4.3. Results

### 4.3.1. Mineral film characterization

The 2-step biomimetic technique employed for preparation of the CaP coatings resulted in the formation of a uniform crystalline CaP layer that covered the entire surface of the Ti plates (Figure 1.a, b and c). The SEM micrographs showed CaP crystals with a plate-like morphology, which formed perpendicular to the surface of the Ti plates. The morphology of the crystals was modified by addition of  $\text{Sr}^{2+}$  to the initial CPS solution.  $\text{Sr}^{2+}$ -added CPS solution resulted in smaller and less sharp CaP crystals (Figure 1. c).

The presence of the CaP film was confirmed by EDS spectra of the samples, in which sharp peaks of calcium, phosphorous, and oxygen were visible (Figure 1. d-f). EDS elemental maps also showed that Ca and P elements were homogeneously distributed on the surface (Figure 1. g-l). EDS results showed presence of  $\text{Sr}^{2+}$  in the CaP coatings prepared with a concentration of 1000  $\mu\text{M}$   $\text{Sr}^{2+}$  in the CPS solution (Figure 1. f). The EDS strontium elemental maps indicated that  $\text{Sr}^{2+}$  was homogeneously distributed within the coating (Figure 1. m, n, o). Quantification of the EDS results indicated an incorporation of approximately 3 at% of strontium into CaP coatings at the highest concentration of  $\text{Sr}^{2+}$  in CPS solution (Table 3.). EDS did not detect  $\text{Sr}^{2+}$  in the coating with low  $\text{Sr}^{2+}$  incorporation. However, ICP measurements showed the presence of 0.44 and 16.49 mg/l  $\text{Sr}^{2+}$  in the coatings with low and high incorporation of  $\text{Sr}^{2+}$  dissolved in  $\text{HNO}_3$ , respectively (Table 3). Calculation of atomic ratios indicated that the ratio of Sr/P increased from 0.021 to 0.098 by increasing the concentration of  $\text{Sr}^{2+}$  in CPS solution from 0  $\mu\text{M}$  to 1000  $\mu\text{M}$ . The Ca/P ratio in these conditions, however, was calculated to be 1.197 and 1.091, respectively. The (Ca+Sr)/P ratios remained constant at approximately 1.2.

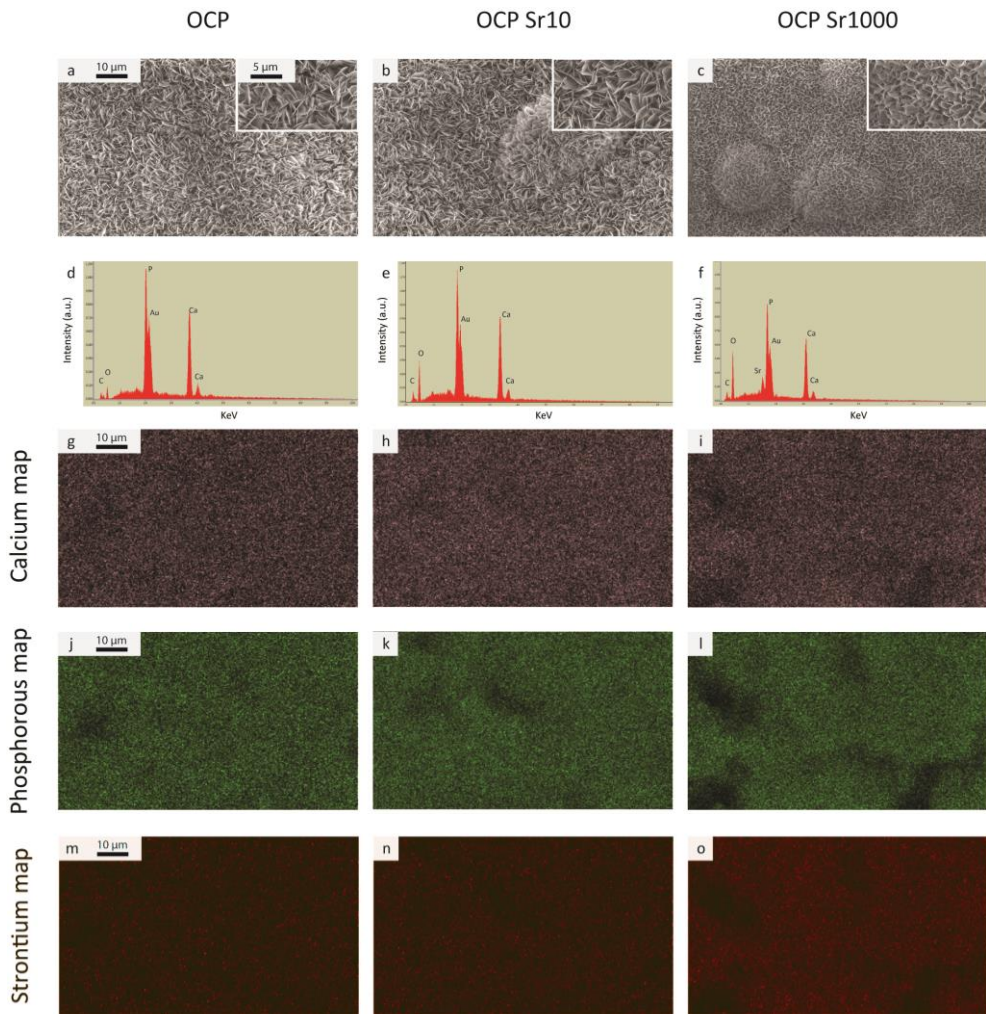


Figure 1. SEM images (a,b,c), EDS spectra (d,e,f), Ca elemental map (g,h,i), P elemental map (j,k,l) and Sr elemental map (m,n,o) of OCP, OCP Sr10 and OCP S1000, respectively. A crystalline CaP layer was formed on the surface of Ti plates with a homogenous distribution of all the elements. Presence of  $\text{Sr}^{2+}$  in higher concentration was detected in EDS spectrum and Sr elemental map of OCP Sr1000. Moreover, the morphology of the coatings changed upon addition  $1000 \mu\text{Sr}^{2+}$  to CPS solution resulting in smaller and less sharp crystals.

The results of the XRD and FTIR analyses for CaP coatings without and with Sr<sup>2+</sup> (Figure 2) were in accordance with data obtained in earlier studies when similar biomimetic coating method was applied [37-39]. The XRD patterns (Figure 2. a) of the coatings exhibited peaks at 2 $\theta$ =4.7° corresponding to (010) diffraction line and at 2 $\theta$ =25.8° corresponding to (002) plane, both typical of triclinic octacalcium phosphate (OCP) crystals. The peaks observed at 2 $\theta$ =9.8° and at 2 $\theta$ =27-28.5° can also be attributed to the OCP structure. The broad set of peaks at approximately 2 $\theta$ =31.5° to 32.5° are common for both OCP and apatitic structures. A small shift of approximately 2 $\theta$ =0.1° towards lower degrees was observed in some of the characteristic OCP peaks, when the OCP Sr1000 coating was analyzed. Supplementary figure 1 summarizes the position of the main peaks in the XRD patterns of the coatings without and with Sr<sup>2+</sup> incorporation.

The FTIR spectra of the coatings (Figure 2. b) exhibited sharp P-O bands at 560 cm<sup>-1</sup> and 600 cm<sup>-1</sup>. Moreover, the bands at 906 cm<sup>-1</sup> and 850 cm<sup>-1</sup> were typical HPO<sub>4</sub><sup>2-</sup> bands in the OCP phase. Nevertheless the vibration bands observed between 1020 cm<sup>-1</sup> and 1070 cm<sup>-1</sup> were less sharp and less numerous as compared to phase-pure OCP [38-39]. The small bands observed at 1450 cm<sup>-1</sup> and at 1480 cm<sup>-1</sup> corresponded to the carbonate group typical of A-B carbonated apatite, suggesting that apart from the OCP, the coating comprised a carbonated apatitic phase. The typical PO<sub>4</sub><sup>3-</sup> and HPO<sub>4</sub><sup>-</sup> bands of the coatings prepared in presence of higher concentration of Sr<sup>2+</sup> were less sharp, suggesting a decrease in crystallinity.

Table 3. Sr content measured by EDS and ICP, and atomic ratios quantified based on EDS data in CaP coatings. The Sr content in OCP Sr1000 was approximately 3 at%, whereas the content of both OCP and OCP Sr10 coating was within the background noise, below 1 at%.

Increasing the concentration of Sr<sup>2+</sup> in CPS solution resulted in increasing in Sr/P and a slight decrease in the Ca/P ratios, while (Ca+Sr)/P ratio constantly remained at approximately 1.2.

Sample	Sr content (at%)	Sr content (mg/l)	Ca/P ratio	Sr/P ratio	(Ca+Sr)/P ratio
OCP Sr0	0.780	0.024	1.197	0,021	1,218
OCP Sr10	0,698	0.444	1,168	0,021	1,189
OCP Sr1000	2.964	16.490	1.091	0,097	1,189

### 4.3.2. Cell morphology

Cells cultured on TCPs with 1000  $\mu\text{M}$   $\text{Sr}^{2+}$  in the basic medium appeared to have a higher aspect ratio compared to cells cultured in basic medium without  $\text{Sr}^{2+}$  addition, while no apparent differences were observed between the control, and the cells treated with 10  $\mu\text{M}$  of  $\text{Sr}^{2+}$  (figure 3.a-c).

Quantification of the cell parameters using CellProfiler based on immunofluorescent images showed that the cell area was reduced dose-dependently when  $\text{Sr}^{2+}$  was added to cell medium. The eccentricity was however significantly increased upon addition of  $\text{Sr}^{2+}$  to cell medium in a dose-dependent manner, confirming increase in elongation of the cells treated with  $\text{Sr}^{2+}$ .

Similar results were obtained when cells were cultured on OCP coatings. After 1 day, cells cultured on OCP Sr1000 coatings appeared more elongated in their morphology compared to the cells cultured on OCP and OCP Sr10 coatings (Figure 3.d-f). The adhesion points were observed in the cells cultured on all the coatings (Figure 3.g-i).

Quantification of the morphology parameters of the cells cultured on CaP coatings based on immunofluorescent images indicated that area of the cells cultured on OCP Sr10 was significantly higher than the area of those cultured on OCP without strontium incorporation. The eccentricity of cells cultured on OCP Sr1000 was also significantly higher than the one of the cells cultured on OCP and OCP Sr10 coatings.

### 4.3.3. DNA content and ALP activity

At 7 days, the addition of 1000  $\mu\text{M}$   $\text{Sr}^{2+}$  to the osteogenic media increased the hMSC DNA content in both donors when cultured on TCPs, however, this increase was only significant in cells of Donor 1. A similar trend was seen when 1000  $\mu\text{M}$  of  $\text{Sr}^{2+}$  was added to basic media in Donor 1 cultures, but not when cells from Donor 2 were cultured (Figure 4. a and b). The DNA content of the cells did not increase between 7 and 14 days, suggesting the formation of a confluent monolayer before the second time point analysis.

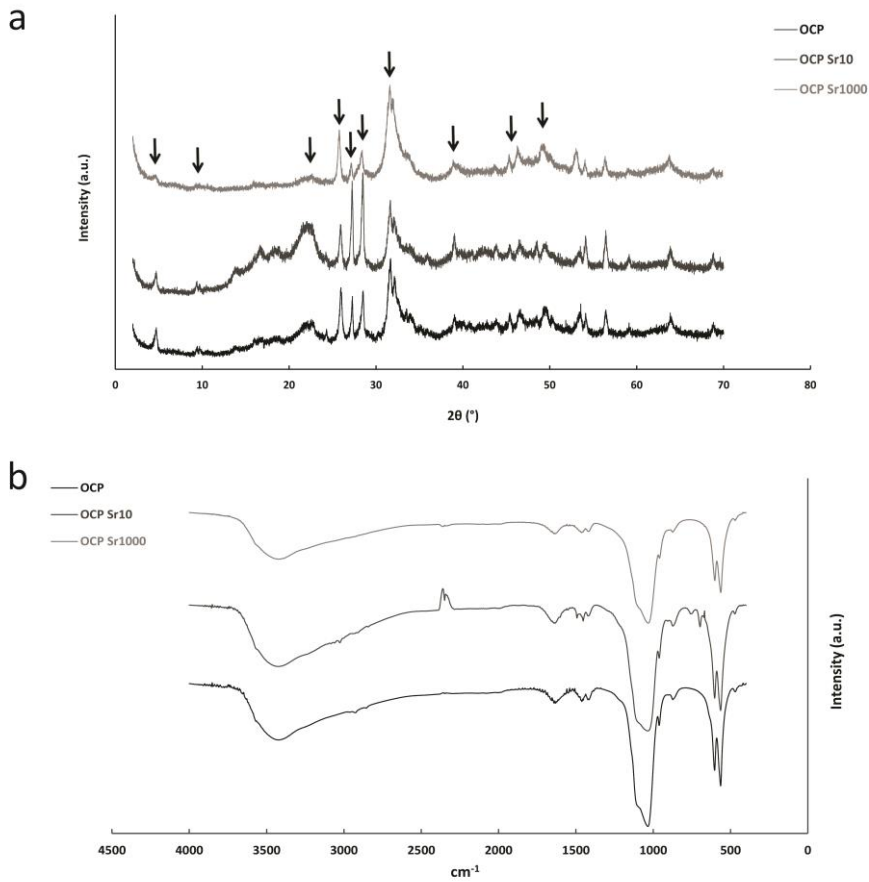


Figure 2. XRD patterns (a) and FTIR Spectra (b) of the coatings. The XRD peaks of OCP structure. The XRD patterns and the FTIR spectra suggested that the coatings predominantly consisted of OCP, with presence of some carbonated apatite. Furthermore, the data suggested that an increase of  $\text{Sr}^{2+}$  content of the coating led to a limited decrease in crystallinity.

While at 7 days no significant differences in ALP activity were seen among the conditions, at 14 days, the addition of either 10  $\mu\text{M}$  or 1000  $\mu\text{M}$   $\text{Sr}^{2+}$  to osteogenic media increased the normalized ALP activity of hMSCs. This result was statistically significant for cells of Donor 1, and for 1000  $\mu\text{M}$  in Donor 2 cells (Figure 4. c and d).

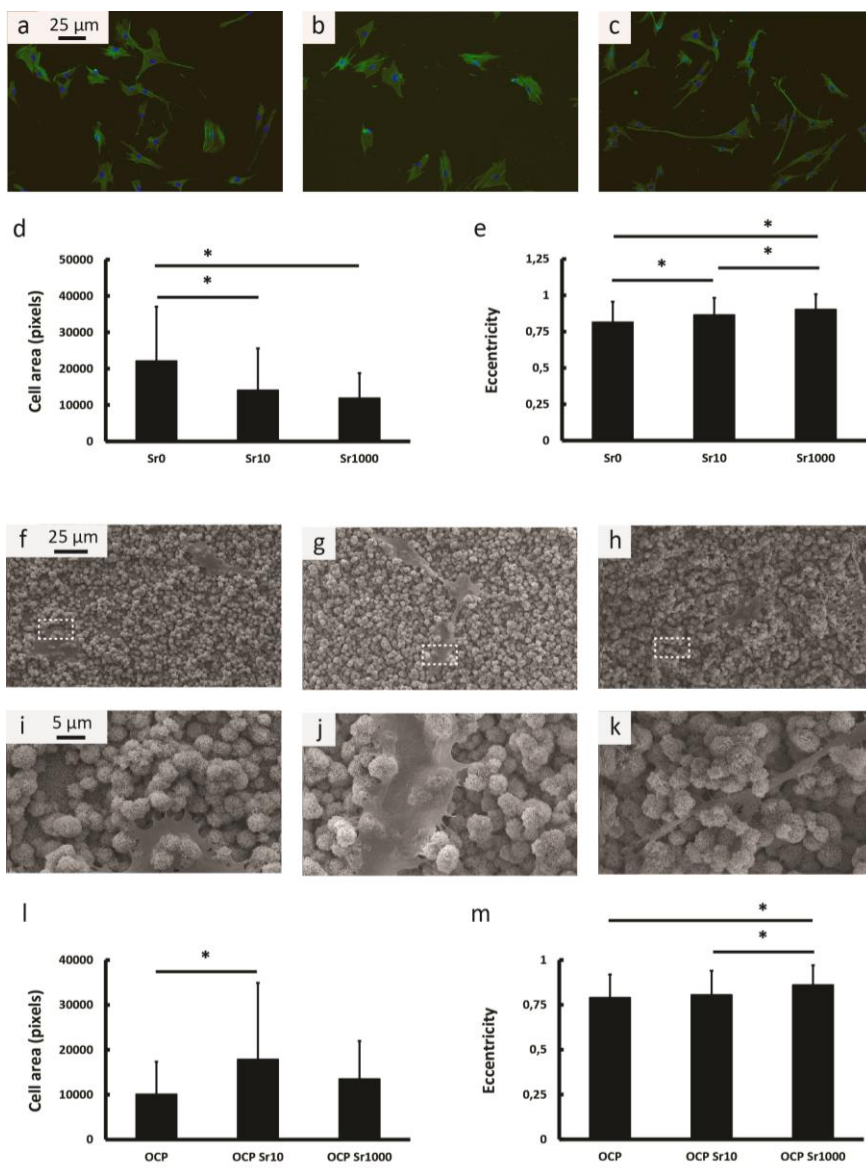


Figure 3. Fluorescent microscopy images of the cells cultured for 1 day on TCPs in basic medium without 0 (a), and supplemented with 10 (b) or 1000 (c)  $\mu\text{M}$   $\text{Sr}^{2+}$ , quantification of cell area (d) and eccentricity (e) of these cells, SEM images of the cells cultured for 1 day in basic medium on OCP (f), OCP Sr10 (g) and OCP Sr1000 (h) coatings with (i), (j) and (k) magnified images of the areas marked with dashed lines in (f), (g) and (h) images, respectively and quantification of cell area (l) and eccentricity (m) of these cells. In fluorescent images, the cells were stained with Dapi (in blue) and Phalloidin (in green) showing cell nuclei and cytoskeleton, respectively.

No differences in DNA content were seen when cells were cultured on coatings for 7 days, however, at 14 days in Donor 2 cells, the incorporation of  $\text{Sr}^{2+}$  into OCP increased the DNA content, with this result being statistically significant for both basic and osteogenic media at both incorporation concentrations. This effect, however, was not observed in Donor 1 cells. A difference in proliferation profile was observed between the cells from the two donors, with an increase in DNA content between day 7 and day 14 for the cells from Donor 2 but not for the Donor 1 cells (Figure 5. a and b).

At 14 days, the incorporation of  $\text{Sr}^{2+}$  into OCP at the higher concentration (OCP Sr1000) increased the ALP activity in Donor 1, with this result being statistically significant in both basic and osteogenic media. This effect was also observed in osteogenic medium in Donor 2 cells (Figure 5. c and d).

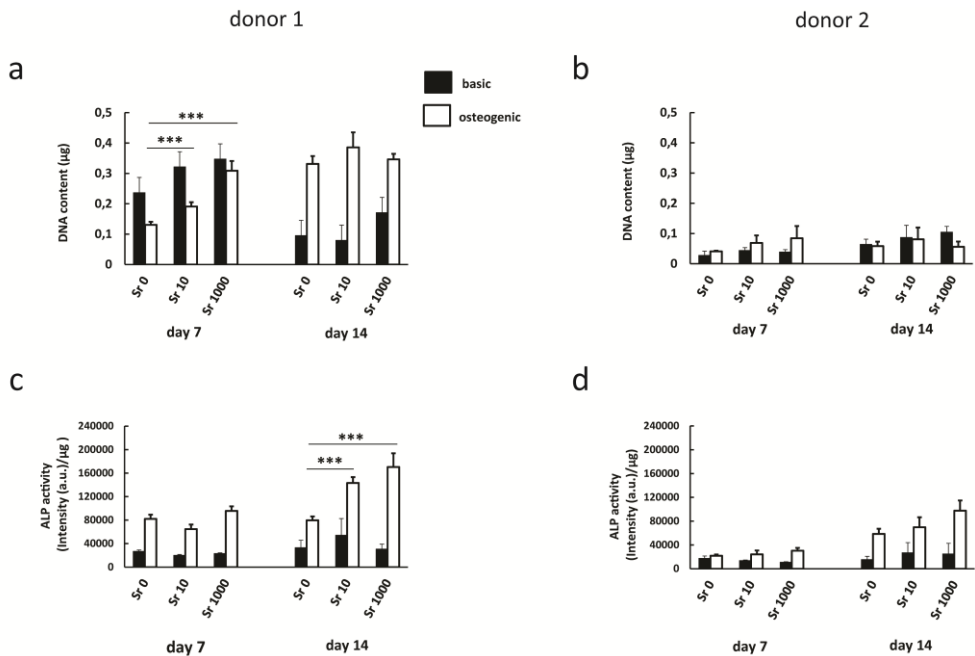


Figure 4. DNA content (a, c) and ALP activity (b, d) of hMSCs of respectively Donor 1 and Donor 2 cultured on TCPs.  $\text{Sr}^{2+}$  supplementation in cell culture medium slightly increased the DNA content of the Donor 1 cells at day 7, while no differences were observed for the other conditions. At day 14, addition of  $\text{Sr}^{2+}$  to osteogenic medium resulted in increasing ALP activity of hMSCs in a dose-dependent manner.

#### 4.3.4. Expression of osteogenic markers at mRNA level

While in basic medium, no significant differences in ALP mRNA expression of cells cultured on TCPs were observed among the conditions at either time point, at 7 days, the addition of 1000  $\mu\text{M}$  of  $\text{Sr}^{2+}$  to the osteogenic media significantly increased the ALP expression in Donor 1 cells. At 14 days, the addition of  $\text{Sr}^{2+}$  to osteogenic media increased the ALP expression, however, this effect was not consistent between the donors (Figure 6. a-b).

At day 7, no differences among the conditions were observed in the BSP expression when cells were cultured on TCPs in basic medium. However, at day 14,  $\text{Sr}^{2+}$  supplementation in both basic and osteogenic media resulted in an ascending trend in expression of BSP dependent on  $\text{Sr}^{2+}$  dose, with a significant effect in osteogenic medium in donor 1 and in basic medium in donor 2 cells (Figure 6. c-d).

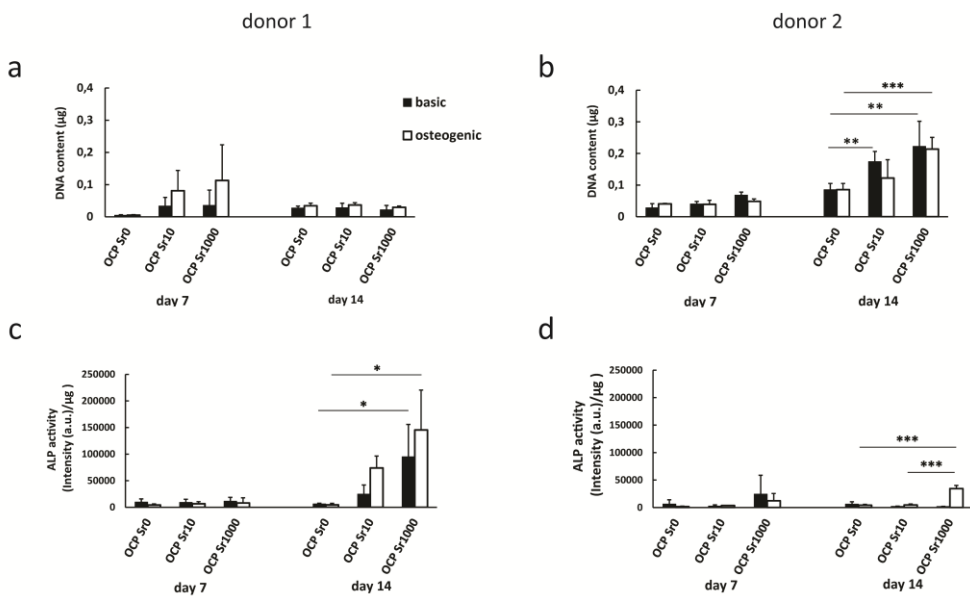


Figure 5. DNA content (a, c) and ALP activity (b, d) of hMSCs of respectively Donor 1 and Donor 2 cultured on the coatings. At day 14, an increase in DNA content of the cells of Donor 2 was observed upon incorporation of  $\text{Sr}^{2+}$  into the coatings. At day 14, addition of  $\text{Sr}^{2+}$  to either medium in cultures of Donor 1 cells and to osteogenic medium in cultures of Donor 2 cells resulted in an increase in ALP activity in a strontium dose-dependent manner.

At days 7 and 14, the addition of  $Sr^{2+}$  to basic media only appeared to influence BMP2 expression, however, this result was statistically significant only between 0 and 1000  $\mu M$  in Donor 1, and 10 and 1000  $\mu M$  in Donor 2. A similar trend was observed in OP expression in basic media, with significant difference between 10 and 1000  $\mu M$  in Donor 2 cells. The addition of 1000  $\mu M$  to osteogenic media significantly increased OP expression in Donor 1, however, this result was not observed in Donor 2 cells (Figure 6. e-f).

No significant differences among the conditions were observed in OC expression at 7 days in either medium. At day 14, the addition of  $Sr^{2+}$  to both basic and osteogenic media appeared to decrease OC expression in a dose dependent manner in donor 1, however, this result was statistically significant only in osteogenic medium. Unlike in Donor 1 cells, the OC expression by the cells of Donor 2 was significantly increased upon addition of 1000  $\mu M$  of  $Sr^{2+}$  to basic medium at day 14, while no effect was seen in osteogenic medium. (Figure 6. g-j). At day 14, hMSCs of donor 1 only, cultured on OCP Sr1000 expressed slightly higher ALP mRNA levels compared to the cells cultured on OCP and OCP Sr10 in basic medium. A similar effect was detected in osteogenic medium, however, this was only significant between OCP and OCP Sr1000. (Figure 7. a-b).

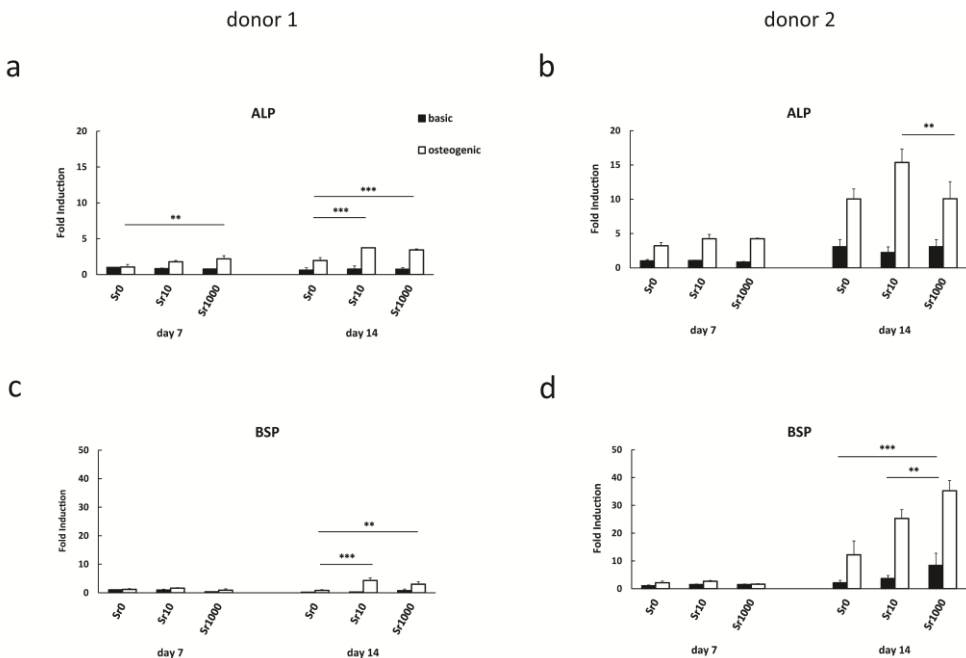
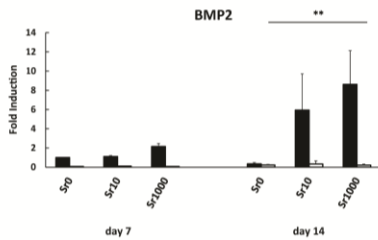
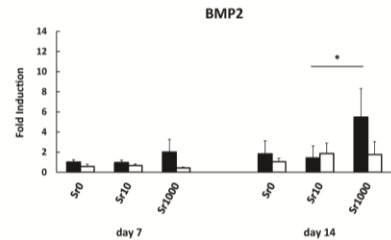


Figure 6. Continues in the next page.

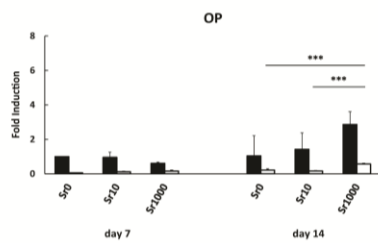
e



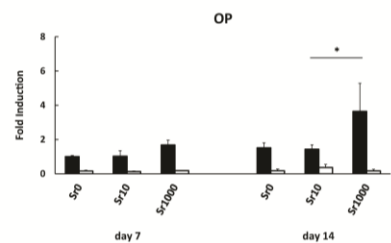
f



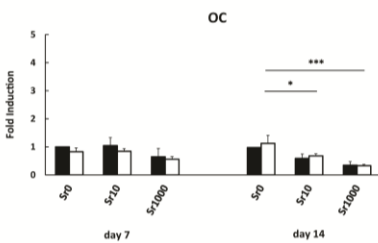
g



h



i



j

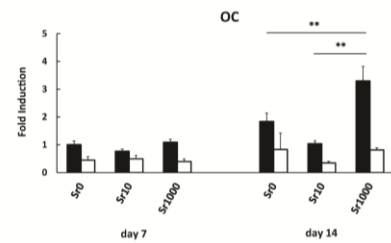


Figure 6. mRNA expression of ALP (a,b), BSP (c,d), BMP2 (e,f), OP (g,h) and OC (i,j) by respectively hMSCs of Donor 1 and Donor 2 cultured on TCPs. The results are normalized for the mRNA level of GAPDH as a housekeeping gene and calibrated for the mRNA level of each gene of hMSCs cultured in basic medium without supplementation for 7 days. mRNA expression of all the osteogenic markers was altered upon addition of  $\text{Sr}^{2+}$  to cell culture medium.  $\text{Sr}^{2+}$  ions generally increased the expression of ALP, BSP, BMP2 and OP, with comparable trends in both donors. Opposing trends were however, observed in the expression of OC from Donor 1 and Donor 2 cells.

Differences in the expression of BSP of cells cultured on different coatings were only observed for Donor 1. At days 7 and 14, incorporation of  $\text{Sr}^{2+}$  into OCP coatings increased the expression of BSP in basic medium in a dose-dependent manner. (Figure 7. c-d).

While low BMP2 levels were observed for all conditions in osteogenic medium, at day 14, hMSCs of donor 1 cultured on OCP Sr1000 coating showed higher BMP2 expression compared to the ones cultured on OCP and OCP Sr10 in basic medium. A similar effect, however not significant, was observed in donor 2 as well (Figure 7. e-f).

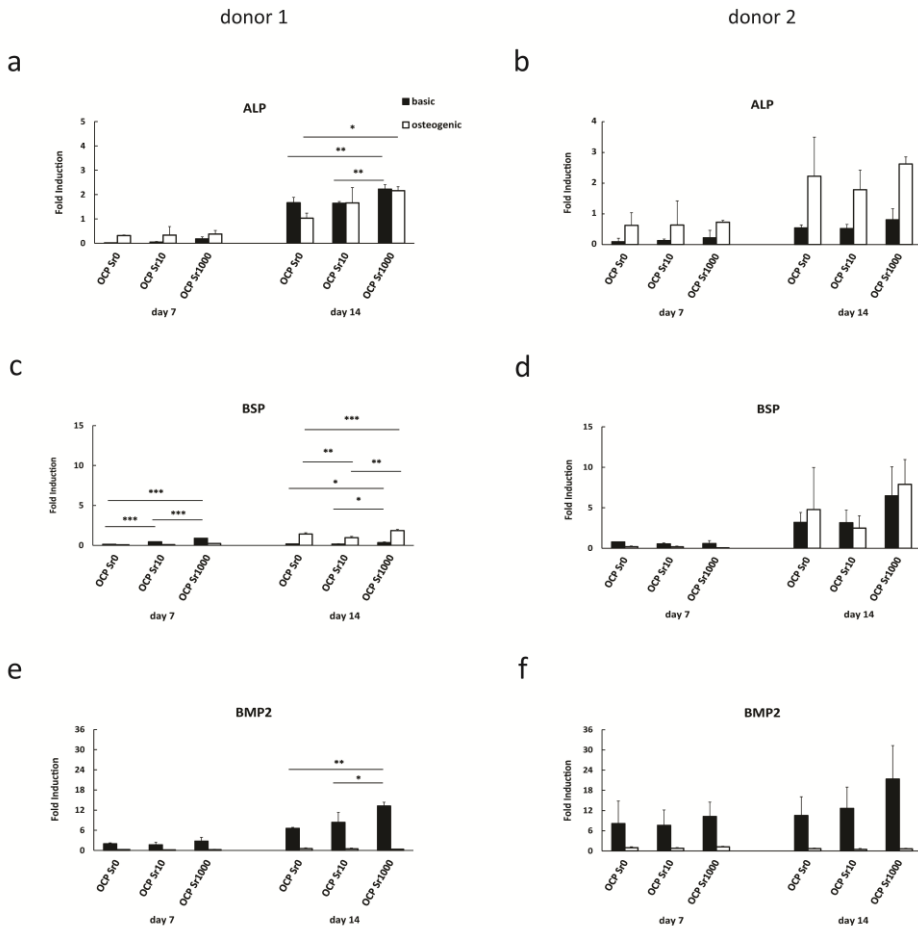
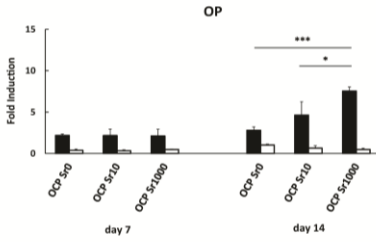
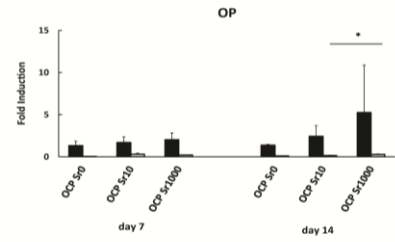


Figure 7. Continues in the next page.

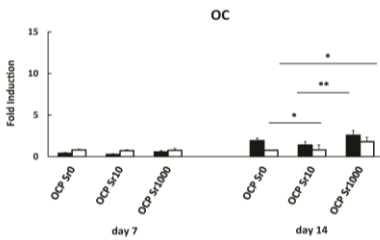
g



h



i



j

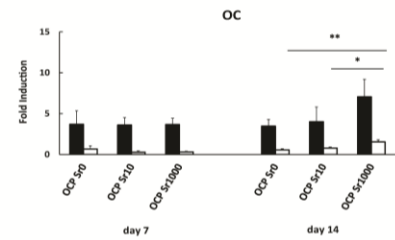


Figure 7. mRNA expression of ALP (a,b), BSP (c,d), BMP2 (e,f), OP (g,h) and OC (i,j) by respectively hMSCs of Donor 1 and Donor 2 cultured on CaP coatings. The results are normalized for the mRNA level of GAPDH as a housekeeping gene and calibrated for the mRNA level of each gene in hMSCs cultured in basic medium on OCP coating for 7 days. In general, presence of Sr<sup>2+</sup> in the CaP coatings positively affected the expression of osteogenic markers. Similar trends were observed in the two donors, with the effects being stronger in Donor 1 cells.

Similar to BMP2, expression of OP was low in osteogenic medium in all the conditions. At day 14, expression of OP in basic medium was higher in OCP Sr1000 coatings compared to OCP and OCP Sr10 in donor 1. A similar, but non-significant effect was observed in donor 2 at similar conditions (Figure 7. g-h).

While at 7 days, no significant differences were observed, at day 14, in donor 1, higher OC levels were seen in both media when cells were cultured on OCP Sr1000 coatings compared to OCP and OCP Sr10, however, in basic medium this effect was only significant between OCP Sr1000 and OCP Sr10. In donor 2, OC was upregulated in osteogenic medium in the cells cultured on OCP Sr1000 compared to the cells cultured on OCP and OCP Sr10 (Figure 7. i-j).

### 4.3.5. Ion concentrations in cell medium

Concentrations of  $\text{Ca}^{2+}$  and  $\text{Sr}^{2+}$  ions in basic medium up to day 7 were measured using ICP-MS (Table 4).  $\text{Ca}^{2+}$  content of control cell culture medium, not containing cells or coatings, slightly decreased after 2 days. However, this concentration reached the original values at later time points. A major decrease of more than 1  $\mu\text{M}$  in  $\text{Ca}^{2+}$  content of cell medium incubated with CaP coatings cultured with cells was detected after 2 days of culture.  $\text{Ca}^{2+}$  content of the medium remained constant at this level at later time points. This effect was independent of  $\text{Sr}^{2+}$  incorporation.

A  $\text{Sr}^{2+}$  release of approximately 12  $\mu\text{M}$  was observed in cell medium conditioned with OCP Sr1000  $\mu\text{M}$  after 2 days. The  $\text{Sr}^{2+}$  release was calculated as approximately 5 and 2  $\mu\text{M}$  for 4 and 7 days, respectively. The  $\text{Sr}^{2+}$  release was negligible in the medium conditioned with OCP and OCP Sr10 samples.

Table 4.  $\text{Ca}^{2+}$  and  $\text{Sr}^{2+}$  concentration (based on  $\mu\text{M}$ ) of basic medium collected during the culture of hMSCs on CaP coatings with, as a control, basic medium without materials or cells. A decrease of  $\text{Ca}^{2+}$  concentration was observed after 2 days in all the samples, after which a plateau at about 700  $\mu\text{M}$  was reached. A release of 12, 5 and 3  $\mu\text{M}$   $\text{Sr}^{2+}$  after 2, 4 and 7 days, respectively was detected during cell culture of OCP Sr1000, suggesting dissolution/precipitation events occurring on the coating surface.

Day	Incubated medium		OCP Sr0		OCP Sr10		OCP Sr1000	
	$\text{Ca}^{2+}$ content	$\text{Sr}^{2+}$ content						
0	1720.50	0.55	1720.50	0.55	172.50	0.55	1720.50	0.55
2	1226.97	0.57	790.99	0.33	769.39	0.48	820.54	12.22
4	1373.85	0.61	773.75	0.34	707.84	0.40	735.46	5.02
7	1757.04	0.69	769.44	0.60	714.88	0.37	770.47	3.22

## 4.4. Discussion

Among the trace elements within bone mineral, strontium is of particular interest due to its reported osteogenic and anti-resorptive effects [17-18]. Pasqualetti et al. suggested that, while absolute levels of strontium influence the embryonic mineralization, the actual strontium-to-calcium ratio may also have an important role in the mineralization process [40]. In addition to the chemical interplay, strontium has been suggested to influence cellular responses by affecting the

physicochemical properties of the mineral [11]. In this manner, strontium ranelate is thought to prevent osteoporotic fractures via an increase in bone hardness due to the  $\text{Sr}^{2+}$  ionic substitution [41-42]. In order to further develop strontium-based treatments, the exact mechanisms of strontium's actions are yet to be fully elucidated.

In the current study, a biomimetic approach was taken to prepare strontium-incorporated CaP coatings on Ti substrates. The results indicated that a predominantly crystalline OCP layer formed which was not inhibited by the lower concentration of strontium, though the crystal morphology was influenced at higher strontium concentrations. The presence of strontium was confirmed using EDS and ICP. The decrease in the Ca/P ratio, and increase in the Sr/P ratio, with a constant (Ca+Sr)/P ratio (1.2) may be due to ionic substitution of  $\text{Ca}^{2+}$  by  $\text{Sr}^{2+}$ , however the data presented here is not sufficient to strongly confirm this. While the calculated ratio of Ca/P of 1.2 in this study differs to the theoretical OCP value of 1.33, this value may have been affected by the semi-quantitative nature of the elemental analysis used. Additionally, the FTIR data indicated the presence of carbonate bands, suggesting the coating formed was not phase-pure. Further, when compared to the coatings formed in absence of  $\text{Sr}^{2+}$  ions, the small shift to smaller angles that was observed in the XRD pattern of OCP Sr1000 coatings also indicated a possible change in the lattice parameters of OCP crystals due to the incorporation of strontium ions into the OCP lattice [43]. This however may be due to broadening of the diffraction peaks upon addition of the  $\text{Sr}^{2+}$  or the overall structural change towards a more apatitic phase resulting in modification of the XRD pattern. Nevertheless, physical entrapment of strontium acetate or another strontium salt into the coating during deposition cannot be fully excluded. Regardless, this data proved the formation of an OCP phase with varying  $\text{Sr}^{2+}$  content which was directly dependent on the impregnation concentration of  $\text{Sr}^{2+}$ . The results indicated a release of strontium from OCP Sr1000 coatings into basic cell medium at 12, 5 and 3  $\mu\text{M}$  after 2, 4 and 7 days, respectively. A relatively high release of  $\text{Sr}^{2+}$  after 2 days was accompanied by a pronounced uptake of  $\text{Ca}^{2+}$  ions from the medium, while at the later time points, the  $\text{Ca}^{2+}$  concentration remained constant and release of  $\text{Sr}^{2+}$  decreased. This may have been due to reprecipitation of a new biological apatite layer formed through dissolution/reprecipitation events occurring on the coating surface [44]. The maximum amount of strontium in the prepared OCP coatings was approximately 8.9 % of the calcium content, which aligns with the percentage reported for a similar method of production

[11]. These values are also in the range reported for that of human bone, being 3.9 at% [45]. However, due to ion release via CaP dissolution, it is difficult to relate total incorporated percentage to the actual ion concentration exposed to the cell.

Cytoskeletal components such as actin have been reported to be involved in mediating hMSC proliferation and differentiation toward osteogenic lineage, with early cytoskeletal organization reportedly having a major effect on cell fate [46]. Baradas et al. [47], for example, have shown that the  $\text{Ca}^{2+}$  induced morphological changes began to happen in the cytoskeleton after 12 hours. Therefore we have selected a 24 hours time point for studying the early morphological organization induced by  $\text{Sr}^{2+}$ .

The presence of strontium appeared to influence cell shape, with a more elongated morphology observed as compared to cells cultured in absence of strontium. In particular, a dose-dependent effect on cell eccentricity was detected upon increasing strontium concentration. Similar changes in eccentricity have previously been identified as important parameters for interpreting changes in cellular responses [36]. In this study, elongated cells generally corresponded to a higher expression of osteogenic markers at mRNA level. While changes in cell morphology are often considered to relate to cell fate, the morphology corresponding to specific lineages remains uncertain [47-50]. As such, while shape differences were noted in this study, further investigation is needed to provide a more detailed context for these results.

A different trend in the changes in cell area as a function of  $\text{Sr}^{2+}$  content was observed on TCPs compared to the coatings. Firstly, it should be kept in mind the released  $\text{Sr}^{2+}$  from the coating is at much lower level as compared to the ones added to cells cultured TCPs, and it is not possible to fairly compare these two conditions. Furthermore, the cell microenvironment provided by the CaP coatings included the presence of other ions as well as the topographical cues of the substrate which is substantially different from that of the cultures on TCPs, which may have resulted in different morphological organization in the cells cultured in these two microenvironment.

The addition of strontium appeared to influence the DNA production of hMSCs, which is considered an indicator of cell proliferation. However, these changes were relatively small, being less than two-fold.  $\text{Sr}^{2+}$  ions have previously shown to increase the proliferation of human osteoblasts [51], and increase the production of collagen matrix in murine pre-osteoblast cells [52]. Therefore, enhancing the

proliferation and survival of bone forming cells has been proposed as a mechanism in which  $\text{Sr}^{2+}$  favors bone formation [4,53]. While the results did not reject this hypothesis, this study could not strongly support this statement.

ALP enzyme activity of hMSCs was generally increased upon exposure to  $\text{Sr}^{2+}$  ions via both delivery methods, although there was some variation between donors. This finding is consistent with previously reported data [26-28, 51-52].

The effect of strontium on the expression of osteogenic markers at the mRNA level appeared to be dose dependent. This suggests that within the limits of this study, a higher dose of strontium used was favorable. This result aligns with previously published data, in which strontium was reported to have a dose dependent effect on the ALP activity of hMSCs [28, 51, 54]. Similarly, Brennan et al. [51] and Bonnelye et al. [17] detected the biologic effects of  $\text{Sr}^{2+}$  in the form of strontium ranelate on osteogenic markers at a minimum concentration of 1000  $\mu\text{M}$ . Therefore, strontium release and dose should be considered in future strategies.

The expression of osteogenic markers was also highly dependent on the medium used. Generally, expression of BMP2, OP and OC was higher in basic medium, whereas ALP and BSP genes were more highly expressed in osteogenic medium. The osteogenic medium used in the present study contained 10 nM dexamethasone, a concentration previously shows to be optimal for formation of mineralized nodules in human osteoblast precursor cell culture [55]. At this concentration, dexamethasone has also been reported to increase the expression of ALP and RUNX2 of human primary bone cells at mRNA and protein level [47, 55-57]. Conversely, evidence exists for the negative effects of glucocorticoids, such as dexamethasone, on bone mineralization, which may lead to lower bone mineral density [58]. Wiontzek et al. also demonstrated the inhibitory effects of dexamethasone, in which intracellular  $\text{Ca}^{2+}$  concentration increased in MG63 shortly after dexamethasone treatment [59]. It appears that in this study, the addition of dexamethasone to cell medium inhibited the regulatory effects of  $\text{Ca}^{2+}$ , resulting in down-regulation of  $\text{Ca}^{2+}$ -dependent osteogenic markers including BMP2, OP and OC [47].  $\text{Sr}^{2+}$  ions, as a divalent cation similar to  $\text{Ca}^{2+}$ , may act on similar cellular targets as  $\text{Ca}^{2+}$ , and similar effects are expected to occur [47].

Generally, hMSCs cultured on OCP coatings with and without Sr incorporation had a higher expression of BMP2, OP and OC, and lower expression of ALP and BSP, when compared to cells cultured on TCPs in strontium supplemented media. This is likely due to the regulatory effects of  $\text{Ca}^{2+}$  ions on BMP2, OP and OC expression.

The  $\text{Ca}^{2+}$  level in cell medium containing the different coatings was similar and independent of  $\text{Sr}^{2+}$  incorporation, while the  $\text{Sr}^{2+}$  concentration differed, which may explain differences in the expression of the osteogenic markers in coatings with and without strontium and suggests the combined effects of both ions. This is further highlighted by the fact that, while the medium concentration of strontium was similar between the OCP Sr1000 and  $10 \mu\text{M Sr}^{2+}$  supplemented media, the hMSC response in these conditions was very different. The expression of BMP2, OP and OC in OCP Sr1000 was substantially higher than that for the cells cultured with 10 and 1000  $\mu\text{M Sr}^{2+}$  salt, indicating a combinatory effect of strontium and calcium ions on the osteogenic markers, which are known to be  $\text{Ca}^{2+}$ -dependent. As expected, such an effect was not observed on ALP and BSP expression, even when the presence of strontium in the coatings resulted in upregulating these genes.

It is worth mentioning that the expression of the osteogenic biomarkers at mRNA level does not necessarily translate to production of these protein. Therefore, the study of the effects of  $\text{Sr}^{2+}$  addition to the CaPs on production of the osteogenic matrix proteins is highly recommended for future experiments.

It should be noted that changes in calcium content of the medium in presence of OCP coating are expected to be accompanied by the changes in inorganic phosphate concentration, also known to affect the hMSCs behavior [60] and this effect needs further investigation. Furthermore, possible direct effects of changes in crystal structure upon incorporation of strontium into the coating require further investigation, since the cell fate can be affected by the physical properties of the material surface [61], such as roughness, micro- and macro-porosity [62], grain size [63] and topography [50-51, 64].

#### 4.5. Conclusion

This study confirms that strontium promotes the osteogenic differentiation of bone marrow derived hMSCs, when introduced to the cells as either dissolved salt or incorporated into CaP coatings. Importantly, the positive effect of strontium appears to synergistically increase when used in combination with CaP coatings. Overall, this study supports the use of  $\text{Sr}^{2+}$ -incorporated CaPs as potential synthetic bone graft substitutes.

Supplementary data 1. Position of the main XRD peaks (based on  $2\theta$ ) appeared in OCP coatings without and with  $\text{Sr}^{2+}$  incorporation. The results showed a small shift to smaller  $2\theta$  degrees in many of the diffraction peaks upon addition of  $\text{Sr}^{2+}$  to the coatings, especially at higher concentrations.

Peak number	Position of the peak ( $2\theta$ )		
	OCP	OCP Sr10	OCP Sr1000
<b>1</b>	4.71	4.7	4.63
<b>2</b>	9.43	9.39	9.28
<b>3</b>	22.73	22.67	22.66
<b>4</b>	25.95	25.91	25.81
<b>5</b>	27.28	27.24	27.14
<b>6</b>	28.47	28.46	28.42
<b>7</b>	31.62	31.64	31.6
<b>8</b>	31.74	31.73	31.67
<b>9</b>	39.04	39.03	38.88
<b>10</b>	43.3	43.25	43.25
<b>11</b>	45.29	45.24	45.25
<b>12</b>	46.46	46.44	46.42
<b>13</b>	49.28	49.3	49.29
<b>14</b>	53,57	53,52	53,48
<b>15</b>	54.12	54.12	54.11
<b>16</b>	56.4	56.4	56.37
<b>17</b>	59.08	59.08	59.08
<b>18</b>	63.88	63.87	63.87
<b>19</b>	68.83	68.81	68.76

## References

1. J. Braux, F. Velard, C. Guillaume, S. Bouthors, E. Jallot, J. Nedelec, D. Laurent-Maquin, P. Laquerrière, A New Insight into the Dissociating Effect of Strontium on Bone Resorption and Formation., *Acta Biomater.* 7 (2011) 2593–2603.
2. M. Bohner, L. Galea, N. Doebelin, Calcium Phosphate Bone Graft Substitutes: Failures and Hopes, *J. Eur. Ceram. Soc.* 32 (2012) 2663–2671.
3. A. Bigi, G. Cojazzi, S. Panzavolta, A. Ripamonti, N. Roveri, M. Romanello, K. Noris Suarez, L. Moro, Chemical and Structural Characterization of the Mineral Phase from Cortical and Trabecular Bone, *J. Inorg. Biochem.* 68 (1997) 45–51.
4. L. Yang, B. Harink, P. Habibovic, Calcium Phosphate Ceramics with Inorganic Additives, Elsevier Ltd. (2011) 229–312.
5. T.N. Vo, F. Kurtis Kasper, A.G. Mikos, Strategies for Controlled Delivery of Growth Factors and Cells for Bone Regeneration, *Adv. Drug Delivery Rev.* 64 (2012) 1292–1309.
6. Y. Liu, K. de Groot, E.B. Hunziker, BMP-2 Liberated from Biomimetic Implant Coatings Induces and Sustains Direct Ossification in an Ectopic Rat Model, *Bone.* 36 (2005) 745 – 757.
7. A. Malhotra, M. Pelletier, R. Oliver, C. Christou, W.R. Walsh, Platelet-Rich Plasma and Bone Defect Healing, *Tissue Eng., Part A.* 20 (2014) 2614–2633.
8. M. Jäger, P. Hernigou, C. Zilkens, M. Herten, X. Li, J. Fischer, R. Krauspe, Cell Therapy in Bone Healing Disorders, *Orthop. Rev.* 2 (2010) 79–87.
9. D.J. Mooney, H. Vandenburgh, Cell Delivery Mechanisms for Tissue Repair, *Cell Stem Cell.* 2 (2008) 205–213.
10. E. Boanini, M. Gazzano, A. Bigi, Ionic Substitutions in Calcium Phosphates Synthesized at Low Temperature, *Acta Biomater.* 6 (2010) 1882–1894.
11. L. Yang, S. Perez-Amodio, F.Y. Barrère-de Groot, V. Everts, C.A. van Blitterswijk, P. Habibovic, The Effects of Inorganic Additives to Calcium Phosphate on In Vitro Behavior of Osteoblasts and Osteoclasts, *Biomaterials.* 31 (2010) 2976–2989.
12. A. Hoppe, N.S. Güldal, A.R. Boccaccini, A Review of the Biological Response to Ionic Dissolution Products from Bioactive Glasses and Glass-ceramics, *Biomaterials.* 32 (2011) 2757–2774.
13. P. Habibovic, J.E. Barralet, *Bioinorganics and Biomaterials: Bone Repair*, *Acta Biomater.* 7 (2011) 3013–3026.
14. S.D. Bain, C. Jerome, V. Shen, I. Dupin-Roger, P. Ammann, Strontium ranelate improves bone strength in ovariectomized rat by positively influencing bone resistance determinants. *Osteoporosis International*, 20 (2009) 1417–1428.
15. P.J. Meunier, C. Roux, E. Seeman, S. Ortolani, J.E. Badurski, T.D. Spector, J. Cannata, A. Balogh, E.M. Lemmel, S. Pors-Nielsen, The Effects of Strontium Ranelate on the Risk of Vertebral Fracture in Women with Postmenopausal Osteoporosis, *N. Engl. J. Med.* 350 (2004) 459–468.
16. S. O'donnell, A. Cranney, G. Wells, J. Adachi, J.Y. Reginster, Strontium Ranelate for Preventing and Treating Postmenopausal Osteoporosis, *Cochrane. Database. Syst. Rev.* 4 (2006) CD005326.
17. E. Bonnelye, A. Chabadel, F. Saltel, P. Jurdic, Dual Effect of Strontium Ranelate: Stimulation of Osteoblast Differentiation and Inhibition of Osteoclast Formation and Resorption In Vitro, *Bone.* 42 (2008) 129–138.
18. P.J. Marie, Strontium Ranelate: a Dual Mode of Action Rebalancing Bone Turnover in Favour of Bone Formation, *Curr. Opin. Rheumatol.* 18 (2006) S11–S15.
19. A. Sabareeswaran, B. Basu, S.J. Shenoy, Z. Jaffer, N. Saha, A. Stamboulis, Early Osseointegration of a Strontium Containing Glass Ceramic in a Rabbit Model. *Biomaterials.* 34 (2013) 9278–9286.
20. E. Gentleman, Y.C. Fredholm, G. Jell, N. Lotfibakhshaiesh, M.D. O'Donnell, R.G. Hill, M.M. Stevens, The Effects of Strontium-Substituted Bioactive Glasses on Osteoblasts and Osteoclasts In Vitro, *Biomaterials.* 31 (2010) 3949–3956.

21. J. Zhang, S. Zhao, Y. Zhu, Y. Huang, M. Zhu, C. Tao, C. Zhang, Three-Dimensional Printing of Strontium-Containing Mesoporous Bioactive Glass Scaffolds for Bone Regeneration. *Acta Biomater.* 10 (2014) 2269–2281.
22. O.Z. Andersen, V. Offermanns, M. Sillassen, K.P. Almqvist, I.H. Andersen, S. Sørensen, C.S. Jeppesen, D.C.E. Kraft, J. Bøttiger, M. Rasse, F. Kloss, M. Foss, Accelerated Bone Ingrowth by Local Delivery of Strontium from Surface Functionalized Titanium Implants, *Biomaterials.* 34 (2013) 5883-5890.
23. L. Zhao, H. Wang, K. Huo, X. Zhang, W. Wang, Y. Zhang, Z. Wu, P.K. Chu, The osteogenic Activity of Strontium Loaded Titania Nanotube Arrays on Titanium Substrates, *Biomaterials.* 34 (2013) 19-29.
24. K. Lin, L. Xia, H. Li, X. Jiang, H. Pan, Y. Xu, W.W. Lu, Z. Zhang, J. Chang, Enhanced Osteoporotic Bone Regeneration by Strontium-Substituted Calcium Silicate Bioactive Ceramics, *Biomaterials.* 34 (2013) 10028-10042.
25. S. Singh, A. Roy, B.E. Lee, J. Ohodnicki, A. Loghmanian, I. Banerjee, P.N. Kumta, A Study of Strontium Doped Calcium Phosphate Coatings on AZ31, *Mater. Sci. Eng., A.* 40 (2014) 357–365.
26. W. Zhang, Y. Shen, H. Pan, K. Lin, X. Liu, B.W. Darvell, W.W. Lu, J. Chang, L. Deng, D. Wang, W. Huang, Effects of Strontium in Modified Biomaterials, *Acta Biomater.* 7 (2011) 800–808.
27. [26] E. Boanini, P. Torricelli, M. Fini, F. Sima, N. Serban, I.N. Mihailescu, A. Bigi, Magnesium and Strontium Doped Octacalcium Phosphate Thin Films by Matrix Assisted Pulsed Laser Evaporation, *J. Inorg. Biochem.* 107 (2012) 65–72.
28. C. Capuccini, P. Torricelli, F. Sima, E. Boanini, C. Ristoscu, B. Bracci, G. Socol, M. Fini, I.N. Mihailescu, A. Bigi, Strontium-Substituted Hydroxyapatite Coatings Synthesized by Pulsed-Laser Deposition: In Vitro Osteoblast and Osteoclast Response, *Acta Biomater.* 4 (2008) 1885–1893.
29. U. Thormann, S. Ray, U. Sommer, T. ElKhassawna, T. Rehling, M. Hundgeburth, A. Henß, M. Rohnke, J. Janek, K.S. Lips, C. Heiss, G. Schlewitz, G. Szalay, M. Schumacher, M. Gelinsky, R. Schnettler, V. Alt, Bone Formation Induced by Strontium Modified Calcium Phosphate Cement in Critical-Size Metaphyseal Fracture Defects in Ovariectomized Rats, *Biomaterials.* 34 (2013) 8589-8598.
30. Y. Li, Q. Li, S. Zhu, E. Luo, J. Li, G. Feng, Y. Liao, J. Hu, The Effect of Strontium-Substituted Hydroxyapatite Coating on Implant Fixation in Ovariectomized Rats, *Biomaterials.* 31 (2010) 9006-9014.
31. G.X. Ni, K.Y. Chiu, W.W. Lu, Y. Wang, Y.G. Zhang, L.B. Hao, Z.Y. Li, W.M. Lam, S.B. Lu, K.D.K. Luk, Strontium-Containing Hydroxyapatite Bioactive Bone Cement in Revision Hip Arthroplasty, *Biomaterials.* 27 (2006) 4348–4355.
32. S. Patntirapong, P. Habibovic, P.V. Hauschk, Effects of Soluble Cobalt and Cobalt Incorporated into Calcium Phosphate Layers on Osteoclast Differentiation and Activation, *Biomaterials.* 30 (2009) 548–555.
33. H. Fernandes, A. Mentink, R. Bank, R. Stoop, C. van Blitterswijk, J. de Boer, Endogenous Collagen Influences Differentiation of Human Multipotent Mesenchymal Stromal Cells, *Tissue Eng., Part A.* 16 (2010) 1693-1702.
34. S.K. Both, A.J.C. van der Muijsenberg, C.A. van Blitterswijk, J. de Boer, J.D. de Bruijn, A Rapid and Efficient Method for Expansion of Human Mesenchymal Stem Cells, *Tissue Eng.* 13 (2007) 3-9.
35. A.E. Carpenter, T.R. Jones, M.R. Lamprecht, C. Clarke, I. Han Kan†, O. Friman, D.A. Guertin, J. Han Chang, R.A. Lindquist, J. Moffat, P. Golland, D.M. Sabatini, “CellProfiler: image analysis software for identifying and quantifying cell phenotypes”, *Genome Biology* 7 (10) (2006) R100.1-11.
36. H. Erbil Abaci, Y. Shen, S. Tan, S. Gerecht, “Recapitulating physiological and pathological shear stress and oxygen to model vasculature in health and disease”, *Scientific Reports* 4 (4951) (2014), DOI: 10.1038/srep04951.

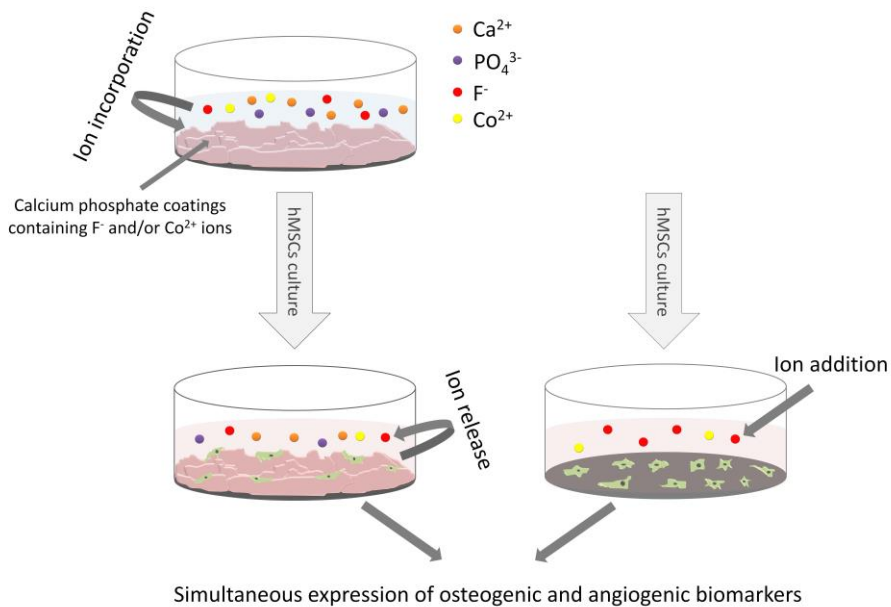
37. P. Habibovic, J. Li, C.M. van der Valk, G. Meijer, P. Layrolle, C.A. van Blitterswijk, K. de Groot, Biological Performance of Uncoated and Octacalcium Phosphate-Coated Ti6Al4V, *Biomaterials*. 26 (2005) 23–36.
38. F. Barrère, P. Layrolle, C.A. van Blitterswijk, K. de Groot, Biomimetic Calcium phosphate Coatings on Ti6Al4V: a Crystal Growth Study of Octacalcium Phosphate and Inhibition by  $Mg^{2+}$  and  $HCO_3^-$ , *Bone*. 25 (1999) 1075-1115.
39. F. Barre`re, P. Layrolle, C.A. van Blitterswijk, K. de Groot, Biomimetic Coatings on Titanium: a Crystal Growth Study of Octacalcium Phosphate, *J. Mater. Sci.: Mater. Med.* 12 (2001) 529-534.
40. S. Pasqualetti, G. Banfi, M. Mariotti, The Effects of Strontium on Skeletal Development in Zebrafish Embryo, *J. Trace Elem. Med. Biol.* 27 (2013) 375–379.
41. G.M. Blake, I. Fogelman, Strontium Ranelate Does not Have an Anabolic Effect on Bone, *Bone*. 9 (2013) 696-670.
42. P. Chavassieux, P.J. Meunier, J.P. Roux, N. Portero-Muzy, M. Pierre, R. Chapurlat, Bone Histomorphometry of Transiliac Paired Bone Biopsies After 6 or 12 Months of Treatment with Oral Strontium Ranelate in 387 Osteoporotic Women: Randomized Comparison to Alendronate, *J. Bone Miner. Res.* 29 (2014) 618–628.
43. D. Guo, K. Xu, X. Zhao, Y. Han, Development of a Strontium-Containing Hydroxyapatite Bone Cement, *Biomaterials*. 26 (2005) 4073–4083.
44. F. Barrère, C.M. van der Valk, R.A.J. Dalmeijer, C.A. van Blitterswijk, K. de Groot, P. Layrolle, In Vitro and In Vivo Degradation of Biomimetic Octacalcium Phosphate and Carbonate Apatite Coatings on Titanium Implants, *J. Biomed. Mater. Res., Part A*. 64A (2002) 378-387.
45. S. Pors Nielsen, The Biological Role of Strontium, *Bone*. 35 (2004) 583– 588.
46. M.D. Treiser, E.H. Yang, S. Gordonov, D.M. Cohen, I.P. Androulakis, J. Kohn, C.S. Chen, P.V. Moghe, Cytoskeleton-Based Forecasting of Stem Cell Lineage Fates, *Proc. Natl. Acad. Sci. U. S. A.* 107 (2010) 610-615.
47. A.M.C. Barradas, H.A.M. Fernandes, N. Groen, Y. Chai, J. Schrooten, J. van de Peppel, J.P.T.M. van Leeuwen, C.A. van Blitterswijk, J. de Boer, A Calcium-Induced Signaling Cascade Leading to Osteogenic Differentiation of Human Bone Marrow-Derived Mesenchymal Stromal Cells, *Biomaterials*. 33 (2012) 3205-3215.
48. M.D. Treiser, E.H. Yang, S. Gordonov, D.M. Cohen, I.P. Androulakis, J. Kohn, C.S. Chen, P.V. Moghe, Cytoskeleton-Based Forecasting of Stem Cell Lineage Fates, *Proc. Natl. Acad. Sci. U.S.A.* 107 (2010) 610-615.
49. R. McBeath, D.M. Pirone, C.M. Nelson, K. Bhadriraju, C.S. Chen, Cell Shape, Cytoskeletal Tension, and RhoA Regulate Stem Cell Lineage Commitment, *Dev. Cell*. 6 (2004) 483–495.
50. M.J. Dalby, N. Gadegaard, R. Tare, A. Andar, M.O. Riehle, P. Herzyk, C.D.W. Wilkinson, R.O.C. Oreffo, The Control of Human Mesenchymal Cell Differentiation Using Nanoscale Symmetry and Disorder. *Nat. Mater.* 6 (2007) 997 – 1003.
51. T.C. Brennan, M.S. Rybchyn, W. Green, S. Atwa, A.D. Conigrave, R.S. Mason, Osteoblasts Play Key Roles in the Mechanisms of Action of Strontium Ranelate, *Br. J. Pharmacol.* 157 (2009) 1291–1300.
52. A. Barbara, P. Delannoy, B.G. Denis, P.J. Marie, Normal Matrix Mineralization Induced by Strontium Ranelate in MC3T3-E1 Osteogenic Cells, *Metabolism*. 53 (2004) 532-537.
53. Z. Saidak, P.J. Marie, Strontium Signaling: Molecular Mechanisms and Therapeutic Implications in Osteoporosis, *Pharmacol. Ther.* 136 (2012) 216–226.
54. S. Choudhary, P. Halbout, C. Alander, L. Raisz, C. Pilbeam, Strontium Ranelate Promotes Osteoblastic Differentiation and Mineralization of Murine Bone Marrow Stromal Cells: Involvement of Prostaglandins, *J. Bone Miner. Res.* 22 (2007) 1002-1010.
55. S. Walsh, G.R. Jordan, C. Jefferiss, K. Stewart, J.N. Bresford, High Concentrations of Dexamethasone Suppress the Proliferation but not the Differentiation or Further Maturation of

Human Osteoblast Precursors In Vitro: Relevance to Glucocorticoid-Induced Osteoporosis, *Rheumatology*. 40 (2001) 74–83.

56. J.N. Beresford, C.J. Joyner, C. Devlin, J.T. Triffitt, The Effects of Dexamethasone and 1,25-Dihydroxyvitamin D on Osteogenic Differentiation of Human Marrow Stromal Cells In Vitro, *Archs. onrl. Bid.* 39 (1994) 941-947.
57. F. Langenbach, J. Handschel, Effects of Dexamethasone, Ascorbic Acid and  $\beta$ -Glycerophosphate on the Osteogenic Differentiation of Stem Cells In Vitro, *Stem Cell Res. Ther.* 4 (2013) 117-123.
58. H.A. Weiler, Z. Wang, S.A. Atkinson, Dexamethasone Treatment Impairs Calcium Regulation and Reduces Bone Mineralization in Infant, *Am. J. Clin. Nutr.* 61 (1995) 805-811.
59. M. Wiontzek, G. Matziolis, S. Schuchmann, T. Gaber, D. Krockner, G. Duda, G.R. Burmester, C. Perka, F. Buttgereit, Effects of Dexamethasone and Celecoxib on Calciumhomeostasis and Expression of Cyclooxygenase-2 mRNA in MG-63 Human Osteosarcoma Cells, *Clin. Exp. Rheumatol.* 24 (2006) 366-372.
60. C.B.S.S. Danoux, D.C. Bassett, Z. Othman, A.I. Rodrigues, R.L. Reis, J.E. Barralet, Cl.A. van Blitterswijk, P. Habibovic, Elucidating the individual effects of calcium and phosphate ions on hMSCs by using composite materials, *Acta Biomaterialia* 17 (2015) 1–15.
61. A.M.C Barradas, H. Yuan, C.A. van Blitterswijk, P. Habibovic, Osteoinductive biomaterials: current knowledge of properties, experimental models and biological mechanisms, *Eur Cell Mater* 21 (2011) 407–29.
62. P. Habibovic, H. Yuan, C.M. van der Valk, G. Meijer, C.A. van Blitterswijk, K. de Groot, 3D microenvironment as essential element for osteoinduction by biomaterials, *Biomaterials* 26 (2005) 3565–3575.
63. J. Zhang, X. Luo, D. Barbieri, A.M.C. Barradas, J.D. de Bruijn, C.A. van Blitterswijk, H. Yuan, The size of surface microstructures as an osteogenic factor in calcium phosphate ceramics, *Acta Biomaterialia* 10 (2014) 3254–3263.
64. H.V. Unadkat, M. Hulsman, K. Cornelissen, B.J. Papenburg, R.K. Truckenmüller, A.E. Carpenter, M. Wessling, G.F. Post, M. Uetz, M.J.T. Reinders, D. Stamatialis, C.A. van Blitterswijk, J. de Boer, An Algorithm-Based Topographical Biomaterials Library to Instruct Cell Fate, *PNAS* 108 (2011) 16565–1657.

## Chapter 5

### Combinatorial incorporation of fluoride and cobalt ions into calcium phosphates to stimulate osteogenesis and angiogenesis



## Abstract

Bone healing requires two critical mechanisms, angiogenesis and osteogenesis. In order to improve bone graft substitutes, both mechanisms should be addressed simultaneously. While the individual effects of various bioinorganics have been studied, an understanding of the combinatorial effects is lacking. Cobalt and fluoride ions, in appropriate concentrations, are known to individually favor the vascularization and mineralization processes, respectively. This study investigated the potential of using a combination of fluoride and cobalt ions to simultaneously promote osteogenesis and angiogenesis in human mesenchymal stromal cells (hMSCs). Using a two-step biomimetic method, wells of tissue culture plates were coated with a calcium phosphate (CaP) layer without or with the incorporation of cobalt, fluoride, or both. In parallel, hMSCs were cultured on uncoated well plates, and cultured with cobalt and/or fluoride ions within the media. The results revealed that cobalt ions increased the expression of angiogenic markers, with the effects being stronger when the ions were added as a dissolved salt in cell medium as compared to incorporation into CaP. Cobalt ions generally suppressed the ALP activity, the expression of osteogenic genes, and the level of mineralization, regardless of delivery method. Fluoride ions, individually or in combination with cobalt, significantly increased the expression of many of the selected osteogenic markers, as well as mineral deposition. This study demonstrates an approach to simultaneously target the two essential mechanisms in bone healing: angiogenesis and osteogenesis. The incorporation of cobalt and fluoride into CaPs is a promising method to improve the biological performance of fully synthetic bone graft substitutes.

## 5.1. Introduction

Approximately 69 weight% of bone is comprised of mineral that is a calcium phosphate (CaP) in the form of AB type carbonated apatite [1]. Inspired by this bone composition, CaP-based materials have been successfully used as synthetic bone graft substitutes, and for improving the performance of orthopedic implants [2]. In addition to CaP, the inorganic component of bone contains a number of elements in trace quantities, such as magnesium ( $Mg^{2+}$ ), strontium ( $Sr^{2+}$ ), copper ( $Cu^{2+}$ ), fluoride (F), etc. [1,3]. While these elements are known to play vital roles in bone healing, formation, and remodeling [4,5], their clinical use is often the result of serendipity, observations based on nutritional deficiencies, or genetic disorders [5]. In comparison to growth factors and other biologics, the advantage of such compounds is their stability, while being relatively inexpensive. Further research is needed to explore the possibilities of these compounds when incorporated into bone graft substitutes.

Several studies have demonstrated that the introduction of relevant bioinorganics to bone graft substitutes may change not only chemistry, but also other properties such as crystallinity, degradation and mechanical properties, thereby also influencing the biological response. More recently, mechanistic studies have shed light into how these elements function individually by altering osteogenesis and bone formation, as summarized in previous review papers [2,4-7]. However, it is not clear what effect the combinations of bioinorganics have on bone regeneration, and how these combinations may affect the overall biological response to bone graft substitutes. Therefore, this study was designed to assess the combinatorial effects of two types of bioinorganics, being cobalt ( $Co^{2+}$ ) and fluoride (F) ions, on the osteogenic and angiogenic differentiation of human mesenchymal stromal cells (hMSCs).

Being an integral component of vitamin B12 complex and involved in the production of red blood cells,  $Co^{2+}$  ion is an essential element in physiological mechanisms in humans and other mammals [7-8]. As a main component of cobalt-chromium metal alloys, cobalt has been commonly used in several orthopedic applications such as total joint replacement and dentistry castings [9]. While cobalt-based alloys offer a high corrosion resistance, chemical stability and excellent mechanical properties [9], there are issues related to the toxicity resulting from wear debris and elevated levels of soluble  $Co^{2+}$  ions [2,10].  $Co^{2+}$  ion supplementation has been shown to substantially reduce the viability of osteoblastic cells [11-12], and was reported to reduce the expression of

osteogenic makers, such as alkaline phosphatase (ALP) and other markers of osteogenesis [11,13-14].  $\text{Co}^{2+}$  ions, in solution or incorporated into CaP, have been shown to activate and increase osteoclast cell differentiation, which may, in part, explain the aseptic loosening of cobalt-based implants in vivo [15]. At higher concentrations ( $>10 \mu\text{M}$ ), however,  $\text{Co}^{2+}$  ions may result in a reduction in osteoclast cell number and resorption activity [11].

Several mechanisms have been proposed to describe the toxic effects of  $\text{Co}^{2+}$  at higher concentrations, including oxidative damage to DNA, proteins and lipids, putative inhibition of  $\text{Ca}^{2+}$  entry and  $\text{Ca}^{2+}$ -signaling, competition with  $\text{Ca}^{2+}$  for intracellular binding to proteins and inhibition of activity of crucial enzymes [10].

There is evidence that  $\text{Co}^{2+}$  ions, by inducing hypoxia conditions [16], increase expression of angiogenic genes and proteins such as vascular endothelial growth factor (VEGF) [14,17]. It has been also shown that the addition of  $\text{Co}^{2+}$  ions and cells treated with  $\text{Co}^{2+}$  ions to tissue engineered scaffolds promotes neovascularization in animal models, which, contrary to in vitro results mentioned above, may indirectly benefit in vivo bone formation [12,17]. Therefore, combining  $\text{Co}^{2+}$  ions with factors, which directly promote expression of osteogenic markers, may be a promising strategy for inducing formation of vascularized bone.

Fluoride ( $\text{F}^-$ ) has been recognized as an essential element in mineralized tissues, including bone and teeth [4,8], with the use of fluoride as an additive in the formulation of toothpaste being an example of the daily use of bioinorganics [5,19]. While  $\text{F}^-$  ions in the form of sodium fluoride has been used clinically for the treatment of osteoporosis [4], in vitro results have shown a dose-dependent effect of  $\text{F}^-$  ions on proliferation and osteogenic differentiation of various relevant cell types [20-22]. These results revealed that doses lower than  $100 \mu\text{M}$  promoted osteogenic differentiation and osteoblast proliferation, whereas doses higher than  $500 \mu\text{M}$  induced apoptosis and inhibition of osteogenic markers [21]. Moreover, sodium fluoride has been reported to be involved in the initiation of osteogenesis from the embryonic mesenchyme, and in the formation of a bone-like matrix [22]. As with other bioinorganics, the incorporation of  $\text{F}^-$  ions into synthetic bone graft substitutes has been previously explored, especially in association with CaPs and bioactive glasses [23-30]. This incorporation of  $\text{F}^-$  ions has been shown to promote the proliferation and osteogenic differentiation of different cell types, with the cell response being substantially dependent on the fluoride concentration, the substrate material and cell source [25-33]. In addition to these biological effects, many studies have demonstrated significant changes in the biomaterial's

physicochemical properties, including crystallinity, dissolution rate, mechanical properties and coating-substrate adhesion when  $F^-$  was incorporated into CaPs [23-27].

While both  $Co^{2+}$  and  $F^-$  ions individually have beneficial effects that can promote bone healing, their use in combination needs greater investigation in order to develop improved bone graft substitutes with the ability to simultaneously induce osteogenic and angiogenic responses. This study was set up in such a way. Firstly, the effect of  $Co^{2+}$  ions on the expression of angiogenic markers was investigated. Secondly,  $F^-$  ions were added and proliferation and osteogenic differentiation was studied and compared to the sole effects of fluoride and cobalt ions. This was done in order to investigate whether the presence of  $Co^{2+}$  ions would compromise the effect of  $F^-$  ions on the proliferation and osteogenic differentiation of hMSC.

## 5.2. Materials and Methods

### 5.2.1. Preparation of $Co^{2+}$ and $F^-$ stock solutions

A Tris buffer solution was prepared by dissolving 6.05 g Tris base (Sigma), 41 ml 1 M HCl (Sigma) in pure MilliQ water to a total volume of 1L (pH= 7.4) as was previously described [15, 32].  $Co^{2+}$  and  $F^-$  stock solutions were prepared by dissolving appropriate amounts of  $CoCl_2$  (Sigma) and NaF (Sigma) salts in Tris buffer to reach the concentration of 10 mM and 100 mM of  $Co^{2+}$  and  $F^-$ , respectively, representing a low and high dose. For sterilization, the stock solutions were filtered using 0.22  $\mu$ M filters and kept at 4°C.

### 5.2.2. Coating preparation

The CaP coatings were deposited on the surface of treated tissue culture 24- well plates (Nunc). The deposition of CaP coating was achieved via a 2-step biomimetic coating approach, which has been previously described [15,32]. Briefly, in the first step, a concentrated simulated body fluid solution (SBF 2.5x) was prepared with ionic content of 733.5 mM  $Na^+$ , 7.5 mM  $Mg^{2+}$ , 12.5 mM  $Ca^{2+}$ , 720 mM  $Cl^-$ , 5 mM  $HPO_4^{2-}$  and 21 mM  $HCO_3^-$ . 1 ml of SBF 2.5X was added to each well, and refreshed daily, for three days at room temperature. In the second step, a calcium phosphate solution (CPS) was prepared consisting of 140 mM  $Na^{2+}$ , 4 mM  $Ca^{2+}$ , 2 mM  $HPO_4^{2-}$  and 144 mM  $Cl^-$  (buffered at pH 7.4). Appropriate volumes of  $Co^{2+}$  and  $F^-$  stock solutions were added to the CPS solution to reach the desired concentrations of ions in the CPS solutions (Table 1). According to the groups, 1 ml

of the CPS solution with varying concentrations of ions was added to each well, and refreshed daily, for three days at room temperature. The coatings were then washed three times with demineralized water and dried overnight in an air oven.

### 5.2.3. Coating characterization

The chemistry of the mineral phase was characterized by Fourier transform infrared spectroscopy (FTIR, Perkin-Elmer Spectrum 1000) and x-ray diffraction (XRD, Miniflex, Rigaku).

The morphology of the mineral films was characterized using scanning electron microscopy (SEM, XL-30 ESEM-FEG, Philips) in the secondary electron mode, coupled with an energy dispersive X-ray spectroscopy analyzer (EDS, EDAX, AMETEK Materials Analysis Division) at the accelerator voltage of 10 KeV and working distance of 10 mm. The samples were sputtered with a thin gold layer prior to imaging. Quantification of the EDS data was achieved using the TEAM™ EDS V2.2 software provided by the EDS manufacturer.

Table 1. An overview of samples with  $\text{Co}^{2+}$  and/or  $\text{F}^-$  ion concentrations in cell culture medium and in the CaP solution used for coating preparation.

Ions directly supplemented to the medium	Sample label	Concentration of $\text{Co}^{2+}$ in cell medium ( $\mu\text{M}$ )	Concentration of $\text{F}^-$ in cell medium ( $\mu\text{M}$ )
	Co 0	0	0
	Co 0.1	0.1	0
	Co 20	20	0
	F 1000	0	1000
	F1000 Co 0.1	0.1	1000
	F1000 Co 20	20	1000
Ions incorporated into CaP coatings	Sample label	Concentration of $\text{Co}^{2+}$ in CPS solution ( $\mu\text{M}$ )	Concentration of $\text{F}^-$ in CPS solution ( $\mu\text{M}$ )
	CaP Co 0	0	0
	CaP Co 0.1	0.1	0
	CaP Co 20	20	0
	CaP F 1000	0	1000
	CaP F1000 Co0.1	0.1	1000
	CaP F1000 Co0.1	20	1000

#### 5.2.4. Cell subculture

Human mesenchymal stromal cells (hMSCs) were isolated from bone marrow aspirates (5–20 ml) obtained from one donor with written informed consent [34–35]. Aspirates were resuspended using 20 G needles, plated at a density of  $5 \times 10^5$  cells per  $\text{cm}^2$ , and cultured in proliferation medium (consisting of  $\alpha$ -MEM (Gibco) supplemented with 10% fetal bovine serum (Lonza), 2 mM L-glutamine (Gibco), 0.2 mM ascorbic acid (Sigma),  $100 \text{ U ml}^{-1}$  penicillin and  $100 \mu\text{g ml}^{-1}$  streptomycin (Gibco) and  $1 \text{ ng ml}^{-1}$  rhbFGF (AbDSerotec)). The medium was refreshed every 2–3 days. The cells were harvested using the standard trypsinization method at approximately 80% confluency for subculture until passage 3.

#### 5.2.5. Cell culture

CaP coatings were sterilized with ethanol prior to cell culture. To sterilize, the CaP-coated wells were washed three times with 70% ethanol followed by 15 min of drying inside the flow cabinet after each washing step. In the last step of sterilization, 100% ethanol was added to the samples and allowed to evaporate in the flow cabinet for at least 2 hours. The wells were then washed twice with sterile PBS. 1 ml of basic medium ( $\alpha$ -MEM (Gibco) supplemented with 10% fetal bovine serum (Lonza), 2 mM L-glutamine (Gibco), 0.2 mM ascorbic acid (Sigma),  $100 \text{ U ml}^{-1}$  penicillin and  $100 \mu\text{g ml}^{-1}$  streptomycin (Gibco)) was added to each sterilized sample, and then incubated overnight in a 5%  $\text{CO}_2$  humid atmosphere at  $37^\circ\text{C}$ .

hMSCs ( $n=3$ ) were cultured on the coated plates for the analysis of DNA amounts, ALP activity, the expression of a set of osteogenic markers on mRNA level and mineralization. For mineralization assessment in the trans-well set-up  $n=2$  was used as a sample size. All the measurements were performed twice on the same set of samples.

hMSCs of passage 3 were seeded on treated tissue culture plates (TCPs) with and without CaP coatings at a density of  $10000 \text{ cells/cm}^2$  in approximately  $50 \mu\text{l}$  of basic medium. 2 ml of either basic, osteogenic (basic medium supplemented with 10 nM dexamethasone (Sigma)) or mineralization medium (osteogenic medium supplemented with 0.01 M beta-glycerophosphate (Sigma)) was directly added to each treated well with and without CaP coating. Appropriate volumes of ion stock solutions were also added to each well without CaP coating to reach  $\text{Co}^{2+}$

concentrations of 0, 0.1 and 20  $\mu\text{M}$ , and  $\text{F}^-$  concentrations of 0 and 1000  $\mu\text{M}$  in cell culture mediums (Table 1.). The medium was refreshed every 2-3 days.

A parallel cell culture in a trans-well set up was performed to investigate the mineralization of hMSCs when exposed to ion-incorporated CaP coatings. Glass coverslips were coated with  $\text{Co}^{2+}$  and  $\text{F}^-$ -incorporated CaP coatings using the method described above. The coated coverslips were then sterilized, and conditioned overnight in basic medium similar to the coated well plates. hMSCs were cultured on the bottom compartment of trans-wells in either basic or mineralization medium. The CaP-coated coverslips were placed in the top compartment of trans-wells, sharing the medium with cells. The medium was refreshed every 2-3 days.

### 5.2.6. DNA content and ALP activity quantification

Total DNA was assessed with CyQuant Cell Proliferation Assay kit (Invitrogen) at days 7 and 14. After 3 cycles of freeze/thaw at  $-80^\circ\text{C}$ , 500  $\mu\text{l}$  lysis buffer (lysis buffer provided in the kit diluted in a buffer of NaCl-EDTA solution) was added to each well. The samples were ultra-sonicated and incubated at room temperature for 1 hour. After centrifugation, the lysis buffer was collected and the DNA content was measured in accordance with manufacturer's protocol. Briefly, 100  $\mu\text{l}$  of the supernatant was mixed with the same volume of CyQuant GR dye in a 96 well micro-plate and incubated for 15 min. Fluorescence measurements for DNA quantification were done at excitation and emission wavelengths of 480 and 520 nm, respectively, using a spectrophotometer (Perkin Elmer). ALP activity of the cells was measured using a CDP-star kit (Roche Applied Science) at days 7 and 14. 10  $\mu\text{l}$  of the lysis buffer used for quantifying DNA content was mixed with 40  $\mu\text{l}$  CDP-star reagent in a 96 well micro-plate and incubated for 30 min. After incubation, chemiluminescence measurements were completed at 466 nm. Results of the DNA assays are presented based on average  $\mu\text{g}$  of DNA detected in each condition normalized for DNA content of hMSCs cultured on TCPs in basic medium without ion addition for 7 days. Results of ALP activity were normalized per DNA content of each culture and ALP activity of hMSCs cultured on TCPs in basic medium without ion addition for 7 days and presented as the average of normalized ALP activity.

### 5.2.7. RNA extraction and gene expression (qPCR) assay

Total RNA was isolated by using a NucleoSpin® RNA II isolation kit (Macherey Nagel) for cells cultured on TCPs and in combination with NucleoSpin® RNA II isolation kit and Trizol method for cells cultured on CaP coatings, in accordance with the manufacturer's protocol at days 7 and 14. RNA was collected in RNase-free water and the total concentration was measured using nano-drop measurement equipment (ND1000 spectrophotometer, Thermo Scientific). The cDNA of the cultures were then prepared using an iScript kit (Bio-Rad) according to the manufacturer's protocol and diluted 10 times in RNase-free water to be used for quantitative real-time PCR (qPCR). The qPCR measurements were completed using Bio-Rad equipment using Syber green I master mix (Invitrogen) and the primers (Sigma) the sequences of which are listed in table 2. Expression of the osteogenic marker genes were normalized to GAPDH levels and hMSCs cultured on TCPs in basic medium for 7 days, and the fold inductions were calculated by using the  $\Delta\Delta CT$  method.

### 5.2.8. Mineralization assay

Alizarin Red staining was done at day 21 in order to investigate the mineralization of hMSCs. The cultures were washed twice with PBS after aspirating the medium, fixed with 4% paraformaldehyde (PFA) (Sigma) in phosphate buffered saline (PBS), buffered at pH 7.4 for 30 minutes and washed at least twice with PBS. The cells were stained with 2% Alizarin red solution (Sigma) for 5 minutes, washed with PBS and imaged using a stereomicroscope (SMZ-10A, Nikon).

In order to quantify the mineralization of hMSCs, 200  $\mu$ L of 1M HCl (Sigma) was added to each well and collected after 1 minute. The calcium content in the acid was then quantified using QuantiChrom™ calcium assay kit (BioAssay Systems) according to manufacturer's protocol. A spectrophotometric plate-reader (Thermo Scientific MultiscanGo) was used to read the optical density of calcium complexes at 612 nm.

Table 2. Primer sequence of the angiogenic and osteogenic genes investigated.

Gene	Primer sequence
GAPDH (housekeeping gene)	5'-CCATGGTGTCTGAGCGATGT 5'-CCATGGTGTCTGAGCGATGT
Vascular endothelial growth factor (VEGF)	5'-AGGTCTCGATTGGATGGCA 5'-AGGGCAGAATCATCACGAAGT
CD31	5'-GAACGGTGTCTTCAGGTTGGTATTTCA 5'-TCTATGACCTCGCCCTCCACAAA
Alkaline phosphatase (ALP)	5'-TTCAGCTCGTACTGCATGTC 5'-ACAAGCACTCCCACCTTCATC
Bone sialoprotein (BSP)	5'-TCCCGTTCTCACTTTTCATA 5'-CCCCACCTTTTGGGAAAAC
Bone morphogenetic protein 2 (BMP2)	5'-GCATCTGTTCTCGGAAAACCT 5'-ACTACCAGAAACGAGTGGGAA
Osteocalcin (OC)	5'-CGCCTGGGTCTCTTCACTAC 5'-TGAGAGCCCTCACACTCCTC
Osteopontin (OP)	5'-CCAAGTAAGTCCAACGAAAG 5'-GGTGATGTCCTCGTCTGTA

### 5.2.9. Statistical analysis

Statistical comparisons were performed using One-way Analysis of Variance (ANOVA) followed by a Tukey's multiple comparison test. For all analyses, the following p-value applies: \* p < 0.05.

## 5.3. Results

### 5.3.1. Coating characterization

To analyze the morphology and chemical composition of the different coatings, SEM imaging and EDS elemental analysis were performed, respectively (Figure 1.a1-f1). A homogenous crystalline mineral layer composed of globules with a diameter of approximately 5  $\mu\text{m}$ , was observed in all conditions. The crystals of CaP coatings without additives exhibited a flat plate-like morphology oriented perpendicular to the surface of the substrate (Figure 1.a2). The presence of  $\text{Co}^{2+}$  ions did not alter the morphology of the crystals in the coatings (Figure 1.b2-c2).

Upon  $F^-$  incorporation, the size of coating globules did not change, however, instead of a plate-like morphology, the individual crystals exhibited a rod-shaped morphology (Figure 1.d2-f2).

EDS spectra of all the coatings showed sharp peaks of calcium, phosphorous and oxygen (Figure 1.a3-f3), confirming the formation of a CaP layer. Sodium and chlorine peaks were observed in the spectra of CaP coatings, suggesting incomplete washing. Within the energy range of 0-10 KeV, the most intense peak of cobalt appears at 0.776 KeV. In the EDS spectra of CaP and CaP Co0.1, such a peak was not observed, whereas, a small peak at approximately 0.7-0.8 KeV was observed in EDS spectrum of CaP Co20. Fluorine peak was observed in all the CaP coatings with  $F^-$  incorporation (Figure 1.a3-f3).

Semi-quantitative analysis of EDS data (Figure 1.g) revealed a Ca/P ratio of approximately 1.3-1.5 in all the coatings (atomic ratios are listed in Supplementary data 1.). The mean Co content of the CaP coatings without  $Co^{2+}$  incorporation and with low concentration of  $Co^{2+}$  was calculated to be lower than 0.05 atomic percent (at%), whereas, CaP Co20 and CaP F1000 Co20 coatings contained  $0.18 \pm 0.04$  at% and  $0.15 \pm 0.02$  at% cobalt, respectively. The results of fluorine quantification showed a value of  $1.15 \pm 0.02$  at% for F content in the coatings without  $F^-$  incorporation, while addition of  $1000 \mu M F^-$  to CPS solution resulted in  $5.10 \pm 0.66$ ,  $4.19 \pm 0.95$  and  $3.79 \pm 1.06$  at% fluorine in the CaP F1000, CaP F1000 Co 0.1 and CaP F1000 Co20 coatings, respectively (Figure 1.g).

The composition of the coating and the effect of ion incorporation on the crystalline structure were further investigated by FTIR and XRD analyses (Figure 2). All the FTIR spectra were typical of CaPs prepared using the biomimetic coating method [36-37]. The FTIR spectra of all CaP coatings exhibited phosphate peaks at 568, 605 and a set of peaks at approximately  $1040 \text{ cm}^{-1}$ . The small peaks observed at  $1410-1450 \text{ cm}^{-1}$  are attributed to carbonate groups, which may be incorporated into the crystalline lattice during coating deposition. Moreover, two small bands appeared at  $860$  and  $910 \text{ cm}^{-1}$ , which are typical of  $HPO_4^{2-}$  bands in octacalcium phosphate (OCP) structure. The band at approximately  $1650 \text{ cm}^{-1}$  represents presence of water. The broad band at approximately  $3400 \text{ cm}^{-1}$  also belongs to absorbed  $H_2O$  groups and the small shoulder at  $3550 \text{ cm}^{-1}$  represents  $OH^-$  groups [38]. Addition of  $Co^{2+}$  to CPS solution did not affect the FTIR spectra of CaP coatings. However, upon  $F^-$  incorporation, the  $HPO_4^{2-}$  peak at  $910 \text{ cm}^{-1}$  disappeared and the intensity of the  $HPO_4^{2-}$  peak at  $860 \text{ cm}^{-1}$  was reduced.

Moreover, the  $\text{OH}^-$  peak at  $3550\text{ cm}^{-1}$  disappeared upon addition of  $\text{F}^-$  to the coatings (Figure 2.a).

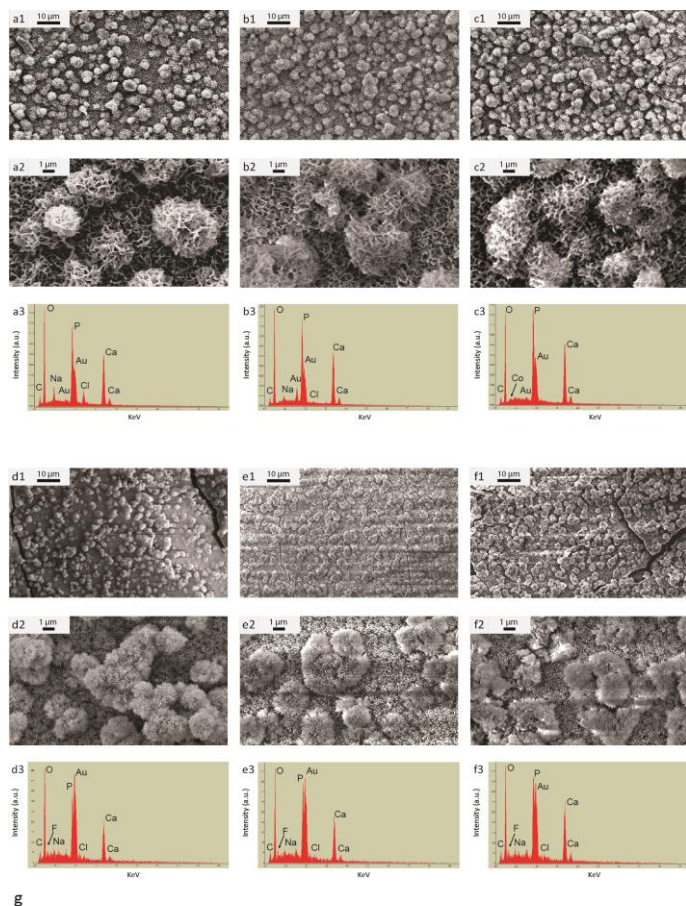


Figure 1. SEM images at low (a1-f1) and high (a2-f2) magnifications, and EDS spectra (a3-f3) of CaP, CaP Co0.1, CaP Co20, CaP F1000, CaP F1000 Co 0.1 and CaP F1000 Co 20, respectively, and Ca, P, Co and F content (g) in CaP coatings quantified based on EDS analysis. A homogenous low-crystallinity CaP layer was formed on the surface of tissue culture well plates.  $\text{Co}^{2+}$  and  $\text{F}^-$  content of approximately 0.15-0.18 at% and 3.79-5.1 at% was detected in the coatings upon addition of  $20\ \mu\text{M}$  of  $\text{Co}^{2+}$  and  $1000\ \mu\text{M}$  of  $\text{F}^-$  to CPS solution, respectively.

Sample	Ca	P	Co	F
CaP	21.54±1.49	15.20±0.89	0.04±0.04	1.25±0.26
CaP Co 0.1	24.37±4.70	16.53±1.75	0.01±0.01	1.00±0.22
CaP Co20	22.09±1.30	16.42±0.80	0.18±0.04*	1.19±0.34
CaP F 1000	17.59±1.43	13.27±1.00	0.04±0.02	5.13±0.66*
CaP F1000 Co 0.1	18.61±1.32	14.19±0.61	0.02±0.00	4.19±0.95*
CaP F1000 Co 20	25.53±8.51	16.09±2.55	0.15±0.02*	3.79±1.06*

The XRD patterns of the coatings showed only peaks with very low intensity in the  $2\theta$  range of  $5\text{--}70^\circ$ . A larger peak appeared at  $5.6^\circ$  theta, which may represent the 010 crystalline plane in the OCP structure that is expected at approximately  $4^\circ$  theta. The less intense peak appearing at  $25.7^\circ$  theta are also observed in the XRD pattern of OCP as a less intense peak that is attributed to plane 002. The small peak observed at approximately  $32^\circ$  theta is typical for XRD patterns of both apatite and OCP. No substantial changes were observed in the XRD patterns of the CaP coatings upon addition of  $\text{Co}^{2+}$  and  $\text{F}^-$  ions to CPS solution (Figure 2.b).

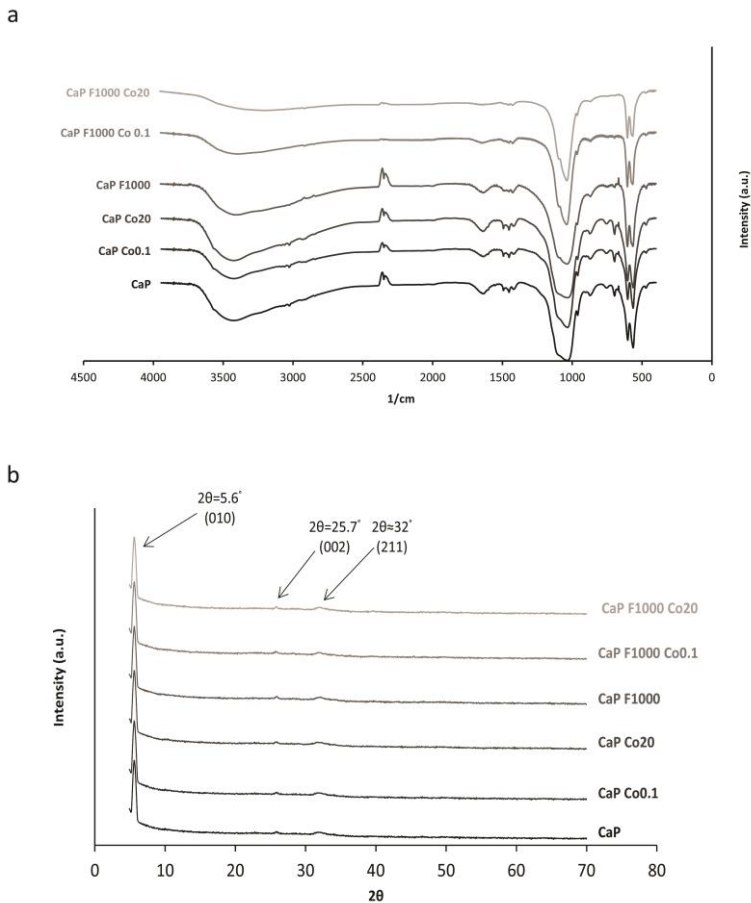


Figure 2. XRD patterns (a) and FTIR spectra (b) of the CaP coatings without and with additives. The XRD patterns and the FTIR spectra suggested that the predominant phase was octacalcium phosphate, with a limited presence of carbonate. Addition of  $\text{F}^-$  ions to the coating solution rendered the CaP phase more apatitic.

### 5.3.2. Effect of $\text{Co}^{2+}$ on the expression of angiogenic genes

The angiogenic effect of  $\text{Co}^{2+}$  ions on hMSC was analyzed with qPCR, using VEGF and CD31 as angiogenic markers (Figure 3). At day 7, no significant differences were observed in the expression of VEGF upon addition of  $\text{Co}^{2+}$  to basic medium. At day 14, the addition of  $\text{Co}^{2+}$  to basic medium in both concentrations led to a significant increase in the expression of VEGF (Figure 3.a1). A similar trend was observed in the expression of CD31, however, this result was not statistically significant at either time point (Figure 3.a2). Similar to medium conditioning with  $\text{Co}^{2+}$  ions,  $\text{Co}^{2+}$  ions incorporated into CaP coatings did not affect the expression of VEGF at mRNA level at day 7. At day 14, a small increase in the expression of VEGF and CD31 was observed in the hMSCs cultured on CaP  $\text{Co}^{2+}$ , however, this difference was not statistically significant for either marker (Figure 3.b1 and 3.b2).

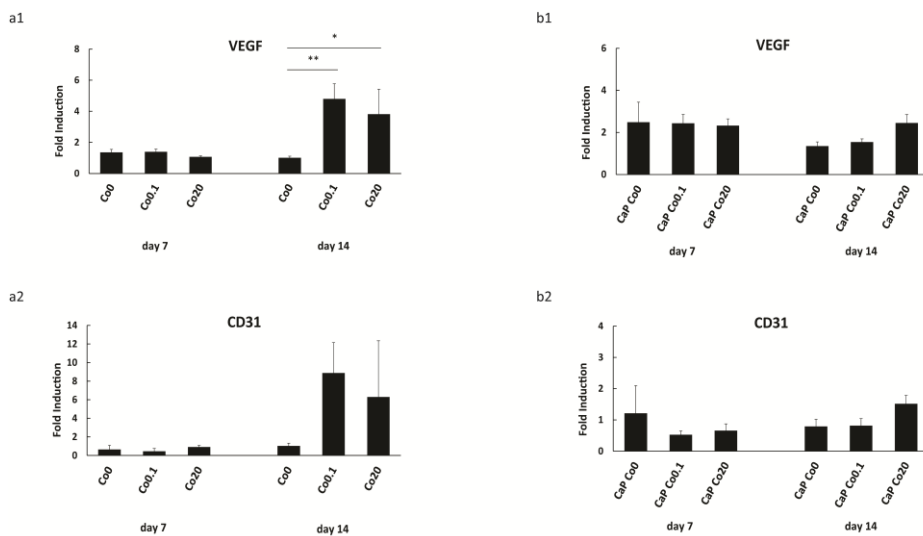


Figure 3. mRNA expression of VEGF (a1,b1) and CD31 (a2,b2) in hMSCs (n=3) cultured on uncoated tissue culture plastic and on CaP coatings, respectively.  $\text{Co}^{2+}$  ions increased the expression of both markers after 14-day culture via both delivery methods with the effects being stronger when the ions were directly added to cell culture medium.

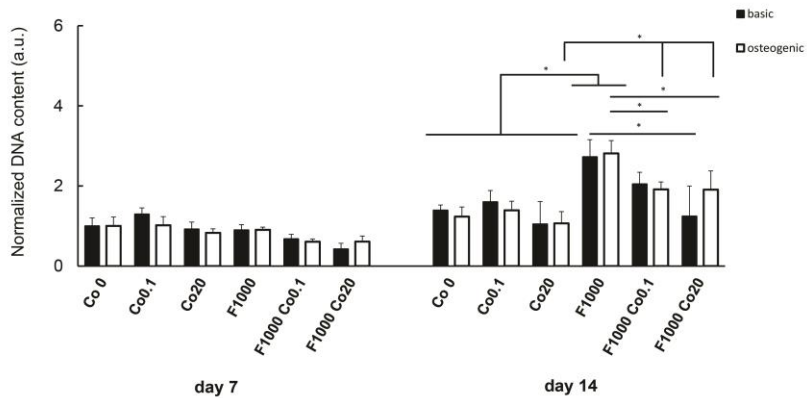
### 5.3.3. Effect of $\text{Co}^{2+}$ and $\text{F}^-$ on DNA content

When added to cell culture medium,  $\text{Co}^{2+}$  and  $\text{F}^-$  ions did not significantly affect the DNA content of hMSCs at day 7. At day 14 in both basic and osteogenic

medium, F1000 showed significantly higher DNA content compared to all the other conditions, except F1000 Co0.1 in basic medium. Moreover, hMSCs cultured with 20  $\mu\text{M}$   $\text{Co}^{2+}$  showed significantly lower DNA content compared to all conditions containing  $\text{F}^-$ , while no differences were seen with cells cultured in media without additives (Figure 4.a1).

When  $\text{Co}^{2+}$  and  $\text{F}^-$  ions were incorporated into CaP coatings, no significant differences were detected on the DNA content of hMSCs at day 7. At day 14, the incorporation of  $\text{F}^-$  into the CaP coating in general decreased the DNA content of the cells in both basic and osteogenic media, as compared to the control and coatings with only  $\text{Co}^{2+}$ , which was in contrast to the findings of conditioned media (Figure 4.b1).

a1



a2

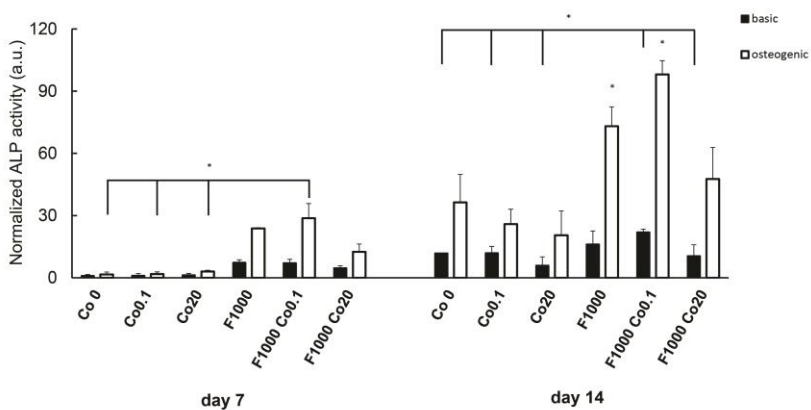
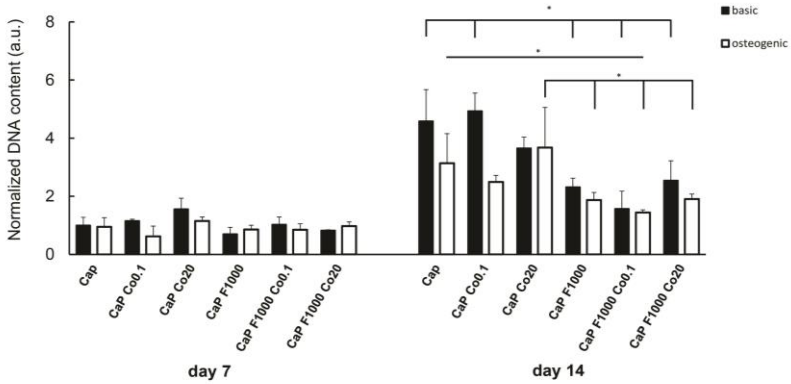


Figure 4. Continues in the next page.

b1



b2

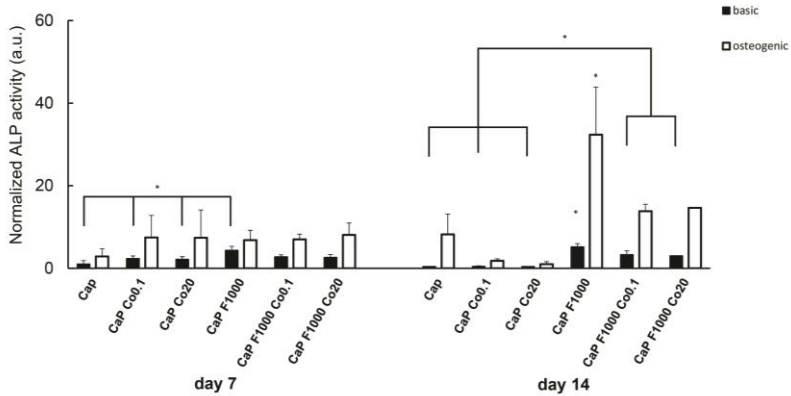


Figure 4. DNA content (a1, b1) and ALP activity (a2, b2) of hMSCs (n=3) cultured on uncoated tissue culture plastic and on CaP coatings, respectively. DNA content of the cells did not change upon exposure to  $\text{Co}^{2+}$ , whereas  $\text{F}^-$  ions increased the DNA content of the cells at day 14 when added to the medium, and decreased it when incorporated into CaP coatings. While a slight decrease in ALP activity of hMSCs was observed upon exposure to  $\text{Co}^{2+}$ ,  $\text{F}^-$  ions favored the expression of ALP activity.

### 5.3.4. Effect of $\text{Co}^{2+}$ and $\text{F}^-$ on ALP activity

Enzymatic ALP activity of hMSCs, as an early marker of osteogenesis, was quantified at days 7 and 14, normalized for DNA content and expressed in relation to the ALP activity in basic medium at 7 days (Figure 4.a2-b2). ALP levels measured in cells cultured on tissue culture plastic without coating were found to be higher than those measured in cells cultured on CaP coatings, independent of

the medium used. The addition of  $F^-$  ions to cell culture medium (Figure 4.a2) generally increased the ALP activity in hMSCs compared to control sample and samples containing only  $Co^{2+}$  ions, an effect that was independent of cell medium or time point.  $Co^{2+}$  ions, when added individually to cell medium, did not alter the ALP activity at day 7 and reduced the ALP activity at day 14 with a dose-dependent trend. The combination of  $F^-$  with  $Co^{2+}$  in higher concentration decreased the ALP activity as compared to  $F^-$  alone, however, this activity was still greater than that measured upon addition of only  $Co^{2+}$ .

In the CaP group, at day 7, the cells cultured in basic media on CaP F1000 had significantly higher ALP activity than the ones cultured of CaP, CaP Co0.1 and CaP Co20 (Figure 4.b2), though the differences were relatively small. At day 14, a general observation was that ALP activity in all the  $F^-$ -incorporated samples was higher than the one quantified in CaP, CaP Co0.1 and CaP Co20, independent of medium type, with CaP F1000 always resulting in highest ALP activity. Individual incorporation of  $Co^{2+}$ , however, reduced the ALP activity independent of cell medium. In combination with  $F^-$  incorporation,  $Co^{2+}$  incorporation also resulted in a reduction in ALP activity, however, in this case, the ALP activity was still higher than the one in CaP coatings without ion incorporation and with only  $Co^{2+}$  incorporation.

### 5.3.5. Effect of $Co^{2+}$ and $F^-$ on expression of osteogenic genes

Expression of osteogenic markers including ALP, BSP, BMP2, OC and OP of hMSCs in ions-conditioned media and upon culture on coatings incorporating ions was quantified via qPCR analysis after 7 and 14 days of culture (Figure 5.).

Addition of  $Co^{2+}$  ions to cell culture medium resulted in a dose-dependent reduction of ALP expression, independent of medium and time point. Addition of  $F^-$  to cell medium, however, strongly enhanced expression of ALP at all the time points, the effect which was more pronounced in osteogenic medium. Combination of dissolved  $Co^{2+}$  and  $F^-$  ions decreased ALP expression when compared to addition of  $F^-$  ions alone, however, the expression of ALP was still significantly higher compared to control and  $Co^{2+}$ -added samples (Figure 5.a1).

Also in the CaP coating group, it was generally observed that expression of ALP in hMSCs cultured on  $F^-$ -incorporated CaP coatings was higher than on CaP and  $Co^{2+}$ -incorporated CaP coatings, with this effect being stronger in osteogenic than in basic medium. Addition of  $Co^{2+}$  decreased the positive effect on  $F^-$  in a dose dependent manner (Figure 5.b1).

Similar to the ALP expression, BSP gene was also upregulated when F<sup>-</sup> ions, individually or in combination with Co<sup>2+</sup> ions, were added to cell media at both time points. Addition of Co<sup>2+</sup> to F<sup>-</sup> inhibited somewhat its effect in a dose dependent manner, though not to the level of the control medium without additives (Figure 5.a2).

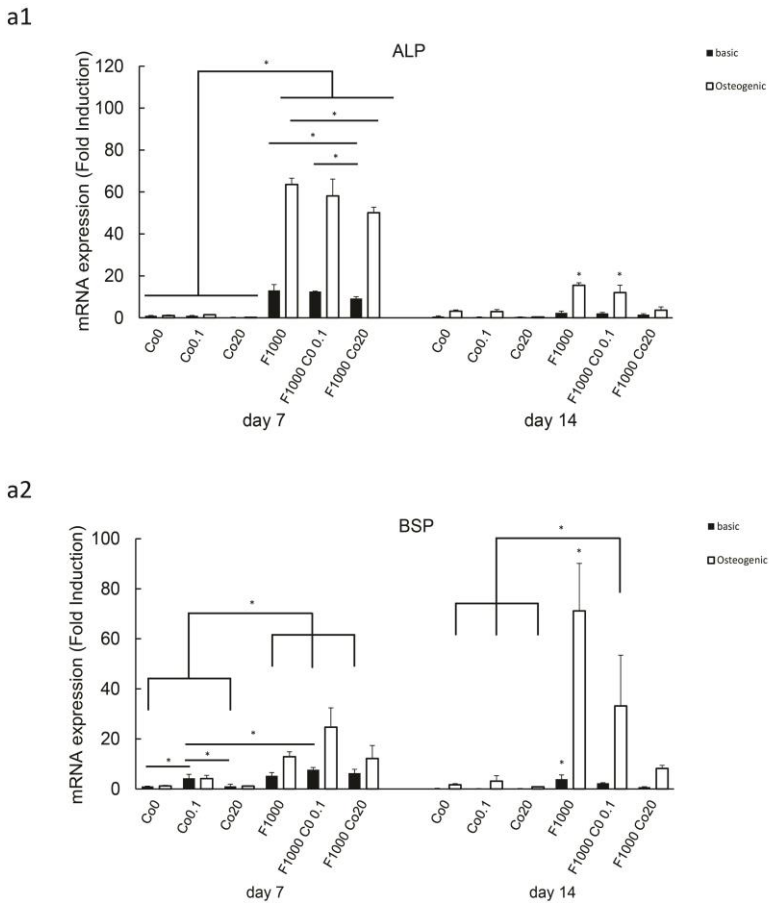
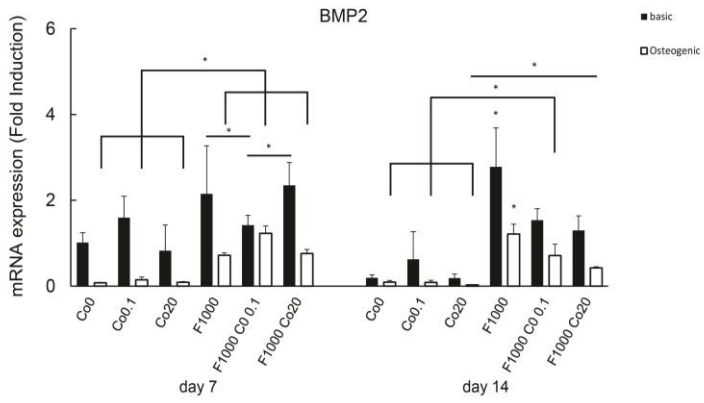
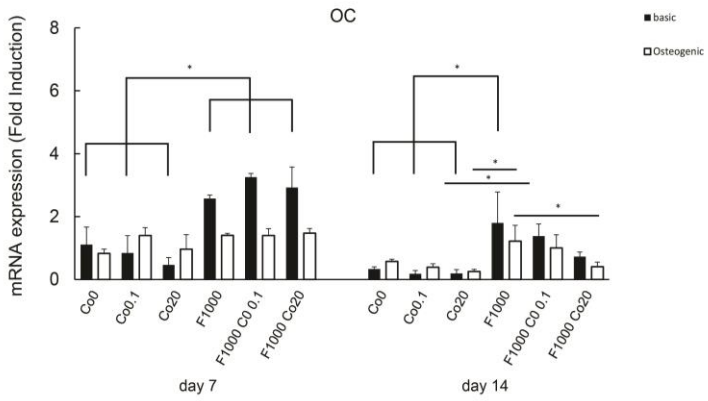


Figure 5. Continues in the next page.

a3



a4



a5

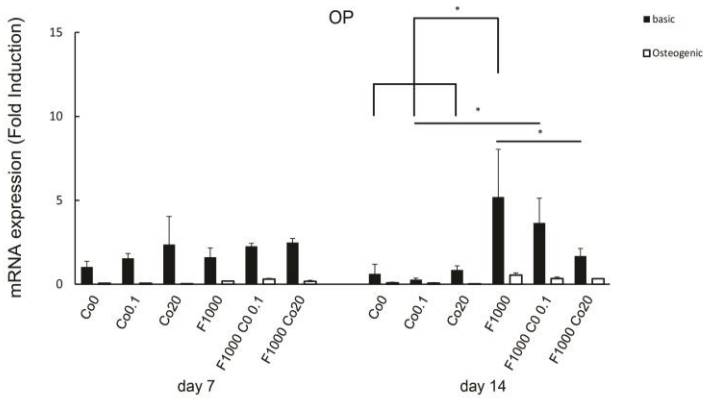


Figure 5. Continues in the next page.

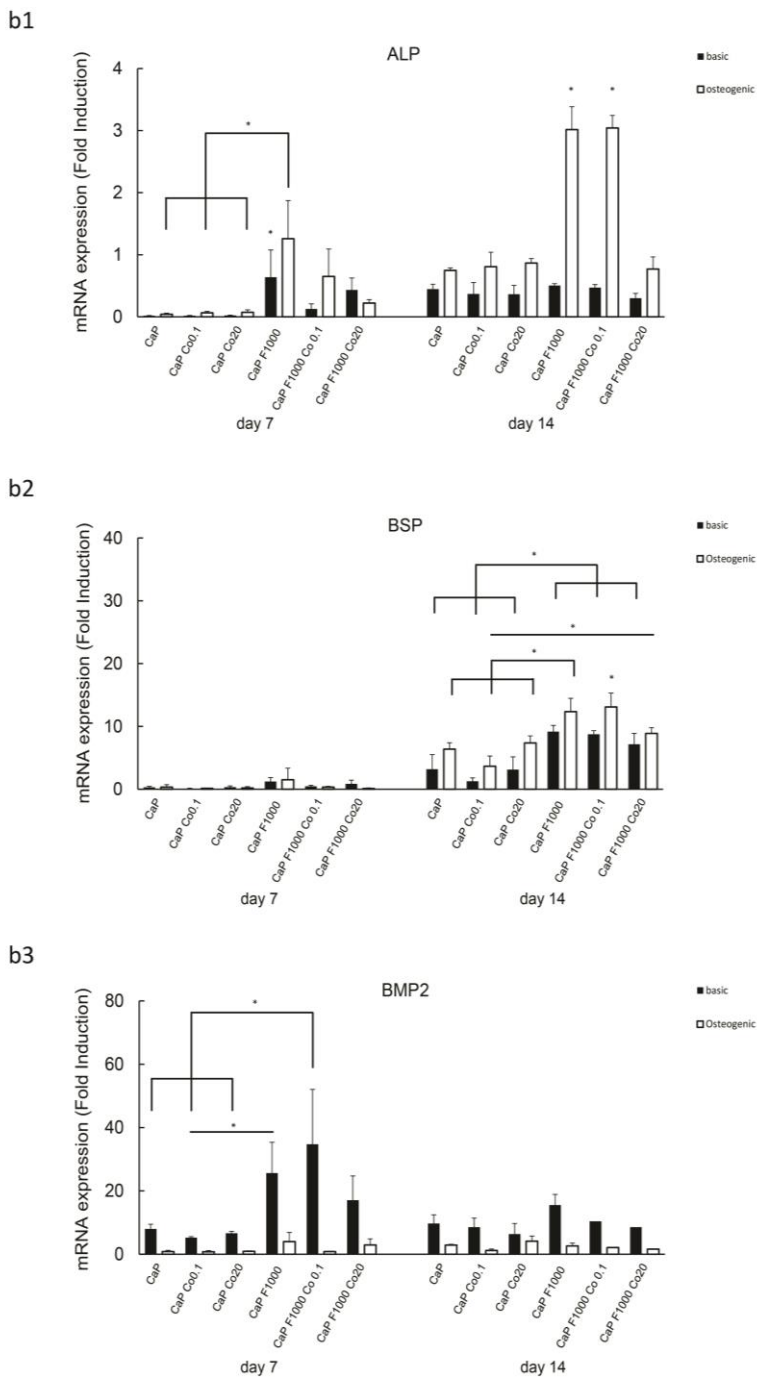


Figure 5. Continues in the next page.

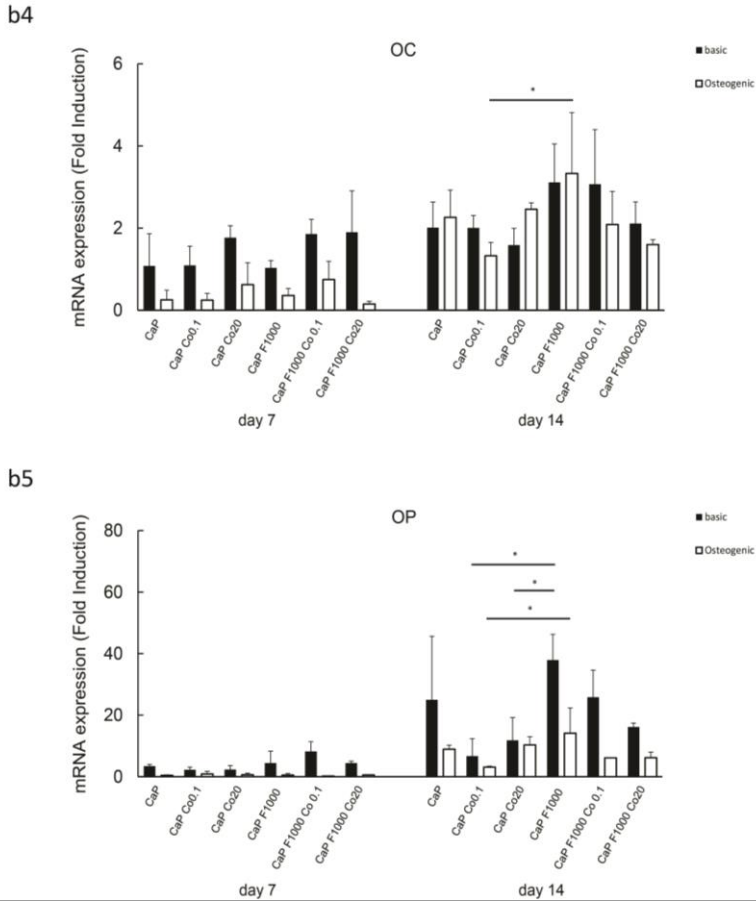


Figure 5. mRNA expression of ALP (a1, b1), BSP (a2, b2), BMP2 (a3, b3), OC (a4, b4) and OP (a5, b5) in hMSCs (n=3) cultured on uncoated tissue culture plastic and on CaP coatings, respectively. Limited to no effect of  $\text{Co}^{2+}$  was detected on the expression of osteogenic genes. In contrast, introduction of  $\text{F}^-$  ions to hMSCs in general substantially promoted the expression of osteogenic genes. Combined supplementation/incorporation of both ions had a less stimulatory effect on osteogenic differentiation than the use of  $\text{F}^-$  ions alone.

In the CaP group, no significant differences were detected in the expression of BSP gene among different samples at day 7. At day 14,  $\text{F}^-$ -incorporated CaP coatings generally led to a higher BSP expression in both media as compared to coatings without or with only  $\text{Co}^{2+}$  and the adverse effect of the addition of  $\text{Co}^{2+}$

was only seen at higher concentration and only in osteogenic medium (Figure 5.b2).

Regarding BMP2 expression by cells cultured in ion-conditioned media, no significant effect among different conditions was observed at day 7 in basic medium. However, in osteogenic medium at day 7 and in both media at day 14, supplementation by  $F^-$  ions resulted in a higher BMP2 expression, as compared to control media, or media containing only  $Co^{2+}$ . A decrease in the BMP2 expression was observed in combined ion condition as compared to the condition with  $F^-$  only (Figure 5.a3).

Also on CaP coatings, a positive effect of  $F^-$ -incorporation was observed on the BMP2 expression, with significant differences between CaP F1000 and CaP Co0.1 and between CaP F1000 Co0.1 and CaP, CaP Co0.1 and CaP Co20 in basic medium at 7 days (Figure 5.b3).

OC expression by cells cultured on uncoated and on coated tissue culture plastic remained relatively low for all conditions. All  $F^-$  supplemented basic media significantly increased OC gene expression compared to control basic medium and  $Co^{2+}$  supplemented media at 7 days. At day 14, the  $F^-$ -supplemented media showed a positive effect on OC expression, as compared to the conditions without  $F^-$ , in both types of media. A decrease in the expression was observed upon addition of  $Co^{2+}$  to  $F^-$  conditioned medium, in particular at higher concentrations (Figure 5.a4).

The effect of ion supplementation of the CaP coating on the OC expression was relatively small, with the only significant difference being between CaP F1000 and CaP Co0.1 in osteogenic medium at 14 days of culture (Figure 5.b4).

While no significant differences were detected in the expression of OP at day 7 among different conditions, at day 14, a general trend was that addition of  $F^-$  individually or in combination with  $Co^{2+}$  ions increased OP expression compared to the other samples. This effect was observed in both media even though the expression of OP was lower in osteogenic medium. Combining  $Co^{2+}$  ions with  $F^-$  ions reduced the expression of OP, dose-dependently. However, even in the highest concentration of  $Co^{2+}$ , this combination led to higher OP expression compared to the control samples, as well as when  $Co^{2+}$  ions were added individually (Figure 5.a5).

Also in the case of cells cultured on CaP coatings, at day 14, a beneficial effect of  $F^-$  incorporation was observed, in particular as compared to the coatings where only  $Co^{2+}$  was incorporated (Figure 5.b5).

### 5.3.6. Effect of $\text{Co}^{2+}$ and $\text{F}^-$ on hMSCs mineralization

Mineralization of hMSCs cultured on tissue culture plastic in basic or mineralization medium supplemented with  $\text{Co}^{2+}$  and/or  $\text{F}^-$  and on CaP coated tissue culture plastic without and with ion incorporation in basic and mineralization medium was analyzed after a 21-day culture period by staining the cells with Alizarin red solution.

When cultured on uncoated tissue culture plastic, hMSCs did not show any signs of mineralization in basic medium (data not shown). However, mineralization of the cells cultured in mineralization medium was detected (Figure 6.a-f). Supplementing the medium with  $20 \mu\text{M Co}^{2+}$  reduced the visible mineralized area (Figure 6.a-c), while the mineralized area was increased when the cells were exposed to  $1000 \mu\text{M F}^-$  ions (Figure 6.d). Although the combination of  $\text{Co}^{2+}$  and  $\text{F}^-$  ions showed less pronounced mineralization compared to the condition where only  $\text{F}^-$  ions were added, they resulted in a mineralization comparable to that observed in the control medium and medium supplemented with  $0.1 \mu\text{M Co}$  (figure 6.e-f). Calcium content quantification confirmed these results, however, the differences were relatively small and the only significant difference was found between F1000 and Co20 condition (Figure 6.g).

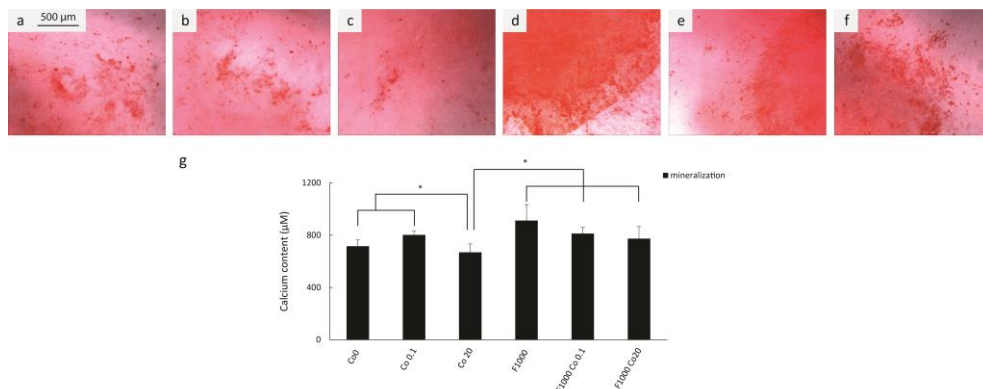


Figure 6. Light microscopy images of mineral formation by hMSCs ( $n=3$ ) cultured in mineralization medium without supplements (a) and with  $0.1 \mu\text{M Co}^{2+}$  (b),  $20 \mu\text{M Co}^{2+}$  (c),  $1000 \mu\text{M F}^-$  (d),  $1000 \mu\text{M F}^-$  and  $0.1 \mu\text{M Co}^{2+}$  (e) and  $1000 \mu\text{M F}^-$  and  $20 \mu\text{M Co}^{2+}$  (f), and quantification of calcium content in the cultures at day 21 (g). Presence of  $\text{Co}^{2+}$  ions reduced the amount of mineralization in the cultures, however, addition of  $\text{F}^-$  ions, individually or in combination with  $\text{Co}^{2+}$  ions, enhanced the mineralization of hMSCs.

Since Alizarin red staining of cells cultured on CaP coatings does not allow reliable quantification of cell mineralization, the culture was also performed in a trans-well set up in which the cells were cultured on the surface of the well while sharing a medium with a CaP-coated cover slip placed in the inset of the trans-well.

The culture in basic medium did not result in a high amount of mineralization. Small nodules of mineralization were, however, detected in hMSCs cultured with CaP coatings as shown by arrows in Figure 8.a1. Mineralization nodules did not form when cells were cultured with  $\text{Co}^{2+}$ -incorporated CaP coatings (Figure 7.b1-c1). When cultured with  $\text{F}^-$ -incorporated and  $\text{F}^-$  and  $\text{Co}^{2+}$ -incorporated CaP coatings, the mineralization nodules were found in larger numbers, however, they did not grow into mineralized areas (Figure 7.d1-f1). Quantification of the mineralization showed a slight increase in the calcium level in  $\text{F}^-$  containing coatings compared to the coatings without  $\text{F}^-$  incorporation (Figure 7.g).

In mineralization medium, cells cultured with CaP coatings showed extensive mineralization (Figure 7.a2-f2). In CaP Co0.1 and CaP Co20 coatings, the nodules were observed, however, they appeared dispersed over the surface (Figure 7.b2-c2). In contrast, in CaP F1000 samples, larger dense mineralization areas were observed (Figure 7.d2). The density of the mineralized layer reduced upon addition of both  $\text{Co}^{2+}$  and  $\text{F}^-$  ions into the coating as compared to the coating only containing  $\text{F}^-$ , but the mineralized area was still larger than in the CaP Co0.1 and CaP Co20 condition (Figure 7.e2-f2). Quantification of calcium content in the cultures showed that indeed  $\text{F}^-$ -incorporated CaP coatings resulted in higher calcium levels compared to CaP coatings with  $\text{Co}^{2+}$  incorporation (Figure 7.g).

#### 5.4. Discussion

The current use of bioinorganics in the field of orthopedics and dentistry ranges from anti-osteoporotic and anti-cariogenic treatments, to their incorporation into bone graft substitutes, with the aim of improving the properties and performance of the latter. As single trace elements incorporated into synthetic materials have demonstrated positive results to date, incorporating multiple bioinorganics may further enhance the biological performance. Several attempts have been made to incorporate multiple bioinorganics into various CaP-based materials [39-45], revealing enhanced impact of multiple bioinorganics on bone formation processes. In the present study, we have investigated the combined effect of  $\text{Co}^{2+}$

and  $F^-$  ions, which have been suggested to positively influence angiogenesis and osteogenesis, respectively.

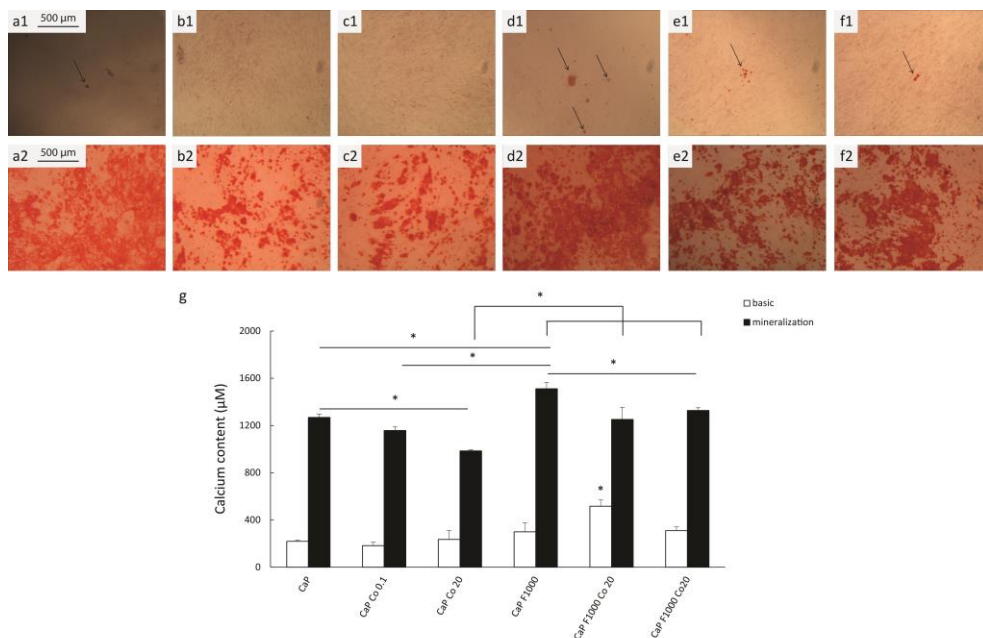


Figure 7. Mineralization of hMSCs (n=2) in basic (a1- f1) and mineralization medium (a2, - f2) in a trans-well set-up in the presence of CaP coating prepared without and with 0.1  $\mu\text{M}$   $\text{Co}^{2+}$ , 20  $\mu\text{M}$   $\text{Co}^{2+}$ , 1000  $\mu\text{M}$   $\text{F}^-$ , 1000  $\mu\text{M}$   $\text{F}^-$  and 0.1  $\mu\text{M}$   $\text{Co}^{2+}$  and 1000  $\mu\text{M}$   $\text{F}^-$  and 20  $\mu\text{M}$   $\text{Co}^{2+}$ , respectively, and quantification of calcium content in the cultures at day 21 (g). In mineralization medium, while presence of  $\text{Co}^{2+}$  in the coatings decreased the mineralized area in the coatings, incorporation of  $\text{F}^-$  ions in the coatings resulted in larger mineralization areas and higher calcium content in the cultures.

For  $\text{Co}^{2+}$ , a low (0.1  $\mu\text{M}$ ) and a higher (20  $\mu\text{M}$ ) concentration were used, above which cytotoxic effects of the ion were reported<sup>11</sup>. A constant  $\text{F}^-$  concentration of 1000  $\mu\text{M}$  was selected based on a preliminary study, at which the strongest positive effect on ALP activity of hMSCs was observed (data not shown), while avoiding cytotoxicity that has been reported above this concentration range [20-21]. In parallel with studies on direct ions supplementation of the cell culture medium, the ions were incorporated into a CaP coating using a previously

described method [32]. Similar concentrations of cobalt and fluoride salts were used as described for direct medium supplementation, without issues with stability of the CaP solution. However, since the efficiency of incorporation is never 100%, it should be noted that the amount of ions presented to the cells upon culture on CaP coatings is always lower than that achieved through direct supplementation of the medium. Furthermore, the concentrations selected in this study were optimized for in vitro experiments and the optimal ion content in the coatings may be different in the in vivo situation.

Physico-chemical characterization of the coatings revealed homogenous deposition of a low-crystalline CaP that predominantly consisted of an OCP phase with incorporation of some carbonate, which is in accordance with results previously obtained by applying the same technique [36-37]. Within the applied concentration range, the addition of  $\text{Co}^{2+}$  ions did not have an apparent effect on CaP coating properties, confirming the data previously presented by Patntirapong et al. [15]. Conversely, when  $\text{F}^-$  ions were added to the coating solution, significant changes were observed in the morphology of the CaP crystals, decreasing in size and becoming more rod-shaped as shown in previous studies [32,46-48], which is closer to apatitic crystal morphology [32]. This observation was confirmed by the changes observed in FTIR spectra after  $\text{F}^-$  incorporation.

5 The effect of  $\text{Co}^{2+}$  on the expression of angiogenic markers was measured as a first test to determine whether this ion could aid angiogenesis in a bone graft substitute. Vascularization is critical for the process of bone formation and remodeling, both in the development stage and during repair [49-50]. The absence of adequate blood supply, for example, in critically sized bone defects, may result in pathological conditions during the bone formation process.

The addition of  $\text{Co}^{2+}$  ions, both as direct supplement to the medium or incorporated into CaP coatings, upregulated the expression of VEGF and CD31 in hMSCs as compared to the control without  $\text{Co}^{2+}$ , although, in general, the expression of these markers was relatively low. A low expression of CD31 of hMSCs cultured in basic or osteogenic medium was expected based on an earlier study [51]. Higher marker expression was found when  $\text{Co}^{2+}$  was added to cell medium as a dissolved salt, which may be due to differences in concentration. These results are in accordance with those previously reported in literature. Supplementation of  $\text{Co}^{2+}$  ions in cell medium as well as the release of  $\text{Co}^{2+}$  from bioactive glass was shown to result in a significant increase in VEGF gene expression and/or protein release [14,17]. Furthermore, the implantation of  $\text{Co}^{2+}$ -

treated cells seeded on a collagen scaffold resulted in enhanced vascularized bone formation [17]. Cobalt, in ionic form, has been shown to induce hypoxia conditions by directly binding to and stabilizing hypoxia inducible factor- $\alpha$  [16-17]. Cells compensate for the low oxygen levels by expressing angiogenic markers and increasing blood vessel formation, which is the suggested mechanism behind the positive effect of  $\text{Co}^{2+}$  ions on angiogenesis [2].

The addition of  $\text{Co}^{2+}$  ions did not significantly change the DNA content of the cells. As DNA content can be considered an indication of cell number and growth, this result indicated that the presence of  $\text{Co}^{2+}$  ions did not have adverse effects on the cell viability. Although the toxic effects of  $\text{Co}^{2+}$  on various cell types have been reported, these effects were substantially dependent on the locally delivered dose, as well as the cell type [11-14].

The addition of 1000  $\mu\text{M}$   $\text{F}^-$  ions to cell medium did not appear to affect the DNA content of the cells at day 7 either. However, at day 14, there was a small increase in the DNA content compared to control and  $\text{Co}^{2+}$ -containing samples. Previous studies, however, have reported opposing results using similar concentrations of  $\text{F}^-$  ions, emphasizing different responses depending on the cell type [20-21].

While no effect was observed on the DNA content upon direct addition of  $\text{F}^-$  to the cell culture medium, incorporation into CaP coatings generally resulted in a reduction of the DNA content of the cells at later time points compared to CaP and  $\text{Co}^{2+}$ -incorporated CaP. This effect is possibly a result of the change of CaP coating morphology upon  $\text{F}^-$  ions incorporation.

Regarding the effect on the osteogenic differentiation of hMSCs,  $\text{Co}^{2+}$  ions suppressed the ALP enzymatic activity as well as the ALP expression at mRNA level, with the effect being more pronounced with direct addition to cell medium condition compared to the incorporation into the CaP coating, possibly due to differences in concentrations. Similar results were found for the expression of BSP gene, whereas no strong effect was found on the expression of BMP2, OC and OP using either delivery method. ALP and BSP genes are directly related to mineralization of the cells [52-53] and it was therefore not surprising to observe that direct addition, as well as incorporation of  $\text{Co}^{2+}$ , reduced the mineralization of hMSCs in terms of number and size of mineralization nodules and calcium content. These findings are consistent with earlier studies on the effect of cobalt on the osteogenic differentiation of osteoblastic progenitor and ligament cells. Andrews et al. [11] also observed a reduction in ALP activity of SaOS-2 cells upon  $\text{Co}^{2+}$  supplementation at concentrations higher than 10  $\mu\text{M}$ , and attributed this

effect to the potential cytotoxicity of the ions observed at these concentrations. Our data, however, did not show a reduction in cell proliferation in the examined range of concentrations. Similarly, Osathanon et al. [13] reported reduced ALP activity and expression of osteogenic genes including ALP, OC and RUNX2 as well as a significant reduction in mineralization in human periodontal ligament cells when cultured with 50 and 100  $\mu\text{M}$   $\text{CoCl}_2$ . These effects were attributed to the ability of  $\text{Co}^{2+}$  ions to maintain the stemness of the cells.

Exposure of hMSCs to  $\text{F}^-$  ions resulted in a strong increase in ALP activity, expression of osteogenic markers at mRNA level, as well as the formation and growth of mineralization nodules. Similar results have been previously obtained for both studies with and without CaP materials [20-22,24,26-29,31-33]. Several mechanisms have been proposed to describe the effects of fluoride on bone cells, in which many proteins and signaling pathways are involved [54]. The effects are, however, commonly attributed to fluoride's anabolic role on bone metabolism which increases the proliferation of bone cells, in addition to its potential in stimulating osteogenic differentiation, resulting in the deposition of bone matrix [21-22]. Besides these direct effect, the change of crystal morphology upon incorporation of  $\text{F}^-$  ions into the CaP coatings may also affect the osteogenic differentiation, as has been previously proposed by Yang et al. [32]. Regardless of the mechanism, these results support the use of  $\text{F}^-$  ions as means to enhance osteogenic differentiation of hMSCs.

Regarding the effect of the combination of the two ions on proliferation, osteogenic differentiation and mineralization of hMSCs, the general trend observed was that the addition of  $\text{Co}^{2+}$  weakened the positive effect of  $\text{F}^-$  ions, independent of the method of delivery. Nevertheless, even at higher  $\text{Co}^{2+}$  concentrations, a combination of the two ions indicated a more pronounced osteogenic differentiation and mineralization than the control without ionic additives.

While  $\text{Co}^{2+}$  and  $\text{F}^-$  release into cell culture medium has not been quantified in this study, in an earlier study, the effect of  $\text{Co}^{2+}$  ions incorporated into similar CaP coatings as used here was studied on osteoclastic resorption. In this study a gradual release of  $\text{Co}^{2+}$  into cell culture medium was observed over a 9-day culture period [15]. Similarly, we have observed the release of  $\text{Sr}^{2+}$  from similar CaP coatings into cell culture medium (unpublished data). Therefore, it is assumed that both  $\text{Co}^{2+}$  and  $\text{F}^-$  were released into the cell culture medium during culture of hMSCs here. This is in contrast to calcium ( $\text{Ca}^{2+}$ ) and inorganic phosphate (Pi) ions,

which are actually taken up from the medium, probably as a result of their high concentration in the medium. Clearly, the dynamics of this ion exchange on the surface is complex and requires further investigation.

While our results suggest that  $\text{Co}^{2+}$  ions promote the expression of angiogenic markers by hMSCs, and that  $\text{F}^-$  alone and in combination with  $\text{Co}^{2+}$  favors osteogenesis, further investigation is needed to confirm that the combination is also beneficial for angiogenesis. While enhanced expression of VEGF has been reported in rats upon treatment with  $\text{F}^-$  [55-56], the possibility of some antagonistic effects on vascularization from the combination of  $\text{Co}^{2+}$  and  $\text{F}^-$  remains, and further investigation is justified.

## 5.5. Conclusion

This study investigated the combined effects of two bioinorganics,  $\text{Co}^{2+}$  and  $\text{F}^-$  ions, as a means to stimulate both angiogenesis and osteogenesis. While  $\text{Co}^{2+}$  can stimulate angiogenesis, its detrimental effects on osteogenesis can be overruled by the addition of  $\text{F}^-$ . The combination of  $\text{Co}^{2+}$  and  $\text{F}^-$  resulted in higher expression of osteogenic markers and mineralization compared to the controls without ionic additives. This effect was obtained by direct addition of the ions to the cell culture medium, as well as through incorporation into CaP. Such approaches can be used to improve the performance of the bone graft substitutes.

Supplementary data 1. Atomic ratios in CaP coatings measured by EDS.

sample	Ca/P	Co/Ca	F/Ca
CaP	1.41	0.0019	0.05
CaP Co0.1	1.47	0.0004	0.04
CaP Co20	1.34	0.0081	0.05
CaP F1000	1.32	0.0022	0.29
CaP F1000 Co0.1	1.31	0.0010	0.22
CaP F1000 Co20	1.58	0.0058	0.14

## References

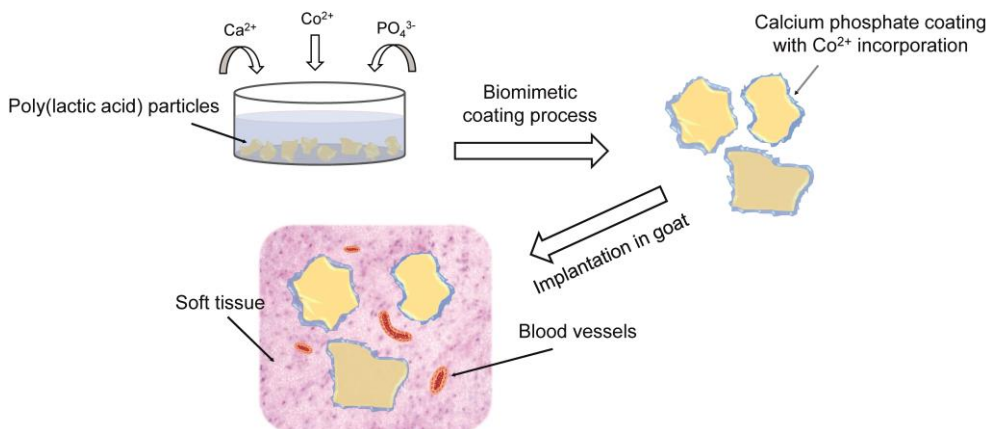
1. S. Bose, S. Tarafder, Calcium phosphate ceramic systems in growth factor and drug delivery for bone tissue engineering: A review, *Acta Biomaterialia* 8 (2012) 1401–1421.
2. S. Bose, G. Fielding, S. Tarafder, A. Bandyopadhyay, Understanding of dopant-induced osteogenesis and angiogenesis in calcium phosphate ceramics, *Trends in Biotechnology* 31 (10) (2013) 594–605.
3. J. Aaseth, G. Boivin, O. Andersen, Osteoporosis and trace elements – An overview, *Journal of Trace Elements in Medicine and Biology* 26 (2012) 149–152.
4. L. Yang, B. Harink, P. Habibovic, Calcium phosphate ceramics with inorganic additives, ed. P. Ducheyne, Elsevier Ltd., Oxford, 2011, chapter 1.118, 229–312.
5. P. Habibovic, J.E. Barralet, Bioinorganics and biomaterials: Bone repair, *Acta Biomaterialia* 7 (2011) 3013–3026.
6. E. Boanini, M. Gazzano, A. Bigi, Ionic substitutions in calcium phosphates synthesized at low temperature, *Acta Biomaterialia* 6 (2010) 1882–1894.
7. V. Mourino, J.P. Cattalini, A.R. Boccaccini, Metallic ions as therapeutic agents in tissue engineering scaffolds: an overview of their biological applications and strategies for new developments, *Journal of the Royal Society Interface* 6 (11) (2012) 1–19.
8. J. Gál, A. Hursthouse, P. Tatner, F. Stewart, R. Welton, Cobalt and secondary poisoning in the terrestrial food chain: Data review and research gaps to support risk assessment, *Environment International* 34 (2008) 821–838.
9. Q. Chen, G.A. Thouas, Metallic implant biomaterials, *Materials Science and Engineering R* 87 (2015) 1–57.
10. L.O. Simonsen, H. Harbak, P. Bennekou, Cobalt metabolism and toxicology—A brief update, *Science of the Total Environment* 432 (2012) 210–215.
11. R.E. Andrews, K.M. Shah, J.M. Wilkinson, A. Gartland, Effects of cobalt and chromium ions at clinically equivalent concentrations after metal-on-metal hip replacement on human osteoblasts and osteoclasts: Implications for skeletal health, *Bone* 49 (2011) 717–723.
12. N. Ignjatovic', Z. Ajdukovic', V. Savic', S. Najman, D. Mihailovic', P. Vasiljevic', Z. Stojanovic', V. Uskokovic', D. Uskokovic, Nanoparticles of cobalt-substituted hydroxyapatite in regeneration of mandibular osteoporotic bones, *Journal of Materials Science: Materials in Medicine* 24 (2013) 343–354.
13. T. Osathanon, P. Vivatbutsiri, W. Sukarawan, W. Sriarj, P. Pavasant, S. Soompon, Cobalt chloride supplementation induces stem-cell marker expression and inhibits osteoblastic differentiation in human periodontal ligament cells, *Archives of Oral Biology* 60 (2015) 29 – 36.
14. C. Wu, Y. Zhou, W. Fan, P. Han, J. Chang, J. Yuen, M. Zhang, Y. Xiao, Hypoxia-mimicking mesoporous bioactive glass scaffolds with controllable cobalt ion release for bone tissue engineering, *Biomaterials* 33 (2012) 2076–2085.
15. S. Patntirapong, P. Habibovic, P.V. Hauschka, Effects of soluble cobalt and cobalt incorporated into calcium phosphate layers on osteoclast differentiation and activation, *Biomaterials* 30 (2009) 548–555.
16. Y. Yuan, G. Hilliard, T. Ferguson, D.E. Millhorn, Cobalt inhibits the interaction between hypoxia-inducible factor- $\alpha$  and von Hippel-Lindau protein by direct binding to hypoxia-inducible factor- $\alpha$ , *The Journal Of Biological Chemistry* 178 (18) (2003) 15911–15916.
17. W. Fan, R. Crawford, Y. Xiao, Enhancing in vivo vascularized bone formation by cobalt chloride-treated bone marrow stromal cells in a tissue engineered periosteum model, *Biomaterials* 31 (2010) 3580–3589.
18. R.A. Surmenev, M.A. Surmeneva, A. A. Ivanova, Significance of calcium phosphate coatings for the enhancement of new bone osteogenesis – A review, *Acta Biomaterialia* 10 (2014) 557–579.
19. F. N. Hattab, The state of fluorides in toothpastes, *Journal of Dentistry* 17 (1989) 47–54.

20. C.G Bellows, J.N. Heersche, J.E. Aubin, The effects of fluoride on osteoblast progenitors in vitro, *Journal of Bone Mineralization Research* 5 (1990) 101-105.
21. W.Qu, D. Zhong, P. Wu, J. Wang, B. Han, "Sodium fluoride modulates caprine osteoblast proliferation and differentiation", *Journal of Bone Mineralization and Metabolism* 26 (2008) 328-334.
22. B.K. HALL, Sodium fluoride as an initiator of osteogenesis from embryonic mesenchyme in vitro, *Bone* 8 (1987) 111-116.
23. E.J. Lee, S.H. Lee, H.W. Kim, Y.M. Kong, H.E. Kim, Fluoridated apatite coatings on titanium obtained by electron-beam deposition, *Biomaterials* 26 (2005) 3843-3851.
24. Y.S. Wang, S. Zhang, X.T. Zeng, L.L. Ma, W.J. Weng, W.Q. Yan, Osteoblastic cell response on fluoridated hydroxyapatite coatings, *Acta Biomaterialia* 3 (2007)191-197.
25. Z. Sam, X.T. Zeng, Y.S. Wang, K.L. Cheng, W.J. Wenig, Adhesion strength of sol-gel derived fluoridated hydroxyapatite coatings, *Surface Coating Technology* 200 (2006) 6350-6354.
26. B. Hahn, Y. Cho, D. Park, J. Choi, J.Ryu, J. Kim, C. Ahn, C. Park, H. Kim, S. Kim, Effect of fluorine addition on the biological performance of hydroxyapatite coatings on Ti by aerosol deposition, *Journal of Biomaterials Applications* 27 (2011) 587-594.
27. J. Wang, Y. Chao, Q. Wan, Z. Zhu, H. Yu, Fluoridated hydroxyapatite coatings on titanium obtained by electrochemical deposition, *Acta Biomaterialia* 5 (2009) 1798-1807.
28. H. Kim, H. Kim, J.C. Knowles, Fluor-hydroxyapatite sol-gel coating on titanium substrate for hard tissue implants, *Biomaterials* 25 (2004) 3351-3358.
29. J. Li, Y. Song, S. Zhang, C. Zhao, F. Zhang, X. Zhang, L. Cao, Q. Fan, T. Tang, In vitro responses of human bone marrow stromal cells to a fluoridated hydroxyapatite coated biodegradable MgZn alloy, *Biomaterials* 31 (2010) 5782-5788.
30. H. Kim, Y. Kong, C. Bae, Y. Noh, H. Kim, Sol-gel derived fluor-hydroxyapatite biocoatings on zirconia substrate, *Biomaterials* 25 (2004) 2919-2926.
31. H. Qu, M. Wei, The effect of fluoride contents in fluoridated hydroxyapatite on osteoblast behavior, *Acta Biomaterialia* 2 (2006) 113-119.
32. L. Yang, S. Perez-Amodio, F.Y.F. Barre` re-de Groot, V. Everts, C.A. van Blitterswijk, P. Habibovic, The effects of inorganic additives to calcium phosphate on in vitro behavior of osteoblasts and osteoclasts, *Biomaterials* 31 (2010) 2976-2989.
33. E. Gentleman, M.M. Stevens, R.G. Hill, D.S. Brauer, Surface properties and ion release from fluoride-containing bioactive glasses promote osteoblast differentiation and mineralization in vitro, *Acta Biomaterialia* 9 (2013) 5771-5779.
34. H. Fernandes, A. Mentink, R. Bank, R. Stoop, C. van Blitterswijk, J. de Boer, Endogenous Collagen Influences Differentiation of Human Multipotent Mesenchymal Stromal Cells, *Tissue Engineering: Part A* 16 (2010) 1693-1702.
35. S.K. Both, A.J.C. van der Muijsenberg, C.A. van Blitterswijk, C.A., J. de Boer, J.D. de Bruijn, A rapid and efficient method for expansion of human mesenchymal stem cells, *Tissue Engineering* 13 (2007) 3-9.
36. P. Habibovica, J. Li, C.M. van der Valk, G. Meijer, P. Layrolled, C.A. van Blitterswijk, K. de Groot, Biological performance of uncoated and octacalcium phosphate-coated Ti6Al4V, *Biomaterials* 26 (2005) 23-36.
37. F. Barrère, P. Layrolle, C.A. van Blitterswijk, K. de Groot, Biomimetic Calcium phosphate Coatings on Ti6Al4V: a Crystal Growth Study of Octacalcium Phosphate and Inhibition by  $Mg^{2+}$  and  $HCO_3^-$ , *Bone* 25 (1999) 107S-111S.
38. L.L. Hench, S.M. Best, *Ceramic, glasses and glass ceramics: Basic principles*, ed. B.D. Ratner, Academic Press, 3<sup>rd</sup> edition, 2013, Chapter I.2.4, 128-151.
39. M.S. Sadera, K. Lewis , G.A. Soares , RZ. LeGeros, Simultaneous Incorporation of Magnesium and Carbonate in Apatite: Effect on Physico-chemical Properties, *Materials Research* 16 (2013) 779-784.

40. F. Yao, R.Z. LeGeros, Carbonate and fluoride incorporation in synthetic apatites: Comparative effect on physico-chemical properties and in vitro bioactivity in fetal bovine serum, *Materials Science and Engineering C* 30 (2010) 423–430.
41. B. Badraoui, A. Aissa, A. Bigi, M. Debbabi, M. Gazzano, Synthesis and characterization of Sr(10x)Cdx(PO<sub>4</sub>)<sub>6</sub>Y<sub>2</sub>(Y=OH and F): A comparison of apatites containing two divalent cations, *Materials Research Bulletin* 44 (2009) 522–530.
42. M. Roy, G.A. Fielding, A. Bandyopadhyay, S. Bose, Effects of zinc and strontium substitution in tricalcium phosphate on osteoclast differentiation and resorption, *Biomaterial Science* 1 (2013) 74–82.
43. S. Tarafder, N.M. Davies, A. Bandyopadhyay, S. Bose, 3D printed tricalcium phosphate bone tissue engineering scaffolds: effect of SrO and MgO doping on in vivo osteogenesis in a rat distal femoral defect model, *Biomaterial Science* 1 (2013) 1250–1259.
44. G. Fielding, S. Bose, SiO<sub>2</sub> and ZnO dopants in three-dimensionally printed tricalcium phosphate bone tissue engineering scaffolds enhance osteogenesis and angiogenesis in vivo, *Acta Biomaterialia* 9 (2013) 9137–9148.
45. S. Bose, S. Tarafder, S.S. Banerjee, N.M. Davies, A. Bandyopadhyay, Understanding in vivo response and mechanical property variation in MgO, SrO and SiO<sub>2</sub> doped β-TCP, *Bone* 48 (2011) 1282–1290.
46. Y. Shiwaku, T. Anada, H. Yamazaki, Y. Honda, S. Morimoto, K. Sasaki, O. Suzuki, Structural, morphological and surface characteristics of two types of octacalcium phosphate-derived fluoride-containing apatitic calcium phosphates, *Acta Biomaterialia* 8 (2012) 4417–4425.
47. W. Xia, C. Lindahl, C. Persson, P. Thomsen, J. Lausmaa, H. Engqvist, Changes of surface composition and morphology after incorporation of ions into biomimetic apatite coatings, *Journal of Biomaterials and Nanobiotechnology* 1 (2010) 7–16.
48. Y. Fan, Z. Sun, J. Moradian-Oldak, Effect of fluoride on the morphology of calcium phosphate crystals grown on acid-etched human enamel, *Caries Research* 43 (2009) 32–136.
49. H. Gerber, N. Ferrara, Angiogenesis and Bone Growth, *Trends in Cardiovascular Medicine* 10( 5) ( 2000) 223–228.
50. R.A.D. Carano, E.H. Filvaroff, Angiogenesis and bone repair, *Drug Discovery Today* 8 (2003) 980–989.
51. J. Rouwkema, J. de Boer, C.A. van Blitterswijk, Endothelial cells assemble into a 3-dimensional prevascular network in a bone tissue engineering construct, *Tissue Engineering* 12 (2006) 2685–2693.
52. H. Orimo, The mechanism of mineralization and the role of alkaline phosphatase in health and disease, *Journal of Nippon Medical School* 77 (2010) 4–12.
53. J.A.R. Gordon, C.E. Tye, A.V. Sampaio, T.M. Underhill, G.K. Hunter, H.A. Goldberg, Bone sialoprotein expression enhances osteoblast differentiation and matrix mineralization in vitro, *Bone* 41 (2007) 462–473.
54. K.H.W. Lau, D.J. Baylink, Molecular Mechanism of Action of Fluoride on Bone Cells, *Journal of Bone and Mineral Research* 13 (1998) 1660–1667.
55. G. Liua, W. Zhang, P. Jiang, X. Li, C. Liua, C. Chai, Role of nitric oxide and vascular endothelial growth factor in fluoride-induced goitrogenesis in rats, *Environmental Toxicology and Pharmacology* 34 (2012) 209–217.
56. A.Y. Alhijazi, A. Dheyaa Neamah, Expression of and BMP7 in bone healing after Topical, systemic fluoride application (experimental study in rats), *International Research Journal of Natural Sciences* 2 (2014) 52–68.

## Chapter 6

### Stimulatory effect of cobalt ions incorporated into calcium phosphate coatings on neovascularization in an in vivo intramuscular model in goats



## Abstract

Rapid vascularization of bone graft substitutes upon implantation is one of the most important challenges to overcome in order to achieve successful regeneration of large, critical-size bone defects. One strategy for stimulating vascularization during the regeneration process is to create a hypoxic microenvironment by either directly lowering the local oxygen tension or by applying hypoxia-mimicking factors. Cells compensate for the hypoxic condition by releasing angiogenic factors and forming new blood vessels. In the present study, we explored the potential of cobalt ions ( $\text{Co}^{2+}$ ), known chemical mimickers of hypoxia, to stimulate vascularization inside a bone graft substitute in vivo. To this end,  $\text{Co}^{2+}$  ions were incorporated into calcium phosphate (CaPs) coatings deposited on poly(lactic acid) (PLA) particles and their effect on the formation of new blood vessels was studied upon intramuscular implantation in goats. PLA particles and CaP-coated particles without  $\text{Co}^{2+}$  ions served as controls. Pathological scoring of the inflammatory response following a 12-week implantation period showed no significant differences between the four types of materials. Histological and immunohistochemical analyses revealed higher values for both blood vessel area and number of blood vessels in CaP-coated PLA particles containing  $\text{Co}^{2+}$  as compared to the uncoated PLA particles and CaP-coated PLA particles without  $\text{Co}^{2+}$ . Analysis of blood vessel size distribution indicated abundant formation of small blood vessels in all the samples, while large blood vessels were predominantly found in PLA particles coated with CaP containing  $\text{Co}^{2+}$  ions. The results of this study supported the use of CaPs containing  $\text{Co}^{2+}$  ions to enhance vascularization in vivo.

## 6.1. Introduction

Angiogenesis plays a pivotal role in skeletal development and regenerative fracture repair [1-2]. It has been shown that inadequate or abnormal vascularization negatively affects the bone healing process, leading to inferior bone formation or formation of fibrous tissue in the bone defect area [2-3]. Therefore, establishment and maintenance of vasculature remains an important challenge in bone regenerative strategies, especially when large, critical-size bone defects are considered.

Surgical approaches such as induced membrane and distraction osteogenesis have been traditionally used as methods for increasing the vascularization of natural or synthetic bone graft substitutes. Although such techniques have shown some successes, their use is associated with important drawbacks including the need for a second surgery, pain, extended surgical procedure and recovery time, etc. [4].

Bone regenerative strategies based on biomaterials and tissue-engineered constructs have offered a number of interesting solutions to couple processes of angiogenesis and osteogenesis, as in detail reviewed by Mercado-Pagán et al. [4], Laschke and Menger [5], Lovett et al. [6] and Nguyen et al. [7]. A common strategy to improve vascularization in bone graft substitutes revolves around tuning of the scaffold properties such as chemical composition, porosity and mechanical strength [4-5, 8]. Functionalization of scaffolds by growth- and other stimulatory factors such as vascular endothelial growth factor (VEGF) [9-11] and fibroblast growth factor (FGF) [12] and incorporation of blood vessel forming cells such as endothelial cells and pericytes [4,13-15] are typical tissue engineering approaches to achieve angiogenesis and establish vascularization of bone graft substitutes. Complementary techniques such as mechanical [16-18] and electrical stimulation [19], and microfabrication techniques [20] have also been investigated. Alternatively, induction of angiogenesis by lowering the oxygen tension or incorporating the hypoxia mimicking factors into the scaffold has also been recognized as a promising approach [21]. It has been shown that cells respond to hypoxia by producing higher levels of pro-angiogenic factors such as VEGF and erythropoietin (EPO) and forming more blood vessels in order to compensate for the low oxygen tension [22]. For example, Doorn et al. showed that a small molecule phenanthroline, a hypoxia-mimicking factor, upregulated the expression of hypoxia-target genes in human mesenchymal stromal cells. Furthermore, they showed that the release of phenanthroline from Matrigel plugs resulted in induction of blood vessel formation *in vivo* in a mouse model [21].

Cellular response to low oxygen tension can be mimicked by cobalt ions ( $\text{Co}^{2+}$ ), a process sometimes referred to as chemical hypoxia [23-24]. Being a transition metal,  $\text{Co}^{2+}$  can replace  $\text{Fe}^{2+}$  from the catalytic sites of the Hypoxia Inducible Factor (HIF) prolyl-hydroxylases (PHDs), leading to inhibition of its enzymatic function [25]. As a result, the continuous destruction of HIF1- $\alpha$ , a key transcription factor is stopped and HIF-responsive gene expression is upregulated [26].  $\text{Co}^{2+}$  has previously been shown to induce the in vitro angiogenesis in 3D scaffolds [27], as well as to promote neovascularization in vivo, upon direct addition to or after treatment of cells by  $\text{Co}^{2+}$  in bone tissue-engineered constructs [28-29].

Calcium phosphates (CaPs) are the most widely used family of biomaterials in the field of bone regeneration, owing to their chemical resemblance to the mineral portion of bone [30]. CaP ceramics are, however, intrinsically brittle, which is why they are often combined with other materials, like polymers, which are more versatile in terms of mechanical properties [31-32]. CaPs and CaP-based hybrid systems are biocompatible, osteoconductive and, in some cases, even osteoinductive [33-34], and they have the advantage of being relatively inexpensive and available in large quantities, however, they are still not considered a full alternative to the golden standard for bone regeneration, i.e. autograft [35]. One of the promising methods to improve the bioactivity of CaPs, while retaining their synthetic character, is the use of bioinorganics [36] such as  $\text{Mg}^{2+}$ ,  $\text{Zn}^{2+}$ ,  $\text{Sr}^{2+}$ , etc. Many of these elements are present in bone mineral, often in trace amounts, and are known for their role in bone formation and remodeling processes [36-38]. Few studies have also explored the possibility of incorporating  $\text{Co}^{2+}$  into CaPs and investigate their effect in vitro [39-40].

In an attempt to develop bone graft substitutes that stimulate angiogenesis, in the current study, we have deposited CaP coatings with or without  $\text{Co}^{2+}$  on particles of poly(lactic acid) (PLA), a widely used aliphatic polyester in biomedical application [41], by employing the previously described biomimetic method [39, 42]. The constructs were implanted intramuscularly in 9 goats, and formation of new blood vessels was assessed using histological and immunohistochemical techniques.

## 6.2. Materials and Methods

### 6.2.1. Material production

CaP-coated poly(D,L-lactic acid) (PLA) particles without and with  $\text{Co}^{2+}$  incorporation in the CaP phase were used in this study, and uncoated PLA particles served as a control.

A low molecular weight PLA (Purasorb PDL05, Purac, MW: 59000 g/mole) was used to produce polymeric particles by means of extrusion as described previously [43]. In short, PLA was extruded using a twin-screw extruder with conical non-converging screws (Artecs BV, Enschede, the Netherlands) at 150 °C and the screw rotation speed of 100 rpm. After 5 minutes, the rod-shaped polymer was allowed to flow out of the extruder. The rods were ground and sieved to obtain particles with the size in the range 0.5-1 mm.

The PLA particles were coated with a CaP layer by applying a two-step biomimetic procedure as described earlier [39, 42]. In short, the particles were first immersed in a 2.5 times concentrated Simulated Body Fluid (SBF 2.5x) with ionic content of 733.5 mM  $\text{Na}^{2+}$ , 7.5 mM  $\text{Mg}^{2+}$ , 12.5 mM  $\text{Ca}^{2+}$ , 720 mM  $\text{Cl}^-$ , 5 mM  $\text{HPO}_4^{2-}$  and 21 mM  $\text{HCO}_3^-$ , while stirring at 37 °C for three days with daily refreshment. In the second step, the particles were incubated with a calcium phosphate solution (CPS) consisting of 140 mM  $\text{Na}^{2+}$ , 4 mM  $\text{Ca}^{2+}$ , 2 mM  $\text{HPO}_4^{2-}$  and 144 mM  $\text{Cl}^-$  (buffered at pH 7.4), under stirring at 37 °C for three days with daily refreshments. A stock solution of cobalt chloride (Sigma) in a Tris buffer (pH=7.4) with concentration of 10 mM was prepared. In order to incorporate the ion into CaP coatings, appropriate volumes of  $\text{Co}^{2+}$  stock solution were combined with the CPS solution to reach varying concentrations of  $\text{Co}^{2+}$  in CPS (0, 0.1 and 20  $\mu\text{M}$ ). The  $\text{Co}^{2+}$  concentration was selected based on an earlier in vitro study [39] on hypoxia-mimicking by Co to investigate the effect on osteoclastic resorption that showed a successful incorporation of the ion into CaP using a similar technique. The coated PLA particles were washed three times with MilliQ water and dried at least overnight in an air oven.

PLA particles were prepared using the same extrusion procedure and served as control in all the experiments.

### 6.2.2. Material Characterization

The surface morphology and the presence of calcium, phosphorous carbon and cobalt were investigated on gold-sputtered PLA and CaP-coated PLA particles

without  $\text{Co}^{2+}$  (CaP-PLA), with low  $\text{Co}^{2+}$  concentration (CaP Co0.1-PLA) and with high  $\text{Co}^{2+}$  concentration (CaP Co20-PLA) using scanning electron microscopy (SEM, XL-30 ESEM-FEG, Philips) in the secondary electron mode, coupled with energy dispersive X-ray spectroscopy analyzer (EDS, EDAX, AMETEK Materials Analysis Division) at the accelerator voltage of 10 KeV and working distance of 10 mm. The chemical composition of the particles was characterized using Fourier transform infrared spectroscopy (FTIR, Perkin-Elmer Spectrum 1000) in transmission mode. Furthermore, the total amount of Co, as well as Ca/P ratio in CaP-PLA, CaP Co0.1-PLA and CaP Co20-PLA (n=3) were determined using ICP-MS analysis (Agilent 7700 ICP-MS), upon dissolution of the CaP coating in ultra-pure nitric acid. Briefly, 1 ml ultra-pure nitric acid (10 v/v%) was added to approximately 100  $\mu\text{l}$  of particles of each of the four types for approximately 5 minutes. The solution was then diluted 10 times using MilliQ water, prior to the ICP-MS analysis.

### 6.2.3. Implantation

Prior to implantation, approximately 1 ml of particles of each PLA, CaP-PLA, CaP Co0.1-PLA and CaP Co20-PLA were sterilized inside histological tissue bags by using ethylene oxide (Isotron Nederland BV). The animal study was approved by the animal ethical committee of the University of Utrecht, Utrecht, the Netherlands (DEC 2012. III.04.040). In total, 10 Dutch milk goats were used for the study. One animal died of pneumonia before the implantations started, and the remaining animals received one implant of each type (n=9). The animals also received other implants, both intramuscularly and on the transverse processes of the lumbar spine. These implantations were not related to this study, and their results will be published separately. The surgical procedures were performed under general anesthesia of the animals, which was achieved and maintained by isoflurane under sterile condition. Before surgery, the skin of the back of animals was shaved and disinfected with a 10% povidone-iodine solution. A longitudinal incision followed by a blunt separation was made in the paraspinal area to expose the muscles. Fascia incisions were created in the muscles. Intramuscular pockets were created bilaterally by blunt dissection, and each pocket was filled with about 1 ml of the material by using an open syringe. A randomization scheme was used to minimize location-induced effects. Then, fascias were closed with nonresorbable sutures to facilitate implant localization at explantation. The skin was closed in two layers. All animals received a subcutaneous injection of

Albipen® (7.5 ml/50kg, Intervet BV, Boxmeer, The Netherlands) for five consecutive days after surgery to eliminate the risk of post-operative infections.

#### **6.2.4. Implant retrieval, histological and immunohistochemical evaluation**

Twelve weeks after the implantation, the animals were sacrificed by an overdose of Nembutal® (Apharmo, Arnhem, The Netherlands) and the samples with surrounding tissue were harvested. The explants were stored in 4% formaldehyde at 4° C for at least one week. They were then trimmed to remove the surrounding muscle tissue and each sample was cut into two equal parts, one of which was used for histological and immunohistochemical evaluation of blood vessel formation. For histology, the samples were first decalcified in 125 gr/l ethylenediaminetetraacetic acid solution (EDTA, Sigma) for one week and then dehydrated using a series of ethanol solutions (70%, 80%, 90%, 96%, 100%) for at least 5 days per step. They were then placed in polymeric holders, kept in melted paraffin overnight and embedded in paraffin using an automatic embedding apparatus (Excelsior ES, Thermo Scientific). The paraffin blocks were then cut in 5-8 µm thick sections using a microtome (HM355, Microm, Belgium) and dried overnight at room temperature on objective glasses.

Immunohistochemical staining of actin fibers in smooth muscle cells was performed on 4 sections per sample. Briefly, the sections were deparaffinized and rehydrated in xylene and ethanol series, respectively. After washing with milliQ water, the sections were blocked for 1 hour with a blocking solution (0.5 W/V% bovine serum albumin (BSA) and 0.1 v/v% Triton X-100 in PBS). Subsequently, 100 µl Monoclonal Mouse Anti-Human Actin Smooth Muscle antibody (asma, Clone 1A4, Dako, Belgium) diluted in blocking buffer (1:200) was added to each section, and incubated overnight at room temperature in dark. After incubation, the sections were washed with blocking solution, and the anti-goat secondary antibody diluted in blocking solution (1:1000) was added for 1 hour. The sections were then washed twice with PBS and dried in dark in a fume hood for few minutes. The slides were then mounted using a mounting medium containing DAPI to stain the nuclei (VectaShield, Vector Laboratories, Burlingame, USA) prior to imaging using the NanoZoomer both in brightfield mode (data not shown) and in fluorescent mode in DAPI- (data nor shown) and FITC channels.

Hematoxylin and eosin (H&E, Sigma) staining was performed on 2 sections per sample. In short, the sections were first deparaffinized in xylene (Klinpath) and then rehydrated in a series of ethanol solutions (100%, 96%, 90%, 80% and 70%)

and stained with hematoxylin solution for 5 minutes, rinsed with tap water, counterstained with eosin solution for 2 minutes and fixed in xylene. Masson's trichrome (MT, Merck chemicals) staining was performed on 6 sections per sample. After deparaffinization and rehydration, the sections were stained according to the manufacturer's protocol. The H&E and the MT stained sections were then mounted on coverslips and dried overnight in a fume hood. The slides were imaged using a NanoZoomer (NanoZoomer 2.0 RS, Hamamatsu, Japan) in the brightfield mode.

The extent of the inflammatory response was evaluated by an experienced pathologist. Randomly selected H&E-stained slides of each sample type from all animals were used for scoring the presence of inflammatory cells in the connective tissue between the material particles as well as in the connective tissue around the implant. When 40-60% of the connective tissue contained inflammatory cells, the sample received score 2. Samples with inflammatory cells present in less than 40% of the connective tissue area received score 1, and above 60%, score 3.

Number of blood vessels and blood vessel area were quantified on 6 MT-stained slides per sample selected from different areas (2 from the top, 2 from the middle and 2 from the bottom). Quantification of the blood vessel area per sample area was performed using Adobe Photoshop CS6 by first determining the sample area (per pixel) and then manually selecting and quantifying the red-stained area (per pixel). Quantification of the vessel number was done semi-automatically by using ImageJ 1.48 by first adjusting the color thresholds to eliminate the noise of the background and then quantifying the number of cells. The results were then normalized for the sample area and presented as number of vessels per 1000 pixels area.

### **6.2.5. Statistical analysis**

For the statistical analysis of the scores for inflammatory response to the four material types, the Kruskal-Wallis test was performed. Histomorphometrical data on blood vessel area and blood vessel number were analyzed by using the One-way Analysis of Variance (ANOVA) followed by a Tukey's multiple comparison post-hoc test. Differences were considered statistically significant at  $p < 0.05$ .

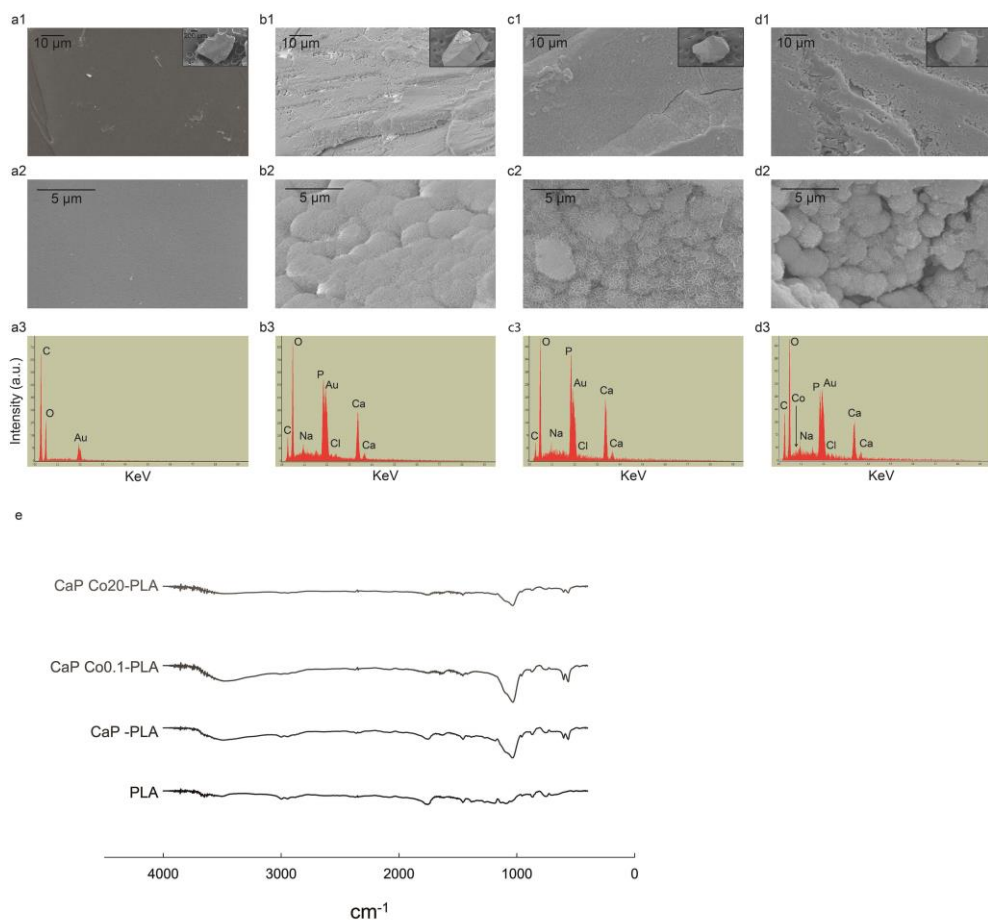
## 6.3. Results

### 6.3.1. Material characterization

The extrusion-grinding technique used for the production of implants resulted in the formation of irregularly shaped dense PLA particles with a diameter of 0.5-1mm (Figure 1.a1-d1, insets). Upon the two-step biomimetic coating process, a uniform mineral layer was formed on the surface of PLA particles, covering it completely. Addition of  $\text{Co}^{2+}$  to the CPS solution did not prevent the formation of the mineral coating on the particles. Microscopically, while the PLA particles exhibited a relatively smooth surface, the CaP-coated particle surface appeared rougher and more porous. The coating consisted of mineral globules with a diameter below  $1\ \mu\text{m}$  that were built of small plate-shaped crystals. The presence of  $\text{Co}^{2+}$  in CPS solution did not have an obvious effect on the size or the morphology of the crystals (Figure 1.a1-d2). The EDS analysis showed a decrease in the intensity of the carbon peak on the surface of the coated PLA particles as compared to the uncoated PLA. This was accompanied by the appearance of the calcium and phosphorous peaks and an increase in the intensity of oxygen, suggesting the formation of a CaP phase on the surface of PLA particles. A small peak of Co could be detected only at higher concentrations, i.e. in CaP Co20-PLA sample. Appearance of sodium and chlorine peaks in the EDS spectra of CaP-coated PLA particles indicated the presence of residual NaCl in the coating, suggesting incomplete washing (Figure 1.a3-d3).

FTIR analysis of the PLA particles without coating (Figure 1. e) showed typical spectrum of pure PLA including the bands at approximately  $1000\text{-}1100\ \text{cm}^{-1}$  that corresponded to the stretching mode of C-O bond, at  $1370\text{-}1450$  and  $1950\text{-}2000\ \text{cm}^{-1}$  corresponding to bending and stretching modes and at  $1750\ \text{cm}^{-1}$  that is attributed to stretching mode of C=O bond [44-46].

Similar peaks were observed in the FTIR spectra of all CaP-coated PLA particles. The C-O band at  $1000\ \text{cm}^{-1}$  was however modified in these samples due to the presence of  $\text{PO}_4^{3-}$  peak at similar wavelength [43, 46]. The bands at  $560$  and  $604\ \text{cm}^{-1}$  in the FTIR spectra of all CaP-coated PLA particles also corresponded to the P-O bond. The small shoulder at  $3565\ \text{cm}^{-1}$  formed on  $\text{H}_2\text{O}$  band at approximately  $3500\ \text{cm}^{-1}$  is attributed to the hydroxyl group. These results confirmed the presence of a CaP coating on the surface of PLA particles independent of the concentration of  $\text{Co}^{2+}$  in the CPS solution.



6

Figure 1. SEM images at low (a1-d1) and high (a2-d2) magnification, EDS spectra (a3-d3) and FTIR spectra (e) of PLA, CaP-PLA, CaP Co0.1-PLA and CaP Co20-PLA particles, respectively. The SEM images showed the presence of a CaP layer consisting of small plate-like crystals, which uniformly covered the surface of the PLA particles. The EDS results confirmed the presence of Ca and P in the CaP-coated samples. The presence of Co was detected by EDS in the CaP Co20-PLA particles. Presence of a CaP phase was further confirmed by the FTIR analysis.

ICP-MS analysis of the coatings dissolved in nitric acid indicated that the amount of Co in the CaP-coated PLA was below 0.01 mg/L, whereas in the CaP Co0.1-PLA and CaP Co20-PLA, the amount was  $0.39 \pm 0.02$  mg/L and  $2.76 \pm 0.21$  mg/L,

respectively. The Ca/P ratio of CaP Co0.1-PLA and (Ca+Co)/P ratios of CaP Co0.1-PLA and CaP Co20-PLA were  $1.27 \pm 0.01$ ,  $1.29 \pm 0.01$  and  $1.28 \pm 0.01$ , respectively.

### 6.3.2. Histological and immunohistochemical analyses

No surgical complications occurred and all animals showed an uneventful recovery from the surgery. At implant retrieval, no visual signs of inflammation or infection, such as redness or swelling, were observed. Representative images of H&E stained tissue sections from one animal (goat #1), showing the overall histological appearance of the implants and the newly formed tissue are presented in Figure 2. Newly formed soft tissue was observed between the materials particles in all cases, with normal cell distribution. No apparent bulk degradation of any of the particles occurred and the size of the particles remained in the range of 0.5-1 mm.

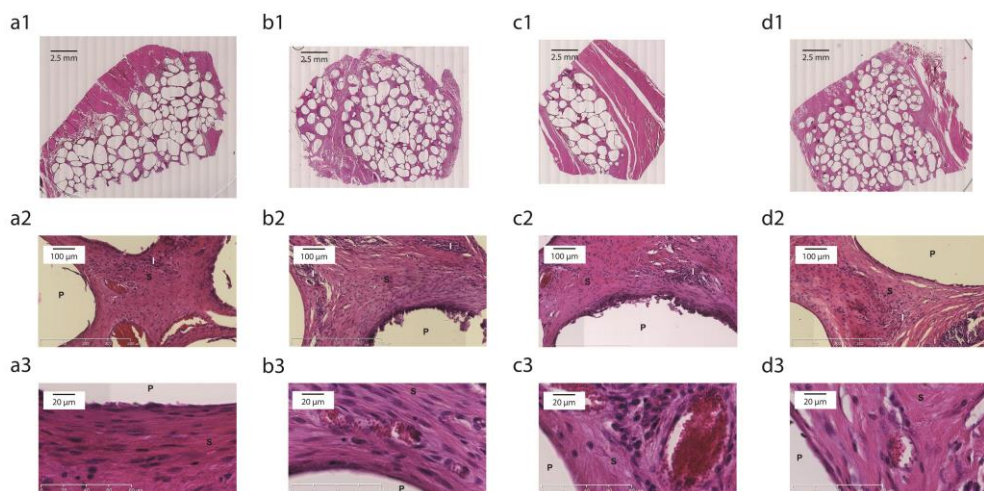


Figure 2. Micrographs of H&E stained histological slides at low (a1-d1), middle (a2-d2) and high (a3-d3) magnification for PLA, CaP-PLA, CaP Co0.1-PLA and CaP Co20-PLA particles, respectively, after 12 weeks of implantation in goat #1. P, S and I indicate particles, soft tissue and inflammatory cells respectively.

The results showed the formation of fibrous tissue among the particles while there were no sign of major degradation of the material. No difference between the inflammatory response to the particles of different types was detected.

Pathological analysis of the inflammatory response indicated presence of macrophages, plasma cells and T-cells, suggesting a mild chronic inflammatory

response. The majority of inflammatory cells were observed in the connective tissue surrounding the implants, close to blood vessels, while fewer inflammatory cells were observed in the connective tissue that was formed between individual particles. The scores of the extent of inflammatory response are shown in Table 1. No significant differences in the extent of inflammatory response were found between the four material types ( $p=0.714$ ).

Table 1. Scores of the inflammatory response to the four materials following 12 weeks of implantation

Inflammatory response score	PLA (number of animals)	CaP-PLA (number of animals)	CaP0.1Co-PLA (number of animals)	CaP20Co-PLA (number of animals)
1 (<40%)	1	2	4	3
2 (40-60%)	5	5	2	5
3 (>60%)	1	0	2	0

Immunohistochemical analysis was performed to locate actin fibers that are present in the smooth muscle cells cytoskeleton. The representative results of this analysis for 3 animals (goats #1, #2 and #3) are shown in Figure 3. Because of the autofluorescence of the materials, especially at the interface with soft tissue, the immunohistochemical analysis could not be reliably used for the quantification of blood vessel parameters. Nevertheless, the images clearly illustrated the presence of blood vessels with high fluorescence intensity and a hollow circular or elliptical morphology. Cell nuclei were detected in DAPI channel at the same location and were arranged in the same circular or elliptical shape (data not shown). The results of the immunohistochemical analysis showed presence of small blood vessels in low numbers in PLA and CaP-PLA samples. On the other hands, the blood vessels found around CaP Co0.1-PLA and CaP Co 20-PLA particles were in general larger in size and appeared in larger amounts.

Figure 4.a1-d3 exhibits representative results of the MT staining for one animal (goat #1), with host muscle tissue surrounding the implant and newly formed fibrous tissue infiltrating the space between material particles. The formation of blood vessels inside the tissue was confirmed by the presence of erythrocytes. Qualitative analysis of the MT-stained sections were in accordance with the results of immunohistochemical analysis and indicated that in general, fewer, and

smaller blood vessels were formed around the PLA and CaP-PLA particles in most animals. On the other hand, in CaP Co 0.1-PLA and CaP Co20-PLA samples, the blood vessels density was higher and the average size of the vessels larger. These qualitative observations were confirmed by the quantification of the average number of blood vessels and their area, normalized for the sample area, that was performed on all samples (Figure 4. e and f). In detail, the normalized blood vessel area was significantly higher in CaP-coated PLA particles containing  $\text{Co}^{2+}$  as compared to PLA and CaP-PLA particles. Similar trend was observed for blood vessel number. While significantly higher number of blood vessels was observed in Co0.1-PLA and Co20-PLA samples as compared to PLA-CaP, the only significant difference with PLA was with Co0.1-PLA.

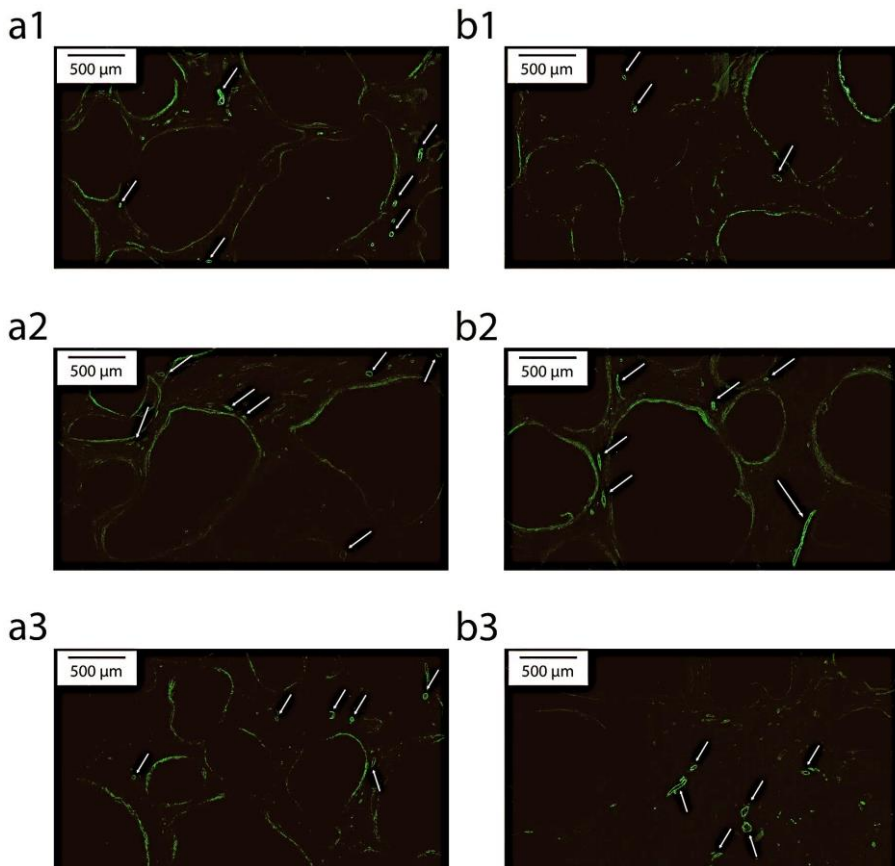


Figure 3. Continues in the next page.

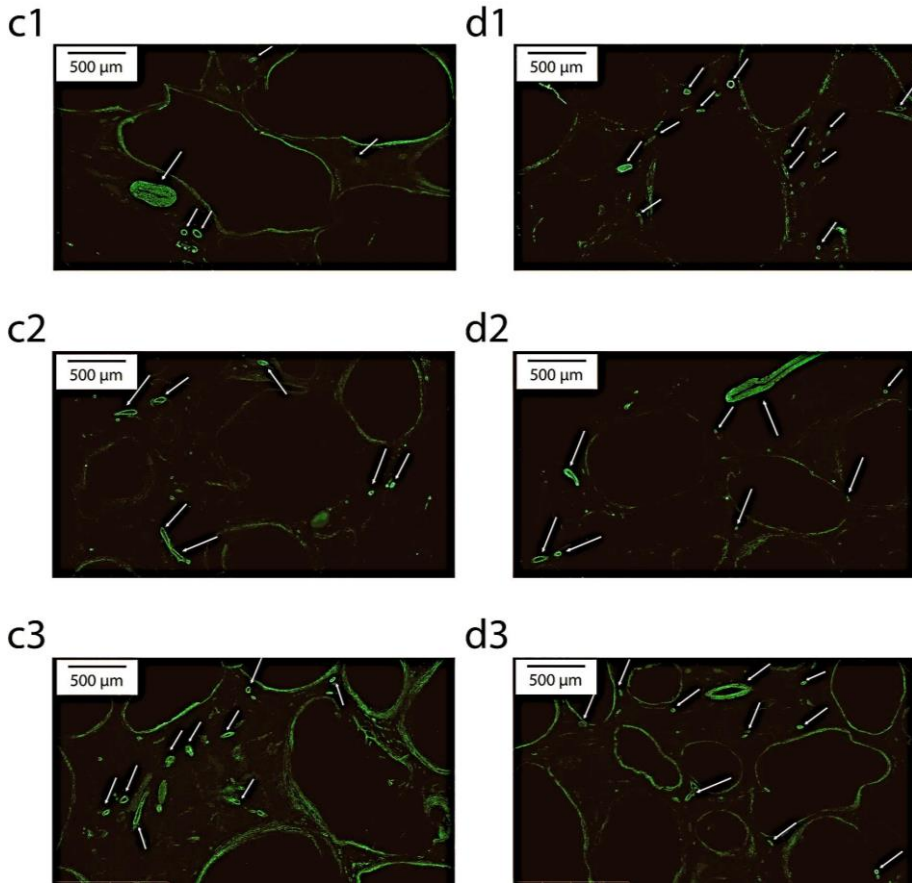


Figure 3. Micrographs showing immunohistochemical staining for  $\alpha$ -actin protein in smooth muscle cells found in tissue surrounding PLA (a1-a3), CaP-PLA (b1-b3), CaP Co0.1-PLA (c1-c3) and CaP Co20-PLA (d1-d3) particles, after 12 weeks of implantation in goats #1, #2 and #3 respectively. Blood vessels are indicated with white arrows. A larger number of blood vessels with varying sizes was formed in tissue surrounding  $\text{Co}^{2+}$  containing particles, whereas fewer, and predominantly smaller blood vessels were formed in PLA and CaP-coated PLA particles

The distribution of the blood vessel size for each sample is shown in figure 5. Small vessels (vessel area  $< 0.01 \text{ mm}^2$ ) were found in similar numbers in all the samples. A clear difference in frequency of occurrence of intermediate size blood vessels ( $0.01 \text{ mm}^2 < \text{vessel area} < 0.05 \text{ mm}^2$ ) was observed between samples with and without  $\text{Co}^{2+}$ . Extra-large vessels (vessel area  $> 0.05 \text{ mm}^2$ ) were rarely present in PLA (Figure 5. a) and CaP-PLA (Figure 5. b) samples, while they were frequently

observed in  $\text{Co}^{2+}$  incorporated samples (Figure 5. c-d), especially at higher  $\text{Co}^{2+}$  concentration (Figure 5. d).

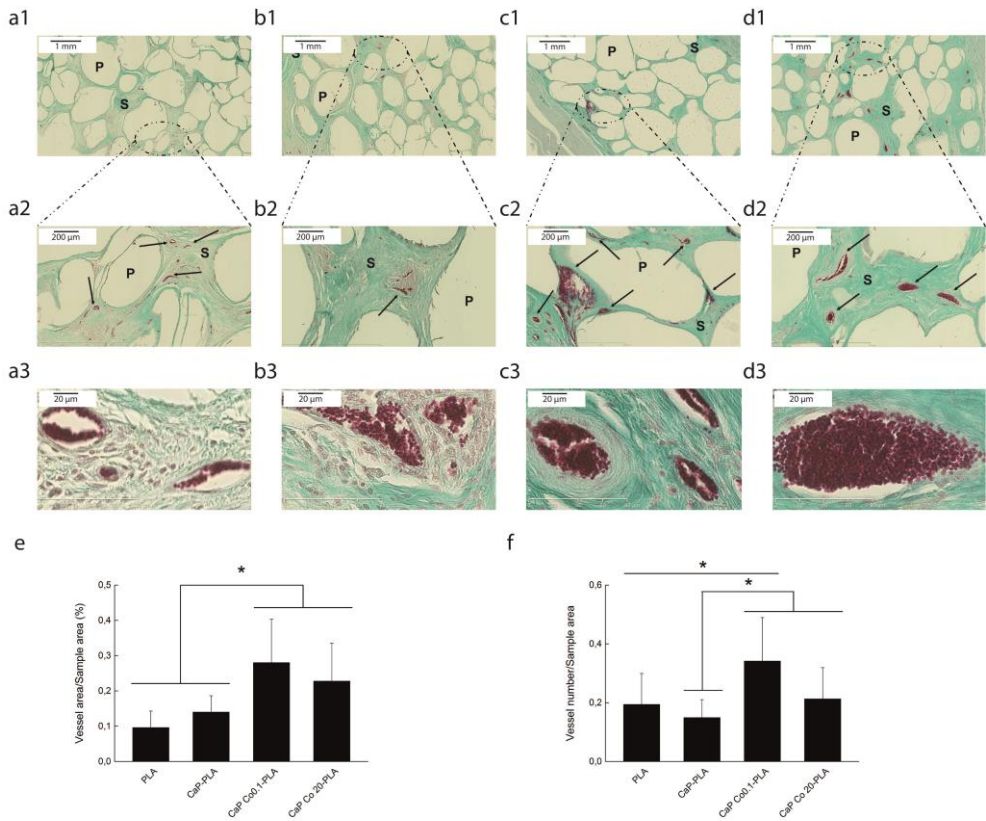


Figure 4. Micrographs of Masson's trichrome stained histological slides at low (a1-d1), middle (a2-d2) and high (a3-d3) magnification for PLA, CaP-PLA, CaP Co0.1-PLA and CaP Co20-PLA particles, respectively, after 12 weeks of implantation in goat #1, and quantification of blood vessel area (e) and vessel number (f) normalized for sample area for all particle types in all the animals. Quantitative data are presented as mean +/- SD. P and S indicate particles and soft tissue, respectively. The vessels are indicated with black arrows. In accordance with the results of immunohistochemical analysis, the histological results showed formation of small blood vessels in all samples, though in larger numbers in  $\text{Co}^{2+}$  containing ones. Larger vessels were detected in CaP Co0.1- and CaP Co20-PLA particles. The quantification of vascularization parameters showed that while there was no difference in vascularization parameters between PLA and CaP-coated PLA particles, a higher number of blood vessels and a larger normalized blood vessel area were detected in CaP Co0.1- and CaP Co20-PLA particles as compared to the samples not containing  $\text{Co}^{2+}$ .

## 6.4. Discussion

The focus of this study was localized delivery of  $\text{Co}^{2+}$  ions to stimulate new blood vessel formation *in vivo*.  $\text{Co}^{2+}$  ions are known as chemical mimickers of hypoxia and the application of this ion has previously been shown to result in higher expression of angiogenic genes [47-48]. Indeed, hypoxic conditions stimulate angiogenesis, with HIFs playing an important role in this mechanism [49-50]. The upregulation of the expression of angiogenic factors such as VEGF and osteoprotegerin (OPG) and enhancement of vascularization are known biological responses to hypoxic condition [22]. Furthermore, hypoxia also affects other aspects of angiogenesis such as vessel pattern, maturation and function [50]. With this important role in mind, hypoxia has been investigated as a strategy to improve angiogenesis in bone graft substitutes [51-52].

Building up on the previously shown effect of  $\text{Co}^{2+}$  on angiogenesis, we hypothesized that combining CaPs, being widely used synthetic bone graft substitutes, with  $\text{Co}^{2+}$  ions is a promising approach to simultaneously stimulate both osteogenesis and angiogenesis during bone regeneration. A CaP coating with or without  $\text{Co}^{2+}$  was applied on a polymeric substrate. The rationale behind the combination of a polymeric substrate and a ceramic coating was the strategy to improve mechanical properties of the ceramic while retaining the bioactivity, a topic that will be discussed separately.

In the current study, paraspinal muscles of goats were used as implantation site to first deliver evidence for an effect and select the right conditions, before moving to a bone defect, the number of which is limited in such an animal model. The intramuscular environment is obviously different than the microenvironment in a bone defect, and the response to the materials tested here may be different in bone. Nevertheless, assessment of newly developed materials *in vivo* in a large animal model provides valuable information that is complementary to *in vitro* studies or studies in smaller animals, owing to a closer resemblance of larger animals to human skeletal structure and metabolism. Furthermore, based on an earlier study in which cobalt-substituted CaP was tested in osteoporotic bone *in vivo* [28], a positive effect of  $\text{Co}^{2+}$  ions on blood vessel formation in bone is expected as well.

The method used to incorporate  $\text{Co}^{2+}$  ions into CaP coating is based on precipitation of the mineral from a CaP solution to which the ion was added, at near physiological conditions, in order to obtain the incorporation throughout the coating and not only on the surface, like, for example, in the case of adsorption-

based methods [39,42]. This approach has been previously shown to result in a more controlled release of incorporated compounds, such as Bone Morphogenetic Protein-2 [53].

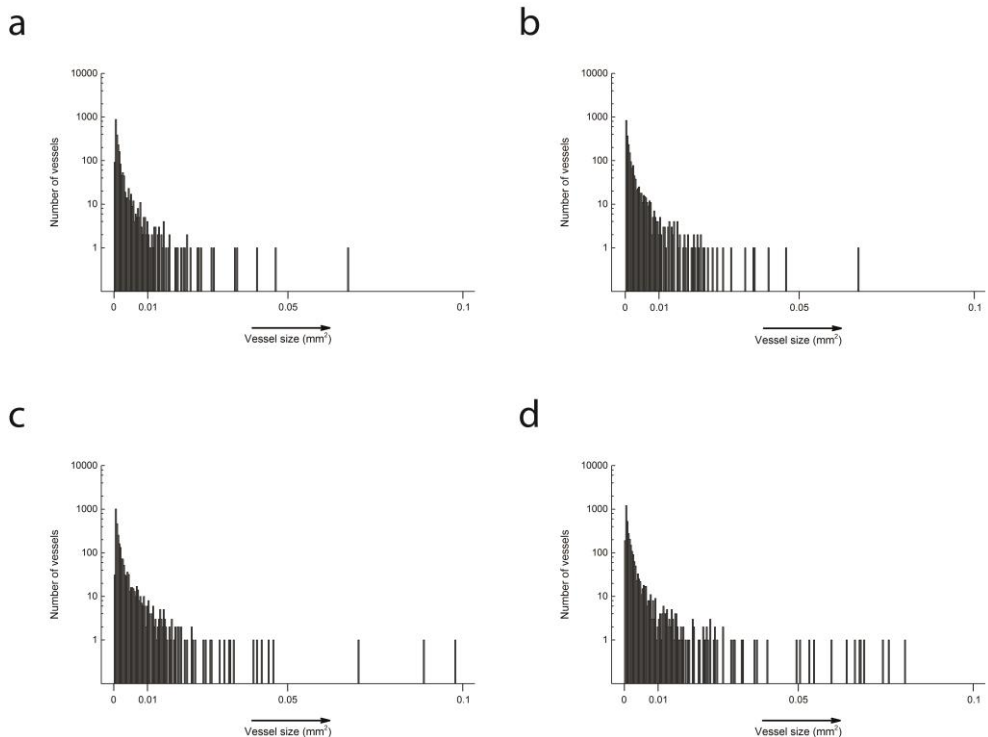


Figure 5. A histogram showing size distribution of blood vessels in PLA (a), CaP-PLA (b), CaP Co0.1-PLA (c) and CaP Co20-PLA (d) particles. Small blood vessels were equally abundant in all the samples, while larger vessels were more frequently observed in  $\text{Co}^{2+}$ -containing particles. Extra-large blood vessels were rarely found in PLA and CaP-PLA samples while they were more frequently observed around CaP Co0.1- and CaP Co20-PLA particles, resulting in the formation of more hierarchical vascular structure in these samples.

Here, we successfully deposited a homogenous mineral layer on the surface of PLA particles, both in the absence and in the presence of  $\text{Co}^{2+}$ . Patntirapong et al. [39] coated the surface of tissue culture well plates with CaP with or without  $\text{Co}^{2+}$  to study the effect of  $\text{Co}^{2+}$  on osteoclastic resorption of the mineral, and their results showed the formation of a CaP coating with a similar crystal morphology, which was shown to predominantly consist of octacalcium phosphate (OCP). In

our study, the difference in  $\text{Co}^{2+}$  concentration between the two  $\text{Co}^{2+}$  containing coating solutions was 200 times. Nevertheless, the Co content of CaP Co20-PLA was only 7 times higher than that of CaP Co0.1, which suggests that there is a maximum amount of the ion that can be incorporated into the CaP coating. Nevertheless, the Ca/P ratio of the coating without and the (Ca+Co)/P ratios of the coating with  $\text{Co}^{2+}$  indicated that the nucleation and growth of the crystals were not affected by the presence of  $\text{Co}^{2+}$ , which was also confirmed by the SEM and FTIR analyses. Partial Co-for-Ca substitution has been previously shown in  $\beta$ -tricalcium phosphate [54], however, based on our data it is difficult to conclude whether all the incorporate Co was actually substituted into the CaP lattice or partially physically entrapped into the coating.

After 12 weeks of intramuscular implantation, the formation of fibrous tissue was detected in the pores between the particles. The results further evidenced that there was no major bulk degradation of the PLA particles with or without the CaP coating, as opposed to the results by Danoux et al. [43] where a substantial degradation of PLA plates prepared using similar technique was observed after 12 weeks of intramuscular implantation in dogs. This difference could be attributed to the physiological differences between the two species as well as the difference in the implant shape. Because the materials were decalcified after explantation, we could not determine the level of degradation of the CaP coating. In a study by Barrere et al., it was shown that an OCP coating that was deposited on titanium plates did not dissolve after 4 weeks of subcutaneous implantation in rats, but instead transformed into a more stable carbonated apatite phase [55]. Although useful, these data cannot be directly extrapolated to our study, because of the difference in animal model and in implantation period. It was also not possible to measure the release profile of  $\text{Co}^{2+}$  in vivo. Nevertheless, the in vitro study by Patntirapong et al. [39] showed that in cell culture medium, a burst release of  $\text{Co}^{2+}$  was observed from CaP coatings deposited on cell culture plastic. After 3 days, about 50% of total  $\text{Co}^{2+}$  was released, and after 6 days another 5% release was measured. Although the environment of a cell culture dish is very different from that in vivo, this may suggest that the majority of the ions are released relatively soon after implantation.

Both histological and immunohistochemical analyses showed the formation of small blood vessels, with a size below  $0.01 \text{ mm}^2$ , in low numbers in the tissue formed around PLA and CaP-PLA particles, while in CaP Co0.1- and CaP Co20-PLA samples both small and larger vessels were frequently found. In accordance with

these results, quantification of blood vessel area and number of vessels showed higher values for both parameters for  $\text{Co}^{2+}$  containing materials as compared to both controls. Fan et al. [29] demonstrated that treating bone marrow stromal cells (BMSCs) with  $\text{Co}^{2+}$  ions resulted in a more pronounced vascularization of collagen scaffolds in which the cells were incorporated upon a 2-week subcutaneous implantation in mice. Subsequent implantation of these scaffolds in an orthotopic site resulted in enhanced neovascularized bone formation. Ignjatović et al. [28] also analyzed the effect of paramagnetic cobalt-substituted hydroxyapatite (HA) nanoparticles on osteoporotic alveolar bone regeneration and blood vessel formation in rats. The results showed an active angiogenesis process and young bone formation 6 and 24 weeks after the implantation of the nanoparticles containing  $\text{Co}^{2+}$ . The in vitro studies showed that treatment of BMSCs with  $\text{Co}^{2+}$  ions increased the expression of VEGF both at mRNA and protein level [27, 29]. In a more recent study, Quinlan et al. [56] demonstrated that the incorporation of cobalt in bioactive glass significantly enhanced the production and expression of VEGF by endothelial cells. Furthermore, they observed that exposing endothelial cells to cell medium conditioned with cobalt incorporated-bioactive glass/collagen glycosaminoglycan scaffold enhanced the tubule formation. In accordance with these previous studies, our findings also indicated that while there was no difference in vascularization between the PLA and CaP-coated PLA particles, incorporation of  $\text{Co}^{2+}$  in the CaP coatings enhanced the vascularization in terms of number of blood vessels and their area.

Because for this study, a relatively long implantation time was selected, early events that may explain the positive effect of  $\text{Co}^{2+}$  on vascularization cannot be determined. While we hypothesize that local hypoxic environment may be a reason for increased vascularization, short-term implantation is needed to analyze the HIF-1 $\alpha$  expression in the surrounding tissue. Furthermore, besides the effect of hypoxia, increased inflammatory response to the  $\text{Co}^{2+}$ -containing materials may be a reason for the enhanced vascularization. Although the pathological analysis after 12 weeks indicated presence of mild chronic inflammatory response in the connective tissue surrounding all materials, no significant differences between the four implant types were observed. While these findings suggest that increased vascularization was not a result of increased inflammatory response, it is important to, on one hand, analyze early events upon implantation of such materials and release of  $\text{Co}^{2+}$  from them, and, on the other hand, the effects on tissue when  $\text{Co}^{2+}$  release is maintained for a longer period of time. This is

particularly important from the safety perspective, as in vitro studies have shown a negative effect of viability upon prolonged exposure of cells to cobalt-substituted hydroxyapatite [28].

The results of this study also showed that incorporation of  $\text{Co}^{2+}$  not only increased the number of blood vessels and their area, but also their size distribution. Blood vessels of different sizes ranging from very large ones with the area larger than  $0.05 \text{ mm}^2$  to small vessels with an average area below  $0.01 \text{ mm}^2$  were formed when  $\text{Co}^{2+}$  was present in the CaP coating. In contrast, in the samples without  $\text{Co}^{2+}$ , with or without CaP, very large vessels did not form and large vessels were less frequent. Similar to this observation, Ignjatović et al. [28] detected the formation of a properly structured vascular network containing both large blood vessels and small capillaries in HA nanoparticles with  $\text{Co}^{2+}$  incorporation implanted in rats. The importance of the size of blood vessels is evident considering that natural bone is highly vascularized from the intramedullary cavity to the periosteal mineral, with a hierarchical vascular structure containing large vessels which further branch out internally into small capillaries [4].

Based on the previously published work, hypoxic environment induced by  $\text{Co}^{2+}$  may have an important effect on the vascular pattern and lumen size of the newly formed blood vessels. It is known that local metabolic and mechanical changes in cell microenvironment including the presence of hypoxic condition substantially influences the formation, maturation, function and remodeling of the vessels of different sizes [50,57]. Stoeltzing et al. [58] studied the effects of inhibition of HIF-1 $\alpha$  activity on angiogenesis in human gastric cancer in vivo and observed the formation of blood vessels with much smaller lumen size in the tumor cells in which the HIF-1 $\alpha$  activity was inhibited compared to those expressing increased level of HIF-1 $\alpha$ . They suggested that HIF-1 $\alpha$  provided a complex proangiogenic microenvironment that influences vessel morphology and function. Based on this argument, the upregulation of HIF-1 $\alpha$  in the muscle tissue as a result of  $\text{Co}^{2+}$ -induced hypoxia may indeed plausibly be the reason for larger lumen size and different vascular structure in the presence of these ions.

## 6.5. Conclusion

This study showed that incorporation of  $\text{Co}^{2+}$  into a CaP coating resulted in the formation of more and larger blood vessels upon intramuscular implantation in goats. Also a wider distribution in size of blood vessels is achieved in presence of

Co<sup>2+</sup>. As such, the results support the use of Co<sup>2+</sup>-containing CaPs as a means to stimulate vascularization of synthetic bone graft substitutes.

## References

1. H.Gerber and N. Ferrara, Angiogenesis and bone growth, *Trends in Cardiovascular Medicine* 10 (2000) 223-228.
2. R.A.D. Carano and E.H. Filvaroff, Angiogenesis and bone repair, *Drug Discovery Today* 8 (2003) 980-989.
3. M.R Hausman, M.B Schaffler, R.J Majeska, Prevention of fracture healing in rats by an inhibitor of angiogenesis, *Bone* 29 (2001) 560–564.
4. A.E. Mercado-Pagán, A.M. Stahl, Y. Shanjani, Y. Yang, Vascularization in bone tissue engineering constructs, *Annual Biomedical Engineering* 43 (2015) 718–729.
5. M.W. Laschke M.D. Menger, Vascularization in tissue engineering: angiogenesis versus inosculation, *European Surgical Research* 48 (2012) 85–92.
6. M. Lovett, K. Lee, A. Edwards, D.L. Kaplan, Vascularization strategies for tissue engineering, *Tissue Engineering Part B* 15 (2009) 353-370.
7. L.H. Nguyen, N. Annabi, M. Nikkhah, H. Bae, L. Binan, S. Park, Y. Kang, Y. Yang, A. Khademhosseini, Vascularized bone tissue engineering: approaches for potential improvement, *Tissue Engineering Part B* 18 (2012) 363-382.
8. Y. Chiu, M. Cheng, H. Engel, S. Kao, J.C. Larson, S. Gupta, E.M. Brey, The role of pore size on vascularization and tissue remodeling in PEG hydrogels, *Biomaterials* 32 (2011) 6045-6051.
9. D. Kaigler, Z. Wang, K. Horger, D.J. Mooney, P.H. Krebsbach, VEGF scaffolds enhance angiogenesis and bone regeneration in irradiated osseous defects, *Journal Bone Mineral Research* 21 (5) (2006) 735-744.
10. A. Kampman, D. Lindhorst, P. Schumann, R. Zimmerer, H. Kokemüller, M. Rücker, N. Gellrich, F. Tavassol, Additive effect of mesenchymal stem cells and VEGF to vascularization of PLGA scaffolds, *Microvascular Research* 90 (2013) 71–79.
11. E. Wernike, M.O. Montjovent, Y. Liu, D. Wismeijer, E.B. Hunziker, K.-A. Siebenrock, W. Hofstetter, F.M. Klenke, VEGF incorporation into calcium phosphate ceramics promotes vascularization and bone formation in vivo, *European Cells and Materials* 19 (2010) 30-40.
12. D. Qu, J. Li, Y. Li, Y. Gao, Y. Zuo, Y. Hsu, J. Hu, Angiogenesis and osteogenesis enhanced by bFGF ex vivo gene therapy for bone tissue engineering in reconstruction of calvarial defects, *Journal Biomedical Materials Research A*. 96 (2011) 543-551.
13. J. Rouwkema, J. de Boer, C.A. van Blitterswijk, Endothelial cells assemble into a 3-dimensional prevascular network in a bone tissue engineering construct, *Tissue Engineering* 12 (2006) 2685–2693.
14. G.E. Amiel, M. Komura, O. Shapira, J.J. Yoo, S. Yazdani, J. Berry, S. Kaushal, J. Bischoff, A. Atala, S. Soker, Engineering of blood vessels from acellular collagen matrices coated with human endothelial cells, *Tissue Engineering* 12 (2006) 2355–2365.
15. C.S.N. Choong, D.W. Hutmacher, J.T. Triffitt, Co-culture of bone marrow fibroblasts and endothelial cells on modified polycaprolactone substrates for enhanced potentials in bone tissue engineering, *Tissue Engineering* 12 (2006) 2521–2531.
16. N. Von Offenberg Sweeney, P.M. Cummins, E.J. Cotter, P.A. Fitzpatrick, Y.A. Birney, E.M. Redmond, P.A. Cahill, Cyclic strain-mediated regulation of vascular endothelial cell migration and tube formation, *Biochemical and Biophysical Research Communication* 329 (2005) 573-582.
17. T. Iba and B.E. Sumpio, Morphological response of human endothelial cells subjected to cyclic strain in vitro, *Microvascular Research* 42 (1991) 245-154.

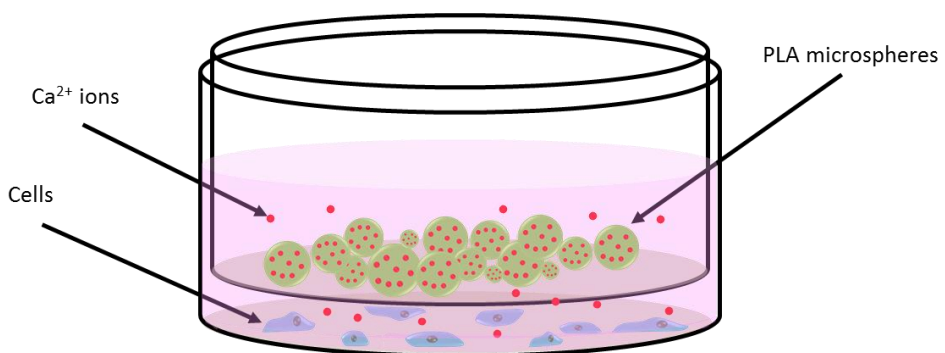
18. Q. Li, T. Hou, J. Zhao, J. Xu, Vascular endothelial growth factor release from alginate microspheres under simulated physiological compressive loading and the effect on human vascular endothelial cells, *Tissue Engineering Part A* 17 (2011) 1777-1785.
19. N. Rahimi, D.G. Molin, T.J. Cleij, M.A. van Zandvoort, M.J. Post, Electrosensitive Polyacrylic Acid/Fibrin Hydrogel Facilitates Cell Seeding and Alignment, *Biomacromolecules* 13 (2012) 1448-1457.
20. J.T. Borenstein, H. Terai, K.R. King, E.J. Weinberg, M.R. Kaazempur-Mofrad, J.P. Vacanti, Microfabrication technology for vascularized tissue engineering, *Biomedical Microdevices* 4 (2002) 167-175.
21. J. Doorn, H. A.M. Fernandes, B.Q. Le, J. van de Peppel, J.P.T.M. van Leeuwen, M.R. De Vries, Z. Aref, P.H.A. Quax, O. Myklebost, D.B.F. Saris, C.A. van Blitterswijk, J. de Boer, A small molecule approach to engineering vascularized tissue, *Biomaterials* 34 (2013) 3053-3063.
22. S. Bose, G. Fielding, S. Tarafder, A. Bandyopadhyay, Understanding of dopant-induced osteogenesis and angiogenesis in calcium phosphate ceramics, *Trends in Biotechnology* 31 (10) (2013) 594-605.
23. A. Grosfeld, V. Zilberfar, S. Turban, J. André, M. Guerre-Millo, T. Issad, Hypoxia increases leptin expression in human PAZ6 adipose cells, *Diabetologia* 45 (2002) 527-530.
24. F. Grasselli, G. Basini, S. Bussolati, F. Bianco, Cobalt chloride, a hypoxia-mimicking agent, modulates redox status and functional parameters of cultured swine granulosa cells, *Reproduction, Fertility and Development* 17 (2005) 715-720.
25. C.J. Schofield, P.J. Ratcliffe, Oxygen sensing by HIF hydroxylases, *Nature Reviews Molecular Cell Biology* 5 (2004) 343-354.
26. G.L. Semenza, HIF-1 and mechanisms of hypoxia sensing, *Curr Opin Cell Biology* 13 (2001) 167-171.
27. C. Wu, Y. Zhou, W. Fan, P. Han, J. Chang, J. Yuen, M. Zhang, Y. Xiao, Hypoxia-mimicking mesoporous bioactive glass scaffolds with controllable cobalt ion release for bone tissue engineering, *Biomaterials* 33 (2012) 2076-2085.
28. N. Ignjatović, Z. Ajduković, V. Savić, S. Najman, D. Mihailović, P. Vasiljević, Z. Stojanović, V. Uskoković, D. Uskoković, Nanoparticles of cobalt-substituted hydroxyapatite in regeneration of mandibular osteoporotic bones, *Journal of Materials Science: Materials in Medicine* 24 (2013) 343-354.
29. W. Fan, R. Crawford, Y. Xiao, Enhancing in vivo vascularized bone formation by cobalt chloride-treated bone marrow stromal cells in a tissue engineered periosteum model, *Biomaterials* 31 (2010) 3580-3589.
30. A. Bigi, G. Cojazzi, S. Panzavolta, A. Ripamonti, N. Roveri, M. Romanello, K. Noris Suarez, L. Moro, Chemical and Structural Characterization of the Mineral Phase from Cortical and Trabecular Bone, *Journal of Inorganic Biochemistry* 68 (1997) 45-51.
31. A.J. Wagoner Johnson, B.A. Herschler, A review of the mechanical behavior of CaP and CaP/polymer composites for applications in bone replacement and repair, *Acta Biomaterialia* 7 (2011) 16-30.
32. C. Canal, M.P. Ginebra, Fibre-reinforced calcium phosphate cements: A review, *Journal of Mechanical Behavior of Biomedical Materials* 4 (2011) 1658-1671.
33. P. Habibovic, M.C. Kruyt, M.V. Juhl, S. Clyens, R. Martinetti, L. Dolcini, N. Theilgaard, C.A. van Blitterswijk, Comparative in vivo study of six hydroxyapatite-based bone graft substitutes, *Journal of Orthopaedics Research* 26 (2008) 1363-1370.
34. H. Yuan, H. Fernandes, P. Habibovic, J. de Boer, A. M.C. Barradas, A. de Ruitter, W.R. Walsh, C.A. van Blitterswijk, J.D. de Bruijn, Osteoinductive ceramics as a synthetic alternative to autologous bone grafting, *Proceeding of the National Academic Science USA* 107 (2010) 13614-13619.
35. M. Bohner, L. Galea, N. Doebelin, Calcium phosphate bone graft substitutes: Failures and hopes, *Journal of European Ceramic Society* 32 (2012) 2663-2671.

36. L. Yang, B. Harink, P. Habibovic, Calcium phosphate ceramics with inorganic additives, in: Paul Ducheyne (Ed.), *Comprehensive biomaterials*, Elsevier Ltd., 2011, p.p. 229-312.
37. P. Habibovic, J.E. Barralet, *Bioinorganics and biomaterials: Bone repair*, *Acta. Biomaterialia* 7 (2011) 3013-3026.
38. J. Wang, K. de Groot, C. van Blitterswijk, J. de Boer, Electrolytic deposition of lithium into calcium phosphate coatings, *Dental Materials* 25 (2009) 353-359.
39. S. Patntirapong, P. Habibovic, P.V. Hauschka, Effects of soluble cobalt and cobalt incorporated into calcium phosphate layers on osteoclast differentiation and activation, *Biomaterials* 30 (2009) 548-555.
40. S. Kulanthaivela, U. Mishra, T. Agarwal, S. Giri, K. Pal, K. Pramanik, I. Banerjee, Improving the osteogenic and angiogenic properties of synthetic hydroxyapatite by dual doping of bivalent cobalt and magnesium ion, *Ceramics International* 41 (2015) 11323-11333.
41. L.S. Nair, C.T. Laurencin, *Biodegradable polymers as biomaterials*, *Progressive Polymer Science* 32 (2007) 762-798.
42. L. Yang, S. Perez-Amodio, F.Y.F. Barre`re-de Groot, V. Everts, C.A. van Blitterswijk, P. Habibovic, The effects of inorganic additives to calcium phosphate on in vitro behavior of osteoblasts and osteoclasts, *Biomaterials* 31 (2010) 2976-2989.
43. C.B Danoux, D. Barbieri, H. Yuan, J.D. de Bruijn, C.A. van Blitterswijk, P. Habibovic, In vitro and in vivo bioactivity assessment of a polylactic acid/hydroxyapatite composite for bone regeneration, *Biomatter* 4 (2014) e27664 1-12.
44. B.W. Chieng, N.A. Ibrahim, W.M.Z.W. Yunus, M.Z. Hussein, Poly(lactic acid)/Poly(ethylene glycol) Polymer Nanocomposites: Effects of Graphene Nanoplatelets, *Polymer* 6 (2014) 93-104.
45. A. Jordá-Vilaplana, V. Fombuena, D. García-García, M.D. Samper, L. Sánchez-Nácher, Surface modification of polylactic acid (PLA) by air atmospheric plasma treatment, *European Polymer Journal* 58 (2014) 23-33.
46. D. Barbieri, A.J.S. Renard, J.D. de Bruijn, H. Yuan, Heterotopic Bone Formation by Nano-Apatite Containing Poly(D,L-Lactide) Composite, *European Cells and Materials* 19 (2010) 252-261.
47. Y. Yuan, G. Hilliard, T. Ferguson, D.E. Millhorn, Cobalt inhibits the interaction between hypoxia-inducible factor- $\alpha$  and von Hippel-Lindau protein by direct binding to hypoxia-inducible factor- $\alpha$ , *Journal of Biological Chemistry* 178 (2003) 15911-15916.
48. K. Peters, H. Schmidt, R.E. Unger, G. Kamp, F. Prols, B.J. Berger, C.J. Kirkpatrick, Paradoxical effects of hypoxia-mimicking divalent cobalt ions in human endothelial cells in vitro, *Molecular Cell Biochemistry* 270 (2005) 157-166.
49. L. Chen, A. Endler, F. Shibasaki, Hypoxia and angiogenesis: regulation of hypoxia-inducible factors via novel binding factors, *Experimental and Molecular Medicine* 41 (2009) 849-857.
50. B.L. Krock, N. Skuli, M.C. Simon, Hypoxia-Induced Angiogenesis: Good and Evil, *Genes and Cancer* 2 (2011) 1117-1133.
51. Y. Liu, J.K.Y. Chan, S. Teoh, Review of vascularised bone tissue-engineering strategies with a focus on co-culture systems, *Journal of Tissue Engineering and Regenerative Medicine* 9 (2015) 85-105.
52. N.C. Rivron, J. Liu, J. Rouwkema, J. de Boer, C.A. van Blitterswijk, Engineering vascularised tissues In vitro, *European Cells and Materials* 15 (2008) 27-40.[53] Y. Liu Y, K. de Groot, E.B.Hunziker, BMP-2 liberated from biomimetic implant coatings induces and sustains direct ossification in an ectopic rat model, *Bone* 36 (2005) 745-757.
53. A. Legrouri, J. Lenzi, M. Lenzi, Isopropanol decomposition over cobalt-substituted calcium phosphate catalysts, *Materials Chemistry and Physics* 38 (1994) 94-97.
54. F. Barre`re, C.M. van der Valk, R.A.J. Dalmeijer, C.A. van Blitterswijk, K. de Groot, P. Layrolle, In vitro and in vivo degradation of biomimetic octacalcium phosphate and carbonate apatite coatings on titanium implants, *Journal of Biomedical Materials Research A*. 64 (2003) 378-387.

55. E. Quinlan, S. Partap, M.M. Azevedo, G. Jell, M.M. Stevens, F.J. O'Brien, Hypoxia-mimicking bioactive glass/collagen glycosaminoglycan composite scaffolds to enhance angiogenesis and bone repair, *Biomaterials* 52 (2015) 358-366.
56. R.K. Jain, Molecular regulation of vessel maturation, *Nature Medicine* 9 (2003) 685-693.
57. O. Stoeltzing, M.F. McCarty, J.S. Wey, F. Fan, W. Liu, A. Belcheva, C.D. Bucana, G.L. Semenza, L.M. Ellis, Role of hypoxia-inducible factor 1 $\alpha$  in gastric cancer cell growth, angiogenesis, and vessel maturation, *Journal of National Cancer Institute* 96 (2004) 946-956.

## Chapter 7

### Poly(lactic acid) microspheres for local delivery of bioinorganics for applications in bone regeneration



## Abstract

Bioinorganics are a family of relatively simple and inexpensive inorganic compounds, which, although often present only in trace amounts, are known to play an important role in the normal functioning of organs and tissues, including bone. Bioinorganics can potentially be used for improving the clinical performance of synthetic bone graft substitutes, as an alternative to growth factors and other biologics. To this end, it is imperative to fully understand their mechanism of action. Currently, bioinorganics are usually incorporated into calcium phosphate and bioglasses. During degradation, these materials release a cocktail of ions, making the study of the effect of the bioinorganic of interest difficult, if not impossible. To overcome this issue, in the present study, we attempted to develop a delivery system for bioinorganics based on polymeric microspheres. Calcium chloride, as a model for bioinorganics, was incorporated into poly(lactic acid) (PLA) microspheres, using a single emulsion-solvent evaporation technique. These microspheres were used to study the effect of the released calcium ions on the proliferation and osteogenic differentiation of human mesenchymal stromal cells (hMSCs) in a trans-well culture system. The results showed that it was possible to incorporate calcium into the microspheres and that the efficiency of incorporation could be increased by increasing the initial amount of PLA, and by using sonication instead of mechanical force during the emulsification step. Furthermore, the release profile of calcium from the microspheres was also dependent on the emulsification method. Cell culture experiments revealed no effect on cell proliferation or ALP activity as a consequence of calcium release, however, the gene expression of Bone Morphogenetic Protein 2 (BMP2) and Osteopontin (OP) was increased when cells were cultured in the presence of calcium containing microspheres. In conclusion, this study demonstrates that it is possible to use the developed polymeric delivery system to study the individual chemical effects of bioinorganics on the cells behavior.

## 7.1. Introduction

The search for successful synthetic alternatives to natural bone grafts has intensified in the past decade as a consequence of an increasing demand for bone regenerative strategies, resulting from a continuous ageing of the population in the developed countries. Synthetic bone graft substitutes, which are available as calcium-phosphate ceramics, bioglass, composites, etc. [1], can be produced in large quantities against acceptable cost, overcoming the most important issues related to the use of auto- or allograft [2]. Nevertheless, the clinical bone regenerative performance of these synthetic bone graft substitutes is in general considered inferior to that of their natural counterparts.

A widely investigated strategy to improve the biological performance of synthetic bone substitutes is the addition of biological compounds such as growth factors (e.g. osteoinductive Bone Morphogenetic Protein-2 and 7) that affect processes related to bone formation directly or indirectly [3]. The use of growth factors is however associated with issues related to their limited stability, and high production and storage cost [4-5]. Therefore less expensive alternatives are sought for.

The inorganic phase of natural bone consists of carbonated-hydroxyapatite [6]. Further elements such as sodium, fluoride, chloride, magnesium, strontium, zinc, copper and iron can also be found in the mineral portion of bone in lower or even trace amounts [7]. The biological roles and effects of these bioinorganics in the human body and, more specifically, in bone metabolism, have been described previously [8-9]. However, the first interest in using bioinorganics as potential therapeutics was based on knowledge obtained from changes in systemic ion levels, such as deficiencies of essential micronutrients, epidemiological studies, nutritional studies of food, animal and tissue health during disease or pharmaceutical treatments [9]. Application of strontium ranelate as anti-osteoporotic agent is an example of a successful clinical application of bioinorganics. Strontium ( $\text{Sr}^{2+}$ ) intake has shown an increase in bone matrix density and reduced bone fracture occurrence in osteoporotic women [10-11]. The addition of fluoride as an anti-cariogenic agent ( $\text{F}^-$ ) to toothpaste formulation is one of the well-known examples of the every-day use of bioinorganics [12]. These examples emphasize on the potential of bioinorganics as therapeutic agents in applications related to bone regeneration or bone-related diseases. Indeed, a number of in vitro and in vivo studies have demonstrated the effect of various

inorganic ions on processes related to bone formation, such as osteogenesis, osteoclastogenesis and angiogenesis [13-15].

Currently, common approaches for using bioinorganics as therapeutic agents include their introduction into either calcium phosphate-based ceramics or bioactive glasses, which are two widely used classes of synthetic bone graft substitutes. In such a way, a carrier or scaffold material is combined with a bioinorganic, which is similar to growth factor based constructs [8, 13, 16]. Delivery of bioinorganic ions from ceramic or bioglass carriers usually relies on the carrier degradation. However, this process is complex, featuring release of a number of ions, and a change of other physico-chemical properties of the carrier, which makes it difficult to evaluate the effects of a single bioinorganic and understand its mechanisms of action.

Delivery systems based on polymers used in biomedical applications are potentially more suitable for studying biological effects of bioinorganics. Polymeric microspheres, for example, are used as carriers and delivery vehicles of growth factors [17] and antibiotics [18], allowing minimally-invasive delivery. Polymeric microspheres have been tested for application as three-dimensional support for cell expansion and differentiation [19-22]. They have also been used for developing composite materials in order to tune the degradation and mechanical properties of bioceramics such as calcium phosphate ceramics [23]. To date, very few studies have explored the possibility of incorporating bioinorganics into polymeric matrices [24].

In the present study, calcium salt was used as a model bioinorganic compound to develop a delivery system based on poly(lactic acid) (PLA) microspheres. Polylactides belong to poly( $\alpha$ -ester) family which is one of the widely studied classes of biodegradable polymers [25]. They are potentially suitable as delivery vehicles, as they degrade hydrolytically due to an ester bond in their backbone [25]. The degradation product of PLA is lactic acid which, is further broken down into water and carbon dioxide in biological systems, hence, it is considered as bio-resorbable [25, 26]. For microsphere preparation in the present study, a single emulsion-evaporation technique was used. Emulsion- solvent evaporation techniques are widely used for microsphere preparation [27, 28]. In both single and double emulsion techniques, microspheres are formed in a two-step process [29]. In the first step, the polymer is dispersed into microdroplets by applying mechanical or ultrasonic shear stress. The second step includes solvent evaporation and polymer precipitation, resulting in microsphere hardening. In this

study, calcium salt was added to the polymer-solvent solution before emulsification. Calcium-containing microspheres were used to study proliferation and osteogenic differentiation of human mesenchymal stromal cells (hMSC) *in vitro*.

## **7.2. Materials and methods**

### **7.2.1. Preparation of PLA microspheres**

PLA microspheres were prepared using a single (oil-in-water) emulsion-solvent evaporation technique. Calcium chloride dihydrate (Merck) was used as model salt to test the incorporation potential into PLA microspheres.

To optimize the process of microsphere preparation, varying amounts of amorphous poly(D,L-lactic acid) (PLA, Purasorb PDL05, Purac, MW: 59000 g/mole) were dissolved in dichloromethane (DCM) (LiChrosolv®, Merck) to reach increasing concentrations of 4, 6, 8 and 10% w/v PLA that served as the oil phase. Calcium chloride was added to the PLA solution to reach a concentration of 200 g/L and stirred magnetically for 30 minutes to prepare a slurry. 25 ml of this mixture with the PLA concentration of 4 or 6% w/v or 20 ml of the mixture with PLA concentrations of for 8 or 10% w/v were added to 25 ml of 1.5% w/v Poly(vinyl alcohol) (PVA) (ACROS ORGANICS) aqueous solution. Ultra-turrax (T25 basic, IKA, Germany) was used to emulsify the mixture for 40 seconds at 8000 rpm before pouring it into 125 ml 1.5% w/v PVA solution. In a parallel experiment, a formulation of 4% w/v PLA was emulsified using an ultra-sonicator (Labsonic M, 50W, Braun) for 90 seconds. A formulation without addition of Ca<sup>2+</sup> salt served as a control for every produced batch of microspheres.

Solvent evaporation and microsphere hardening occurred during magnetic stirring for 2 hours at room temperature. Microspheres were then collected by centrifugation (3900 rpm, 10 minutes, 4°C) and washed 3 times with cold milliQ water. Microspheres were then resuspended in 10 ml milliQ water, freeze-shocked in liquid nitrogen, and stored for at least 30 minutes at -20°C before freeze-drying for at least 48 hours.

### **7.2.2. Characterization of PLA microspheres**

The morphology of the microspheres was analyzed using an environmental scanning electron

microscope (SEM; XL30, ESEM-FEG, Philips) in the secondary electron mode with an acceleration voltage of 10 kV after gold-sputtering for 40 seconds at 30 mA (Cressington sputter coater). To determine the diameter of microspheres from various batches, both SEM images and dynamic light scattering (DLS) equipment (Zetasizer nano ZS, Malvern Instruments, Germany) was used. For the latter analysis, microspheres were re-dispersed in milliQ water in an ultrasonic water bath prior to the measurements.

### 7.2.3. Calcium content and release

10±1 mg of PLA microspheres without or loaded with calcium chloride were completely dissolved in 750 µl DCM under shaking at 80 rpm, for 2h at 37°C. To extract the calcium ions, 150 µl milliQ water was added to the polymer solution and incubated overnight at 37°C. The water phase was then collected and analyzed using a calcium assay kit (QuantiChrom™, BioAssay Systems, USA) to quantify the calcium content of the microspheres. A spectrophotometric plate-reader (Thermo Scientific MultiscanGo) was used to read the optical density of calcium complexes at 612 nm.

Simulated physiological solution (SPS) buffered at pH 7.3 (137 mmol/L Na<sup>+</sup>, 177 mmol/L Cl<sup>-</sup>, 50 mmol/L HEPES in MilliQ water) was used to study the release profile of calcium ions from the microspheres. 10±1 mg of calcium-incorporated microspheres containing varying concentrations of PLA (4, 6, 8, and 10% w/v) were precisely weighed and placed in 500µl tubes. 150 µl of SPS was added to each sample. Triplicates of each sample were then placed in a waterbath at 37°C while shaking at 80 rpm. At dedicated time points between 4 hours to 15 days, three tubes of each condition were removed and centrifuged. The supernatant was collected and calcium content was quantified using the calcium assay kit as was described above.

### 7.2.4. In vitro characterization of PLA microspheres

Human mesenchymal stromal cells (hMSCs) were isolated from bone marrow after written consent as described previously [30-31]. In short, bone marrow aspirates were resuspended in cell culture medium, plated at a density of 5\*10<sup>5</sup> cells per cm<sup>2</sup> and cultured in proliferation medium (α-MEM (Gibco) supplemented with 10% fetal bovine serum (Lonza), 2 mM L-glutamine (Gibco), 0.2 mM ascorbic acid (Sigma), 100 U ml<sup>-1</sup> penicillin and 100 µg ml<sup>-1</sup> streptomycin (Gibco) and 1 ng

ml<sup>-1</sup> rhbFGF (AbDSerotec)). The medium was refreshed every 2-3 days. Cells were harvested at approximately 80% confluency for subculture until passage 3.

In vitro cell culture experiments were performed using hMSCs and microspheres containing 8% or 10% w/v PLA prepared using mechanical emulsification and microspheres containing 4% w/v PLA prepared using ultrasonic emulsification. Polymeric microspheres without the salt served as controls.

42.5±0.5 mg microspheres were placed in 24-well plates (NUNC) and sterilized using isopropanol (Assink Chemie), followed by a three-hour evaporation step. The samples were subsequently washed twice with sterile PBS. Sterilized microspheres were then incubated overnight in 1 ml of basic medium ( $\alpha$ -MEM (Gibco) supplemented with 10% fetal bovine serum (Lonza), 2 mM L-glutamine (Gibco), 0.2 mM ascorbic acid (Sigma), 100 U ml<sup>-1</sup> penicillin and 100  $\mu$ g ml<sup>-1</sup> streptomycin (Gibco)) overnight at 37° C in a humidified atmosphere with 5% CO<sub>2</sub>. To study the effects of products released from the microspheres, cell culture was performed using trans-wells (24-well, Corning) with two compartments. The cells were seeded in the bottom compartment of the trans-wells at a density of 20,000 cells/cm<sup>2</sup> and the microspheres were placed in the top compartment. Cells were cultured for 7 days in either basic or osteogenic medium (Basic medium supplemented with 10 nM dexamethasone (Sigma)) with refreshment every 2-3 days. hMSCs cultured on tissue culture plate, without introducing the microspheres, served as controls. After 7 days, the medium was aspirated, cells were washed with PBS, and DNA content of the cells was quantified using CyQuant Cell Proliferation Assay kit (Invitrogen) according to the manufacturer's protocol. Alkaline phosphatase (ALP) activity, as an early marker of osteogenic differentiation, was assessed and normalized for DNA amounts using CDP-star kit (Roche Applied Science) as per the manufacturer's protocol.

Expression of markers of osteogenesis at the mRNA level was determined using quantitative real-time PCR (QPCR). Total RNA of the cells was isolated by using a combination of TRIzol® (Life technologies) method and NucleoSpin® RNA isolation and purification kit (Macherey-Nagel) according to the manufacturer's protocol. Total RNA content was then measured using a NanoDrop® ND-1000 spectrophotometer. The cDNA of the cultures were then prepared using iScript kit (Bio-Rad) according to the manufacturer's protocol and diluted 10 times in RNase-free water. The qPCR measurements were performed on a Bio-Rad equipment using Syber green I master mix (Invitrogen). The primer (Sigma) sequence of the selected genes (Bone Morphogenetic Protein 2 (BMP2), Osteopontin (OP) and

Osteocalcin (OC) is listed in table 1. Expression of all genes was normalized for the levels of the housekeeping gene GAPDH and corrected for gene expression of hMSCs cultured on tissue culture plastic in basic medium. Induction folds of the target genes were calculated using  $\Delta\Delta CT$  method.

During cell culture, medium was collected at every medium refreshments (2, 4 and 6 days) and its calcium content was measured using calcium assay kit as described above in order to determine the calcium release profile in cell culture medium.

### 7.2.5. Statistical analysis

Statistical analysis was performed using one-way Analysis of Variance (ANOVA) with Tukey's multiple comparison post-hoc test with a significance level of  $p < 0.05$ . For all figures the following applies: \*  $p < 0.05$ , \*\*  $p < 0.01$ , \*\*\*  $p < 0.001$ .

Table 1. Primer sequences of osteogenic markers and housekeeping gene used for qPCR

Gene	Primer sequences
GAPDH (housekeeping gene)	5'-CCATGGTGTCTGAGCGATGT
	5'-CGCTCTCTGCTCCTCCTGTT
Bone morphogenetic protein 2 (BMP2)	5'-GCATCTGTTCTCGGAAAACCT
	5'-ACTACCAGAAACGAGTGGGAA
Osteocalcin (OC)	5'-CGCCTGGGTCTCTTCACTAC
	5'-TGAGAGCCCTCACACTCCTC
Osteopontin (OP)	5'-CCAAGTAAGTCCAACGAAAG
	5'-GGTGATGTCCTCGTCTGTA

## 7.3. Results

### 7.3.1. Microsphere characterization

SEM imaging (Figure 1.a-f) demonstrated formation of microspheres in all conditions tested. No morphological differences were observed between microspheres with and without calcium salt incorporation. Microspheres containing 4% w/v PLA prepared by either mechanical or ultrasonic emulsification

presented small pores with approximate diameter of 0.5-1  $\mu\text{m}$  on the surface, whereas microspheres with higher PLA concentrations showed a smooth surface structure.

Average particle size and size distribution of microspheres (data not shown) with different PLA concentrations (4-10% w/v), without and with calcium chloride incorporation were analyzed using DLS technique. The particles, however, appeared to be polydisperse (which is in accordance with SEM results) and the particle size exceeded the maximum measurable size of 2 micron of the available DLS equipment. In order to get an approximation of the microsphere size, the average particle size of the microspheres obtained from DLS analysis compared with measurements obtained from SEM images. As shown in Figure 1.g, PLA microspheres had an average diameter of 4-6  $\mu\text{m}$ . Increasing the polymer concentration led to a slight increase in average microsphere size. No effect of the emulsification technique was observed on the average microsphere diameter, as both mechanically and ultrasonically prepared microspheres containing 4% PLA possessed a comparable size.

### **7.3.2. Efficiency of calcium incorporation into and release profile from PLA microspheres**

The amount of calcium chloride salt incorporated into PLA microspheres was in the range of 0.5 to 2.2  $\mu\text{g}/\text{mg}$  of microspheres (Figure 2.a). No calcium was detected in microspheres without salt incorporation. A direct positive correlation between PLA concentration and level of calcium was found in the sample prepared by mechanical emulsification; the higher the PLA content the higher the amount of calcium. Interestingly, method of emulsification had a strong effect of the incorporation efficiency. Calcium content of microspheres containing 4% w/v PLA prepared using ultrasonic emulsification was more than four times higher than that of microspheres with the same PLA content prepared using mechanical emulsification.

The calcium release profile of microspheres was investigated in SPS for 15 days. The results are presented as a ratio between  $\text{Ca}^{2+}$  released and the total calcium content ( $M_t/M_\infty$ ) (Figure 2.b). A burst release was observed for all samples prepared using mechanical emulsification, with approximately 80% of the ions released within 4 hours. After 2-4 days the calcium release profile reached a plateau in these conditions, which corresponded to approximately 90% of the

total calcium content. However, the release profile of 4% PLA microsphere prepared using ultrasonic emulsification showed a more sustained release with approximately 5% released after 1 day, increasing to approximately 17 after 10 days in SPS.

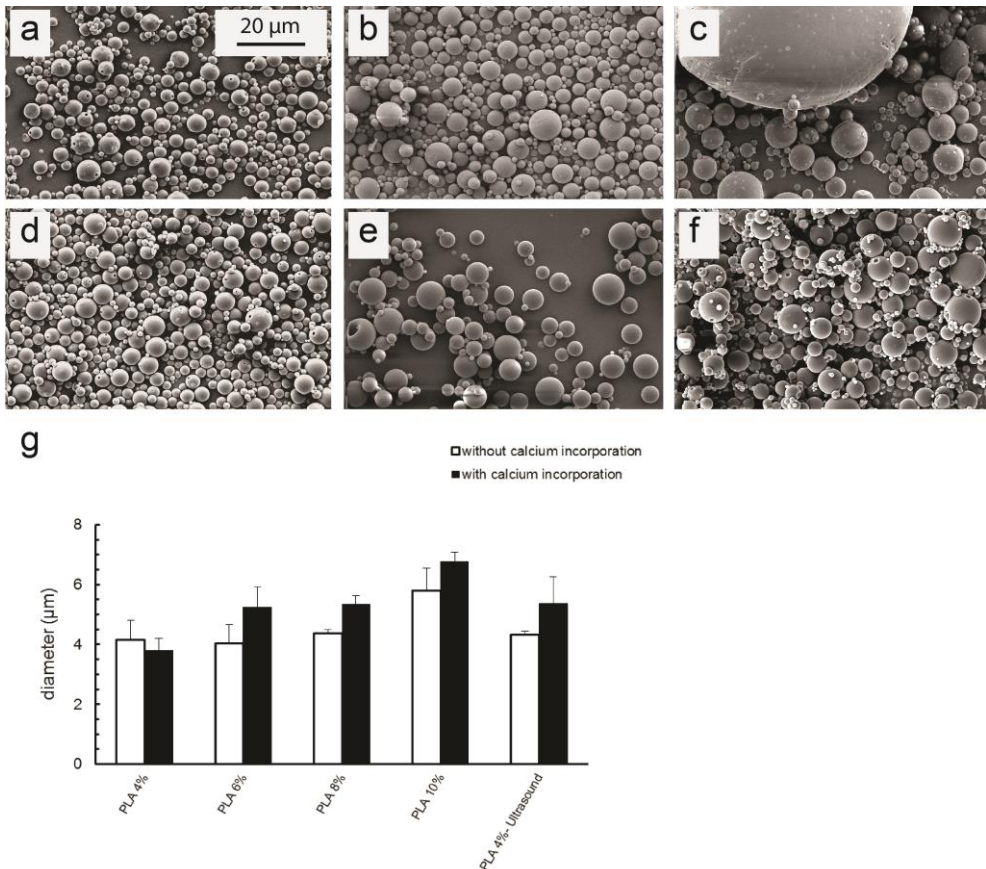
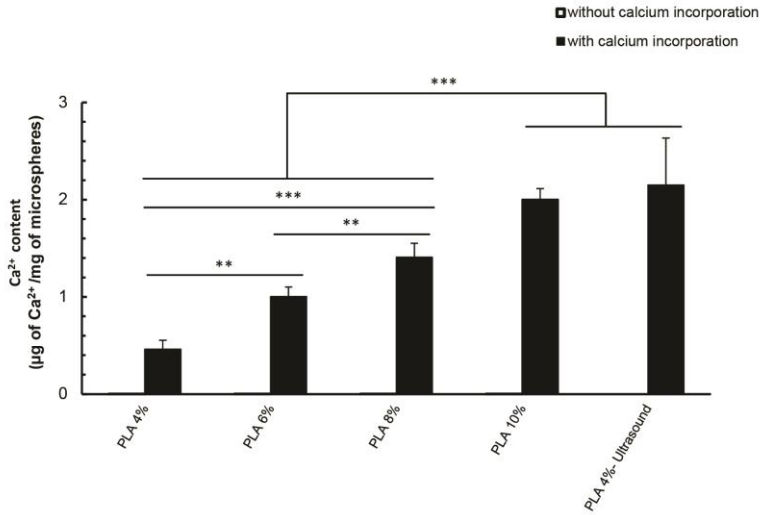


Figure 1. SEM images showing morphology of microspheres prepared by single emulsion technique and mechanical emulsification without calcium incorporation and with a PLA concentration of 4 (a) and 10% (b) w/v PLA, with calcium incorporation and PLA concentration of 4 (d) and 10% (e) w/v PLA and without (c) and with (f) calcium incorporation and a PLA content of 4% w/v prepared by sonication (scale bar=20 µm).

Average diameter of microspheres prepared with various PLA concentrations and emulsification techniques (g). All microsphere batches showed spherical structures with a smooth surface and an average size of 4-6 µm.

a



b

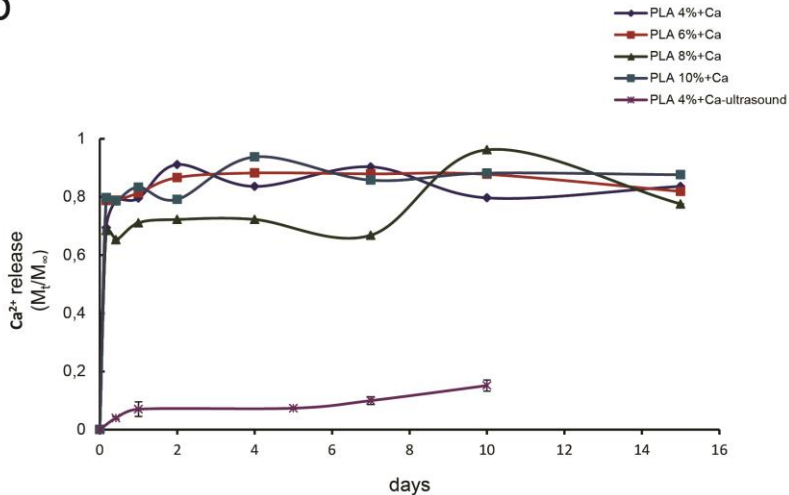


Figure 2. Calcium content of microspheres prepared with either mechanical or ultrasonic emulsification, and with varying PLA concentrations (a) and calcium release profile of 4-10% w/v PLA microspheres in SPS during 15 days (b). In mechanically emulsified microspheres, increasing PLA concentrations correlated with increased calcium incorporation. Ultrasonic preparation of microspheres with 4% w/v PLA resulted in the highest calcium content. All mechanically prepared microspheres showed a burst release of approximately 80% within the first 4 hours while ultrasonically prepared microspheres showed a more sustained release with 17% calcium release after 10 days of immersion.

### 7.3.3. In vitro characterization of PLA microspheres

A trans-well cell culture system (Figure 3.a) was used to study the effect of compounds released from the microspheres on the proliferation and osteogenic differentiation of hMSCs.

As is depicted in Figure 3.b, no significant differences in DNA content were observed among cells cultured on different batches of hMSCs, independent of the medium used. Similarly, there were no differences between cells cultured in presence or in absence of the microspheres.

Also ALP activity was not significantly different among different conditions; only the osteogenic medium seemed to mildly increase the ALP activity (Figure 3.c).

QPCR data showed that both BMP2 and OP genes were upregulated in cells cultured in the presence of calcium chloride containing microspheres as compared to their unloaded counterparts and controls, both in basic and in osteogenic medium (Figure 4.a,b). A significant difference was observed in the expression of BMP2 when hMSCs were cultured with calcium containing 10% w/v PLA microspheres in basic medium compared to other conditions. In osteogenic medium, the expression of BMP2 was significantly higher in Ca<sup>2+</sup> containing 4% w/v and 10% w/v PLA microspheres compared to the control. Ca<sup>2+</sup> containing 8% w/v and 10% w/v PLA microspheres resulted in higher expression of OP in basic medium in comparison with non-loaded microspheres (4% w/v and 10% w/v PLA). OP gene was also upregulated in osteogenic medium when hMSCs were cultured with 10% w/v PLA microspheres compared to non-loaded microspheres (8% w/v and 4% w/v) and control. In contrast to the expression of BMP2 and OP, no significant differences were observed in the expression of OC among different conditions (Figure 4.c)

The calcium ion release profile of calcium chloride-loaded microspheres in basic culture medium after 2, 4, and 6 days is shown in Figure 5.  $\alpha$ -MEM contains 1.8 mM Ca<sup>2+</sup> ions and the FBS added to the medium also contains additional ions. The level of Ca<sup>2+</sup> in the medium was measured using the kit and used as the basic Ca<sup>2+</sup> levels of all the conditions (day 0). After two days of culture in basic medium, Ca<sup>2+</sup> content of the medium increased by 0.5 mM and 0.2 mM in the 8% and 10% w/v PLA conditions, respectively. After 4 and 6 days, a slight decrease of approximately 0.2 mM was observed. A continuous increase of the calcium ion concentration of approximately 0.2 mM at each time point was observed for microspheres with 4% w/v PLA produced using ultrasonic emulsification.

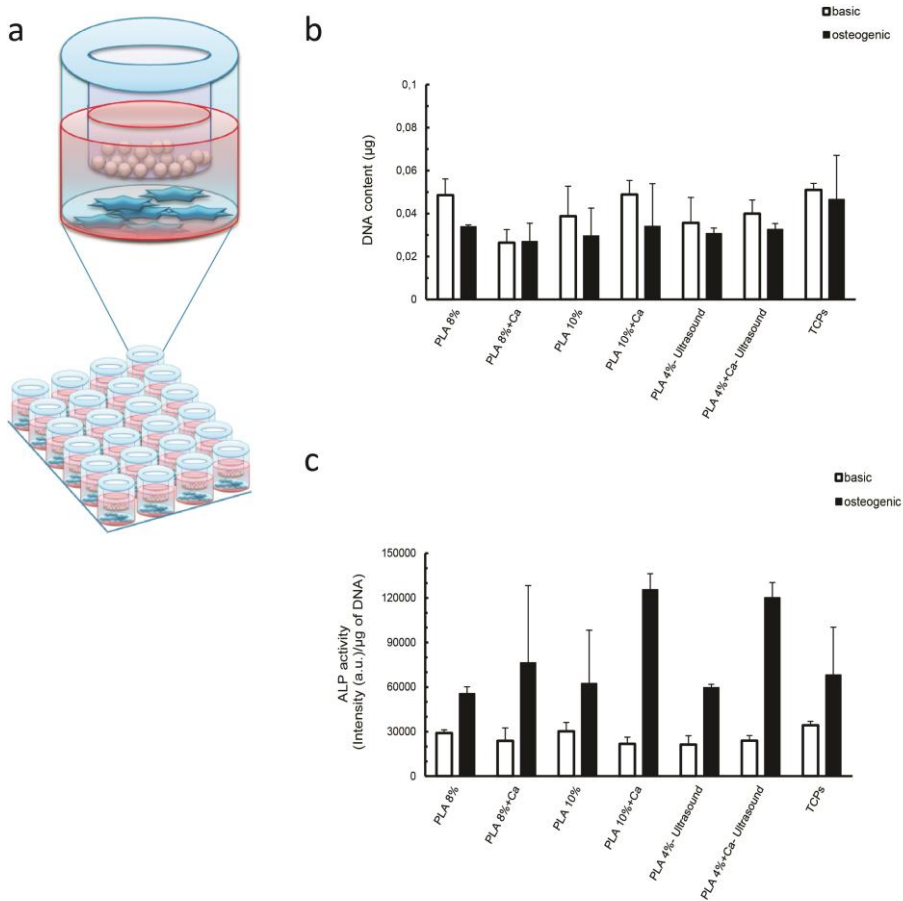


Figure 3. A schematic of cell culture trans-well set up in which the microspheres and the cells were placed in top and bottom compartments, respectively (a), DNA content (b) and ALP activity normalized for DNA (c) of hMSCs cultured in presence of microspheres for 7 days. No significant differences were observed in either DNA content or ALP activity among different conditions.

## 7.4. Discussion

In this study, we have investigated the possibility of incorporation of bioinorganics into and their release from polymeric microparticles. Microparticles were made from PLA, and calcium chloride served as model bioinorganic. Lactic acid, the degradation product of PLA, is a natural metabolite and therefore does not elicit toxic effects [25]. Furthermore, due to the synthetic nature of PLA, batch-to-batch

uniformity of the polymer is high [25]. Calcium was selected as it is one of the constituents of calcium-phosphates, a widely used synthetic bone graft substitute. The microsphere based delivery system as developed here would in the first place allow for studying biological effects of a single bioinorganic on cell behavior since they exclusively release the ions incorporated in them. In contrast, current carriers of bioinorganics, including calcium phosphate and bioactive glass, release a cocktail of ions, making analysis of the effect of individual ions difficult, if not impossible.

The surface morphology of microspheres prepared in this study did not vary upon incorporation of calcium salt. In PLA microspheres containing 4% PLA, a porous surface was observed to be independent of salt incorporation and emulsification technique. Both, spheres with and without salt exhibited a smooth surface structure at higher PLA concentrations. Increasing PLA concentrations from 4 to 10 w/v% increased the average diameter of microspheres from 4 to 6  $\mu\text{m}$  in a relatively linear manner. Nevertheless, the results of SEM imaging and DLS measurements showed polydispersity for all the microsphere batches. Controlling the physical properties of microspheres including particle size and surface roughness was not within the scope of this study, but are obviously properties that can be further modified in order to better control the efficiency of incorporation and release profiles.

Various strategies exist for incorporating inorganic materials into polymer matrices. Inorganics-incorporated interpenetrating polymer networks, incorporation of bioinorganic groups via chemical bonds to the polymer backbone and dual inorganic-organic hybrid polymer are examples of these different strategies [32]. However, different physical and chemical polymer-salt interactions are involved in each of these strategies. In the present study, the inorganic salt is expected to be either adsorbed on the surface, or physically embedded into polymer matrix.

Incorporation of 0.5 - 2.2  $\mu\text{g}$  calcium chloride per mg was achieved in microspheres prepared with 4-10% w/v PLA and mechanical homogenization. It was shown that the calcium incorporation was directly related to the PLA concentration.

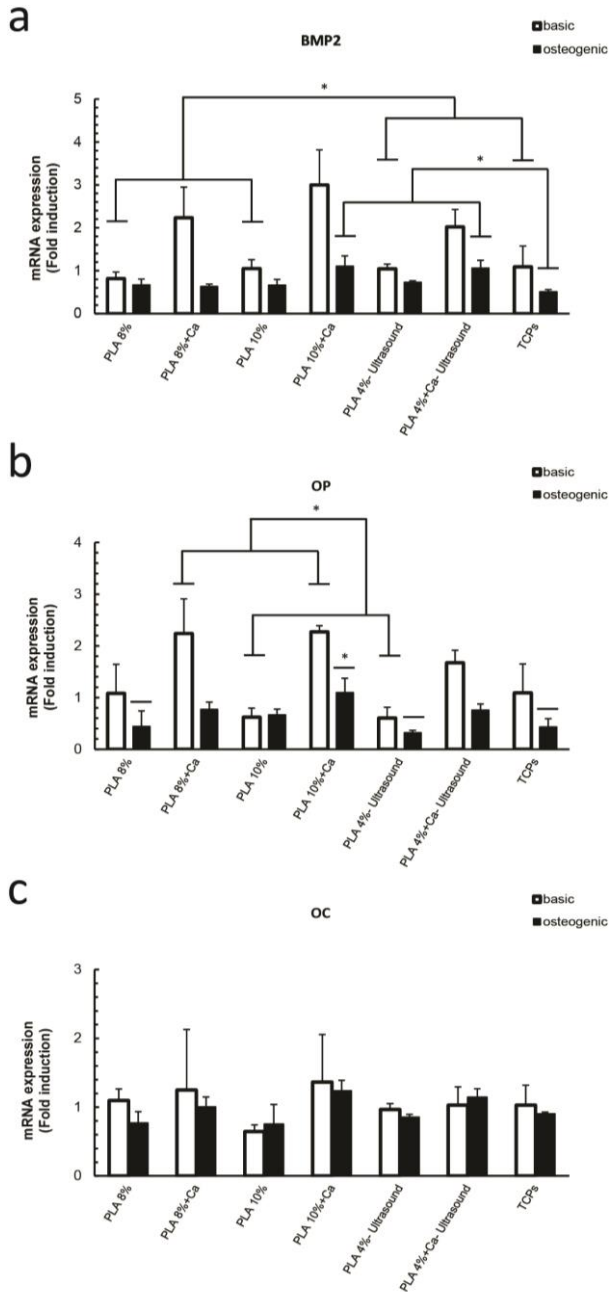


Figure 4. Expression of BMP2 (a), OP (b) and OC (c) genes by hMSCs cultured in presence of different microspheres in trans-wells for 7 days. Generally, higher expression of BMP2 and OP was observed in calcium salt-loaded microspheres compared to non-loaded spheres and control in basic culture medium. Expression of OC gene was similar in all the conditions.

Polymer concentration is known to critically influence the inner porosity and consequently the density of microspheres when a single emulsion technique is used for preparation [33], which correlated to the results of the present study where calcium incorporation increased with increasing PLA content. An absence of micro- and nanopores on the surface of microspheres prepared with higher concentrations of PLA is also due to an increase in the density of the polymer matrix. Density and inner pore structure of microspheres are considered important parameters for achieving a higher incorporation efficiency [33, 34]. Indeed, a maximal salt incorporation and release over longer periods is expected to be achieved by dense microspheres with poorly interconnected pores. Other parameters that play a critical role in incorporation of drugs into microspheres are comprehensively studied by Kumari et al., Kim et al. and O'Donnell et al. [35-37]. The highest efficiency of calcium incorporation into microspheres achieved in this study was approximately 0.2 wt.% for microspheres prepared with 10% w/v PLA using mechanical emulsification and for microspheres containing 4% w/v PLA and ultrasonically emulsified. Although these amounts are relatively low, certainly in comparison with calcium levels found in body fluid, they may be sufficient to mimic the amounts of other trace elements in, for example, bone tissue. Efficiency of incorporation was strongly affected by the method of emulsification, as was demonstrated by microspheres containing 4% of PLA, which were produced using either mechanical or ultrasonic emulsification methods. Calcium content of 4% w/v PLA microspheres was approximately four times higher when emulsification was achieved by sonication compared to mechanical homogenization. The effects of different emulsification techniques on incorporation of bovine serum albumin (BSA) in poly(lactic-co-glycolic acid) (PLGA) matrix using a double emulsion technique was previously studied [38], however, no significant differences between different techniques were observed. The fact that BSA molecules are much larger compared to calcium chloride salt used here, possibly resulting in a higher viscosity of the BSA-polymer mixture, may explain opposing observations in the two studies. An increase in viscosity may limit the shear forces applied to the emulsion in the homogenization step.

Calcium-containing microspheres emulsified mechanically showed a burst  $\text{Ca}^{2+}$  release with approximately 80 wt.% of total calcium content released after 4 hours of immersion in SPS, independent of the initial PLA concentration. However, microspheres prepared by probe sonication showed a  $\text{Ca}^{2+}$  release of only 5 wt.%

of the total amount within the first day, increasing to 17% after 10 days. Comparable results regarding release of BSA were observed in an earlier study [34], where the mechanically homogenized samples released approximately 60% w/v BSA within 24 hours, an amount that was decreased to 14% w/v when sonication of the first emulsion was used [38].

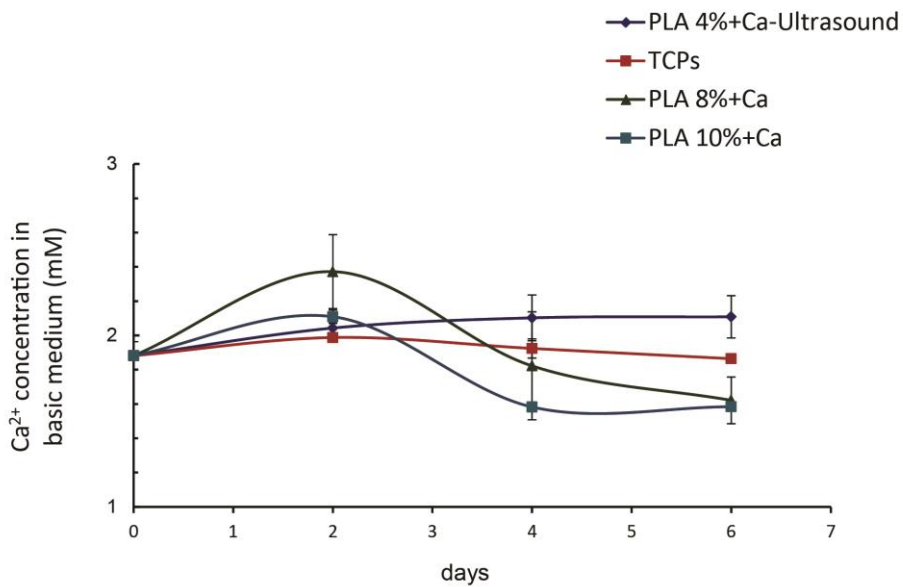


Figure 5. Calcium levels in basic medium during hMSCs culture in the presence of microspheres in trans-well inserts. In the presence of calcium salt-loaded microspheres prepared by mechanical homogenization,  $\text{Ca}^{2+}$  levels were elevated after 2 days, decreasing at the later time points.  $\text{Ca}^{2+}$  levels of cultures containing microsphere prepared by ultrasound showed a gradual increase over time.

Different effects of processing technique including sonication and mechanical homogenization on microsphere characteristics observed here can be explained by differences in efficiency of homogenization, stability of the formed emulsion and polymer density. Microsphere preparation using emulsification techniques is mainly a two-step process [29]. In the first step the polymer solution is dispersed into micro-droplets by either mechanically- or ultrasonically-applied shear stress. The second step is characterized by hardening of the microspheres through evaporation of the solvent and precipitation of the polymer. Homogenization by probe sonication is more effective in micro-droplet formation which consequently

leads to a higher compound distribution throughout the microsphere [38]. The process of solvent elimination and shrinkage of the microsphere critically determines the morphology, compound incorporation and release profile. A homogenous compound distribution results in less salt leaching during harvesting and washing steps of microspheres [29, 38], resulting in a higher inorganic content.

Emulsions prepared by probe sonication are more stable than mechanically homogenized or magnetically stirred ones, as was previously observed [38]. It is critical to limit phase separation of micro-droplets after the emulsification step. This phase separation may occur during the time between homogenization of the sample and pouring and diluting the emulsion in PVA. Separation of micro-droplets in the emulsion decreases the efficiency of mechanical homogenization even more, and consequently the compound distribution in the spheres becomes less homogeneous [38]. Similar to polymer concentration, the emulsification technique can influence the density of the formed microspheres based on the shear forces employed to the bioinorganic-polymer mixture.

Based on the facts mentioned above, adsorption of bioinorganics on the polymer surface is expected to be dominant polymer-bioinorganic interaction when mechanical emulsification is employed. In the case of sonication, the homogenous and stable salt distribution into PLA may result in improved embedding of the bioinorganic into the bulk of the microsphere, leading to a more sustained release of the ions which is controlled by the degradation of the polymer.

The *in vitro* cell culture study was used to investigate whether the delivery system presented here indeed can be used to study the biological effects of a sole ion.  $\text{Ca}^{2+}$  ions were selected here as one of the constituents of calcium phosphate ceramics, and for their earlier demonstrated effects on the osteogenic differentiation of hMSCs [13, 39]. A trans-well system was selected to study the effect of the released ions, independent of the physical contact with the microspheres. Microspheres with the highest calcium content were selected for cell culture experiments.

DNA quantification after 7 days of culture revealed no effect of microspheres, with or without calcium, on cell proliferation. The calcium concentration of the cell culture medium for calcium-loaded microspheres prepared using mechanical homogenization was approximately 2-2.4 mM after 2 days, which is in accordance with the burst release observed upon immersion of microspheres in SPS. At later time points, a plateau was reached at approximately 1.5 mM. The slight decrease

in  $\text{Ca}^{2+}$  level in cell medium at 4 and 6 days is plausibly due to (local) supersaturation of the medium with calcium, that may lead to precipitation of, for example a calcium-phosphate phase on the surface of microspheres, as was previously observed by Barradas et al. [40]. The ultrasonically emulsified samples showed a gradual release of  $\text{Ca}^{2+}$  from polymer matrix, similar to the observation upon immersion in SPS. It was previously shown that a  $\text{Ca}^{2+}$  concentration of 7.8 mM led to a significantly higher cell proliferation [39], which was not observed in the present study, plausibly because of the lower calcium ion levels in the medium. Quantification of ALP activity did not show significant effects of any of the conditions tested, which is in accordance with an earlier study suggesting that calcium is not involved in the pathway that regulates ALP gene expression and protein activity [39].

In an earlier study using hMSCs, in which standard cell culture was performed with medium containing elevated  $\text{Ca}^{2+}$  levels (7.8 mM), increased levels of BMP2, OP and OC were observed as compared to control medium condition [39]. hMSCs cultured in the presence of calcium-containing microspheres generally showed an upregulation of BMP2 and OP in the present study, in comparison to microspheres without the salt. This was not the case for OC, which could be explained by the fact that OC is a late osteogenic marker [41], possibly not yet expressed after 7 days of culture.

It should be emphasized that this study was meant as the development step of a system to study the effects of individual ions on cell behavior. Additional experiments, with microspheres offering distinct release profiles, and extended cell culture study over a longer time period, and including other assays of proliferation, differentiation and mineralization are required to obtain a complete picture of the effects of calcium ions released from PLA microspheres.

## 5. Conclusion

The results of the present study demonstrated that the bioinorganics-containing polymeric microspheres can be used for studying biological effects of individual ions. In conventional cell culture set-ups using ceramics or bioglass, a combination of a number of parameters, including chemical and topographical features is studied simultaneously, making it difficult to study the effect of a single parameter. However, a combination of bioinorganics-containing polymer microspheres and a trans-well cell culture set up offers a platform in which studying the chemical effects of a single bioinorganic independent of other

physico-chemical parameters is possible. Further optimization of the system is needed in terms of incorporation efficiency and release profile, as well as validation of the platform using other bioinorganics.

## References

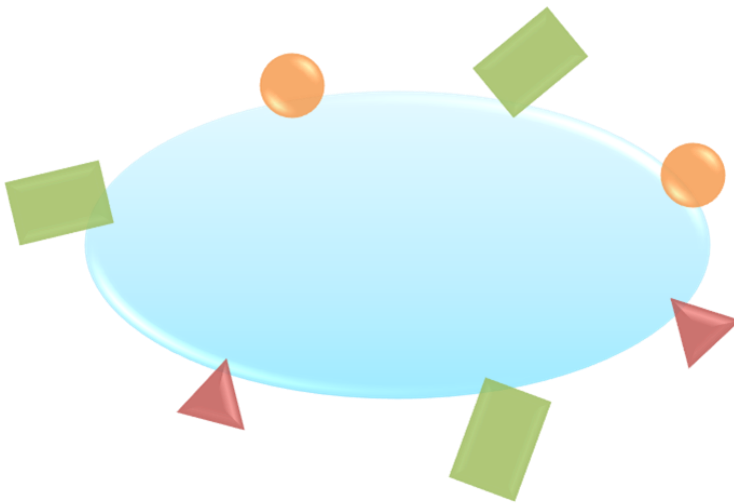
1. B.F. Ricciardi and M.P. Bostrom, Bone graft substitutes: Claims and credibility, *Seminars in arthroplasty* 24 (2013) 119-123.
2. M. Bohner, L. Galea, N. Doebelin, Calcium phosphate bone graft substitutes: Failures and hopes, *Journal of the European Ceramic Society* 32 (2012) 2663-2671.
3. T.N. Vo, F.K. Kasper, A.G. Mikos, Strategies for Controlled Delivery of Growth Factors and Cells for Bone Regeneration, *Advanced Drug Delivery Reviews* 64 (2012) 1292-1309.
4. L. Yang, B. Harink, P. Habibovic, Calcium Phosphate Ceramics with Inorganic Additives, Elsevier Ltd. (2011) 229-312.
5. J. Barralet, U. Gbureck, P. Habibovic, E. Vorndran, C. Gerard, C.J. Doillon, Angiogenesis in calcium phosphate scaffolds by inorganic copper ion release, *Tissue Engineering Part A* 15 (2009) 1601-1609.
6. A. Bigi, G. Cozzani, S. Panzavolta, A. Ripamonti, N. Roveri, M. Romanello, K. Noris Suarez, L. Moro, Chemical and structural characterization of the mineral phase from cortical and trabecular bone, *Journal of inorganic biochemistry* 68 (1997) 45-51.
7. Becker, R.O., Spadaro, J.A., and Berg, E.W. (1968). The trace elements of human bone, *The Journal of Bone & Joint Surgery* 50, 326-334.
8. E. Boanini, M. Gazzano, A. Bigi, Ionic substitutions in calcium phosphates synthesized at low temperature, *Acta Biomaterialia* 6 (2010) 1882-1894.
9. P. Habibovic and J.E. Barralet, Bioinorganics and biomaterials: Bone repair, *Acta Biomaterialia* 7 (2011) 3013-3026.
10. P.J. Meunier, C. Roux, E. Seeman, S. Ortolani, J.E. Badurski, T.D. Spector, J. Cannata, A. Balogh, E.M. Lemmel, S. Pors-Nielsen, The effects of strontium ranelate on the risk of vertebral fracture in women with postmenopausal osteoporosis, *New England Journal of Medicine* 350 (2004) 459-468.
11. S. O'donnell, A. Cranney, G. Wells, J. Adachi, J.Y. Reginster, Strontium ranelate for preventing and treating postmenopausal osteoporosis, *Cochrane Database Systematic Reviews* 19 (2006) CD005326.
12. M. Kleerekoper and R. Vieth, Fluoride and the Skeleton, *Critical Reviews in Clinical Laboratory Sciences* 33 (1996) 139-161.
13. L. Yang, S. Perez-Amodio, F.Y. Barrère-de Groot, V. Everts, C.A., van Blitterswijk, P. Habibovic, The effects of inorganic additives to calcium phosphate on in vitro behavior of osteoblasts and osteoclasts, *Biomaterials* 31 (2010) 2976-2989.
14. W. Fan, R. Crawford, Y. Xiao, Enhancing in vivo vascularized bone formation by cobalt chloride-treated bone marrow stromal cells in a tissue engineered periosteum model, *Biomaterials* 31 (2010) 3580-3589.
15. S. Bose, G. Fielding, S. Tarafder, A. Bandyopadhyay, Understanding of dopant-induced osteogenesis and angiogenesis in calcium phosphate ceramics, *Trends in Biotechnology* 31 (2013) 594-605.
16. A. Hoppe, N.S. Güldal, A.R. Boccaccini, A review of the biological response to ionic dissolution products from bioactive glasses and glass-ceramics, *Biomaterials* 32 (2011) 2757-2774.
17. T.N. Vo, F.K. Kasper, A.G. and Mikos, Strategies for controlled delivery of growth factors and cells for bone regeneration, *Advanced drug delivery reviews* 64 (2012) 1292-1309.

18. S. Ravindra, K. Varaprasad, N.N. Reddy, K. Vimala, K.M. Raju, Biodegradable microspheres for controlled release of an antibiotic ciprofloxacin, *Journal of Polymers and the Environment* 19 (2011) 413-418.
19. R.A. Pérez, J.E. Won, J.C. Knowles, H.W. Kim, Naturally and synthetic smart composite biomaterials for tissue regeneration, *Advanced Drug Delivery Reviews* 65 (2013) 471-496.
20. H.K. Kim, H.J. Gu, H.H. Lee, Microspheres of collagen-apatite nanocomposites with osteogenic potential for tissue engineering, *Tissue engineering* 13 (2007) 965-973.
21. S.J. Hong, H.S. Yu, H.W. Kim, Tissue Engineering Polymeric Microcarriers with Macroporous Morphology and Bone-Bioactive Surface, *Macromolecular bioscience* 9 (2009) 639-645.
22. R.A. Perez, H.W. Kim, M.P. Ginebra, Polymeric additives to enhance the functional properties of calcium phosphate cements, *Journal of tissue engineering* 3 (2012) doi: 10.1177/2041731412439555.
23. R. Félix Lanao, S. Leeuwenburgh, J. Wolke, J. Jansen, In vitro degradation rate of apatitic calcium phosphate cement with incorporated PLGA microspheres, *Acta biomaterialia* 7 (2011) 3459-3468.
24. H. Maeda, T. Kasuga, Preparation of poly (lactic acid) composite hollow spheres containing calcium carbonates, *Acta Biomaterialia* 2 (2006) 403-408.
25. L.S. Nair, C.T. Laurencin, Biodegradable polymers as biomaterials, *Progress in polymer science* 32 (2007) 762-798.
26. P.B. Maurus and C.C. Kaeding, Bioabsorbable implant material review, *Operative Techniques in Sports Medicine* 12 (2004) 158-160.
27. F. Pavanetto, B. Conti, I. Genta, P. Giunchedi, Solvent evaporation, solvent extraction and spray drying for polylactide microsphere preparation, *International journal of pharmaceutics* 84 (1992) 151-159.
28. Vasir, J.K., Tambwekar, K., and Garg, S. (2003). Bioadhesive microspheres as a controlled drug delivery system. *International Journal of Pharmaceutics* 255, 13-32.
29. I.D. Rosca, F. Watari, M. Uo, Microparticle formation and its mechanism in single and double emulsion solvent evaporation, *Journal of controlled release* 99 (2004) 271-280.
30. H. Fernandes, A. Mentink, R. Bank, R. Stoop, C. van Blitterswijk, J. de Boer, Endogenous Collagen Influences Differentiation of Human Multipotent Mesenchymal Stromal Cells, *Tissue Engineering: Part A* 16 (2010) 1693-1702.
31. S.K. Both, A.J.C. van der Muijsenberg, C.A. van Blitterswijk, J. de Boer, J.D. de Bruijn, A rapid and efficient method for expansion of human mesenchymal stem cells, *Tissue Engineering* 13 (2007), 3-9.
32. G. Kickelbick, Concepts for the incorporation of inorganic building blocks into organic polymers on a nanoscale, *Progress in Polymer Science* 28 (2003) 83-114.
33. S. Mao, J. Xu, C. Cai, O. Germershaus, A. Schaper, T. Kissel, Effect of WOW process parameters on morphology and burst release of FITC-dextran loaded PLGA microspheres, *International Journal of Pharmaceutics* 334 (2007) 137-148.
34. Freiberg, S., and Zhu, X. (2004). Polymer microspheres for controlled drug release. *International journal of pharmaceutics* 282, 1-18.
35. A. Kumari, S.K. Yadav, S.C. Yadav, Biodegradable polymeric nanoparticles based drug delivery systems, *Colloids and Surfaces B: Biointerfaces* 75 (2010) 1-18.
36. K.K. Kim, D.W. Pack, Microspheres for drug delivery. In: *BioMEMS and Biomedical Nanotechnology*, Springer, (2006) 19-50.
37. P.B. O'Donnell, J.W. McGinity, Preparation of microspheres by the solvent evaporation technique, *Advanced drug delivery reviews* 28 (1997) 25-42.
38. J.X. Zhang, D. Chen, S.J. Wang, K.J. Zhu, Optimizing double emulsion process to decrease the burst release of protein from biodegradable polymer microspheres, *Journal of Microencapsulation* 22 (2005) 413-422.

39. A. Barradas, H.A., Fernandes, N. Groen, Y.C. Chai, J. Schrooten, J. van de Peppel, J.P. van Leeuwen, C.A. van Blitterswijk, J. de Boer, A calcium-induced signaling cascade leading to osteogenic differentiation of human bone marrow-derived mesenchymal stromal cells, *Biomaterials* 33 (2012) 3205-3215.
40. A.M.C. Barradas, V. Monticone, M. Hulsman, C. Danoux, H. Fernandes, Z.Tahmasebi Birgani, F. Barre`re-de Groot, H. Yuan, M. Reinders, P. Habibovic, C. van Blitterswijk, J. de Boer, Molecular mechanisms of biomaterial-driven osteogenic differentiation in human mesenchymal stromal cells, *Integrative Biology* 5 (2013) 920-931.
41. C. Granéli, A. Thorfvea, U. Ruetschi, H. Brisby, P. Thomsena, A.Lindahl, C. Karlsson, Novel markers of osteogenic and adipogenic differentiation of human bone marrow stromal cells identified using a quantitative proteomics approach, *Stem Cell Research* 12 (2014) 153–165.

## Chapter 8

### General discussion and future perspectives



Bone graft substitutes with bioinorganic modification

## 8.1. Introduction

Despite major scientific efforts in the past decades to develop a comprehensive substitute for the autograft, known as the gold standard for bone regeneration [1], our knowledge about the contributing factors including cells, biological factors and biomaterials, and about their interactions, is still incomplete. As a result, regeneration of bone tissue to a high quality level and with proper functionality, as well as the development of advanced tools for long-term characterization of the regenerated bone, remain an important challenge [2].

As discussed in Chapter 2 of this thesis, various strategies based on combinations of carrier materials with cells and growth factors, physico-chemical modifications of biomaterials and application of external stimuli, have been employed with the aim to develop tissue engineering constructs and synthetic bone graft substitutes with enhanced bone regenerative capacity [1-3]. The basic research into optimization of these strategies and mechanistic studies to unravel the underlying biological processes is ongoing.

This thesis focused on the use of bioinorganic compounds to enhance the bioactivity of synthetic bone graft substitutes, particularly calcium phosphates (CaPs), while retaining their synthetic character. This chapter discusses the results obtained in the experimental chapters in the perspective of the strategies aiming to develop comprehensive synthetic alternatives to natural bone, and gives an outlook toward future developments.

## 8.2. Calcium phosphate-based biomaterials as bone graft substitutes

The work described in this thesis was based on the assumption that an optimal biomaterial intended for bone regeneration should meet a number of requirements as described in Table 1. Besides biocompatibility in an osseous environment, bone regeneration potential through osteoconductivity, osteoinductivity, osteogenesis or osteointegration as well as the ability to initiate and facilitate blood vessel formation, are among the most important requirements for resuming natural bone function. (Temporary) mechanical support and degradability further aid the performance of such a biomaterial. It should be emphasized that all these properties are intertwined, as they are all dependent on physico-chemical and structural properties of the biomaterial [3-7]. CaP bioceramics, having many chemical and structural similarities to bone mineral, are among the most widely used materials as bone graft substitutes and

they naturally fulfill many of the requirements mentioned before. Nevertheless, in general, the clinical performance of CaP bone graft substitutes is considered inferior to that of the autologous bone [3, 8]. Hence, many attempts have been undertaken to add biological functionality to such bone graft substitutes, for example via immobilization of growth factor [9, 10] or incorporation of synthetic compounds [8, 11, 12]. Therefore, the ability of bone graft substitutes to act as carriers or delivery vehicles of (synthetic) growth factors is often considered an added value. Furthermore, CaPs suffer from lack of ductility, which may result in a brittle fracture under tensile load. As a result, CaP-based bone graft substitutes are not suitable for the most load-bearing applications and therefore, combinations with other materials that offer more versatility in mechanical properties (i.e. CaP composites and CaP-coated biomaterials) are extensively researched [13, 14]. Finally, clinical requirements of easy handling, availability and low cost of production and storage need to be taken into account when developing such bone graft substitutes.

The experiments in this thesis were thus based on the requirements for successful bone graft substitutes described above, taking into account the known limitations of the available CaPs. As one of the basic techniques applied throughout the thesis was a previously developed and characterized biomimetic process for depositing CaP coatings on surfaces of other biomaterials [15]. This is a relatively simple technique that is based on immersion of the substrate of interest into aqueous solutions containing calcium and inorganic phosphate, that leads to precipitation of a CaP layer on the substrate surface.

Many other techniques exist, that have been successfully employed to produce different CaP coatings on surfaces of biomaterials including various plasma spraying techniques, pulsed laser deposition (PLD), ion-beam-assisted deposition (IBAD) and radio-frequency (RF) magnetron sputtering [13]. These techniques are, however, often associated with the use of high levels of energy and high temperatures, limiting their use to a few CaP phases and thermally stable substrates.

Conversely, the biomimetic method employed here is conducted at near-physiological conditions and low temperatures, enabling its use for any type of material including polymers sensitive to higher temperature. Considering that the process takes place in an aqueous solution, geometrically complex and porous substrates can be coated, which is in contrast to line-of-sight methods like plasma spraying. Furthermore, it is also possible to add drugs, growth factors and

inorganic compounds such as bioinorganic salts to the solution. This facilitates the immobilization of the drugs and proteins, and ionic substitutions into the CaP coatings for further improvement of their biological properties [12, 16].

Table 1. Required properties of bone graft substitute biomaterials.

<b>Properties of bone graft substitute</b>	
<b>Basics</b>	Biocompatibility Bone regeneration <ul style="list-style-type: none"> <li>- Osteoconductivity</li> <li>- Osteoinductivity</li> <li>- Osteogenesis and osteointegration</li> </ul> Vascularization Degradability Mechanical support
<b>Pros</b>	Ability to deliver biofactors
<b>Clinical aspects</b>	Economical (Off-the-shelf) availability Easy handling during surgery

The precipitation of CaPs coating from the solution containing calcium and inorganic phosphate ions is largely dependent on the thermodynamic conditions. This means that by changing the ionic condition, temperature or pH, different CaP phases with distinct properties can be produced [16].

Owing to these advantages of the biomimetic technique used for the experiments, it was possible to produce CaP coatings predominantly composed of octacalcium phosphate (OCP), a phase that has a higher solubility than, for example hydroxyapatite (HA), thus releasing higher levels of calcium and phosphate ions upon hydrolysis. The coatings were successfully applied on different substrates including titanium (Ti) implants with rough microporous surface (in Chapter 4), flat polystyrene substrate (in Chapter 5) and on three-dimensional poly(lactic acid) (PLA) particles (in Chapters 3 and 6).

The biomimetic CaP coatings prepared using a similar method were previously tested in *in vitro* experiments [17, 18], which showed their compatibility with cultures of both osteoblastic and osteoclastic cells. In order to assess different ways of combining the CaP ceramic with a polymer, to develop a bone graft substitute with improved mechanical properties and an optimal carrier for bioinorganics, PLA particles coated with OCP were compared to conventional PLA/HA composites for their support of proliferation of human mesenchymal stromal cells (hMSCs). The PLA/HA composite used here was previously shown to increase the osteogenic differentiation of hMSCs and induce new bone formation in *in vivo* models [19, 20]. While containing lower amounts of the CaP mineral compared to PLA/HA composite, the OCP coatings supported the osteogenic differentiation of the hMSCs at the same level as the composite, plausibly due to their higher solubility and availability of the CaP phase (Chapter 3). Based on this result, the coating method was used to further improve the bioactivity by incorporation of bioinorganics of interest.

### **8.3. Calcium phosphate-based bone graft substitutes functionalized with bioinorganics**

Chemical functionalization of CaPs is a widely used approach for enhancing their bioactivity *in vitro* and *in vivo*. Two common categories of chemical cues that can be added to CaPs for this purpose include biological growth factors [9, 10] and bioinorganics or synthetic growth factors [8, 11, 12]. While the use of proteins and growth factors in combination with CaPs has shown great promise in development of functional biomaterials for bone regeneration, bioinorganics, being synthetic, offer the off-the-shelf availability and lower cost.

In terms of biological properties, numerous studies have shown that bioinorganics are involved in many signaling pathways and chemical cascades in human body and, alone or released from bone graft substitutes, can alter the bone regeneration-related mechanisms [11, 21].

In the context of bone regeneration, the first route through which bioinorganics may modify the biological response is by altering the osteogenesis process. Strontium ( $\text{Sr}^{2+}$ ) ions, administered as strontium ranelate or incorporated into CaPs, were shown to enhance the attachment and proliferation of pre-osteoblastic cells resulting in higher activity of functional osteoblasts and secretion of matrix proteins. Furthermore, by inducing the expression and

production of osteogenic proteins in osteoblast precursor cells,  $\text{Sr}^{2+}$  ions were shown to modify the osteogenic differentiation program and increase matrix mineralization [22-25]. In this thesis, in Chapter 4, it was reported that  $\text{Sr}^{2+}$  ions have a direct chemical effect on the osteogenic differentiation of the hMSCs, known to be the progenitors of the osteoblasts. Their positive effect on osteogenic differentiation was intensified when  $\text{Sr}^{2+}$  ions were released from CaPs, plausibly due to additional presence of the calcium and inorganic phosphate ions in the medium.

Similar to the effect of  $\text{Sr}^{2+}$ , in previous studies it has been observed that fluoride ( $\text{F}^-$ ) ions addition to CaPs also substantially increased the expression of the osteogenic markers and the production of mineralized matrix [18, 26, 27]. The results presented in Chapter 5 are in accordance with these findings.  $\text{F}^-$  addition to biomimetic CaP coatings had a major effect on osteogenic differentiation of hMSCs. Furthermore, enhanced mineralization of the cells cultured on CaPs containing  $\text{F}^-$  ions was demonstrated.

While the topic of osteoclastogenesis and osteoclastic resorption was not the focus of this thesis, other studies have shown that a number of bioinorganics exists that interfere with the osteoclast-related processes at different levels including osteoclast attachment, growth, differentiation and resorptive activity. Pharmacological effects of  $\text{Sr}^{2+}$  ions, for example, on reducing osteoclast differentiation and mineral resorption were previously observed in vitro. Mechanistic studies showed that these effects were due to disruption of the actin containing sealing zone, inhibiting osteoclast attachments and modulating signaling pathways related to the osteoclastic differentiation [22, 23].

Cobalt ( $\text{Co}^{2+}$ ) ions, used direct as supplement to cell culture medium or combined with CaP coatings also showed to increase the number of attached osteoclasts and their resorptive activity, with certain ranges of concentrations favoring these effects [17]. It was shown that this effect was a result of the hypoxia-mimicking role of  $\text{Co}^{2+}$  ions.

A major challenge in bone regeneration is vascularization of the newly formed tissue, considering that natural bone itself is highly vascularized. The role of vasculature in bone tissue is to provide a platform for the transfer of essential nutrients and  $\text{O}_2\text{-CO}_2$  exchange and to keep the close spatial and temporal connection between the formed vessels and bone cells to maintain skeletal integrity [28]. A few bioinorganics were found to be pro-angiogenic including  $\text{Co}^{2+}$ , copper ( $\text{Cu}^{2+}$ ) and magnesium ( $\text{Mg}^{2+}$ ) ions [21]. As extensively discussed in

Chapters 5 and 6, the induction of hypoxic conditions at cellular level by  $\text{Co}^{2+}$  ions acts as a stimulator for the cells to produce more pro-angiogenic factors and promote the neo-vascularization to compensate for the  $\text{O}_2$  loss [21]. In these two chapters it was first observed that direct supplementation of the medium with  $\text{Co}^{2+}$  ions resulted in an increase of the expression of angiogenic factors such as vascular endothelial growth factor. Then it was demonstrated that incorporation of  $\text{Co}^{2+}$  ions into CaP-coated PLA particles resulted in the formation of more blood vessels with proper hierarchical structure in an intramuscular model in vivo.

Considering the extensive number studies showing promising results with application of bioinorganics in bone regeneration, the question arises why there are only few bone graft substitutes with bioinorganics approved for clinical use. The answer lies, at least partly, in the fact that an optimal formulation of bioinorganics has not been found, yet.

Several parameters need to be considered in the search for such optimal bioinorganics-functionalized bone graft substitutes, being the properties of the bioinorganic, the properties of the carrier and the method of incorporation (Figure 1). The significance of these different parameters will be discussed in the following sections.

### 8.3.1. Choice of bioinorganics

Bone tissue is a complex microenvironment, which is composed of different cell types, proteins and mineral that, besides CaP, contains several bioinorganics. Inspired by such microenvironment, a combination of different bioinorganics in conjunction with CaP carriers can elicit combined, or even synergistic effects on the processes related to bone regeneration [29]. In Chapter 5 for example, an attempt was undertaken to simultaneously induce osteogenesis and angiogenesis by incorporating a cocktail of  $\text{Co}^{2+}$  and  $\text{F}^-$  ions into CaP coatings. It was observed that by using the right concentration of both compounds in the cocktail, it was possible to maintain the osteogenic effect introduced by  $\text{F}^-$  ions, while adding the angiogenic stimulus by the  $\text{Co}^{2+}$  ions. Combinations of bioinorganics, very much like cocktails of biological growth factors, offer a promising approach to provide CaP bone graft substitutes with a complex biofunctionality.

There is no doubt that the cell response to the bioinorganics-functionalized biomaterials is dose dependent, and that wrong doses can lead to a complete absence of an effect on one, or to adverse, cytotoxic event on the other side. Hence, the concentration of bioinorganics used for preparing the biomaterials and

the release profile of bioinorganics are other crucial parameters that still need to be optimized in order to obtain the optimal formulation in a given application.

### **8.3.2. Choice of the carrier biomaterial and its physicochemical properties**

The physicochemical properties of the host material are the main determinant factor in the final cell and tissue response as discussed above and summarized in table 1. Furthermore, the release profile of the bioinorganics and the physicochemical properties of the carrier during and after the release are of great importance for the final outcome of the treatment.

As is discussed in Chapters 3-6, CaP-based biomaterials are the first choice for developing synthetic bone graft substitutes along with bioactive glasses, owing to their intrinsic bioactivity in a bony environment. However, in Chapter 7, the potential of polymeric materials (in this case PLA) as delivery vehicles of bioinorganics was demonstrated. Such a system provides a simpler platform to study the effect of bioinorganics, without interference of other ions that are commonly simultaneously released from CaP carriers. Furthermore, such system is promising for controlled and localized delivery as bioinorganics, similar to what is used for biological growth factors.

### **8.3.3. Incorporation method**

The availability and release profile of bioinorganics from bone graft substitutes are also largely dependent on the methods of their incorporation into biomaterials. Simple adsorption of bioinorganics from a solution on the surface of the carrier substrate is very simple, however, this method only allows for superficial binding and therefore, limited amount of compounds of interest can be loaded, which are usually released in a short period of time following a burst release profile. Incorporation of bioinorganics into CaPs during their production, by either physical entrapment or by substitution into the crystal lattice can be used if sustained release is required [17]. In this thesis, the biomimetic coating method was used for incorporation, but a variety of other methods exist that would allow incorporation of bioinorganics, since they are stable compounds. The possibility of adding bioinorganics into polymers is interesting for developing polymer-ceramic composites, with, in general improved mechanical properties as compared to the ceramic alone.

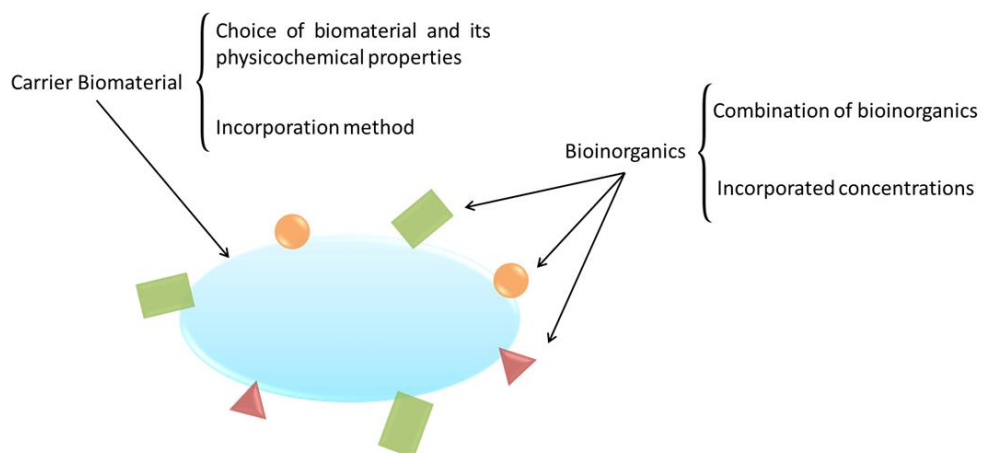


Figure 1. Schematic overview of a system based on bone graft substitute biomaterials as carrier and bioinorganics as synthetic growth factors. On the bioinorganics side, optimized formulation used for functionalization of the carrier including combination and doses of the bioinorganics are important. On the carrier side physicochemical properties of the biomaterial and incorporation method are crucial in defining the profile of local delivery of the bioinorganics and the biological effect of the system.

#### 8.4. Future perspectives

The research presented in this thesis is a valuable contribution to the knowledge of the role of bioinorganics in processes related to bone formation and remodeling as well as the methods to incorporate these compounds into carrier materials to develop improved bone graft substitutes. Despite this scientific advancement, we are still far from defining the optimal synthetic bone graft substitute based on bioinorganics.

Optimizing the selection of bioinorganics formulations and optimizing the properties of the carrier material should be the priorities for further development of bioinorganics-functionalized CaP-based bone graft substitutes having superior biological performance. In this context, a large number of bioinorganics which are known or suspected to be relevant along with a family of potential CaPs and CaP-based carriers result in a massive number of possible combinations. To be able to investigate these great numbers of combinations in a reliable manner, it will be important to develop platforms that are suitable for high-throughput screening of material properties and material-cell interactions. Such platforms should not only identify the hits with excellent performance or remove poorly performing

combinations at the early stage of research, but should also provide insight in the mechanisms governing a cell or tissue response to the material.

In the context of clinical translation of the potentially relevant bioinorganics-functionalized bone graft substitutes, in vivo experiments or experiments able to reliably replace animal research are needed to confirm the long-term safety of the bioinorganics, along with their functionality. In particular compromised animal models, representing challenging cases of diseased bones are of great interest.

## References

1. R. Dimitriou, E. Jones, D. McGonagle, P.V. Giannoudis, Bone regeneration: current concepts and future directions. *BMC Medicine*, 9 (2011) 1-10.
2. A.R. Amini, C.T. Laurencin, S.P. Nukavarapu, Bone Tissue Engineering: Recent Advances and Challenges. *Critical reviews in biomedical engineering*, 40 (2012) 363-408.
3. M. Bohner, L. Galea, N. Doebelin, Calcium phosphate bone graft substitutes: Failures and hopes. *Journal of the European Ceramic Society*, 32 (2012) 2663-2671.
4. A. Beswick and A.W. Blom, Bone graft substitutes in hip revision surgery: a comprehensive overview. *Injury*, 42 Suppl 2 (2011) S40-6.
5. I. Denry and L.T. Kuhn, Design and characterization of calcium phosphate ceramic scaffolds for bone tissue engineering. *Dental Materials*, 32 (2016) 43-53.
6. B.F. Ricciardi and M.P. Bostrom, Bone graft substitutes: Claims and credibility. *Seminars in Arthroplasty*, 24 (2013) 119-123.
7. D. Tang, R.S. Tare, L.-Y. Yang, D.F. Williams, K.-L. Ou, R.O.C. Oreffo, Biofabrication of bone tissue: approaches, challenges and translation for bone regeneration. *Biomaterials*, 83 (2016) 363-382.
8. L. Yang, B. Harink, P. Habibovic, 1.118 - Calcium Phosphate Ceramics with Inorganic Additives A2 - Ducheyne, Paul, in *Comprehensive Biomaterials*. 2011, Elsevier: Oxford. p. 299-312.
9. T.N. Vo, F.K. Kasper, A.G. Mikos, Strategies for controlled delivery of growth factors and cells for bone regeneration. *Advanced Drug Delivery Reviews*, 64 (2012) 1292-1309.
10. S. Bose and S. Tarafder, Calcium phosphate ceramic systems in growth factor and drug delivery for bone tissue engineering: A review. *Acta Biomaterialia*, 8 (2012) 1401-1421.
11. P. Habibovic and J.E. Barralet, Bioinorganics and biomaterials: bone repair. *Acta Biomater*, 7 (2011) 3013-26.
12. E. Boanini, M. Gazzano, A. Bigi, Ionic substitutions in calcium phosphates synthesized at low temperature. *Acta Biomaterialia*, 6 (2010) 1882-1894.
13. R.A. Surmenev, M.A. Surmeneva, A.A. Ivanova, Significance of calcium phosphate coatings for the enhancement of new bone osteogenesis – A review. *Acta Biomaterialia*, 10 (2014) 557-579.
14. H. Zhou, J.G. Lawrence, S.B. Bhaduri, Fabrication aspects of PLA-CaP/PLGA-CaP composites for orthopedic applications: a review. *Acta Biomater*, 8 (2012) 1999-2016.
15. F. Barrere, P. Layrolle, C.A. Van Blitterswijk, K. De Groot, Biomimetic coatings on titanium: a crystal growth study of octacalcium phosphate. *J Mater Sci Mater Med*, 12 (2001) 529-34.
16. X. Lin, K. de Groot, D. Wang, Q. Hu, D. Wismeijer, Y. Liu, A review paper on biomimetic calcium phosphate coatings. *Open Biomed Eng J*, 9 (2015) 56-64.
17. S. Patnirapong, P. Habibovic, P.V. Hauschka, Effects of soluble cobalt and cobalt incorporated into calcium phosphate layers on osteoclast differentiation and activation. *Biomaterials*, 30 (2009) 548-55.

18. L. Yang, S. Perez-Amodio, F.Y. Barrere-de Groot, V. Everts, C.A. van Blitterswijk, P. Habibovic, The effects of inorganic additives to calcium phosphate on in vitro behavior of osteoblasts and osteoclasts. *Biomaterials*, 31 (2010) 2976-89.
19. C.B. Danoux, D. Barbieri, H. Yuan, J.D. de Bruijn, C.A. van Blitterswijk, P. Habibovic, In vitro and in vivo bioactivity assessment of a polylactic acid/hydroxyapatite composite for bone regeneration. *Biomatter*, 4 (2014) e27664.
20. D. Barbieri, A.J. Renard, J.D. de Bruijn, H. Yuan, Heterotopic bone formation by nano-apatite containing poly(D,L-lactide) composites. *Eur Cell Mater*, 19 (2010) 252-61.
21. S. Bose, G. Fielding, S. Tarafder, A. Bandyopadhyay, Understanding of dopant-induced osteogenesis and angiogenesis in calcium phosphate ceramics. *Trends in Biotechnology*, 31 (2013) 594-605.
22. E. Bonnelye, A. Chabadel, F. Saltel, P. Jurdic, Dual effect of strontium ranelate: stimulation of osteoblast differentiation and inhibition of osteoclast formation and resorption in vitro. *Bone*, 42 (2008) 129-38.
23. Z. Saidak and P.J. Marie, Strontium signaling: Molecular mechanisms and therapeutic implications in osteoporosis. *Pharmacology & Therapeutics*, 136 (2012) 216-226.
24. F. Yang, D. Yang, J. Tu, Q. Zheng, L. Cai, L. Wang, Strontium enhances osteogenic differentiation of mesenchymal stem cells and in vivo bone formation by activating Wnt/catenin signaling. *Stem Cells*, 29 (2011) 981-91.
25. M. Schumacher and M. Gelinsky, Strontium modified calcium phosphate cements - approaches towards targeted stimulation of bone turnover. *Journal of Materials Chemistry B*, 3 (2015) 4626-4640.
26. J. Li, Y. Song, S. Zhang, C. Zhao, F. Zhang, X. Zhang, L. Cao, Q. Fan, T. Tang, In vitro responses of human bone marrow stromal cells to a fluoridated hydroxyapatite coated biodegradable Mg–Zn alloy. *Biomaterials*, 31 (2010) 5782-5788.
27. H. Qu and M. Wei, The effect of fluoride contents in fluoridated hydroxyapatite on osteoblast behavior. *Acta Biomaterialia*, 2 (2006) 113-119.
28. J.M. Kanczler and R.O. Oreffo, Osteogenesis and angiogenesis: the potential for engineering bone. *Eur Cell Mater*, 15 (2008) 100-14.
29. S. Bose, G. Fielding, S. Tarafder, A. Bandyopadhyay, Trace element doping in calcium phosphate ceramics to Understand osteogenesis and angiogenesis. *Trends in biotechnology*, 31 (2013) 10.1016/j.tibtech.2013.06.005.

## Summary

Bone tissue is naturally able to regenerate when damaged. However, in many large defects caused by fractures due to aging or osteoporosis, trauma, tumor removal, etc., the natural regenerative ability of bone is not sufficient to fully heal the defect. In such cases, a graft is required to support the process of regeneration. While natural bone grafts, especially autografts, are widely applied in such conditions, their use is associated with important disadvantages, limited availability being the most prominent one. To overcome these limitations, a wide range of natural and synthetic alternatives has been developed, which are available off-the-shelf in large quantities. However their clinical performance has always been considered inferior to that of autografts. Therefore, in the past decades, extensive research efforts have been invested in developing bone graft substitutes with improved properties and clinical performance.

In Chapter 1 of this thesis, the Introduction, the concept of advanced biomaterials and strategies for enhancing the functionality of bone graft substitutes was described. One of these strategies includes chemical modification of the existing bone graft substitutes with bioinorganics such as strontium ( $\text{Sr}^{2+}$ ), magnesium ( $\text{Mg}^{2+}$ ), zinc ( $\text{Zn}^{2+}$ ), etc. Chapter 2 was dedicated to reviewing and analyzing different aspect of this strategy, when used in association with calcium phosphate (CaP)-based bone graft substitutes.

In Chapter 3, a biomimetic method for producing CaP coatings on polymers, that allows the incorporation of bioinorganics, was introduced and the resulting materials were compared to the conventional polymer/ceramic composites. It was shown that the CaP-coated-materials, similar to the conventional composite, are able to trigger the differentiation of human mesenchymal stromal cells (hMSCs) towards the osteogenic lineage.

Although a variety of bioinorganics has been used as a strategy to improve properties of CaPs and their biological performance, the mechanisms of actions of bioinorganics are still not fully understood. Therefore, in Chapters 4 and 5, the effects of  $\text{Sr}^{2+}$ , cobalt ( $\text{Co}^{2+}$ ) and fluoride ( $\text{F}^-$ ) were evaluated on the osteogenic differentiation of hMSCs. The results of these studies showed that cells might be influenced directly by the presence of the bioinorganics in their microenvironment, or indirectly through changes in the physicochemical properties of the CaPs, caused by the incorporation of bioinorganics into their structure. It was also shown that using cocktails of different bioinorganics might be an interesting strategy to affect different biological processes simultaneously.

Although the *in vitro* cell-based tests provide a screening tool for assessing the safety and the initial bioactivity of bioinorganics and bioinorganics-containing bone graft substitutes, *in vivo* models are required to validate this data and bring the treatment a step closer to the clinical application. Therefore, in Chapter 6, the effects of  $\text{Co}^{2+}$  ions incorporated into CaP coatings on vascularization were evaluated in an intramuscular goat model. The results showed that the presence of  $\text{Co}^{2+}$  in CaP coatings enhanced the new blood vessel

formation and maturation, which in itself is considered beneficial in the process of bone regeneration.

CaPs are complex functional materials, with a multitude of properties, which are often intertwined, and this complexity is further increased by the incorporation of bioinorganics into CaPs. This further impedes the full understanding of the mechanisms of action of the incorporated ions. Therefore, in Chapter 7, we developed a model biomaterial based on polymer microspheres, to act as a carrier for bioinorganics. This simplified platform was successfully tested *in vitro* for screening direct effects of bioinorganics on hMSCs, independent of the properties of the carrier material.

Finally, in Chapter 8 some concluding remarks were given as well as a summary of the important parameters that can be tuned to achieve an optimum formulation of bioinorganics-modified bone graft substitute.

## Samenvatting

Botweefsel bezit het natuurlijke vermogen te regenereren wanneer het beschadigd is. In veel grote botbreuken, die een gevolg kunnen zijn van ouder worden of osteoporose, en bij trauma's of verwijdering van bottumoren, faalt dit natuurlijke herstelmechanisme. In deze gevallen is het nodig een bottransplantaat te gebruiken om het proces van regeneratie te ondersteunen. Terwijl natuurlijk bottransplantaten, en in het bijzonder patiënt-eigen bot standaard worden gebruikt in dit soort situaties, wordt hun gebruik vaak geassocieerd met grote nadelen, waarvan de schaarste de belangrijkste is. Dit heeft de ontwikkeling van een groot aantal natuurlijke en synthetische botsubstituten gestimuleerd, die gemaakt kunnen worden in onbeperkte hoeveelheden en direct beschikbaar zijn. Echter worden de klinische resultaten van deze botsubstituten altijd als inferieur gezien ten opzichten van natuurlijke bottransplantaten.

In de afgelopen decennia is er uitgebreid onderzoek gedaan naar de mogelijkheden om nieuwe botsubstituten te ontwikkelen met betere eigenschappen, die in de kliniek betere resultaten leveren. In Hoofdstuk 1 van dit proefschrift, de inleiding, is het concept van geavanceerde materialen geïntroduceerd, en zijn verschillende strategieën bediscussieerd om botsubstituten met verbeterde functionaliteit te ontwikkelen. Een van deze strategieën maakt gebruik van de zogenaamde bioinorganics, zoals strontium ( $\text{Sr}^{2+}$ ), magnesium ( $\text{Mg}^{2+}$ ), zink ( $\text{Zn}^{2+}$ ), etc. die toegevoegd kunnen worden aan botsubstituten. In Hoofdstuk 2 is een overzicht en een analyse gegeven van verschillende aspecten van deze strategie, in het bijzonder wanneer het gebruikt wordt met calciumfosfaat (CaF) keramiek botsubstituten.

In Hoofdstuk 3 is een biomimetische methode geïntroduceerd voor het maken van dunne laagjes CaF op polymeer botsubstituten. Met deze methode is het vrij eenvoudig bioinorganics in zo'n CaF coating op te nemen. De gecoate polymeren zijn in deze studie vergeleken met conventionele polymeer-CaF composieten. De resultaten hebben laten zien dat het stimuleren van humane mesenchymale stromale cellen (hMSCs) richting de osteogene (bot) lijn, even efficiënt is voor beide soorten materialen.

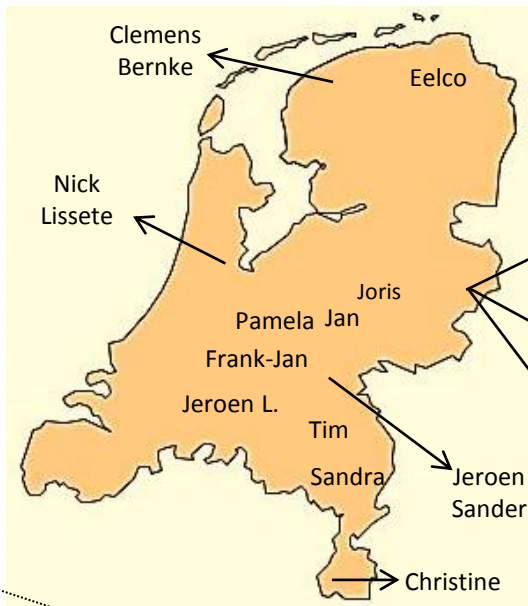
Hoewel verschillende bioinorganics gebruikt worden om de functionaliteit van botsubstituten te verbeteren, zijn de achterliggende mechanismen nog steeds niet volledig bekend. Om dit nader te onderzoeken zijn in Hoofdstukken 4 en 5, de effecten van  $\text{Sr}^{2+}$ , kobalt ( $\text{Co}^{2+}$ ) en fluoride ( $\text{F}^-$ ) op osteogene differentiatie van hMSCs geëvalueerd. De resultaten van deze studies hebben laten zien dat de cellen direct beïnvloed kunnen worden door de aanwezigheid van bioinorganics in hun micro-omgeving, maar ook indirect, door de veranderingen aan fysisch-chemische eigenschappen van CaF dragermateriaal, als gevolg van de toevoeging van bioinorganics aan hun structuur. Deze hoofdstukken hebben ook laten zien dat cocktails van bioinorganics gebruikt kunnen worden om verschillende belangrijke processen van botregeneratie tegelijkertijd te beïnvloeden.

Hoewel de *in vitro* cel testen nuttig zijn om de veiligheid en bioactiviteit van bioorganics en bioorganics-houdende botssubstituten initieel te testen, is het belangrijk deze resultaten *in vivo* te valideren, om ze zo een stap dichterbij de klinische toepassing te brengen. Daarom zijn in Hoofdstuk 6 de effecten van  $\text{Co}^{2+}$  ionen-houdende CaF coatings op vascularisatie getest in een intramusculair model in geiten. De resultaten van deze studie hebben laten zien dat de aanwezigheid van  $\text{Co}^{2+}$  ionen in CaF coatings de groei en maturatie van bloedvaten bevordert, wat als een voordelig effect wordt gezien in de regeneratie van bot.

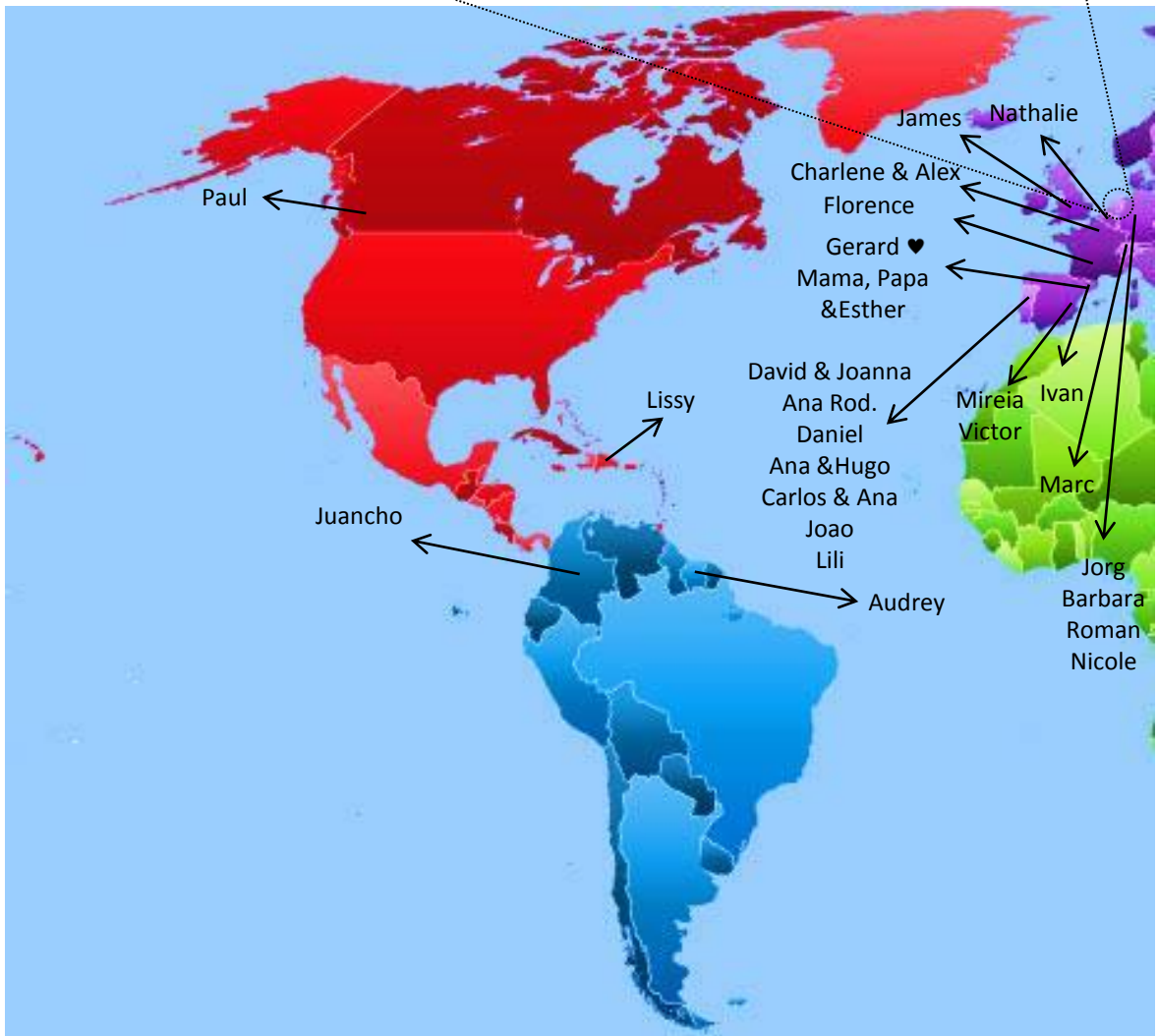
CaF zijn complexe functionele materialen met veel eigenschappen, die vaak met elkaar vervlochten zijn, en deze complexiteit wordt verder vergroot wanneer bioorganics worden toegevoegd. Dit alles maakt het moeilijk om de exacte effecten van bioorganics in botssubstituten volledig te begrijpen. Daarom zijn in Hoofdstuk 7 nieuwe modelmaterialen ontwikkeld op basis van polymere microbolletjes, die als dragermateriaal kunnen dienen voor een of meerdere bioorganics. *In vitro* testen van dit vereenvoudigd systeem hebben laten zien dat het inderdaad mogelijk is de eigenschappen van bioorganics te bestuderen, onafhankelijk van de eigenschappen van het dragermateriaal.

Hoofdstuk 8 bevat een aantal belangrijke overkoepelende conclusies en een samenvatting van belangrijke parameters die aangepast kunnen worden om de optimale samenstelling van bioorganics-houdende botssubstituten te ontwikkelen.

# Acknowledgement



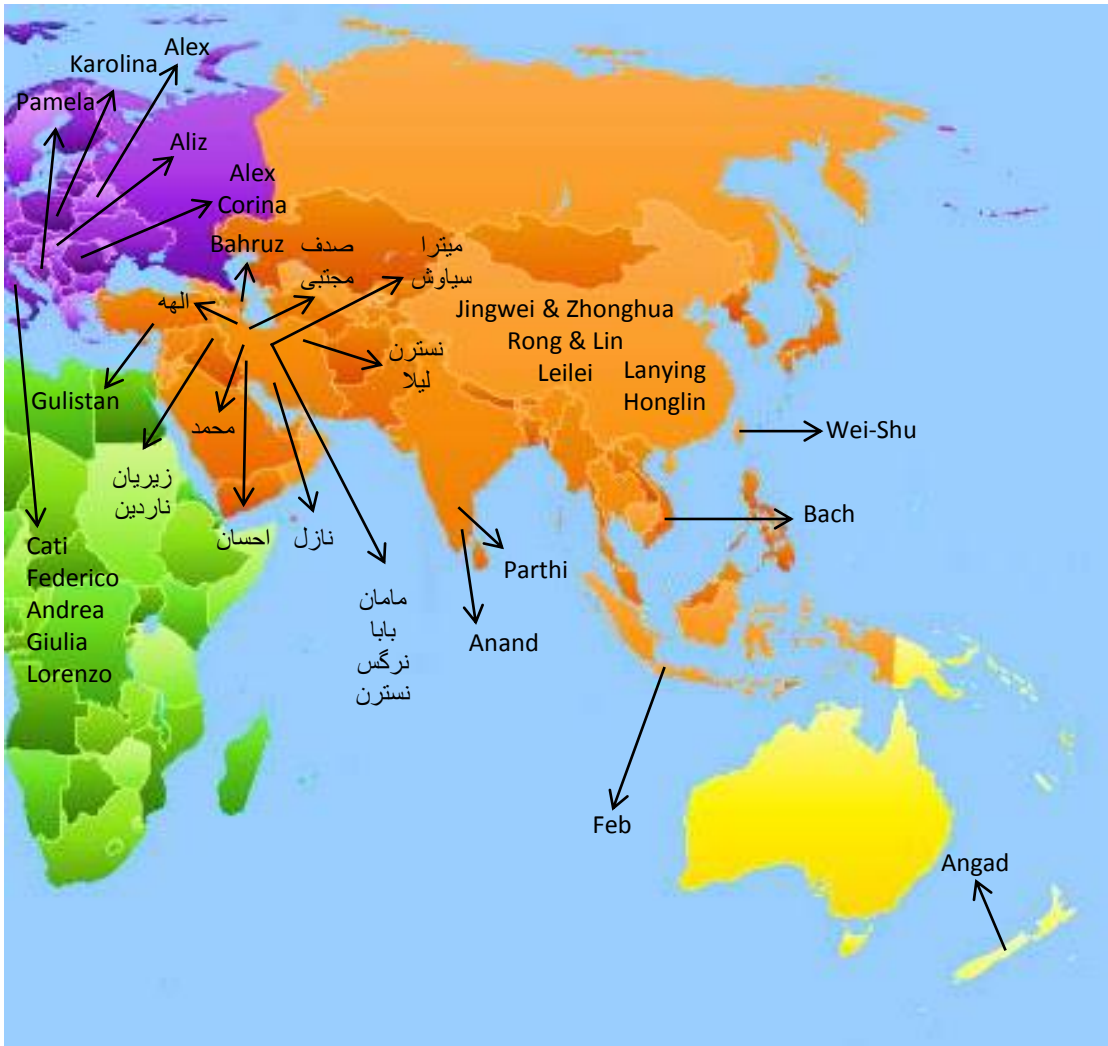
- Erik & Erica
- Anne & Maaïke
- Mijke
- Bjorn
- Anouk
- Jacqueline
- Tom
- Marloes K.
- Marloes L.
- Carola
- Wim
- Frits
- Andre
- Marcel



*I am really grateful for all the help and support from my supervisors, committee members, colleagues, friends, family and partner.*

*You literally make my world.*

**July 2016**  
**Niloofer**



## List of publications

### Publications related to this thesis:

1. Z. Tahmasebi Birgani, A. Malhotra, L. Yang, B. Harink, P. Habibovic, "Calcium phosphate ceramics with inorganic additives", in: Paul Ducheyne, *Comprehensive Biomaterials*, Elsevier Ltd. (2016) accepted for publication.
2. Z. Tahmasebi Birgani, A. Malhotra, C.A. van Blitterswijk, P. Habibovic, "Human mesenchymal stromal cells response to biomimetic calcium-phosphates containing strontium", *Journal of Biomedical Materials Research: Part A* (2016) DOI:10.1002/jbm.a.35725.
3. Z. Tahmasebi Birgani, E. Fennema, M.J. Gijbels, J. de Boer, C.A. van Blitterswijk, P. Habibovic, "Stimulatory effect of cobalt ions incorporated into calcium phosphate coatings on neovascularization in an in vivo intramuscular model in goats", *Acta Biomaterialia* 36 (2016) 267–276.
4. Z. Tahmasebi Birgani, C.A. van Blitterswijk, P. Habibovic, "Monolithic calcium phosphate/poly(lactic acid) composite versus calcium phosphate-coated poly(lactic acid) for support of osteogenic differentiation of human mesenchymal stromal cells", *Journal of material science: Materials in Medicine* 75 (2016) 54-66.
5. Z. Tahmasebi Birgani, N. Gharraee, A. Malhotra, C.A. van Blitterswijk, P. Habibovic, "Combinatorial incorporation of fluoride and cobalt ions into calcium phosphates to stimulate osteogenesis and angiogenesis", *Biomedical Materials* (2016) DOI:10.1088/1748-6041/11/1/015020.
6. Z. Tahmasebi Birgani, B.J. Klotz, C.A. van Blitterswijk, P. Habibovic, "Poly(lactic acid) microspheres for local delivery of bioinorganics for applications in bone regeneration", *Advanced Biomaterials and Devices in Medicine* 1 (2014) 1-10.

### Other publications:

7. B.A.J.A. van Oirschot, R.M. Eman, P. Habibovic, S.C.G. Leeuwenburgh, Z. Tahmasebi, H. Weinans, J. Alblas, G.J. Meijer, J.A. Jansen, J.J.J.P. van den Beucken, "Osteophilic properties of bone implant surface modifications in a cassette model on a decorticated goat spinal transverse process", *Acta Biomaterialia* 37 (2016) 195–205.
8. C. Danoux, L. Sun, G. Koçer, Z. Tahmasebi Birgani, D. Barata, J. Barralet, C. van Blitterswijk, R. Truckenmüller, P. Habibovic, "Development of Highly Functional Biomaterials by Decoupling and Recombining Material Properties" *Advanced Materials* (2015) DOI: 10.1002/adma.201504589.

9. N Groen, N. Tahmasebi, F. Shimizu, Y. Sano, T. Kanda, D. Barbieri, H. Yuan, P. Habibovic, C.A. van Blitterswijk, J. de Boer, "Exploring the Material-Induced Transcriptional Landscape of Osteoblasts on Bone Graft Materials", *Advanced Healthcare Materials* 4 (2015) 1691-1700.
10. S. Amin Yavari, J. van der Stok, Y. Chai, R. Wauthle, Z. Tahmasebi Birgani, P. Habibovic, M. Mulier, J. Schrooten, H. Weinans, A. Zadpoor, "Bone regeneration performance of surface-treated porous titanium", *Biomaterials* 35 (2014) 6172-6181.
11. M. Ventura, Y. Sun, S. Cremers, P. Borm, Z.T. Birgani, P. Habibovic, A. Heerschap, P.M. van der Kraan, J.A. Jansen, X.F. Walboomers, "A theranostic agent to enhance osteogenic and magnetic resonance imaging properties of calcium phosphate cements", *Biomaterials* 35 (2014) 2227-2233.
12. M. Bianchi, E.R. Urquia Edreira, J.G.C. Wolke, Z.T. Birgani, P. Habibovic, J.A. Jansen, A. Tampieri, M. Marcacci, S.C.G. Leeuwenburgh, J.J.J.P. van den Beucken, "Substrate geometry directs the in vitro mineralization of calcium phosphate ceramics", *Acta Biomaterialia* 10 (2014) 661-669.
13. A.W.G. Nijhuis, M.R. Nejadnik, F. Nudelman, X.F. Walboomers, J. te Riet, P. Habibovic, Z. Tahmasebi Birgani, L. Yubao, P.H.H. Bomans, J.A. Jansen, N.A.J.M. Sommerdijk, S.C.G. Leeuwenburgh, "Enzymatic pH control for biomimetic deposition of calcium phosphate coatings", *Acta Biomaterialia* 10 (2014) 931-939.
14. A. Nandakumar, Z. Tahmasebi Birgani, D. Santos, A. Mentink, N. Auffermann, K. van der Werf, M. Bennink, L. Moroni, C. van Blitterswijk, P. Habibovic, "Surface modification of electrospun fibre meshes by oxygen plasma for bone regeneration", *Biofabrication* 5 (2013) 01-14.
15. M. Bongio, J.J.J. van den Beucken, M.R. Nejadnik, Z. Tahmasebi Birgani, P. Habibovic, L.A. Kinard, F.K. Kasper, A.S.G. Mikos, S.C.G. Leeuwenburgh, J. A. Jansen, "Subcutaneous tissue response and osteogenic performance of calcium phosphate nanoparticle-enriched hydrogels in the tibial medullary cavity of guinea pigs", *Acta Biomaterialia* 9 (2013) 5464-5474.
16. A. Nandakumar, C. Cruz, A. Mentink, Z. Tahmasebi Birgani, L. Moroni, C. van Blitterswijk, P. Habibovic, "Monolithic and assembled polymer-ceramic composites for bone regeneration", *Acta Biomaterialia* 9 (2013) 5708-5717.
17. M. Bongio, M.R. Nejadnik, Z. Tahmasebi Birgani, P. Habibovic, L.A. Kinard, F.K. Kasper, A.G. Mikos, J.A. Jansen, S.C.G. Leeuwenburgh, J.J.J.P. van den Beucken, "In Vitro and In Vivo Enzyme-Mediated Biomineralization of Oligo(poly(ethylene glycol) Fumarate Hydrogels", *Macromolecular Bioscience* 13(6) (2013) 777-88.
18. M.R. Nejadnik, X. Yang, T. Mimura, Z. Tahmasebi Birgani, P. Habibovic, K. Itatani, J.A. Jansen, J. Hilborn, D. Ossipov, A.G. Mikos, S.C.G. Leeuwenburgh, "Calcium-Mediated

Secondary Cross-Linking of Bisphosphonated Oligo(poly(ethylene glycol) Fumarate) Hydrogel”, *Macromolecular Bioscience* 13 (2013) 1308–1313.

19. A.M.C. Barradas, V. Monticone, M. Hulsman, C. Danoux, H. Fernandes, Z. Tahmasebi Birgani, F. Barre`re-de Groot, H. Yuan, M. Reinders, P. Habibovic, C. van Blitterswijk, J. de Boer, “Molecular mechanisms of biomaterialdriven osteogenic differentiation in human mesenchymal stromal cells”, *Integrative Biology* 5 (2013) 920-931.



“Look deep into nature, and then you will understand everything better.”

Albert Einstein

ISBN:978-90-365-4153-4